

The Mechanisms of Calcification in Coccolithophores

**The molecular basis of calcium and inorganic carbon
transport in *Emiliana huxleyi***

Dissertation

**in fulfilment of the requirements for the degree “Dr. rer. nat.”
of the Faculty of Mathematics and Natural Sciences
at Kiel University**

submitted by

Luke Colin Martin Mackinder

Kiel

March 2012

First referee: Prof. Dr. Ulf Riebesell

Second referee: Prof. Colin Brownlee

Date of the oral examination: 23rd May 2012

Approved for publication:

Signed (Title, first and surnames), Dean:

Table of Contents

Summary	4
Zusammenfassung	6
CHAPTER 1. General Introduction	9
1.1 Coccolithophores – the rise of <i>Emiliana huxleyi</i>	9
1.2 Coccolithophores and the marine carbon cycle in a changing ocean	10
1.3 Calcification in coccolithophores	13
1.4 Ca²⁺ transport in coccolithophores	16
1.5 Inorganic carbon uptake and usage in coccolithophores	17
1.6 pH homeostasis in coccolithophores	19
1.7 Thesis Outline	20
1.8 List of publications	21
References	23
CHAPTER 2. Molecular Mechanisms Underlying Calcification in Coccolithophores	29
CHAPTER 3. Expression of biomineralization-related ion transport genes in <i>Emiliana huxleyi</i>	41
CHAPTER 4. Calcification and photosynthesis in <i>Emiliana huxleyi</i>: Physiological and genetic responses to individual carbonate system parameters	59
CHAPTER 5. Ion transport associated with calcification and inorganic carbon acquisition in coccolithophores: Insights from the <i>Emiliana huxleyi</i> genome	103
CHAPTER 6. The cloning and partial characterization of two calcification related genes, AEL1 a putative HCO₃⁻ transporter and CAX3 a putative Ca²⁺/H⁺ exchanger, from the coccolithophore <i>Emiliana huxleyi</i>	135
CHAPTER 7. Synthesis and future perspectives	169
7.1 Calcification	169
7.2 Inorganic carbon transport	171
7.3 Coccolithophores in a changing ocean	173
7.4 Future directions	175
References	176
Acknowledgements	178
Declaration of work	179

Summary

Coccolithophores are calcifying marine phytoplankton that through the fixation of inorganic carbon into calcite and particulate organic carbon play a fundamental role in global carbon cycles. As the CO₂ concentration of the surface ocean increases through the anthropogenic release of CO₂ by burning fossil fuels both a decrease in pH (ocean acidification) and an increase in dissolved inorganic carbon (ocean carbonation) are taking place. To understand the impact of these ocean changes on coccolithophores it is essential that we rapidly increase our knowledge of the cellular processes underlying coccolithophore physiology. This doctoral thesis focuses on the cellular and molecular processes involved in the transport of Ca²⁺, inorganic carbon and H⁺ in relation to calcification and photosynthesis in the coccolithophore species *Emiliana huxleyi*. The thesis comprises 7 chapters: Chapter 1 is a general introduction to coccolithophore cellular biology and global carbon cycling; Chapters 2-6 are a combination of publications and data chapters; Chapter 7 provides a synthesis of the results placing the presented data into context of coccolithophores in a changing ocean, highlighting future research areas.

Chapter 2 is a published review of the current literature on the molecular aspects of calcification in coccolithophores. It identifies key gaps in our knowledge of coccolithophore cellular biology and presents new hypotheses for the transport of substrates to the site of calcification. Chapter 3 investigates some of the proposed hypotheses by examining the role of several candidate Ca²⁺, H⁺ and inorganic carbon transport genes in calcifying and non-calcifying cells of *E. huxleyi*, using quantitative reverse transcriptase PCR. The data provides strong evidence that a putative HCO₃⁻ transporter (*AEL1*), a Ca²⁺/H⁺ exchanger (*CAX3*), a vacuolar H⁺-ATPase pump (*ATPvc/c'*) and a gene encoding for a coccolith-associated protein, GPA, play key roles in *E. huxleyi* biomineralization. *CAX3* and *AEL1* were chosen for further analysis and were successfully cloned and expressed in *Saccharomyces cerevisiae* and Human Embryonic Kidney cells (HEK293) respectively (Chapter 6). However complete characterization of *CAX3* and *AEL1* was unsuccessful. *CAX3* failed to complement the Ca²⁺ sensitive phenotype of a *S. cerevisiae* mutant, with further expression in a Ca²⁺ sensitive *Escherichia coli* mutant resulting in a lethal phenotype. The investigation of HCO₃⁻ transport in HEK293 cells expressing *AEL1* gave negative results, potentially due to the poor localization of AEL1 to the plasma membrane. The data highlights the importance of developing genetic transformation techniques in coccolithophores to reduce the dependency of using foreign expression systems for the characterization of genes.

The influence of the individual carbonate system components (CO₂, HCO₃⁻, CO₃²⁻ and H⁺) on coccolithophore physiology and genetic response is relatively unknown. Chapter 4

disentangles the individual carbonate system components investigating their influence on calcification, particulate organic carbon fixation and gene expression in *E. huxleyi*. It identifies, for the first time, the genetic basis of a carbon concentrating mechanism (CCM) in coccolithophores, with the transcription of multiple CCM associated genes up-regulated at low concentrations of HCO_3^- and CO_2 . Physiological data combined with expression data indicates that calcification does not function as a CCM under carbon limitation and is instead reduced to allow the redistribution of inorganic carbon from calcification to photosynthesis. Furthermore, the data confirms previous studies that the substrate for calcification is HCO_3^- and that growth and organic carbon fixation rates are primarily influenced by CO_2 .

The recent sequencing of the *E. huxleyi* genome has provided vast quantities of genetic data that requires detailed analysis to realise its full potential. Chapter 5 analyses the genome for calcification and photosynthesis related transport genes discovering that *E. huxleyi* has a diverse range of inorganic carbon, Ca^{2+} and H^+ transporters, from classical plant, animal and bacterial families. The presence of multiple $\text{Na}^+/\text{Ca}^{2+}$ exchangers, a family of almost exclusively animal transporters indicates that coccolithophores have the potential to use both H^+ and Na^+ electrochemical gradients to drive secondary transport. Furthermore the identification of green algal CCM genes may provide a strong basis for investigating the evolution of CCMs in eukaryotic algae.

The data presented in this thesis provides a significant step in our understanding of coccolithophore physiology at a cellular and molecular level. It offers a solid platform for future research in coccolithophore cell biology an area of research that is essential to comprehend the role of coccolithophores in global carbon cycling and how they will respond and adapt to future ocean changes.

Zusammenfassung

Coccolithophoriden sind kalkbildende marine Phytoplankton. Sie sind von außerordentlicher Bedeutung für den globalen Kohlenstoffkreislauf, da sie inorganischen Kohlenstoff sowohl in Kalzit als auch in organischem Kohlenstoff binden können. Die zunehmende Verbrennung von fossilen Brennstoffen führt zu einem Anstieg der Kohlenstoffdioxid (CO_2) Konzentration im Oberflächenwasser der Ozeane. Das wiederum hat zur Folge, dass deren pH Wert abnimmt (Ozeanversauerung) und die Konzentration von inorganischem Kohlenstoff zunimmt (Ozean carbonation). Um zu verstehen welche Folgen diese Veränderungen auf Coccolithophoriden haben werden ist es unbedingt notwendig dass wir schnellstmöglich unser Verständnis zellulärer und physiologischer Prozesse verbessern.

Diese Doktorarbeit befasst sich mit dem intrazellulären Transport von inorganischem Kohlenstoff, Ca^{2+} und H^+ und wie dieser mit der Kalkbildung und Photosynthese der Coccolithophoride *Emiliana huxleyi* in Zusammenhang steht. Die Doktorarbeit umfasst sieben Kapitel. Kapitel 1 beinhaltet eine Einleitung über die Zellbiologie von Coccolithophoriden und den globalen Kohlenstoffkreislauf. Kapitel 2 bis 6 beinhalten die Publikationen und weitere unveröffentlichte Daten. Kapitel 7 beinhaltet eine Synthese aller Ergebnisse und setzt die erhobenen Daten in Bezug zu den sich wandelnden Ozeanen und hebt zukünftige Forschungsgebiete hervor.

In Kapitel 2 wird das uns bekannte molekularbiologische Wissen über Kalkbildung in Coccolithophoriden zusammengefasst. In der daraus entstandenen Veröffentlichung wird auf entscheidende Verständnislücken intrazellulärer Prozesse aufmerksam gemacht und es werden neue Konzepte erarbeitet wie Coccolithophoriden zur Kalzifizierung benötigte Substrate innerhalb der Zelle transportieren. Kapitel 3 befasst sich mit einigen dieser Konzepte, indem mittels qPCR Techniken mögliche Ca^{2+} , H^+ und $\text{CO}_2/\text{HCO}_3^-$ Transporter in kalzifizierenden und nicht-kalzifizierenden *E. huxleyi* Zellen genauer untersucht werden. Ergebnisse dieser Studie deuten stark darauf hin, dass bestimmte Gene (ein HCO_3^- transport protein (*AELI*), ein $\text{Ca}^{2+}/\text{H}^+$ Tauscher (*CAX3*), eine ATPase (*ATPVc/c'*) und ein Gen was für ein coccolithen-assoziiertes Protein (*GPA*) kodiert), entscheidende Funktionen in der Kalkbildung von *E. huxleyi* übernehmen. *CAX3* und *AELI* wurden daraufhin genauer unter die Lupe genommen. *CAX3* wurde erfolgreich in Hefe (*Saccharomyces cerevisiae*) kloniert und *AELI* in embryonale menschliche Nierenzellen (HEK293). Eine vollständige Charakterisierung der beiden Proteine blieb jedoch erfolglos. Der Einbau von *CAX3* in einen Ca^{2+} sensitiven Hefe Phänotyp führte zu keinem Ergebnis. Auch ein Ca^{2+} sensitiver Phänotyp von *Escherichia coli* konnte durch den Einbau von *CAX3* nicht gerettet werden. Der Einbau von *AELI* in HEK293 Zellen brachte

ebenfalls keine neuen Erkenntnisse. Möglicherweise wurde AEL1 innerhalb der Zelle nicht an der Plasmamembran eingebaut. Diese Ergebnisse zeigen, dass es dringend notwendig ist Klonierungstechniken speziell für Coccolithophoriden zu entwickeln, damit man bei der Charakterisierung von Genen weniger von Methoden abhängt, die auf andere Organismen optimiert sind.

Der Einfluss einzelner Karbonatsystemparameter (CO_2 , HCO_3^- , CO_3^{2-} und H^+) auf die Physiologie und Genregulierung von Coccolithophoriden ist nur in geringem Maße verstanden. In Kapitel 4 wird der individuelle Einfluss dieser Parameter auf *E. huxleyi* genauer untersucht. Besonderes Augenmerk galt dabei deren Einfluss auf Kohlenstofffixierung, Kalkbildung und Genregulierung. Dabei wurde zum ersten mal genauer die genetische Grundlage für die intrazelluläre Anreicherung von CO_2 (CCM) identifiziert. Mehrere Gene die wahrscheinlich im Zusammenhang mit dem CCM stehen wurden, unter geringen CO_2 und HCO_3^- Konzentrationen verstärkt exprimiert. Des Weiteren, konnte klar gezeigt werden, dass Kalkbildung nicht als CCM fungiert, wenn CO_2 und HCO_3^- Konzentrationen gering sind. Stattdessen wurde unter diesen Bedingungen die Kalkbildung eingestellt um mehr inorganischen Kohlenstoff für die photosynthetische Kohlenstofffixierung bereit zu stellen. Außerdem konnte in dieser Studie bestätigt werden, (1) dass HCO_3^- aus Seewasser als Kohlenstoffsubstrat für die Kalkbildung dient und (2) dass Wachstum und photosynthetische Kohlenstofffixierung weitestgehend von der externen CO_2 -Konzentration abhängen.

Die Sequenzierung des *E. huxleyi* Genoms hat eine enorme Menge an genetischen Daten erzeugt, die nun genau analysiert werden müssen, um deren Potenzial voll auszuschöpfen. In Kapitel 5 wird das Genom, mit Schwerpunkt auf Genen die im Zusammenhang mit Photosynthese und Kalkbildung stehen, genauer untersucht. Die Ergebnisse zeigen, dass *E. huxleyi* eine Vielzahl von $\text{CO}_2/\text{HCO}_3^-$, Ca^{2+} und H^+ Transportern hat, die mit denen von Landpflanzen, Tieren und Bakterien verwandt sind. Die Anwesenheit mehrerer $\text{Na}^+/\text{Ca}^{2+}$ Austauscher Proteine (die beinahe ausschließlich aus Tieren bekannt sind) verdeutlicht, dass Coccolithophoriden sowohl H^+ als auch Na^+ Gradienten nutzen können um Transportprozesse durchzuführen. Außerdem wurde ein grünalgen-ähnlicher CCM entdeckt. Dieses Ergebnis könnte die Basis für weitere evolutionsbiologische Studien über eukaryotische Algen bieten.

Die Ergebnisse, die in dieser Doktorarbeit zusammengefasst sind, erhöhen deutlich unser Verständnis über die Physiologie und Zellbiologie von *E. huxleyi*. Sie legen außerdem die Grundlage für weitere zell- und molekularbiologische Untersuchungen. Es wird außerordentlich wichtig sein auf diesem Gebiet weiter zu forschen um zu verstehen welche Rolle Coccolithophoriden im Kohlenstoffkreislauf haben und wie sie auf zukünftige Veränderungen in den Ozeanen reagieren und sich eventuell anpassen werden.

CHAPTER 1. General Introduction

1.1 Coccolithophores – the rise of *Emiliana huxleyi*

The Earth is approximately 4.6 billion years (Gyrs) old (Gradstein et al., 2004). Around 2.4 Gyrs ago prokaryotic oxygenic autotrophs started to take advantage of the virtually infinite supply of reductant in the form of seawater and energy from sunlight to fix CO₂ - initiating the oxidation of the Earth's ocean and atmosphere (Falkowski et al., 2004). This oxidation allowed the evolution of single celled eukaryotes that subsequently ~1.8 Gyrs ago enslaved a cyanobacterium resulting in the forefather of all eukaryotic photosynthetic life (Tirichine and Bowler, 2011). Over time through further secondary and tertiary endosymbiotic events and the advent of multicellularity the diverse terrestrial and marine photosynthetic life forms that shape our planet evolved.

Our present day oceans are dominated by three main groups of eukaryotic algae; the diatoms, dinoflagellates and coccolithophores all with "red" plastids primarily derived from a secondary endosymbiotic event. The rise of this modern day eukaryotic phytoplankton assemblage was initiated in the mid Triassic ~240 million years (Myrs) ago (Falkowski et al., 2004). Of these three principle groups the coccolithophores are unicellular calcifying phytoplankton that evolved ~220 Myrs ago and have since been a significant component of the oceanic phytoplankton and marine sediment (Bown et al., 2004). Through the photosynthetic fixation of carbon and the production of inorganic calcite plates (coccoliths), coccolithophores have had and continue to have an influential impact on the Earth's geology and atmosphere. The production of calcite and its deposition has resulted in the global decrease in the saturation state of carbonate minerals (Ridgwell, 2005) and formation of vast calcareous deposits that define our surrounding geology.

Since the rise of coccolithophores within the Haptophytes during the Triassic, over 4000 morphological distinct coccosphere types (the collective term for the coccoliths surrounding the cell) have been identified in the geological record (De Vargas et al., 2007). From these only ~280 morphologically unique coccospheres are extant (Young et al., 2003). The most abundant extant species is *Emiliana huxleyi* which, along with the genera *Gephyrocapsa* and *Reticulofenestra*, belong to the Noëlaerhabdaceae, a family member of the Isochrysidales which diverged from the other calcifying coccolithophores ~150 Myrs ago (De Vargas et al., 2007). Although only a small proportion of coccolithophore species belong to the Noëlaerhabdaceae, they have dominated coccolithophore communities over the past 20 Myrs (Beaufort et al., 2011).

Of these *E. huxleyi* evolved from the geophyrocapsids ~250,000 years ago and for the last ~70,000 years has been the most abundant coccolithophore forming gigantic blooms up to one million square kilometres in area (Tyrrell and Young, 2009).

The importance of *E. huxleyi* at a global level has resulted in it becoming the most investigated coccolithophore species, with the majority of coccolithophore cell physiological studies focusing on this single species. Although a single species, it is becoming increasingly evident that there are large genetic and physiological variations between *E. huxleyi* strains. This has been highlighted by the large intraspecific variation at the genetic level not only between spatially separated *E. huxleyi* blooms but also within individual blooms (Medlin et al., 1996; Iglesias-Rodríguez et al., 2006). This intraspecific variation is also widely seen at a physiological level with large variations in physiological performance and responses to abiotic changes between *E. huxleyi* strains (Langer et al., 2009). This has resulted in the discussion of the species concept in *E. huxleyi* and the presence of a bacterial-like pan-genome (a genome consisting of a group of core genes (found in all strains) and dispensable genes (genes specific to certain strains) (Medini et al., 2005)) (Joint Genome Institute: Read et al., unpublished). This intraspecific variation adds an extra layer of complexity to coccolithophore research, requiring cautious extrapolation of results from single species experiments to other coccolithophores and ultimately global influences (Ridgwell et al., 2009).

1.2 Coccolithophores and the marine carbon cycle in a changing ocean

Since the beginning of the industrial revolution, the oceans have absorbed ~50% of anthropogenic released CO₂ from fossil fuel burning (Sabine et al., 2004). This is buffering the effects of global warming but is having a profound effect on ocean carbonate chemistry and its biology (Riebesell et al., 2009). Although phytoplankton contribute to only about 0.2% of the Earth's photosynthetic biomass they account for 45% of the Earth's annual net primary production of ~105 petagrams of carbon year⁻¹ (Field et al., 1998). Of this, coccolithophores represent an important group within marine photoautotrophs, comprising in the order of 10% of the phytoplankton biomass (Tyrrell and Young, 2009) and a considerably larger proportion of all modern day CaCO₃ precipitation (Milliman, 1993). This results in them playing a fundamental role in global carbon cycling, a dynamic process set to see dramatic changes in the future (Riebesell et al., 2009).

The global carbon cycle is a complex network interconnected by chemical, biological and physical processes and involving fluxes of carbon between three reservoirs - the terrestrial realm, the atmosphere and the oceans (Fig. 1). The oceans provide a gigantic store for carbon with a

content of reactive carbon that is ~60 times greater than that of the atmosphere (Riebesell et al., 2009). By “pumping” carbon from surface waters, which is in equilibrium with the atmosphere in respect to CO_2 , to the deep ocean they form a gradient removing the greenhouse gas CO_2 from the atmosphere. This oceanic carbon flux from the surface to the deep ocean can be described by two processes, the abiotic solubility pump and the biotic pump, interacting in a nonlinear manner (Riebesell et al., 2009). The abiotic solubility pump is driven by the increasing solubility of CO_2 in cold water and accounts for ~30-40% of the surface-to-deep dissolved inorganic carbon (DIC) gradient (Toggweiler et al., 2003). The biological pump accounts for the other 60-70% and is driven by the fixation of DIC into organic carbon that sinks out of the photic zone below the pycnocline. To some extent the biological pump is counteracted by the carbonate counter pump. This is driven by the formation of carbonates, predominantly by foraminifera, pteropods and coccolithophores and reduces surface water alkalinity leading to an increase in partial CO_2 pressure ($p\text{CO}_2$) and a reduction in the atmosphere-ocean CO_2 flux (Rost and Riebesell, 2004). However, both the biological and counter pump form the surface-to-deep ocean DIC gradient by transporting particulate carbon to the deep ocean (Riebesell et al., 2009).

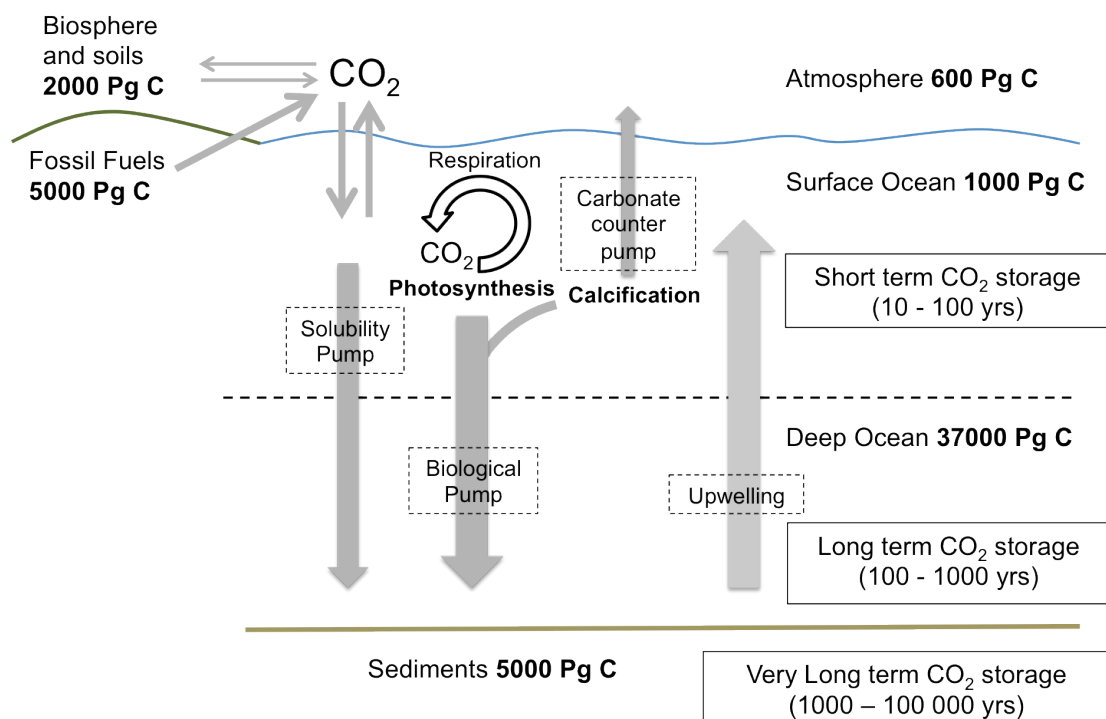
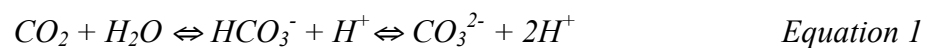


Figure 1. The surface carbon cycle. The approximate reservoir sizes are in bold expressed as petagrams of carbon (Pg C: $1 \text{ Pg} = 10^{15} \text{ g} = 1 \text{ gigaton}$). In solid boxes are the storage time-scales and in dashed boxes are the principal carbon “pumps”. Based on Zeebe and Ridgwell (2011).

Increased atmospheric CO₂ is predicted to cause two principal changes in the ocean: a rise in sea surface temperature (SST) through the greenhouse effect of CO₂ and ocean acidification induced through the absorption of CO₂ by the oceans (Equation 1). The solubility pump will be dominantly affected by increases in SST that will reduce the CO₂ solubility of the oceans and potentially slow down thermohaline circulation leading to a further reduction of solubility gradients (Riebesell et al., 2009). Increasing SST is also expected to have three major impacts on the ocean ecosystem and in turn the biological pump these being: 1) reduced supply of nutrients due to decreased vertical mixing 2) Increased stratification providing more sunlight to surface waters and 3) increased thermal energy to drive biological activity. With the potential effects being highly complex and expected to vary considerably both spatially and temporally (Riebesell et al., 2009).



In addition to SST rise ocean acidification has the potential to result in major changes in ocean chemistry and biological processes. With future anthropogenic driven ocean acidification possibly leading to an upper ocean pH decrease not seen for the past 300 Myrs, excluding rare catastrophic events in the Earth's history (Caldeira and Wickett, 2003). Ocean acidification also results in ocean "carbonation", a concurrent increase in DIC. Together these are expected to result in winners and losers potentially leading to the loss of biodiversity and restructuring of ecosystems (Riebesell et al., 2009). Ocean carbonation may benefit organisms with inefficient DIC uptake and CO₂ fixation mechanisms, stimulating carbon fixation rates and primary production (Riebesell et al., 1993; Hein and Sand-Jensen, 1997; Riebesell et al., 2007), thus increasing the biological pump and acting as a negative feedback on global warming.

By the year 2100, oceanic uptake of anthropogenic CO₂ is predicted to result in a ~0.3-0.5 pH unit decrease in seawater pH (Caldeira and Wickett, 2005). Ocean acidification has primarily been shown to have negative effects on calcifying organisms (Fabry et al., 2008; Riebesell and Tortell, 2011), with coccolithophores generally showing decreased calcification with decreasing pH in laboratory (Riebesell et al., 2000; Feng et al., 2008) and field (Delille et al., 2005; Engel et al., 2005) based studies. This negative influence of low pH on calcification is further supported in a global study of coccoliths isolated from water and sediment samples with a general trend of decreasing coccolith mass seen with decreasing CO₃²⁻ concentration (Beaufort et al., 2011). Contradictory to the majority of data, is an increase in calcification at elevated CO₂ in an over-calcified strain of *E. huxleyi* (PLY M219 (NZEH)) (Iglesias-Rodriguez et al., 2008; Shi et al., 2009). However, the normalization process and methodology of Iglesias-Rodriguez et al.

(2008) has been placed under scrutiny (Riebesell et al., 2008) and data from Shi et al. (2009) is based on only two $p\text{CO}_2$ levels. A recent comprehensive study with the same strain has shown a moderate decrease in calcification with increasing $p\text{CO}_2$ (Hoppe et al., 2011). It is becoming increasingly apparent that the inter- and intra- specific variations in response to increasing $p\text{CO}_2$ (Langer et al., 2006; Langer et al., 2009) can be explained by an optimum response curve that shifts between species and strains (Langer et al., 2006; Langer et al., 2009; Ridgwell et al., 2009; Bach et al., 2011; Krug et al., 2011), with the optimum met at different $p\text{CO}_2$ levels for different strains/species, resulting in variations in observed responses over the same $p\text{CO}_2$ range.

A decrease in calcification in surface waters is predicted to influence the global marine carbon cycle in two ways, both with opposite feedbacks on global warming. Due to the higher density of CaCO_3 compared to particulate organic carbon, calcite produced in surface waters is proposed to act as ballast increasing the downward flux of the biological pump. Therefore a decrease in calcite production due to ocean acidification will lead to a reduction in calcite ballast, reducing the export of organic carbon into the deep (Armstrong et al., 2002; Klaas and Archer, 2002). This will result in positive feedback reducing the air-to-sea CO_2 flux. On the other hand, a decrease in calcification will reduce the carbonate counter pump, increasing the air-to-sea CO_2 flux providing a negative feedback loop (Riebesell et al., 2009). The overall sign and magnitude of the feedback response on global warming by coccolithophores (and other organisms) to a changing ocean is uncertain (Riebesell et al., 2009). There are still key gaps and uncertainties in our knowledge of the response of the biological and carbonate pump to changes in coccolithophore calcification. Furthermore, the response of coccolithophores over longer time-scales and at the community level is uncertain. To understand these responses it is essential that we have a greater understanding of the genetic plasticity of coccolithophores (i.e. how they will adapt to a changing ocean) and the underlying mechanisms of coccolithophore cellular processes (i.e. calcification and DIC acquisition).

1.3 Calcification in coccolithophores

Biom mineralization of calcite in coccolithophores is a complex and highly regulated process, resulting in its biogenic product differing in both morphology and chemical composition from abiotically produced calcite (Westbroek et al., 1989). Coccoliths can fall into two categories, heterococcoliths and holococcoliths. Heterococcoliths are produced intracellularly and consist of complex calcite crystal elements that are routinely used in coccolithophore taxonomy (Young et al., 1992). Holococcoliths are less complex and comprise of uniform-shaped crystals that are thought to be produced extracellularly during certain life-cycle stages (Young et al., 1999). This

thesis focuses on the intracellular formation of heterococcoliths, the more widely abundant and biogeochemically important coccolith form.

The intracellular site of calcite production means that it is completely isolated from the surrounding seawater. This results in the necessity for the transport of the substrates for calcification from the external environment to the site of precipitation along with tight regulation of cellular pH. This has posed three key questions: 1) What is the route and mechanism of cellular Ca^{2+} transport? 2) How does the cell acquire and distribute DIC between calcification and photosynthesis? And 3) How does the cell regulate cytosolic and endomembrane pH - essential for calcification and cellular metabolism? Our current knowledge of these three questions is covered, respectively, in the following sections: **1.4 Ca^{2+} transport in coccolithophores**, **1.5 Inorganic carbon uptake and usage in coccolithophores** and **1.6 pH homeostasis in coccolithophores**.

Evidence from electron microscopy studies have formed the basis of our knowledge of coccolith formation and structure in several coccolithophore species, namely *E. huxleyi* (Wilbur and Watabe, 1963; Klaveness, 1976; van der Wal et al., 1983; Westbroek et al., 1989; Young et al., 1999), *Pleurochrysis carterae* (Manton and Leedale, 1969; van der Wal et al., 1983; van der Wal et al., 1983) and *Coccolithus pelagicus* (Manton and Leedale, 1969; Taylor et al., 2007). Calcification in coccolithophores takes place in a Golgi derived intracellular vesicle termed the coccolith vesicle (CV) that is tightly apposed to the nucleus (Klaveness, 1976; van der Wal et al., 1983). Associated with the distal side of the CV in *E. huxleyi*, *Gephyrocapsa* sp. and *C. pelagicus* is an organelle termed the reticular body (RB), a unique endomembrane network with a large surface area that is hypothesised to play a crucial role in calcification (Klaveness, 1976). In *P. carterae*, there is no defined RB and coccolith production occurs in vesicles that form the trans Golgi, with multiple coccoliths at varying stages of formation seen within a single cell (van der Wal et al., 1983). Once intracellular coccolith formation is complete, the coccolith is transported to the cell cortex and secreted onto the cell surface in a single exocytotic extrusion event (Taylor et al., 2007).

Although variations in coccolith formation occur between species, calcification ubiquitously occurs in Golgi derived vesicles with nucleation of a proto-coccolith ring around an organic base plate. This is followed by growth of crystals in varying directions to form the complex mature coccoliths (Young et al., 1999). In *P. carterae* three highly acidic polysaccharides, PS-1, PS-2 and PS-3, have been identified to play a role in calcite precipitation (Marsh et al., 1992). Golgi derived polysaccharide and Ca^{2+} dense vesicles, termed coccolithosomes, are thought to be involved in the supply of polysaccharide and Ca^{2+} to the coccolith forming vesicles (Outka and Williams, 1971; van der Wal et al., 1983). Using immuno-

localization PS-1 and PS-2 were shown to be synthesised in the Golgi, associate with the organic base plate at the onset of crystallization, and were present in the Golgi- derived coccolith forming vesicle during calcification and to stay associated with the surface of the coccolith after externalization (Marsh, 1994). PS-2 and PS-3 have been shown to be essential for successful nucleation and mineralization in *P. carterae*. With PS-2 mutants producing less than 5% calcite compared to wild-type cells (Marsh and Dickinson, 1997) and PS-3 mutants unable to form mature coccoliths as seen in wild-type cells (Marsh et al., 2002).

In *E. huxleyi* only one polysaccharide (coccolith associated polysaccharide; CAP) has been identified that associates with extracellular coccoliths of *E. huxleyi* (de Jong et al., 1976). This polysaccharide is a galacturonomannan, a complex polysaccharide that consists of a sulphated mannan backbone with a variety of side chains rich in galacturonic acid (Vliegthart et al., 1981), showing similarities to PS-3 (Marsh, 2003). Borman *et al.* (1982) showed that CAP actually inhibits crystal growth in a solution supersaturated for Ca^{2+} and CO_3^{2-} . More recently strong evidence indicates that CAP is involved in the regulation of crystal growth by attaching preferentially to calcite acute edges to induce directional controlled growth (Henriksen et al., 2004). Another interesting macromolecule associated with coccoliths from *E. huxleyi* is GPA (termed GPA due to its high levels of glutamic acid, proline and alanine), a highly acidic protein thought to have potential Ca^{2+} binding properties (Corstjens et al., 1998). GPA has also been tentatively connected to the different morphologies of coccoliths from A and B morphotypes of *E. huxleyi*. Good correlation was shown between variations in the sequence of a unique motif (coccolith morphology motif; CMM) found in the 3'UTR and coccolith morphology (Schroeder et al., 2005).

Interestingly, studies of biomineralization in a wide range of organisms have indicated that biogenic mineral formation proceeds via a disordered interim mineral phase, termed amorphous calcium carbonate (ACC) in CaCO_3 producing organisms. The nature of ACC allows it to be transported and moulded into shape prior to crystalline CaCO_3 formation (Weiner, 2008). Mackinder et al. (2010) first proposed that ACC could be involved in coccolithophore calcification, with further investigation into this mechanism using Fourier Transform Infra-Red (FTIR) spectroscopy providing strong evidence that calcite production proceeds via an ACC phase (Marine Biological Association of the UK: Singleton et al., unpublished). If coccoliths are produced via an ACC phase, it may potentially have considerable impacts on the current concepts of coccolithophore calcification including the regulation of calcite formation and the transport of substrates.

1.4 Ca²⁺ transport in coccolithophores

Ca²⁺ plays an essential role in cell signalling and function. It is involved in many cellular signal transduction processes that rely on free cytosolic Ca²⁺ levels to be highly regulated and maintained at distinct and localized concentrations. As in all eukaryotic cells the free cytosolic Ca²⁺ concentration in *E. huxleyi* is maintained low at ~100 nM, with large changes in external Ca²⁺ not affecting cytosolic Ca²⁺ concentration (Brownlee et al., 1995). The Ca²⁺ concentration of seawater is 10 mM, approximately 10⁵ times greater than that of the cytosol. The ability of coccolithophores to produce coccoliths up to a rate of 1 per hour (Paasche, 1962) requires that large quantities of Ca²⁺ are transported to the CV. Three feasible hypothesis were put forward by Berry et al. (2002), for the trans-cellular transport pathway of Ca²⁺; these being 1) Ca²⁺ diffusion across the cytosol and direct uptake into the RB/CV 2) Fluid phase endocytotic Ca²⁺ uptake and vesicle transport directly to the RB/CV and 3) Ca²⁺ uptake of cytosolic Ca²⁺ via a peripheral endoplasmic reticulum (PER) network adjacent to the plasma membrane (PM), then transport to the CV via vesicle transport or the endomembrane network. Experiments investigating the second hypothesis of fluid phase endocytotic Ca²⁺ uptake have so far proved to be negative indicating that this is an unlikely route for Ca²⁺ uptake (Berry et al., 2002). If endocytosis is not the route for Ca²⁺ uptake, Ca²⁺ entry into the cytosol from the external seawater is almost certainly via Ca²⁺ permeable channels down its electrochemical gradient (Brownlee et al., 1995). Once within the cell either hypothesis 1 or 3 could potentially be feasible. Direct uptake of Ca²⁺ into the CV seems the most unlikely due to energetic constraints discussed in Berry et al. (2002) and limitations in CV surface area (Mackinder et al., 2010), whereas uptake into the endomembrane network then transport to the CV appears the most viable. As discussed above there is strong evidence that large vesicles play a role in Ca²⁺ transport from the Golgi to the site of precipitation in *P. carterae*, but this is not clear in *E. huxleyi* and *C. pelagicus*. In *E. huxleyi* the cellular envelope underlying the coccosphere has been shown to be made up of 3 or 4 membranous layers, which have been proposed to form the PER apposed to the PM (van der Wal et al., 1985). It is hypothesised that the PER could provide a large surface area to rapidly absorb Ca²⁺ into the endomembrane network once it has crossed the PM.

Molecular evidence for mechanisms of coccolithophore Ca²⁺ uptake and transport is very limited. Gene expression data supports the supply of Ca²⁺ for calcification via a Ca²⁺/H⁺ exchanger (CAX). *E. huxleyi* CAX3 has been shown to be exclusively expressed in diploid calcifying cells compared to haploid non-calcifying cells (von Dassow et al., 2009) and down-regulated when calcification was inhibited via Ca²⁺ removal and in a non-calcifying diploid

strain (Mackinder et al., 2011). Apart from this our knowledge of the molecular components is still in its infancy.

1.5 Inorganic carbon uptake and usage in coccolithophores

Unlike most photosynthetic organisms, coccolithophores have two demands for DIC - calcification and photosynthesis. This places a large demand on the cell to maintain sufficient DIC supply. Why coccolithophores produce coccoliths is unknown, it is widely accepted that the ecological success of coccolithophores indicates that the maintenance of coccoliths must be under positive selection. Several proposals have been put forward to explain why coccolithophores calcify. The one that has obtained the majority of attention is that calcification supports photosynthesis by producing protons (H^+) that are used in the dehydration of HCO_3^- to CO_2 . This concept has received strong backing with several physiological studies supporting it (Sikes et al., 1980; Nimer and Merrett, 1992, 1996; Buitenhuis et al., 1999). However, there have always been inconsistencies. In the first comprehensive study (and maybe still the most) on *E. huxleyi* physiology Paasche (1964) comments on the link between calcification and photosynthesis:

“As the work progressed however, it was gradually realized that the link between coccolith formation and photosynthetic CO_2 assimilation might be a less direct one, or that the two processes might even be independent of each other”

More recently the doubts of Paasche (1964) have been strongly supported by recent studies uncoupling photosynthesis and calcification (Herfort et al., 2004; Trimborn et al., 2007; Leonardos et al., 2009). There is also strong evidence that calcification can occur, albeit at lower rates, in the dark (Sekino and Shiraiwa, 1996) and that if calcification is inhibited by hydroxyethylidene bisphonic acid (HEBP) (a inhibitor of the growth of $CaCO_3$ crystals that completely suppresses $CaCO_3$ production) photosynthetic fixation of CO_2 actually increases (Sekino and Shiraiwa, 1994).

The substrate for the principle carbon-fixing enzyme, ribulose biphosphate carboxylase oxygenase (RubisCO) is CO_2 . At current seawater pH ~90% of DIC (concentration ~2mM) is HCO_3^- and less than 1% is CO_2 . This gives a free CO_2 concentration that is significantly lower than the $K_{1/2}$ with respect to CO_2 for RubisCO and may possibly be a limiting factor for phytoplankton productivity in certain environments (Riebesell et al., 1993). To overcome this, most unicellular marine algae have evolved carbon concentrating mechanisms (CCMs)

(Reinfelder, 2011). CCMs function to enhance CO₂ at the active site of RubisCO relative to the external concentration. The operation of a CCM in *E. huxleyi* has been identified, and is regulated by CO₂ limitation, with the K_{1/2} for CO₂ decreasing from 27.3 to 9.6 μmol L⁻¹ CO₂ as cells were cultured at decreasing pCO₂ levels (Rost et al., 2003). Relative to other phytoplankton the *E. huxleyi* CCM appears to be of a low affinity, with the diatom *Skeletonema costatum* and the Prymnesiophyte *Phaeocystis globosa* having K_{1/2}'s for CO₂ ~30 and ~6 times lower, respectively (Rost et al., 2003). The high K_{1/2} for O₂ evolution of *E. huxleyi* implies that photosynthesis is not CO₂ saturated at current oceanic CO₂ levels (~16 μmol L⁻¹). This is supported by other O₂ evolution and ¹⁴C incorporation experiments (Paasche, 1964; Buitenhuis et al., 1999; Herfort et al., 2002). However, neither growth rates nor total particulate organic carbon production increase dramatically above ambient CO₂ conditions (Langer et al., 2009). Why there are these discrepancies is currently unclear.

At ambient DIC there is strong evidence that *E. huxleyi* principally uses external CO₂ for photosynthesis (Sikes et al., 1980; Rost et al., 2003; Schulz et al., 2007) and HCO₃⁻ for calcification (Sikes et al., 1980; Nimer and Merrett, 1992; Buitenhuis et al., 1999; Herfort et al., 2002). Based on membrane inlet mass spectrometry (MIMS) studies, Schulz et al. (2007) further calculated that 70% of carbon for photosynthesis was diffusive CO₂ uptake, 21% active CO₂ uptake and 9% active HCO₃⁻ uptake (Schulz et al., 2007). HCO₃⁻ usage was shown to increase as the CCM was induced due to lower DIC (Rost et al., 2003). Furthermore, HCO₃⁻ usage for photosynthesis has been demonstrated, with inhibitor-based work suggesting that HCO₃⁻ uptake is via a DIDS (4,4'-diisothiocyanato-stibene-2,2'-disulfonic acid) sensitive HCO₃⁻ transporter (Herfort et al., 2002). The involvement of a HCO₃⁻ transporter in DIC uptake for calcification and potentially photosynthesis has been further supported by expression studies. These have shown that an Anion Exchange Like (*AELI*) HCO₃⁻ transporter belonging to the SoLute Carrier 4 (SLC4) family of exchangers is only expressed in the calcifying diploid life-cycle phase (von Dassow et al., 2009; Mackinder et al., 2011) and is regulated in response to the calcification level of cells (Mackinder et al., 2011).

Carbonic anhydrases (CAs) play fundamental roles in DIC uptake for photosynthesis (Badger, 2003) and calcification (Weiss and Marin, 2008) in organisms from all domains of life. Extracellular CA activity is very low in *E. huxleyi* cultured under ambient CO₂ (Nimer et al., 1997; Rost et al., 2003). However, CA has been detected in stationary phase cultures (Nimer et al., 1994) or very low DIC exponential phase cultures (Nimer et al., 1997) although this activity was not detected by Rost et al. (2003). CA activity has been reported in the chloroplast fraction of *Pleurochrysis sp.* (Quiroga and González, 1993) and *E. huxleyi* (Nimer et al., 1994), with the cytosolic fraction inhibiting CA activity indicating the potential absence of cytosolic CA

(Quiroga and González, 1993). Two *E. huxleyi* CAs belonging to the γ and δ families have been partially characterized in *E. huxleyi* with γ CA having a potential CV location (Soto et al., 2006), although its expression appears to be unrelated to cellular calcification (Mackinder et al., 2011).

Compared to cyanobacteria, green algae and diatoms our knowledge of carbon-uptake and CCM function in coccolithophores is very limited (Giordano et al., 2005; Reinfelder, 2011). To fully understand how coccolithophores will respond to ocean carbonation an increased mechanistic understanding at the cellular and molecular level is essential.

1.6 pH homeostasis in coccolithophores

If HCO_3^- is the DIC source for calcification (see above) the production of calcite will produce H^+ at a stoichiometry of 1:1 (Equation 2).



Without H^+ removal or buffering calcifying cells would experience a $\sim 0.3 \text{ pH min}^{-1}$ decrease in cytosolic pH (Taylor et al., 2011). The discovery of PM H^+ conductance in *C. pelagicus* resulted in the cloning and characterization of a voltage-gated H^+ channel from *E. huxleyi* and *C. pelagicus* (Taylor et al., 2011). This study provides strong evidence that excess internal H^+ can be dissipated by release into the extracellular environment via H^+ channels. *E. huxleyi* maintains a cytosolic pH of ~ 7 (Dixon et al., 1989; Anning et al., 1996) with a chloroplast pH of ~ 8 (Anning et al., 1996). Internal pH is strongly dependent on external pH, probably due to the presence of H^+ channels, with an external pH change of 1 pH unit linearly translating to a 0.44 pH unit change in internal pH (Suffrian et al., 2011). A reduction in ocean pH of $\sim 0.3 - 0.5$ by the year 2100 (Caldeira and Wickett, 2003) would result in a 100 – 150% increase in H^+ concentration. This could potentially reverse the H^+ electrochemical gradient across the PM and have a drastic influence on intracellular pH homeostasis, which is likely to disrupt calcification (Taylor et al., 2011). However, the ability of coccolithophores to adapt to a decrease in pH is unknown. As H^+ transport across the PM is dependent on the H^+ electrochemical gradient, changes in external pH could be counteracted by adjustments in membrane potential, therefore maintaining intracellular pH.

Intracellular pH appears to be influenced by changes in external DIC. It is known that HCO_3^- plays an essential role in intracellular pH buffering of mammalian cells (Pushkin and Kurtz, 2006), this also appears to be the case in coccolithophores. Interestingly, intracellular pH decreases with both the complete removal of extracellular HCO_3^- and a large increase in

extracellular HCO_3^- . At pH 8, HCO_3^- removal resulted in an internal acidification of 0.8 pH units (Dixon et al., 1989) and at high HCO_3^- ($\sim 20 \text{ mmol kg}^{-1}$) internal pH dropped slightly by 0.12 units (Suffrian et al., 2011). Unexpectedly high CO_2 ($600 \mu\text{mol kg}^{-1}$) resulted in no change in internal pH, however, this could possibly be explained by CO_2 influx leading to H^+ release and subsequent rapid loss by H^+ channels.

Alongside cytosolic pH regulation coccolithophores require strong control over CV pH and the pH of other endomembrane compartments. For calcite precipitation to occur it was hypothesised that the pH of the CV would have to exceed ~ 8 (Brownlee et al., 1995). However, a CV pH of 7.1 ± 0.3 has been measured (Anning et al., 1996). It is also feasible that CaCO_3 supersaturation in the CV could occur if Ca^{2+} and CO_3^{2-} are in high enough concentration in the CV or the pH of the CV is altered between the substrate “loading” and “precipitation” phases (Mackinder et al., 2010). In fact a vacuolar-type H^+ -ATPase has been associated with the CV (Corstjens et al., 2001) and it has shown calcification related expression patterns (Mackinder et al., 2011), making it a key candidate for pH maintenance of the CV and/or the development of endomembrane H^+ gradients to drive Ca^{2+} transport via $\text{Ca}^{2+}/\text{H}^+$ exchange.

The negative effects of ocean acidification discussed in section 1.2 (Coccolithophores and the marine carbon cycle in a changing ocean) are potentially due to the inability of coccolithophores to respond to changes in external pH over the short-term (10s of generations). How they will respond over longer time spans (100s-1000s of generations) is unknown but it is an essential piece of the jigsaw in understanding how ocean acidification will effect global carbon cycling.

1.7 Thesis Outline

This doctoral thesis focuses on the transport of Ca^{2+} and DIC in coccolithophores at a molecular level, principally using the species *Emiliania huxleyi*. **Chapter 2** is a published literature review focusing on the molecular basis of calcification. It identifies what is currently known about coccolithophore calcification at a molecular level. It then goes on to introduce two new concepts that require further experimental investigation. Firstly that coccolith formation potentially proceeds via an amorphous calcium carbonate (ACC) precursor, as seen in sea urchin larvae spicules and the nacreous layer of mollusc shells. Secondly that Ca^{2+} uptake into the CV precursor compartment is mediated by a $\text{Ca}^{2+}/\text{H}^+$ exchanger driven by a H^+ gradient created from H^+ release from calcification and H^+ pumps. With changes in activity of these transporters influencing the chemistry in the CV resulting in controlled calcite precipitation. **Chapter 3** comprises a publication investigating calcification related gene expression in *E. huxleyi*. The

study uses three calcifying vs. non-calcifying comparisons of genetic isoforms to identify calcification-regulated genes. It provides strong evidence that a HCO_3^- transporter (*AELI*), a $\text{Ca}^{2+}/\text{H}^+$ exchanger (*CAX3*) and a vacuolar H^+ -ATPase (*ATPvc/c'*) play key roles in coccolithophore calcification, supporting the hypothesis put forward in Chapter 2. **Chapter 4** focuses on inorganic carbon transport in *E. huxleyi*. It attempts to disentangle the influence of individual carbonate system parameters on the physiological and genetic responses of *E. huxleyi* to a changing carbonate system by culturing cells over a wide range of DIC at two constant pHs of 7.7 and 8.3 and a constant CO_2 of $\sim 16 \mu\text{mol kg}^{-1}$. The data identifies for the first time the genetic basis of a CCM in Haptophyte algae. With all transcriptional responses to low DIC occurring below present day HCO_3^- and CO_2 values indicating that at a genetic level *E. huxleyi* may not dramatically respond to future predicted increases in CO_2 . Furthermore, it shows that calcification does not support photosynthesis in *E. huxleyi* under low DIC conditions, but is in fact switched off to increase DIC supply to photosynthesis. This chapter is to be submitted to *Plant Physiology*. **Chapter 5** is a genome wide analysis of Ca^{2+} , DIC and H^+ related transport genes in *E. huxleyi*. It identifies a wide range of genes in the genome with potential roles in calcification and DIC uptake. Indicating that many CCM-related genes are shared with other eukaryotic algae including evolutionary distinct species such as *Chlamydomonas reinhardtii*. It also provides a strong basis for future molecular based studies in *E. huxleyi*. This chapter will be submitted to *BMC Genomics*. **Chapter 6** is based on *CAX3* and *AELI* both which were identified in Chapter 3 as having potential roles in calcification. It looks into the molecular characterization of these genes to try and understand their function and roles in coccolithophore calcification. Although in both cases full characterization was unsuccessful it provides a strong basis for future work investigating the function of Ca^{2+} and DIC carbon related transporters in coccolithophores.

1.8 List of publications

First Author Publications:

Chapter 2

I Mackinder, L., Wheeler, G., Schroeder, D., Riebesell, U., and Brownlee, C. (2010) Molecular Mechanisms Underlying Calcification in Coccolithophores. *Journal of Geomicrobiology* 27: 585 - 595.

Chapter 3

II Mackinder, L., Wheeler, G., Schroeder, D., von Dassow, P., Riebesell, U., and Brownlee, C. (2011) **Expression of biomineralization-related ion transport genes in the coccolithophore *Emiliana huxleyi*.** *Environmental Microbiology* 13: 3250–3265

Chapter 4

III *Bach, L., *Mackinder, L., Schulz, K., Wheeler, G., Schroeder, D., P., Brownlee, C. and Riebesell, U. **Calcification and photosynthesis in *Emiliana huxleyi*: Physiological and genetic responses to the individual carbonate system parameters.** To be submitted to *Plant Physiology*.

*Joint first authorship

Chapter 5

IV Mackinder, L., Schroeder, D., Riebesell, U., Brownlee, C and Wheeler, G. **Ion transport associated with calcification and inorganic carbon acquisition in coccolithophores: Insights from the *Emiliana huxleyi* genome.** To be submitted to *BMC Genomics*.

Future publications from work related to this thesis:

V Author on the *Emiliana huxleyi* Genome Paper. The most recent draft: **The Rapidly Evolving Pan Genome of the Globally Distributed Coccolithophore *Emiliana huxleyi*.** I have been involved in analyzing the genome for calcification-related genes.

VI Author on a paper investigating calcification in coccolithophores proceeding via an Amorphous Calcium Carbonate (ACC) precursor phase. In preparation by Chloe Singleton. I have played key role in establishing the concept that calcification in coccolithophores may proceed via an ACC state. And also involved in the design and acquisition of preliminary Fourier Transform Infra-Red spectroscopy (FTIR) data used to identify the presence of ACC.

VII I will be the primary author on a paper analysing the transcriptomic data obtained from Illumina based RNA sequencing of samples from Chapter 4. This data is currently under analysis.

References

- Anning T, Nimer N, Merrett MJ, Brownlee C** (1996) Costs and benefits of calcification in coccolithophorids. *Journal of Marine Systems* **9**: 45-56
- Armstrong RA, Lee C, Hedges JI, Honjo S, Wakeham SG** (2002) A new, mechanistic model for organic carbon fluxes in the ocean based on the quantitative association of POC with ballast minerals. *Deep Sea Research* **49**: 219-236
- Bach LT, Riebesell U, Georg Schulz K** (2011) Distinguishing between the effects of ocean acidification and ocean carbonation in the coccolithophore *Emiliana huxleyi*. *Limnology and Oceanography* **56**: 2040-2050
- Badger M** (2003) The roles of carbonic anhydrases in photosynthetic CO₂ concentrating mechanisms. *Photosynthesis Research* **77**: 83-94
- Beaufort L, Probert I, de Garidel-Thoron T, Bendif EM, Ruiz-Pino D, Metzl N, Goyet C, Buchet N, Coupel P, Grelaud M, Rost B, Rickaby RE, de Vargas C** (2011) Sensitivity of coccolithophores to carbonate chemistry and ocean acidification. *Nature* **476**: 80-83
- Berry L, Taylor AR, Lucken U, Ryan KP, Brownlee C** (2002) Calcification and inorganic carbon acquisition in coccolithophores. *Functional Plant Biology* **29**: 289-299
- Borman AH, de Jong EW, Huizinga M, Kok DJ, Westbroek P, Bosch L** (1982) The role in CaCO₃ crystallization of an acid Ca²⁺-binding polysaccharide associated with coccoliths of *Emiliana huxleyi*. *European Journal of Biochemistry* **129**: 179-183
- Bown PR, Lees JA, Young JR** (2004) Calcareous nannoplankton evolution and diversity through time. In HR Thierstein, JR Young, eds, *Coccolithophores: From Molecular Processes to Global Impact*. Springer Verlag, pp 481–505.
- Brownlee C, Davies M, Nimer N, Dong LF, Merrett MJ** (1995) Calcification, photosynthesis and intracellular regulation in *Emiliana huxleyi*. *Bulletin Institute Oceanographique Monaco* **14**: 19-35
- Buitenhuis E, de Baar H, Veldhuis M** (1999) Photosynthesis and calcification by *Emiliana huxleyi* (Prymnesiophyceae) as a function of inorganic carbon species. *Journal of Phycology* **35**: 949-959
- Caldeira K, Wickett ME** (2003) Anthropogenic carbon and ocean pH. *Nature* **425**: 365
- Caldeira K, Wickett ME** (2005) Ocean model predictions of chemistry changes from carbon dioxide emissions to the atmosphere and ocean. *Journal of Geophysical Research* **110**: C09S04
- Corstjens P, van der Kooij A, Linschooten C, Brouwers GJ, Westbroek P, de Vrind-de Jong EW** (1998) GPA, a calcium-binding protein in the coccolithophorid *Emiliana huxleyi* (Prymnesiophyceae). *Journal of Phycology* **34**: 622-630
- Corstjens PLAM, Araki Y, González EL** (2001) A coccolithophorid calcifying vesicle with a vacuolar-type ATPase proton pump: cloning and immunolocalization of the V₀ subunit c¹. *Journal of Phycology* **37**: 71-78
- de Jong EW, Bosch L, Westbroek P** (1976) Isolation and characterization of a Ca²⁺-binding polysaccharide associated with coccoliths of *Emiliana huxleyi* (Lohmann) Kamptner. *European Journal of Biochemistry* **70**: 611-621
- De Vargas C, Aubry M-P, Probert I, Young J** (2007) Origin and evolution of coccolithophores: From coastal hunters to Oceanic farmers. In PG Falkowski, AH Knoll, eds, *Evolution of primary producers in the sea*. Elsevier, London
- Delille B, Harlay J, Zondervan I** (2005) Response of primary production and calcification to changes of pCO₂ during experimental blooms of the coccolithophorid *Emiliana huxleyi*. *Global Biogeochemical Cycles* **19**: GB2023, 2010.1029/2004GB002318
- Dixon GK, Brownlee C, Merrett MJ** (1989) Measurement of internal pH in the coccolithophore *Emiliana huxleyi* using 2',7'-bis-(2-carboxyethyl)-5-(and-

- 6)carboxyfluorescein acetoxymethylester and digital imaging microscopy. *Planta* **178**: 443-449
- Engel A, Zondervan I, Aerts K, Beaufort L** (2005) Testing the direct effect of CO₂ concentration on a bloom of the coccolithophorid *Emiliana huxleyi* in mesocosm experiments. *Limnology and Oceanography* **50**: 493-504
- Fabry VJ, Seibel BA, Feely RA, Orr JC** (2008) Impacts of ocean acidification on marine fauna and ecosystem processes. *ICES Journal of Marine Science* **65**: 414-432
- Falkowski PG, Katz ME, Knoll AH, Quigg A, Raven JA, Schofield O, Taylor FJR** (2004) The Evolution of Modern Eukaryotic Phytoplankton. *Science* **305**: 354-360
- Feng Y, Warner ME, Zhang Y, Sun J, Fu F-X, Rose JM, Hutchins DA** (2008) Interactive effects of increased pCO₂, temperature and irradiance on the marine coccolithophore *Emiliana huxleyi* (Prymnesiophyceae). *European Journal of Phycology* **43**: 87-98
- Field CB, Behrenfeld MJ, Randerson JT, Falkowski P** (1998) Primary Production of the Biosphere: Integrating Terrestrial and Oceanic Components. *Science* **281**: 237-240
- Giordano M, Beardall J, Raven JA** (2005) CO₂ concentrating mechanisms in algae: Mechanisms, Environmental Modulation, and Evolution. *Annual Review of Plant Biology* **56**: 99-131
- Gradstein FM, Ogg JG, Smith AG** (2004) A Geologic Time Scale 2004. Cambridge University Press, Cambridge
- Hein M, Sand-Jensen K** (1997) CO₂ increases oceanic primary production. *Nature* **388**: 526-527
- Henriksen K, Stipp SLS, Young JR, Marsh ME** (2004) Biological control on calcite crystallization: AFM investigation of coccolith polysaccharide function. *American Mineralogist* **89**: 1709-1716
- Herfort L, Loste E, Meldrum F, Thake B** (2004) Structural and physiological effects of calcium and magnesium in *Emiliana huxleyi* (Lohmann) Hay and Mohler. *Journal of Structural Biology* **148**: 307-314
- Herfort L, Thake B, Roberts J** (2002) Acquisition and use of bicarbonate by *Emiliana huxleyi*. *New Phytologist* **156**: 427-436
- Hoppe CJM, Langer G, Rost B** (2011) *Emiliana huxleyi* shows identical responses to elevated pCO₂ in TA and DIC manipulations. *Journal of Experimental Marine Biology and Ecology* **406**: 54-62
- Iglesias-Rodríguez DM, Schofield OM, Batley J, Medlin LK, Hayes PK** (2006) Intraspecific genetic diversity in the marine coccolithophore *Emiliana huxleyi* (Prymnesiophyceae): the use of microsatellite analysis in marine phytoplankton population studies. *Journal of Phycology* **42**: 526-536
- Iglesias-Rodríguez MD, Halloran PR, Rickaby RE, Hall IR, Colmenero-Hidalgo E, Gittins JR, Green DR, Tyrrell T, Gibbs SJ, von Dassow P, Rehm E, Armbrust EV, Boessenkool KP** (2008) Phytoplankton calcification in a high-CO₂ world. *Science* **320**: 336-340
- Klaas C, Archer DE** (2002) Association of sinking organic matter with various types of mineral ballast in the deep sea: Implications for the rain ratio. *Global Biogeochemical Cycles* **16**: 1116-1129
- Klaveness D** (1976) *Emiliana huxleyi* (Lohmann) Hay and Mohler .3. Mineral deposition and origin of matrix during coccolith formation. *Protistologica* **12**: 217-224
- Krug SA, Schulz KG, Riebesell U** (2011) Effects of changes in carbonate chemistry speciation on *Coccolithus braarudii*: a discussion of coccolithophorid sensitivities. *Biogeosciences* **8**: 771-777
- Langer G, Geisen M, Baumann K-H, Kläs J, Riebesell U, Thoms S, Young JR** (2006) Species-specific responses of calcifying algae to changing seawater carbonate chemistry. *Geochemistry Geophysics Geosystems* **7**: 10.1029/2005gc001227

- Langer G, Nehrke G, Probert I, Ly J, Ziveri P** (2009) Strain-specific responses of *Emiliana huxleyi* to changing seawater carbonate chemistry. *Biogeosciences* **6**: 4361–4383
- Leonardos N, Read B, Thake B, Young JR** (2009) No mechanistic dependence of photosynthesis on calcification in the coccolithophorid *Emiliana huxleyi* (Haptophyta). *Journal of Phycology* **45**: 1046-1051
- Mackinder L, Wheeler G, Schroeder D, Riebesell U, Brownlee C** (2010) Molecular Mechanisms Underlying Calcification in Coccolithophores. *Geomicrobiology Journal* **27**: 585 - 595
- Mackinder L, Wheeler G, Schroeder D, von Dassow P, Riebesell U, Brownlee C** (2011) Expression of biomineralization-related ion transport genes in *Emiliana huxleyi*. *Environmental Microbiology* **13**: 3250–3265
- Manton I, Leedale GF** (1969) Observations on the microanatomy of *Coccolithus pelagicus* and *Cricosphaera carterae*, with special reference to their origin and nature. *Journal of the Marine Biological Association of the UK* **49**: 1-16
- Marsh M** (2003) Regulation of CaCO₃ formation in coccolithophores. *Comparative Biochemistry and Physiology Part B* **136**: 743-754
- Marsh M, Dickinson D** (1997) Polyanion-mediated mineralization — mineralization in coccolithophore (*Pleurochrysis carterae*) variants which do not express PS2, the most abundant and acidic mineral-associated polyanion in wild-type cells. *Protoplasma* **199**: 9-17
- Marsh ME** (1994) Polyanion-mediated mineralization — assembly and reorganization of acidic polysaccharides in the Golgi system of a coccolithophorid alga during mineral deposition. *Protoplasma* **177**: 108-122
- Marsh ME, Chang DK, King GC** (1992) Isolation and characterization of a novel acidic polysaccharide containing tartrate and glyoxylate residues from the mineralized scales of a unicellular coccolithophorid alga *Pleurochrysis carterae*. *Journal of Biological Chemistry* **267**: 20507-20512
- Marsh ME, Ridall AL, Azadi P, Duke PJ** (2002) Galacturonomannan and Golgi-derived membrane linked to growth and shaping of biogenic calcite. *Journal of Structural Biology* **139**: 39-45
- Medini D, Donati C, Tettelin H, Massignani V, Rappuoli R** (2005) The microbial pan-genome. *Current Opinion in Genetics; Development* **15**: 589-594
- Medlin LK, Barker GLA, Campbell L, Green JC, Hayes PK, Marie D, Wrieden S, Vaultot D** (1996) Genetic characterization of *Emiliana huxleyi* (Haptophyta). *Journal of Marine Systems* **9**: 13-31
- Milliman JD** (1993) Production and Accumulation of Calcium Carbonate in the Ocean: Budget of a Nonsteady State. *Global Biogeochemical Cycles* **7**: 927-957
- Nimer NA, Guan Q, Merrett MJ** (1994) Extracellular and intracellular carbonic-anhydrase in relation to culture age in a high-calcifying strain of *Emiliana huxleyi* Lohmann. *New Phytologist* **126**: 601-607
- Nimer NA, IglesiasRodriguez MD, Merrett MJ** (1997) Bicarbonate utilization by marine phytoplankton species. *Journal of Phycology* **33**: 625-631
- Nimer NA, Merrett MJ** (1992) Calcification and utilization of inorganic carbon by the coccolithophorid *Emiliana huxleyi* Lohmann. *New Phytologist* **121**: 173-177
- Nimer NA, Merrett MJ** (1996) The development of a CO₂-concentrating mechanism in *Emiliana huxleyi*. *New Phytologist* **133**: 383-389
- Outka DE, Williams DC** (1971) Sequential Coccolith Morphogenesis in *Hymenomonas carterae*. *Journal of Eukaryotic Microbiology* **18**: 285-297
- Paasche E** (1962) Coccolith Formation. *Nature* **193**: 1094-1095
- Paasche E** (1964) A tracer study of the inorganic carbon uptake during coccolith formation and photosynthesis in the coccolithophorid *Coccolithus huxleyi*. *Physiologia Plantarum* **3(suppl)**: 1-82

- Pushkin A, Kurtz I** (2006) SLC4 base (HCO_3^- , CO_3^{2-}) transporters: classification, function, structure, genetic diseases, and knockout models. *AJP-Renal Physiology* **290**: F580-599
- Quiroga O, González EL** (1993) Carbonic anhydrase in the chloroplast of a coccolithophorid (Prymnesiophyceae). *Journal of Phycology* **29**: 321-324
- Reinfelder JR** (2011) Carbon Concentrating Mechanisms in Eukaryotic Marine Phytoplankton. *Annual Review of Marine Science* **3**: 291-315
- Ridgwell A** (2005) A Mid Mesozoic Revolution in the regulation of ocean chemistry. *Marine Geology* **217**: 339-357
- Ridgwell A, Schmidt DN, Turley C, Brownlee C, Maldonado MT, Tortell P, Young JR** (2009) From laboratory manipulations to earth system models: predicting pelagic calcification and its consequences. *Biogeosciences Discussions* **6**: 3455-3480
- Riebesell U, Bellerby RGJ, Engel A, Fabry VJ, Hutchins DA, Reusch TBH, Schulz KG, Morel FMM** (2008) Comment on "Phytoplankton Calcification in a High-CO₂ World". *Science* **322**: 1466-1466
- Riebesell U, Kortzinger A, Oschlies A** (2009) Sensitivities of marine carbon fluxes to ocean change. *Proceedings of the National Academy of Sciences of the United States of America* **106**: 20602-20609
- Riebesell U, Schulz KG, Bellerby RG, Botros M, Fritsche P, Meyerhofer M, Neill C, Nondal G, Oschlies A, Wohlers J, Zollner E** (2007) Enhanced biological carbon consumption in a high CO₂ ocean. *Nature* **450**: 545-548
- Riebesell U, Tortell PD** (2011) Effects of Ocean Acidification on Pelagic Organisms and Ecosystems. *In* J-P Gattuso, L Hansson, eds, *Ocean Acidification*, Ed 1. Oxford University Press, Oxford, pp 99-121
- Riebesell U, Wolfgladrow DA, Smetacek V** (1993) Carbon-dioxide limitation of marine-phytoplankton growth-rates. *Nature* **361**: 249-251
- Riebesell U, Zondervan I, Rost B, Tortell PD, Zeebe RE, Morel FMM** (2000) Reduced calcification of marine plankton in response to increased atmospheric CO₂. *Nature* **407**: 364-367
- Rost B, Riebesell U** (2004) Coccolithophores and the biological pump: responses to environmental change *In* H Thierstein, J Young, eds, *Coccolithophores: From Molecular Processes to Global Impact*. Springer, Berlin, pp 99-125
- Rost B, Riebesell U, Burkhardt S, Sültemeyer D** (2003) Carbon Acquisition of Bloom-Forming Marine Phytoplankton. *Limnology and Oceanography* **48**: 55-67
- Sabine CL, Feely RA, Gruber N, Key RM, Lee K, Bullister JL, Wanninkhof R, Wong CS, Wallace DW, Tilbrook B, Millero FJ, Peng TH, Kozyr A, Ono T, Rios AF** (2004) The oceanic sink for anthropogenic CO₂. *Science* **305**: 367-371
- Schroeder DC, Biggi GF, Hall M, Davy J, Martínez J, Richardson AJ, Malin G, Wilson WH** (2005) A genetic marker to separate *Emiliana huxleyi* (Prymnesiophyceae) morphotypes. *Journal of Phycology* **41**: 874-879
- Schulz KG, Rost B, Burkhardt S, Riebesell U, Thoms S, Wolfgladrow DA** (2007) The effect of iron availability on the regulation of inorganic carbon acquisition in the coccolithophore *Emiliana huxleyi* and the significance of cellular compartmentation for stable carbon isotope fractionation. *Geochimica et Cosmochimica Acta* **71**: 5301-5312
- Sekino K, Shiraiwa Y** (1994) Accumulation and utilization of dissolved inorganic carbon by a marine unicellular coccolithophorid, *Emiliana huxleyi*. *Plant and Cell Physiology* **35**: 353-361
- Sekino K, Shiraiwa Y** (1996) Evidence for the involvement of mitochondrial respiration in calcification in a marine coccolithophorid, *Emiliana huxleyi*. *Plant and Cell Physiology* **37**: 1030-1033
- Shi D, Xu Y, Morel FMM** (2009) Effects of the pH/pCO₂ control method on medium chemistry and phytoplankton growth. *Biogeosciences* **6**: 1199-1207

- Sikes CS, Roer RD, Wilbur KM** (1980) Photosynthesis and coccolith formation - inorganic carbon-sources and net inorganic reaction of deposition. *Limnology and Oceanography* **25**: 248-261
- Soto AR, Zheng H, Shoemaker D, Rodriguez J, Read BA, Wahlund TM** (2006) Identification and preliminary characterization of two cDNAs encoding unique carbonic anhydrases from the marine alga *Emiliana huxleyi*. *Applied and Environmental Microbiology* **72**: 5500-5511
- Suffrian K, Schulz KG, Gutowska MA, Riebesell U, Bleich M** (2011) Cellular pH measurements in *Emiliana huxleyi* reveal pronounced membrane proton permeability. *New Phytologist*: DOI: 10.1111/j.1469-8137.2010.03633.x
- Taylor AR, Chrachri A, Wheeler G, Goddard H, Brownlee C** (2011) A voltage-gated H⁺ channel underlying pH homeostasis in calcifying coccolithophores. *PLoS Biology* **9**: e1001085
- Taylor AR, Russell MA, Harper GM, Collins TT, Brownlee C** (2007) Dynamics of formation and secretion of heterococcoliths by *Coccolithus pelagicus* ssp. *Braarudii*. *European Journal of Phycology* **42**: 125 - 136
- Tirichine L, Bowler C** (2011) Decoding algal genomes: tracing back the history of photosynthetic life on Earth. *The Plant Journal* **66**: 45-57
- Toggweiler JR, Gnanadesikan A, Carson S, Murnane R, Sarmiento JL** (2003) Representation of the carbon cycle in box models and GCMs: 1. Solubility pump. *Global Biogeochemical Cycles* **17**: 1026
- Trimborn S, Langer G, Rost B** (2007) Effect of varying calcium concentrations and light intensities on calcification and photosynthesis in *Emiliana huxleyi*. *Limnology and Oceanography* **52**: 2285-2293
- Tyrrell T, Young JR** (2009) Coccolithophores. In JH Steele, KK Turekian, SA Thorpe, eds, *Encyclopedia of Ocean Sciences*, Ed 2. Academic Press, San Diego, pp 3568-3576
- van der Wal P, de Jong EW, Westbroek P, de Bruijn WC** (1983) Calcification in the coccolithophorid alga *Hymenomonas carterae*. *Ecological Bulletins* **35**: 251-258
- van der Wal P, de Jong EW, Westbroek P, de Bruijn WC, Mulderstapel AA** (1983) Polysaccharide localization, coccolith formation, and golgi dynamics in the coccolithophorid *Hymenomonas carterae*. *Journal of Ultrastructure Research* **85**: 139-158
- van der Wal P, de Jong EW, Westbroek P, de Bruijn WC, Mulderstapel AA** (1983) Ultrastructural polysaccharide localization in calcifying and naked cells of the coccolithophorid *Emiliana huxleyi*. *Protoplasma* **118**: 157-168
- van der Wal P, Leunissen-Vijvelt JJM, Verkleij AJ** (1985) Ultrastructure of the membranous layers enveloping the cell of the coccolithophorid *Emiliana huxleyi*. *Journal of Ultrastructure Research* **91**: 24-29
- Vliegenthart JFG, Fichtinger-Schepman AMJ, Kamerling JP, Versluis C** (1981) Structural studies of the methylated, acidic polysaccharide associated with coccoliths of *Emiliana huxleyi* (Lohmann) Kamptner. *Carbohydrate research* **93**: 105-123
- von Dassow P, Ogata H, Probert I, Wincker P, Da Silva C, Audic S, Claverie JM, de Vargas C** (2009) Transcriptome analysis of functional differentiation between haploid and diploid cells of *Emiliana huxleyi*, a globally significant photosynthetic calcifying cell. *Genome Biology* **10**: R114
- Weiner S** (2008) Biomineralization: A structural perspective. *Journal of Structural Biology* **163**: 229-234
- Weiss IM, Marin F** (2008) The Role of Enzymes in Biomineralization Processes. In *Biomineralization*. John Wiley & Sons, Ltd, pp 71-126
- Westbroek P, Young JR, Linschooten K** (1989) Coccolith production (biomineralization) in the marine alga *Emiliana huxleyi*. *Journal of Protozoology* **36**: 368-373

-
- Wilbur KM, Watabe N** (1963) Experimental studies on calcification in molluscs and the alga *Coccolithus huxleyi*. *Annals of the New York Academy of Sciences* **109**: 82-112
- Young JR, Davis SA, Bown PR, Mann S** (1999) Coccolith Ultrastructure and Biomineralization. *Journal of Structural Biology* **126**: 195-215
- Young JR, Didymus JM, Brown PR, Prins B, Mann S** (1992) Crystal assembly and phylogenetic evolution in heterococcoliths. *Nature* **356**: 516-518
- Young JR, Geisen M, Cros L, Kleijne A, Sprengel C, Probert I** (2003) A guide to extant calcareous nannoplankton taxonomy. *Journal of Nannoplankton Research*: 1-125
- Zeebe R, Ridgwell A** (2011) Past changes in ocean carbonate chemistry. *In* J-P Gattuso, L Hansson, eds, *Ocean Acidification*, Ed 1. Oxford University Press, Oxford, pp 21-40

CHAPTER 2. Molecular Mechanisms Underlying Calcification in Coccolithophores

Molecular Mechanisms Underlying Calcification in Coccolithophores

Luke Mackinder,^{1,2} Glen Wheeler,^{1,3} Declan Schroeder,¹ Ulf Riebesell,² and Colin Brownlee¹

¹Marine Biological Association, The Laboratory, Citadel Hill, Plymouth, United Kingdom

²Leibniz Institute of Marine Science, IFM-GEOMAR, D-24105, Kiel, Germany

³Plymouth Marine Laboratory, Prospect Place, Plymouth, United Kingdom

A number of studies are providing increasing genomic and transcriptomic information on the molecular components of transport, and biochemical control in the cell biology of calcification in coccolithophores. In this review we summarise recent evidence for molecular components involved in the trans-cellular transport of Ca²⁺, inorganic carbon and H⁺ between the external medium and the intracellular calcification compartment. We present new hypotheses for the transport of substrates to the site of calcification and for the removal of products, highlighting key gaps in our current knowledge. We also discuss how a cellular and molecular approach will improve abilities to understand and predict responses and adaptation to changing ocean chemistry of this important group of microorganisms.

Keywords biogeochemical cycling, biomineralization, coccolithophores, molecular, transport

INTRODUCTION

The bulk of global calcification can be attributed to corals, foraminifera and coccolithophores. Although estimates vary, coccolithophores (division Haptophyta class Prymnesiophyceae), are believed to attribute up to half of current oceanic CaCO₃ production (Milliman 1993), playing a major role in the earth's carbon cycle both in terms of long term sequestration of inorganic carbon and providing ballast for sedimentation of organic carbon production. Coccolithophore calcification may influence sea surface carbonate chemistry in a number of ways, including reduction of draw down of atmospheric CO₂ by reducing sea surface alkalinity (Riebesell et al. 2009). Coccolithophores are widespread and locally abundant in all of the

world's oceans, with *Emiliana huxleyi* being the most abundant calcifying phytoplankton on earth (Westbroek et al. 1993), forming vast blooms at temperate latitudes (Holligan et al. 1983; Fernandez et al. 1993; Holligan et al. 1993).

Biomineralization of calcite in coccolithophores is a stringently controlled biological process, with its biogenic product differing in both morphology and chemical composition from abiogenically produced calcite (Westbroek et al. 1989). Individual calcitic coccoliths, termed heterococcoliths, which are made up of calcite crystal elements of complex shape, are produced in intracellular compartments where they are subjected to numerous cellular control mechanisms during maturation and growth before secretion onto the cell surface (Brownlee and Taylor 2005; Taylor et al. 2007; Figure 1).

This highly controlled intracellular production allows accurate replication of intricately formed coccoliths within individuals and strains and has resulted in considerable inter- and intraspecific differences in coccolith morphology (Young et al. 1999). During certain stages in their life cycle some coccolithophore species may also form holococcoliths that comprise uniform-shaped crystallites. Holococcoliths are thought to be produced extracellularly (Young et al. 1999), though very little is known about the mechanism underlying their formation.

A mechanistic understanding of calcification and its links with photosynthesis, nutrient acquisition, physiological benefits and other cellular processes is essential if we want to fully understand coccolithophore ecological success, their roles in climatic processes and the effect of climate change on this group of organisms. Better understanding of the numerous processes that are involved in the formation of highly organised crystal structures within the cellular calcification compartment is required to allow the disentangling of the "vital effect" (e.g., Rickaby et al. 2002). With a good understanding of coccolithophore biology, their ease of culture, their importance in climatic functioning and the anticipated availability of the *E. huxleyi* genome sequence, the coccolithophores represent ideal candidates for the detailed studies of biomineralization.

Received 13 December 2009; accepted 5 February 2010.

Address correspondence to Colin Brownlee, Marine Biological Association, The Laboratory, Citadel Hill, Plymouth PL1 2PB, UK. E-mail: cbr@mba.ac.uk

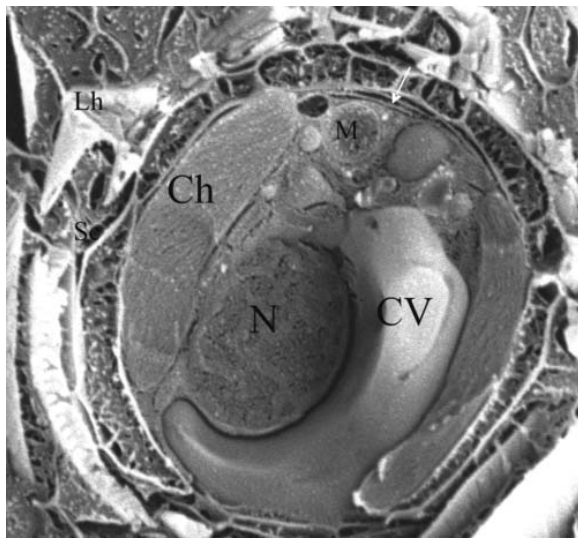


FIG. 1. Freeze fracture through the centre of a whole *C. pelagicus* cell showing fractured external interlocking coccoliths (Lh), layer of organic scales (Sc) connected to the plasma membrane by columnar strands and local adhesions spanning the periplasmic space (examples indicated with white arrow). The nucleus (N), chloroplast (Ch), mitochondria (M) and coccolith vesicle (CV) are also easily distinguished. (Reproduced with permission from Taylor et al. 2007).

Coccolith formation and structure has been well documented in several coccolithophore species. In particular an abundance of electron microscopical observations has provided the basis of our knowledge of coccolith formation and structure in *E. huxleyi* (Wilbur and Watabe 1963; Klaveness 1976; van der Wal et al. 1983c; Westbroek et al. 1989; Young et al. 1999), *Pleurochrysis carterae* (Manton and Leedale 1969; van der Wal et al. 1983a, 1983bb) and *Coccolithus pelagicus* (Manton and Leedale 1969; Taylor et al. 2007). Calcification in coccolithophores takes place in a Golgi-derived intracellular vesicle, the coccolith vesicle (CV). In *E. huxleyi* the CV is tightly apposed to the nucleus (Klaveness 1976; van der Wal et al. 1983c).

Associated with the distal side of the CV is a unique membranous structure that is clearly distinguishable in *E. huxleyi* and *Gephyrocapsa oceanica* termed the reticular body (RB). Although the RB has not been observed in all coccolithophore species, there is evidence for similar membranous structures in *C. pelagicus* (Taylor et al. 2007). In *P. carterae* (van der Wal et al. 1983b) and *C. pelagicus* (Manton and Leedale 1969) coccolith production can be observed in trans Golgi cisternae, with coccoliths at varying stages of formation seen within a single cell (van der Wal et al. 1983b).

In *P. carterae* dense vesicles termed coccolithosomes appear to play an essential role in calcium transport to the coccolith forming vesicles (Outka and Williams 1971; van der Wal et al. 1983b). In all coccolithophore species complete intracellular formation of coccoliths takes place before transport to the cell cortex and secretion to the cell surface in a single exocytotic

extrusion event (Taylor et al. 2007). Calcification in coccolithophores initiates with nucleation of a proto-coccolith ring around an organic base plate. This is followed by growth of crystals in varying directions to form the complex mature coccoliths (Young et al. 1999).

Calcification in coccolithophores involves the cellular uptake of dissolved inorganic carbon (DIC) and Ca^{2+} from the extracellular medium into the Golgi-derived coccolith vesicle. The cell physiological evidence for the transport pathways supplying the substrates and removing the products have been discussed in a number of recent reviews (e.g., Paasche 2001; Berry et al. 2002; Brownlee and Taylor 2005).

Although there are extensive studies on the ultrastructure and formation of coccoliths and increased numbers of publications that provide a broad understanding of the underlying physiology, our knowledge of genetic regulation and molecular and biochemical processes of coccolith formation is still in its infancy, with very limited knowledge of the functions of the genes and proteins involved in the transport of Ca^{2+} and dissolved inorganic carbon (DIC) to the site of coccolith formation, intracellular pH regulation and the controlled formation of calcite. In this review we will summarise more recent evidence based on biochemical and molecular studies that sheds additional light on the mechanisms underlying coccolithophore calcification.

Identification of Calcification-Related Genes

Over the last decade a number of studies using expressed sequence tags (ESTs), suppressive subtractive hybridization (SSH), serial analysis of gene expression (SAGE) and cDNA microarrays have made comparisons of gene expression in *E. huxleyi* strain under a range of conditions that bring about changes in calcification rate in order to identify genes that are associated with the calcification mechanism. A number of studies have utilized *E. huxleyi* strain 1516 using phosphate depletion to increase calcification rate relative to organic carbon fixation (Wahlund et al. 2004; Nguyen et al. 2005; Dyhrman et al. 2006; Quinn et al. 2006).

Although phosphate depletion increases calcification (Paasche 2001), it causes limitation of growth and metabolism, holding cells in the G1 phase of the cell cycle (Müller et al. 2008) and reducing cell division rates. Phosphate depletion was shown to increase expression of numerous genes associated with cell stress and cell defence including heat shock proteins, co-chaperonins and programmed cell death and apoptosis related genes (Wahlund et al. 2004). Although it is difficult to disentangle genes related to phosphate scavenging and calcification these studies have identified numerous potential genes involved in calcification that are expressed at higher levels in phosphate-depleted conditions.

These include genes encoding Ca^{2+} -binding proteins such as the coccolith-associated glutamic acid, proline and alanine-rich protein GPA (Corstjens et al. 1998), calreticulin and calnexin (Wahlund et al. 2004, Quinn et al. 2006) which are involved in a range of Ca^{2+} -dependent cellular processes, carbonic anhydrase

(Quinn et al. 2006) and several proteins that showed features similar to biomineralization proteins seen in other marine organisms (Nguyen et al. 2005).

Richier et al. (2009) carried out a quantitative PCR comparison of expression of three putative calcification-related genes, by comparing expression in a haploid, non-calcifying strain with a diploid calcifying strain. These included calmodulin (CaM), a γ carbonic anhydrase (CA), previously shown to be up-regulated in calcifying cells of *Pleurochrysis haptanemofera* (Fujiwara et al. 2007) and GPA. CaM and GPA were expressed to significantly higher levels in the diploid strain both in the light and dark. CA showed increased expression in the diploid strain only in the light. All 3 genes showed increased expression in the diploid strain in the light compared with darkness.

A comprehensive analysis of expressed sequence tags (ESTs) of normalized cDNA libraries from pure clonal, genetically identical haploid and diploid *E. huxleyi* strains by von Dassow et al. (2009) has provided additional insights into genes that are specifically associated with calcification. The study identified clear differences in the transcriptomes of the different cell types, with particular 1N- or 2N-specific clusters that related to the motility of the non-calcifying haploid strain (flagellar function and cell signalling) and calcification of the diploid strain.

Of particular interest were highly 2N-specific gene clusters that included homologues of a number of membrane transporters including a Solute Carrier 4 (SLC4) family $\text{Cl}^-/\text{HCO}_3^-$ exchanger, a vacuolar $\text{Ca}^{2+}/\text{H}^+$ (VCX) exchanger with greatest similarity to the *Arabidopsis thaliana* cation exchanger CAX2_ARATH, a putative NCKX family $\text{Na}^+/\text{Ca}^{2+}$ exchanger and a putative subunit of a vacuolar V-type ATPase as well as a homologue of a syntaxin-1 SNARE that functions in exocytotic vesicle fusion. A number of other transporters were identified, including other family members of the above groups, that were shown not to be specific to 2N cells, including sarcoplasmic/endoplasmic reticulum (SERCA)-type ATPases.

Interestingly, this study showed that the coccolith-associated GPA protein was expressed in both 1N and 2N cells. Moreover, this study did not confirm 2N-specific expression of the transcripts that were putatively indicated to be calcification-related in earlier subtractive cDNA library studies (Quinn et al. 2006). Understanding the functions of these and other genes is clearly a priority for further mechanistic understanding of calcification (Figure 2).

Ca^{2+} Transporters

Ca^{2+} is involved in many cellular signal transduction processes. For these signalling systems to function correctly requires tight regulation of free cytosolic Ca^{2+} levels to allow reversible and often localized changes in Ca^{2+} that are used to encode signalling information. As in all eukaryotic cells the free cytosolic $[\text{Ca}^{2+}]$ in *E. huxleyi* is maintained low, with large changes in external $[\text{Ca}^{2+}]$ not affecting cytosolic $[\text{Ca}^{2+}]$ (Brownlee et al. 1995). Fundamental questions concerning the mechanism of Ca^{2+} delivery to the CV relate to how large fluxes

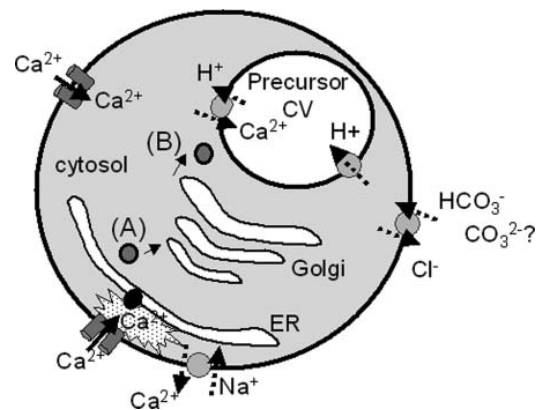


FIG. 2. Schematic of the putative roles of transporters and channel in the major fluxes of Ca^{2+} , DIC and H^+ in the calcification process. Potential endomembrane transport and accumulation pathways via the ER-Golgi and/or Golgi-CV precursor compartment are shown. Dashed arrows represent putative fluxes through transporters and pumps that have recently been identified in transcriptomics analyses (see text for details). Only a single CV precursor compartment is shown though accumulative Ca^{2+} and DIC fluxes may also occur at stages (A) and (B) along the transport pathway.

of Ca^{2+} from the surrounding environment to the CV can be supported whilst maintaining the stringent requirements of Ca^{2+} as an intracellular signal (Raven 1980).

Ca^{2+} -permeable channels allow the flux of Ca^{2+} into the cytosol from outside the cell or from intracellular stores down its electrochemical potential gradient. Such channel-mediated fluxes play key roles in rapid Ca^{2+} fluxes essential for cell signalling (Berridge 2002; Sanders et al. 2002). Ca^{2+} almost certainly diffuses across the coccolithophore plasma membrane (PM) into the cytosol down an electrochemical gradient through, as yet unidentified, Ca^{2+} -permeable channels and is removed from the cytosol by the action of Ca^{2+} -ATPases and/or cation/ Ca^{2+} exchangers. However, kinetic considerations suggest that a straightforward entry of Ca^{2+} into the cytosol across the PM, followed by diffusion across the cytosol and uphill transport into the coccolith-forming compartment is unlikely (Brownlee and Taylor 2005).

If Ca^{2+} diffused through the cytosol to the CV, large quantities of calcium sequestering proteins would likely be required to maintain low cytosolic Ca^{2+} levels. With a coccolith mass of 0.9 pg (Young and Ziveri 2000) and a coccolith production rate of approx 1 per hour (Paasche, 1962) approximately 5.36×10^6 Ca^{2+} ions per second would have to be moved into the *E. huxleyi* CV from the cytosol. Direct uptake of Ca^{2+} into the CV (Araki and González 1998) via Ca^{2+} -ATPases would require around 250,000 Ca^{2+} -ATPase molecules since a typical SERCA-type Ca^{2+} -ATPase can transport ~ 20 Ca^{2+} per second (Bartolommei et al. 2006).

By comparison, the sarcoplasmic reticulum of rat skeletal muscle has an estimated 4000 Ca^{2+} -ATPase molecules per μm^2 , (Dulhunty et al. 1993). Assuming a similar ATPase density in

588

L. MACKINDER ET AL.

the CV membrane, a membrane surface area of around $70 \mu\text{m}^2$ would be required to effect uphill Ca^{2+} transport into the CV. This is significantly higher than the estimated $16 \mu\text{m}^2$ membrane surface area of a CV, based on the dimensions of a mature *E. huxleyi* coccolith.

More rapid uphill transport of Ca^{2+} could occur more feasibly through the action of higher capacity exchangers such as $\text{Ca}^{2+}/\text{H}^+$ exchangers or $\text{Ca}^{2+}/\text{Na}^+$ exchangers (VCX/CAX- and NCX/NCKX-like proteins respectively) to transport Ca^{2+} into an endomembrane precursor CV compartment. A low affinity, high capacity (Sze et al. 2000) CAX-based transporter could in principle fulfil at least part of the endomembrane Ca^{2+} transport requirements of calcification. However, $\text{Ca}^{2+}/\text{H}^+$ exchangers work with a stoichiometry of $1\text{Ca}^{2+}/3\text{H}^+$ (Sze et al. 2000) and would require a substantial H^+ electrochemical gradient to be established across the precursor CV membrane.

Therefore, their function alone would only allow the transport of one third of the Ca^{2+} needed for calcite production if Ca^{2+} was exchanged only for H^+ produced during the calcification reaction, inside the CV or precursor compartment, assuming HCO_3^- as the DIC substrate for calcification (see next). However, the action of V-type H^+ -ATPases maintains H^+ electrochemical gradients (inside acidic) in endomembrane compartments, including Golgi-derived compartments. Conceivably, Ca^{2+} accumulation into an acidic endomembrane compartment could occur prior to the biomineralization step.

Progressive alkalization of this Ca^{2+} -charged compartment, possibly resulting from down-regulation of V-type H^+ ATPase activity as the compartment matured into the CV could then create conditions favourable for controlled precipitation of calcite (Figure 3).

CAX genes are found in various plant, fungal and bacterial species, with 12 genes in *Arabidopsis* predicted to encode CAX-type exchangers (Maser et al. 2001). Heterologous expression in yeast has been the main molecular tool for characterization of these exchangers. Several *Arabidopsis* CAX proteins have been characterised showing that they are vacuolar-located with varying Ca^{2+} affinities and transport capacities (Hirschi et al. 1996). The nature of CAX proteins in relation to their involvement in Ca^{2+} transport as well as pH control makes them ideal candidates for further investigation in their role in calcification in coccolithophores.

Currently, there is no localization data for the CAX-like gene product identified in the EST analysis of 1N and 2N cells of *E. huxleyi* (von Dassow et al. 2009). The roles of CAX-driven Ca^{2+} uptake into endomembrane compartments and possible role in calcification remain to be investigated.

The cellular envelope underlying the extracellular coccosphere has been shown to be made up of 3 or 4 membranous layers (van der Wal et al. 1985b). We have previously argued that these layers represent the PM and the peripheral endoplasmic reticulum (PER) (Berry et al. 2002). The proximity of the PER to the PM may form a microenvironment in the region of

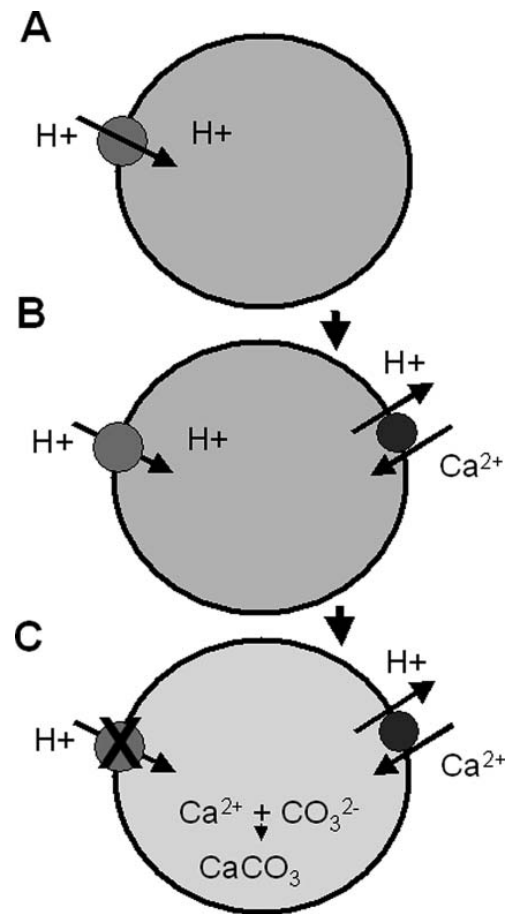


FIG. 3. Schematic hypothesis for the roles of V-type ATPases and $\text{Ca}^{2+}/\text{H}^+$ (VCX)-like exchangers in the accumulation of Ca^{2+} into precursor CV endomembrane compartments such as coccolithosomes. (A) The activity of V-type ATPases maintains an acidic endomembrane compartment. (B) $\text{Ca}^{2+}/\text{H}^+$ (VCX)-like exchangers utilize the H^+ electrochemical gradient to accumulate Ca^{2+} in the endomembrane lumen. (C) As the compartment matures into the CV, V-type ATPase activity is shut down, leading to alkalization of the lumen and precipitation of CaCO_3 .

the cytosol between the PM and PER in which $[\text{Ca}^{2+}]$, through the activity of PM Ca^{2+} channels could potentially reach values significantly higher than mean cytosolic $[\text{Ca}^{2+}]$, leading to energetically more favourable conditions for Ca^{2+} uptake into the ER across a large membrane surface area.

The nature of any Ca^{2+} transporters that may be involved in uptake of Ca^{2+} into the coccolithophore PER is currently unknown. To date, the generally accepted mechanism for Ca^{2+} uptake across the ER membrane is via P-type ATPases. Recently PM Ca^{2+} -ATPase (PMCA) and sarcoplasmic reticulum Ca^{2+} -ATPase (SERCA) pumps have been shown to operate with antiport activity, exchanging Ca^{2+} for H^+ (Niggli and Sigel 2008). The use of Na^+ electrochemical gradients to drive secondary

membrane transport is widespread amongst animals. The calcifying 2N cell-specific expression of an NCKX-like transporter in *E. huxleyi* raises very interesting questions concerning its functional role. Von Dassow et al. (2009) have argued that its role may be to regulate $[Ca^{2+}]$ in the space between the PM and PER.

Ca²⁺-Permeable Channels

Ca²⁺ permeable channels allow the flow of Ca²⁺ down an electrochemical gradient. Ca²⁺ channels can be regulated by a wide range of electrical and chemical stimuli (Berridge 2002; Sanders et al. 2002; Hetherington and Brownlee 2004). Although there is evidence for PM depolarization-activated cation entry from patch clamp electrophysiological experiments with *C. pelagicus* (Taylor and Brownlee 2003), the physiological and molecular characteristics of the primary Ca²⁺ influx pathway for Ca²⁺ in coccolithophores has yet to be established. It is worthy of note here that our previous attempts to determine whether Ca²⁺ entry may occur via a “fluid phase” endocytotic mechanism have all produced negative results (Berry et al. 2002).

This is in contrast to recent evidence from foraminiferal studies (Bentov et al. 2010) that have shown significant fluid-phase endocytosis and the demonstration of an endocytotic transport pathway from the external medium to the site of calcification in the shallow water benthic foraminifera *Amphistegina lobifera*.

Dissolved Inorganic Carbon (DIC) Transport

Coccolithophores need to sustain large influxes of DIC for photosynthesis and calcite formation. Whereas the substrate for the principle carbon fixing enzyme, ribulose biphosphate carboxylase oxygenase (Rubisco) is CO₂, and while early experiments indicated that *E. huxleyi* used CO₂ as the external DIC species for photosynthesis (Sikes et al. 1980), there is substantial evidence that coccolithophores can utilize both CO₂ and HCO₃⁻ as the external DIC source for photosynthesis (e.g., Sekino and Shirawa 1994; Buitenhuis et al. 1999; Herfort et al. 2002; Rost et al. 2003; Trimborn et al. 2007). There is substantial physiological evidence that indicates HCO₃⁻ use for calcification (Sikes et al. 1980; Nimer et al. 1997; Buitenhuis et al. 1999; Herfort et al. 2002). However, virtually none of the physiological studies to date do allow the distinction between HCO₃⁻ and CO₃²⁻ (see later) as the external DIC substrate.

The relationship between photosynthesis and calcification has been under discussion for several decades (Paasche 1964; Sikes et al. 1980; Nimer et al. 1997; Herfort et al. 2002; Leornados et al. 2009; see Berry et al. 2002; Brownlee and Taylor 2005 for reviews). If it is assumed that HCO₃⁻ is the main DIC substrate for calcification, an ultimate product of the calcification reactions is CO₂ (see equations [1] and [2] here). Although there is some evidence that can be interpreted in terms of calcification providing a source of CO₂ for Rubisco (e.g., Buitenhuis et al. 1999), more recent studies that have monitored photosynthesis in the absence of calcification (by removal of Ca²⁺ from the medium) have provided strong evidence that

there is no mechanistic dependence of photosynthesis on calcification (Herfort et al. 2002; Leornados et al. 2009).

Moreover, it has been shown that if calcification is inhibited by hydroxyethylidene bisphonic acid (HEBP) (an inhibitor of the growth of CaCO₃ crystals that completely suppresses CaCO₃ production) photosynthetic fixation of CO₂ was actually increased (Sekino and Shiraiwa 1994).

E. huxleyi cytosolic [HCO₃⁻] has been estimated to be 0.3–0.5 mM (Nimer and Merrett 1992). With external [HCO₃⁻] at 2 mM, HCO₃⁻ can be considered to move passively across the PM at membrane potentials more positive than estimated PM potential (–60 mV; Anning et al. 1996; Brownlee et al. 1995). However, other studies have shown that *E. huxleyi* can accumulate DIC in internal pools up to 10x that of ambient seawater concentrations, suggesting that additional transport mechanisms may operate to bring about intracellular accumulation (Sekino and Shiraiwa 1994).

Determining whether these differences are the result of different methodologies for determining intracellular DIC or an indication of significant differences in the ability of different *E. huxleyi* strains to accumulate DIC (see later) will require further investigation.

More recent inhibitor-based work has indicated the involvement of Cl⁻/HCO₃⁻ exchangers in DIC uptake in *E. huxleyi* (Herfort et al. 2002). This work showed that photosynthesis, growth rates and calcification rates were not saturated at ambient DIC concentrations of sea water, in concordance with Paasche (1964) who showed that photosynthesis required 15 times the ambient DIC concentration to reach saturation. DIC uptake showed biphasic kinetics, with both ¹⁴C uptake and O₂ evolution showing high affinity, low V_{max} below 1 mM DIC and low affinity, high V_{max} above 1mM, suggesting the operation of two mechanisms of DIC uptake.

Use of SLC4 anion exchanger AE1-type inhibitors, SITS (4-acetamido-4'-isothiocyanato-stilbene-2,2'-disulfonic acid) and DIDS (4,4'-diisothiocyanato-stilbene-2,2'-disulfonic acid) and the CA inhibitor, acetazolamide provided strong evidence that at high DIC concentration an AE1-type Cl⁻/HCO₃⁻ exchanger imports DIC across the PM and at lower [DIC] a CA is also activated to aid in DIC transport. These findings are compatible with the demonstration of expression of an SLC4-like homologue that is specific to 2N calcifying cells of *E. huxleyi* (von Dassow et al. 2009).

The SLC4 family of proteins are involved in base (HCO₃⁻, CO₃²⁻) transport across membranes. In eukaryotes these proteins play an important role in maintaining the HCO₃⁻/CO₃²⁻/CO₂ buffer system essential for short-term intracellular pH control as well as the transport of DIC (Pushkin and Kurtz 2006). The SLC4 family can be sub-divided into three groups based on their function (Alper 2006; Pushkin and Kurtz 2006). (1) The Na⁺-independent Cl⁻/HCO₃⁻ exchangers (also known as anion exchangers (AE)) are electroneutral, exchanging Cl⁻ for HCO₃⁻ at an equal stoichiometry. (2) Na⁺-HCO₃⁻ cotransporters (NBC) mediate the co-transport of Na⁺ with

HCO_3^- and/or CO_3^{2-} at a ratio that can be electroneutral or electrogenic. (3) Na^+ -driven $\text{Cl}^-/\text{HCO}_3^-$ exchangers (NDCBE) transport Na^+ and HCO_3^- in exchange for Cl^- , with their electroneutrality still unclear (Pushkin and Kurtz 2006). Whether the identified *E. huxleyi* 2N calcifying cell-specific SLC4-like homologue is able to transport HCO_3^- and/or CO_3^{2-} is unknown.

Although the bulk of experimental work with coccolithophores identifies HCO_3^- rather than CO_2 as the external substrate for calcification, the assumption that it is HCO_3^- rather than CO_3^{2-} that is primarily transported is largely based on the fact that HCO_3^- is the most abundant DIC species available for transport. However, as outlined below, distinguishing between HCO_3^- and direct CO_3^{2-} uptake will be critical for understanding the issue of pH regulation in calcifying coccolithophore cells and the impacts of reduced ocean surface pH on calcification, since predicted changes in ocean surface pH will bring about significant reductions in ocean surface $[\text{CO}_3^{2-}]$.

Increased expression of a CA has been seen in *E. huxleyi* grown in cultures where calcification was stimulated by phosphate-depletion (Quinn et al. 2006) and in 2N calcifying cells in the light (Richier et al. 2009). Two CAs from *E. huxleyi* have been cloned and sequenced revealing two distinct CAs belonging to the delta (δ -EhCA1) and gamma (γ -EhCA2) classes of CAs (Sotoj et al., 2006). Their cellular localization has not yet been determined. Interestingly δ -EhCA1 has an N-terminal transmembrane region that shows high similarity to $\text{Cl}^-/\text{HCO}_3^-$ exchangers, similar δ -CA fused transport proteins are seen in prokaryotes (Smith and Ferry 2000).

$\text{Cl}^-/\text{HCO}_3^-$ exchangers in animal cells play roles in either the uptake and efflux of HCO_3^- in different cell types. In mammalian cell lines the cytoplasmic carboxy terminal of AE1 has a carbonic anhydrase II (CAII) binding site that upon inhibition reduces AE1-mediated $\text{Cl}^-/\text{HCO}_3^-$ exchange by 50–60% (Sterling et al. 2001). Also identified on the extracellular surface of AE1 and NBC1 bicarbonate transporters are carbonic anhydrase IV (CAIV) interaction sites (McMurtrie et al. 2003). CAII and IV increase HCO_3^- transport by altering localised HCO_3^- levels enhancing the HCO_3^- concentration gradient (McMurtrie et al. 2003).

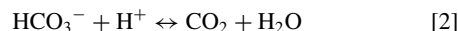
A similar function may occur in coccolithophores with the CA region of δ -EhCA1 or a CA interacting with the $\text{Cl}^-/\text{HCO}_3^-$ exchanger facilitating the localized inter-conversion of HCO_3^- and CO_2 at the cytosolic face of the PM and decreasing the local $[\text{HCO}_3^-]$ at the cytosolic transport site. However, it should be noted that this mechanism would also increase $[\text{CO}_2]$ at the cytoplasmic membrane face, leading to increased diffusive CO_2 loss, which while compatible with a role in cellular pH regulation, may compromise its role in DIC accumulation.

H⁺ Transport

If HCO_3^- is the DIC source for calcification the production of calcite will produce H^+ with a stoichiometry of 1.



H^+ will react with HCO_3^- to generate CO_2 intracellularly.



To maintain a cytosolic pH homeostasis near neutrality, H^+/CO_2 must be removed or neutralised. In principle, photosynthesis could play a role as a net sink for H^+ via removal of CO_2 .

HCO_3^- plays an essential role in pH regulation through the intracellular $\text{HCO}_3^-/\text{CO}_3^{2-}/\text{CO}_2$ buffer system. The importance of this buffer system is demonstrated by the effects of removal of DIC from the external medium which leads to a drop in intracellular pH which can be rapidly resurrected upon the addition of HCO_3^- to the medium (Dixon et al. 1989; Brownlee et al. 1995). This was not a function of photosynthesis as the photosynthetic inhibitor DCMU did not affect the response (Brownlee et al., 1995).

Although the photosynthetic CO_2 affinity of *E. huxleyi* has been reported to be low (Shirawa et al. 2004) if coccolithophores are able to acquire sufficient CO_2 for photosynthesis through diffusion from external seawater, uncatalysed CO_2 production in the cytosol and/or CA-catalysed production of CO_2 at the chloroplast envelope (Brownlee et al. 1995; Nimer et al. 1995), excess H^+ produced from calcification would need to be neutralised, compartmentalised or externalised to maintain a constant cytosolic pH. Although the intracellular $\text{HCO}_3^-/\text{CO}_3^{2-}/\text{CO}_2$ system may act as a transient buffer for H^+ production, this could not be an effective way to buffer a sustained production of H^+ since it would inevitably involve a shift in the $\text{HCO}_3^-/\text{CO}_3^{2-}/\text{CO}_2$ equilibrium that is unfavourable for calcification.

To maintain an environment in the developing CV that is favourable for CaCO_3 precipitation, H^+ have to be removed from the site of CaCO_3 production. Both Ca^{2+} stimulated vacuolar (V type)-ATPase and P-type ATPase activity have been demonstrated on the CV and PM membranes of *P. carterae* (Araki and González 1998). The major subunit (subunit c) of the transmembrane sector, V_0 , was cloned and identified as a subunit of the V-type H^+ -ATPase that subsequently was immuno-localised to the coccolith-producing membrane fraction (Corstjens et al. 2001). In eukaryotes V-type H^+ -ATPases pump protons uphill from the cytosol into organelles (Finbow and Harrison 1997).

If a H^+ -ATPase pump was involved in de-protonation of the coccolith producing organelle it would be the first identified V-type H^+ -ATPase to pump protons across an endomembrane into the cytosol. Cytosolic H^+ would need to be removed into organelles by V-ATPases and V-PPases (inorganic pyrophosphate driven H^+ pumps) or removed from the cell entirely across the PM. At the pH of seawater (pH 8.2) and at PM potentials more positive than -60mV (see preceding) this process would be down the H^+ electrochemical gradient, and could occur via H^+ -permeable channels.

Although it has been hypothesised that a CV pH of >8 may be required to achieve CaCO_3 supersaturation (Brownlee et al.

1995) calcite precipitation could take place in more acidic environments if Ca^{2+} and HCO_3^- concentrations were high enough to ensure the solution is saturated with respect to CaCO_3 . Calcite saturation state (Ω_{calcite}) is related to $[\text{Ca}^{2+}]$, $[\text{HCO}_3^-]$ and pH as follows:

$$[\text{H}^+] = \frac{[\text{Ca}^{2+}][\text{HCO}_3^-]K_2}{K_{\text{calcite}}^*} = [\text{Ca}^{2+}][\text{HCO}_3^-]1.75 \times 10^{-3} \quad [3]$$

where K_2 is the apparent HCO_3^- dissociation constant with a value of 7.68×10^{-10} M at a salinity of 35 and 25°C (Mehrbach et al. 1973) and K_{calcite}^* is the apparent solubility product of calcite with a value of $4.39 \times 10^{-7}\text{M}^2$ (Morse et al. 1980), with $\Omega_{\text{calcite}} \geq 1$ for a saturated solution. Calcite saturation would require a CV pH more alkaline than 7.2 (or 7.38 at typical seawater temperature of 15°C) if $[\text{Ca}^{2+}]$ and $[\text{HCO}_3^-]$ were similar to seawater concentrations. If either HCO_3^- or Ca^{2+} in the CV were significantly elevated above these concentrations, calcite precipitation could occur at lower pH values.

A plausible scenario that allows Ca^{2+} accumulation and CaCO_3 precipitation in the CV could involve Ca^{2+} accumulation into a Golgi- or ER-derived compartment that has an acidic lumen maintained by a V-type ATPase. Simply down-regulating the V-type ATPase activity as the Ca^{2+} -loaded compartment matures into the coccolith vesicle could achieve an appropriate intra-compartmental pH for CaCO_3 precipitation, particularly if the compartment maintained a cytoplasmic side-negative membrane potential, through the action of electrogenic transporters and the establishment of electrochemical potential gradients of other ions, that itself would drive out H^+ into the cytosol (Figure 3).

Mineral CaCO_3 Phases and Coccolithophore Calcification

Our understanding of biomineralization in different groups of microorganisms has changed over recent years. Identification of amorphous precursor phases, multi-macromolecular scaffolds and transport mechanisms have highlighted numerous differences between abiogenic and biogenic mineralization (Weiner and Dove 2003). Evidence from SEM, TEM, cross-polarised light microscopy and selected area electron diffraction (SAED) studies indicates that coccoliths are formed by the assembly of two types of alternating crystal on an organic base plate. These crystals are orientated radially and vertically relative to the base plate margin (Young et al. 1992). The nature of the molecules involved in the nucleation step and the control of crystal growth is unclear.

Studies of biomineralization in a range of organisms has revealed a widespread strategy whereby a disordered mineral phase is initially formed. This transient precursor mineral phase can be transported into place and moulded into shape then induced to crystallise into its final structure (Weiner 2008). The presence of a transient mineral phase has been shown in many different phyla with varying minerals. Examples include disordered hydrated iron oxide (ferrihydrite) transforming into

the crystalline iron oxide in the teeth of chitons (Towe and Lowenstam 1967), mollusc larval shells that contain amorphous calcium carbonate (ACC) that transforms into aragonite (Weiss et al. 2002) and the spicules of sea urchin larvae that also use the precursor ACC but form calcite (Beniash et al. 1997).

The ACC phase is more soluble than calcite or aragonite (Weiner 2008). The idea of an amorphous disordered phase for crystal growth is contrary to the idea that crystals nucleate and grow from a saturated solution. In many biologically controlled environments it appears that crystals grow out of an unstable dehydrated colloidal phase (Weiner 2008). Biomineral nucleation and growth requires a localised zone that initially achieves and maintains a critical level of super-saturation. Controlled biomineralization is brought about by modifying at least one component of the biomineralising compartment (Weiner and Dove 2003). Thus by actively supplying cations to the site of crystallization or to a precursor phase, anions will passively accumulate to maintain electroneutrality (Weiner and Dove 2003).

Biomineralization via a transient precursor phase has been shown to take place on a preformed organic matrix. The matrix of the mollusc shell nacreous layer consists of an ordered β -chitin framework (Levi-Kalisman et al. 2001), with an associated assemblage of highly acidic glycoproteins rich in aspartic acid (Weiner 1979). The β -chitin framework forms layers which are filled with hydrophobic silk-like proteins (silk fibron proteins) (Weiner et al. 1984) and acidic glycoproteins. This silk fibron-glycoprotein network forms a hydrated gel matrix that creates an appropriate micro-environment for controlled crystal growth (Lia Addadi 2006).

Specific acidic proteins within this matrix allow crystal nucleation and control crystal growth and morphology. Crystal growth in the hydrogel region leads to the displacement of the silk fibron gel (although some silk fibron and glycoprotein is incorporated into the crystal lattice) compacting it between the newly formed crystal and the β -chitin framework (Nudelman et al. 2008). It is believed that all the CaCO_3 required for crystal formation is present in the matrix in an amorphous form before crystal nucleation, with the supply of this ACC to the nacreous layer possibly via vesicle transport (Lia Addadi 2006).

Vesicle transport of ACC is seen in echinoderm larvae where the transient amorphous precursor phase appears to be formed in vesicles in cells adjacent to spicule formation, with these ACC-containing vesicles transported to the site of spicule growth (Beniash et al. 1999). ACC forms from a supersaturated solution in which organic and inorganic molecules prevent the deposition of the crystalline phase. Mg^{2+} has been shown to be an important element of ACC stabilization, possibly acting both as a transient phase stabiliser and in control of the precipitation process (Bentov and Erez 2006).

In coccolithophores there is currently no direct evidence for an ACC precursor phase in calcification. However, several indirect lines of evidence point to the operation of a mechanism that could involve an ACC phase. Calcite nucleation in coccoliths takes place on an organic base plate. In *P. carterae* three

highly acidic polysaccharides, PS-1, 2 and 3, have been identified (Marsh et al. 1992). PS-1 and 2 were shown to be synthesised in the Golgi and were associated with the organic base plate at the onset of crystallization (Marsh 1994).

PS-2 was also shown to be essential for successful nucleation and mineralization in *P. carterae* while PS-3 was essential for growth of proto-crystals into the double disc of calcite of the coccolith (Marsh et al. 2002). In *E. huxleyi* a single complex galacturonomannan polysaccharide (coccolith associated polysaccharide; CAP) that consists of a sulphated backbone with a variety of side chains rich in galacturonic acid (Vliegthart et al. 1981) with similarities to PS-3 (Marsh 2003) polysaccharide associates with coccoliths (de Jong et al. 1976).

Borman et al. (1982) showed that CAP inhibits crystal growth from solutions of Ca^{2+} and HCO_3^- . More recently strong evidence was provided for CAP involvement in the regulation of directional crystal growth by attaching preferentially to calcite acute edges (Henriksen et al. 2004). It is clear that acidic polysaccharides play an essential role in calcification. The three polysaccharides identified in *P. carterae* have been localised to the Golgi, coccolithosomes, immature coccoliths and external coccoliths (Marsh 1994; Marsh and Dickinson 1997; Marsh et al. 2002).

During coccolith growth a polysaccharide component forms a closely associated coat that is tightly associated with the surface of the CV membrane (van der Wal et al. 1983b; Marsh et al. 2002). Coccolithosomes appear to be delivered to the organic base plate-containing cisternae prior to and during calcification (van der Wal et al. 1983b). As the coccolith increases in size this polysaccharide coat becomes more pronounced and thicker, showing that coat formation and calcification are simultaneous (van der Wal et al. 1983b). The externalised coccolith has an organic coat between 280 and 350 nm thick (Godoi et al. 2009).

The potential role of coccolithosomes observed in *P. carterae* in the deposition of calcite is particularly intriguing (Outka and Williams 1971). TEM studies show they are electron dense after Pb staining, possibly indicating the presence of high levels of anionic organic matter. X-ray microanalysis has shown them to have a Ca^{2+} concentration of at least 6 M and a high Mg^{2+} content (van der Wal et al. 1983a). It is highly unlikely that Ca^{2+} is free in the coccolithosome, so to maintain a high $[\text{Ca}^{2+}]$ and electroneutrality acidic polysaccharides and proteins are likely to bind the Ca^{2+} or potentially bind both Ca^{2+} and CO_3^{2-} maintaining it in an ACC, and presumably osmotically inactive, phase. Elevated Mg^{2+} levels within the coccolithosome may aid in ACC stabilization as discussed earlier.

The coccolith-associated protein GPA (Corstjens et al. 1998) is highly acidic with Asp and Glu residues accounting for 24% of the total amino acid complement (Corstjens et al. 1998). GPA sequences are correlated with the different morphologies of coccoliths from A and B morphotypes of *E. huxleyi* with a unique motif (coccolith morphology motif; CMM) found in the 3'UTR (Schroeder et al. 2005). Our unpublished studies indicate that GPA bears certain superficial similarities to the silk fibron

proteins that are involved in crystal formation from an ACC phase.

In summary, several aspects of the coccolithophore biomineralization process show strong analogies to biomineralization in the mollusc shell nacreous layer and the spicules of echinoderm larvae. (1) The constituents for CaCO_3 are delivered to the site of mineralization via vesicles (in the form of ACC in molluscs and echinoderms; (2) Highly acidic macromolecules are involved; (3) The compartment where crystallization occurs is isolated and tightly associated with either a membrane (echinoderm larvae; (Beniash et al. 1999)) or a chitin framework cell (mollusc nacreous layer); (4) As crystallization proceeds the organic matrix associated with the CaCO_3 precursors is displaced to the surface of the crystallising unit; (5) The site of crystallization is a non-aqueous environment, this is highly likely in coccolithophores as the membrane of the coccolith-forming compartment is juxtaposed to the coccolith surface; and, (6) The crystallization is a highly regulated process.

Coccolithophore Calcification and Elevated CO_2

Recent studies, have indicated that coccolithophores may respond to altered ocean chemistry in a variety of ways that are not understood. Riebesell et al. (2000) first showed that increased pCO_2 gave rise to reduced calcification relative to organic carbon fixation and on a per-cell basis in *E. huxleyi* and its close relative *Gephyrocapsa oceanica*. Langer et al. (2006) examined the effects of elevated CO_2 on three different species of coccolithophore, showing little effect of elevated CO_2 on *C. pelagicus* calcification, a CO_2/pH optimum for *Calcidiscus leptoporus* with a maximum value at present day CO_2 levels, and decreased calcification with elevated CO_2 for *G. oceanica*. Iglesias Rodriguez et al. (2008) reported increased calcification by cells of *E. huxleyi* in cultures grown in media bubbled with CO_2 levels that mimicked future scenarios.

However, on a per biomass basis, these CO_2 -enriched cultures did not show elevated calcification (Riebesell et al. 2008; Ridgwell et al. 2009). Evidence for higher calcification rate at elevated CO_2 was observed in *E. huxleyi* by Shi et al. (2009) when calculated on a per cell basis. When normalized to algal biomass, no significant difference existed between the two CO_2 treatments. A further analysis of all published responses of coccolithophore calcification to pH manipulation experiments by Ridgwell et al. (2009) suggests that experimental design, in particular whether CO_2/pH manipulations involve acid/base addition or CO_2 bubbling is not a key factor in determining coccolithophore calcification responses to elevated CO_2 , since both increases and decreases in relative calcification rate can be observed in CO_2 bubbling experiments. Rather, it has been argued (Ridgwell et al. 2009) that strain type and prior culture history may be important factors, along with growth conditions, such as light intensity, temperature, nutrient availability, and mixing, in determining responses to elevated CO_2 during CO_2 perturbation experiments

CONCLUSIONS

The precipitation of calcite by coccolithophores occurs as a multi-molecule controlled process that allows the highly regulated precipitation of calcite with stringent control over crystal shape and size. The accumulation of the organic molecules and the inorganic ions necessary for calcification requires complex metabolic and ion transport pathways. Identifying and elucidating them at a molecular and genetic level is essential for understanding of the process of calcification.

The anticipated release of the *E. huxleyi* genome sequence will be key to understanding and interpreting the rapidly increasing information being gained from transcriptomics studies. Clearly there is a need to understand the components of the calcification process and how these may acclimate or adapt to changing ocean chemistry. A major challenge will be to scale up from a rapidly improving cellular and molecular level understanding of calcification to understand population, community and ecosystem responses to projected future CO₂ scenarios.

REFERENCES

- Addadi L. 2003. Taking advantage of disorder: amorphous calcium carbonate and its roles in biomineralization. *Adv Mater* 15:959–970.
- Addadi L. 2006. Mollusk shell formation: A source of new concepts for understanding biomineralization processes. *Chem Euro J* 12:981–987.
- Alper SL. 2006. Molecular physiology of SLC4 anion exchangers. *Exper Physiol* 91:153–161.
- Anning T, Nimer N, Merrett MJ, Brownlee C. 1996. Costs and benefits of calcification in coccolithophorids. *J Mar Syst* 9:45–56.
- Araki Y, González EL. 1998. V- and P-type Ca²⁺ stimulated ATPases in a calcifying strain of *Pleurochrysis* sp. (Haptophyceae). *J Phycol* 34:79–88.
- Bartolomei G, Tadini-Buoninsegni F, Hua S, Moncelli MR, Inesi G, Guidelli R. 2006. Clotrimazole inhibits the Ca²⁺-ATPase (SERCA) by interfering with Ca²⁺ Binding and Favoring the E2 Conformation. *J Biol Chem* 281:9547–9551.
- Beniash E, Addadi L, Weiner S. 1999. Cellular control over spicule formation in sea urchin embryos: A structural approach. *J Struct Biol* 125:50–62.
- Beniash E, Aizenberg J, Addadi L, Weiner S. 1997. Amorphous calcium carbonate transforms into calcite during sea urchin larval spicule growth. *Proc Roy Soc Lond Ser B Biol Sci* 264:461–465.
- Bentov S, Brownlee C, Erez J. 2010. The role of seawater endocytosis in the biomineralization process in calcareous foraminifera. *Proc Natl Acad Sci USA* 106:21500–21504.
- Bentov S, Erez J. 2006. Impact of biomineralization processes on the Mg content of foraminiferal shells: A biological perspective. *Geochem Geophys Geosys* 7:Q01P08.
- Berridge MJ. 2002. Unlocking the secrets of cell signalling. *Ann Rev Physiol* 67:1–21.
- Berry L, Taylor AR, Lucken U, Ryan KP, Brownlee C. 2002. Calcification and inorganic carbon acquisition in coccolithophores. *Funct Plant Biol* 29:289–299.
- Borman AH, de Jong EW, Huizinga M, Kok DJ, Westbroek P, Bosch L. 1982. The role in CaCO₃ crystallization of an acid Ca²⁺-binding polysaccharide associated with coccoliths of *Emiliania huxleyi*. *Euro J Biochem* 129:179–183.
- Borman AH, de Jong EW, Thierry R, Westbroek P, Bosch L, Gruter M, Kamerling JP. 1987. Coccolith-associated polysaccharides from cells of *Emiliania huxleyi* (Haptophyceae). *J Phycol* 23:118–123.
- Brownlee C, Davies M, Nimer N, Dong LF, Merrett M. 1995. Calcification, photosynthesis and intracellular regulation in *Emiliania huxleyi*. *Bull Inst Oceanogr Monaco* 14:19–35.
- Brownlee C, Taylor AR. 2005. Calcification in coccolithophores: a cellular perspective. In Thierstein H, Young J, editors. *Coccolithophores: From Molecular Processes to Global Impact*. Springer, Berlin, P 31–50.
- Buitenhuis E, de Baar H, Veldhuis M. 1999. Photosynthesis and calcification by *Emiliania huxleyi* (Prymnesiophyceae) as a function of inorganic carbon species. *J Phycol* 35:949–959.
- Cai X, Lytton J. 2004. The Cation/Ca²⁺ exchanger superfamily: Phylogenetic analysis and structural Implications. *Mol Biol Evol* 21:1692–1703.
- Corstjens P, Araki Y, González EL. 2001. A coccolithophorid calcifying vesicle with a vacuolar-type ATPase proton pump: cloning and immunolocalization of the V₀ subunit c. *J Phycol* 37:71–78.
- Corstjens P, Van Der Kooij A, Linschooten C, Brouwers GJ, Westbroek P, de Vrind-de Jong EW. 1998. GPA, a calcium-binding protein in the coccolithophorid *Emiliania huxleyi* (Prymnesiophyceae). *J Phycol* 34:622–630.
- de Jong EW, Bosch L, Westbroek P. 1976. Isolation and characterization of a Ca²⁺-binding polysaccharide associated with coccoliths of *Emiliania huxleyi* (Lohmann) Kämtner. *Euro J Biochem* 70:611–621.
- Dixon GK, Brownlee C, Merrett MJ. 1989. Measurement of internal pH in the coccolithophore *Emiliania huxleyi* using 2',7'-bis-(2-carboxyethyl)-5-(and-6) carboxyfluorescein acetoxymethyl ester and digital imaging microscopy. *Planta* 178:443–449.
- Dolman NJ, Tepikin AV. 2006. Calcium gradients and the Golgi. *Cell Calcium* 40:505–512.
- Dulhunty AF, Junankar PR, Stanhope C. 1993. Immunogold labelling of calcium-ATPase in sarcolasmic reticulum of skeletal muscle—use of 1 nm, 5 nm and 10 nm gold. *J Histochem Cytochem* 41:1459–1466.
- Dyhrman ST, Haley ST, Birkeland SR, Wurch LL, Cipriano MJ, McArthur AG. 2006. Long serial analysis of gene expression for gene discovery and transcriptome profiling in the widespread marine coccolithophore *Emiliania huxleyi*. *Appl Environ Microbiol* 72:252–260.
- Fernandez E, Boyd P, Holligan PM. 1993. Production of organic and inorganic carbon within a large scale coccolithophore bloom in the North East Atlantic ocean. *Mar Ecol Progr Ser* 3:271–285.
- Finbow ME, Harrison MA. 1997. The vacuolar H⁺-ATPase: A universal proton pump of eukaryotes. *Biochem J* 324:697–712.
- Fujiwara S, Hirokawa Y, Takasuka Y, Suda K, Asamizo E, Takayanaki T, Shibata D, Tabata S, Tsuzuki M. 2007. Gene expression profiling of coccolith-bearing cells and naked cells in haptophyte *Pleurochrysis haptomenofera* with a cDNA microarray system. *Mar Biotechnol* 8:1–11.
- Godoi, RH, Aerts K, Harlay J, Kaegi R, Ro C-U, Chou L, Van Grieken R. 2009. Organic surface coating on Coccolithophores—*Emiliania huxleyi*: Its determination and implication in the marine carbon cycle. *Microchem J* 91:266–271.
- Gussone N, Langer G, Thoms S, Nehrke G, Eisenhauer A, Riebesell U, Wefer G. 2006. Cellular calcium pathways and isotope fractionation in *Emiliania huxleyi*. *Geology* 34:625–628.
- Hetherington AM, Brownlee C. 2004. The generation of calcium signals in plants. *Ann Rev Plant Biol* 55:401–427.
- Henriksen K, Stipp SLS. 2009. Controlling biomineralization: The effect of solution composition on coccolith polysaccharide functionality. *Crystal Growth Design* 9:2088.
- Henriksen K, Stipp SLS, Young JR, Marsh ME. 2004. Biological control on calcite crystallization: AFM investigation of coccolith polysaccharide function. *Amer Mineral* 89:1709–1716.
- Herfort L, Thake B, Roberts J. 2002. Acquisition and use of bicarbonate by *Emiliania huxleyi*. *New Phytol* 156:427–436.
- Hirschi KD, Zhen RG, Cunningham KW, Rea PA, Fink GR. 1996. CAX1, an H⁺/Ca²⁺ antiporter from Arabidopsis. *Proc Natl Acad Sci USA* 93:8782–8786.
- Holligan PM, Voillier M, Harbour DS, Camus P, Champagne-Phillipe M. 1983. Satellite and ship studies of coccolithophore production along a continental shelf edge. *Nature* 304:339–402.
- Igelesias-Rodríguez MD, Halloran PR, Rickaby REM, Hall IR, Colmenero-Hildago E, Gittins JR, Green DRH, Tyrrell, T, Gibbs SJ, von Dassow P,

- Rehm E, Armbrust EV, Boessenkool KP. 2008. Phytoplankton calcification in a high CO₂ world. *Science* 320:336–340.
- Klaveness D. 1976. *Emiliania huxleyi* (Lohmann) Hay and Mohler. 3. Mineral deposition and origin of matrix during coccolith formation. *Protistologica* 12:217–224.
- Leornados N, Read B, Thake B, Young J. 2009. No mechanistic dependence of photosynthesis on calcification in the coccolithophorid *Emiliania huxleyi* (Haptophyta). *J Phycol* 45:1046–1051.
- Levi-Kalishman Y, Falini G, Addadi L, Weiner S. 2001. Structure of the nacreous organic matrix of a bivalve mollusk shell examined in the hydrated state using cryo-TEM. *J Struct Biol* 135:8–17.
- Manton I, Leedale GF. 1969. Observations on the microanatomy of *Coccolithus pelagicus* and *Cricosphaera carterae*, with special reference to their origin and nature. *J Mar Biol Asso UK* 49:1–16.
- Marsh M, Dickinson D. 1997. Polyanion-mediated mineralization—mineralization in coccolithophore (*Pleurochrysis carterae*) variants which do not express PS2, the most abundant and acidic mineral-associated polyanion in wild-type cells. *Protoplasma* 199:9–17.
- Marsh ME. 1994. Polyanion-mediated mineralization—assembly and reorganization of acidic polysaccharides in the Golgi system of a coccolithophorid alga during mineral deposition. *Protoplasma* 177:108–122.
- Marsh ME. 2003. Regulation of CaCO₃ formation in coccolithophores. *Compar Biochem Physiol Part B: Biochem Mol Biol* 136:743–754.
- Marsh ME, Chang DK, King GC. 1992. Isolation and characterization of a novel acidic polysaccharide containing tartrate and glyoxylate residues from the mineralized scales of a unicellular coccolithophorid alga *Pleurochrysis carterae*. *J Biol Chem* 267:20507–20512.
- Marsh ME, Ridall AL, Azadi P, Duke PJ. 2002. Galacturonomannan and Golgi-derived membrane linked to growth and shaping of biogenic calcite. *J Struct Biol* 139:39–45.
- Maser P, Thomine S, Schroeder JI, Ward JM, Hirschi K, Sze H, Talke IN, Amtmann A, Maathuis FJM, Sanders D, Harper JF, Tchieu J, Gribskov M, Persans MW, Salt DE, Kim SA, Guerinot ML. 2001. Phylogenetic relationships within cation transporter families of Arabidopsis. *Plant Physiol* 126:1646–1667.
- McMurtrie HL, Cleary HJ, Alvarez BV, Loisel FB, Sterling D, Morgan PE, Johnson DE, Casey JR. 2003. The bicarbonate transport metabolon. In 6th International Conference on Carbonic Anhydrases. Taylor & Francis Ltd, Bratislava, Slovakia, 231–236.
- Mehrbach C, Culbertson CH, Hawley JE, Pytkowicz RM. 1973. Measurement of the apparent dissociation constants of carbonic acid in seawater at atmospheric pressure. *Limnol Oceanogr* 18:897–907.
- Milliman JD. 1993. Production and accumulation of calcium carbonate in the ocean: Budget of a nonsteady state. *Glob Biogeochem Cycles* 7:927–957.
- Morse JW, Mucci A, Millero FJ. 1980. The solubility of calcite and aragonite in seawater of 35‰ salinity at 25°C and atmospheric pressure. *Geochim Cosmochim Acta* 44:85–94.
- Müller MN, Antia AN, LaRoche J. 2008. Influence of cell cycle phase on calcification in the coccolithophore *Emiliania huxleyi*. *Limnol Oceanogr* 53:506–512.
- Nguyen B, Bowers RM, Wahlund TM, Read BA. 2005. Suppressive subtractive hybridization of and differences in gene expression content of calcifying and noncalcifying cultures of *Emiliania huxleyi* Strain 1516. *Appl Environ Microbiol* 71:2564–2575.
- Niggl V, Sigel E. 2008. Anticipating antiport in P-type ATPases. *Trends Biochem Sci* 33:156–160.
- Nimer N, Dong LF, Guan Q, Merrett MJ. 1995. Calcification rate, dissolved inorganic carbon utilization and carbonic anhydrase activity in *Emiliania huxleyi*. *Bull Inst Oceanogr Monaco* 14:43–49.
- Nimer NA, Guan Q, Merrett MJ. 1994. Extracellular and intracellular carbonic-anhydrase in relation to culture age in a high-calcifying strain of *Emiliania huxleyi* Lohmann. *New Phytol* 126:601–607.
- Nimer NA, Iglesias-Rodriguez MD, Merrett MJ. 1997. Bicarbonate utilization by marine phytoplankton species. *J Phycol* 33:625–631.
- Nimer NA, Merrett MJ. 1992. Calcification and utilization of inorganic carbon by the coccolithophorid *Emiliania huxleyi* Lohmann. *New Phytol* 121:173–177.
- Nimer NA, Merrett MJ, Brownlee C. 1996. Inorganic carbon transport in relation to culture age and inorganic carbon concentration in a high-calcifying strain of *Emiliania huxleyi* (Prymnesiophyceae). *J Phycol* 32:813–818.
- Nudelmann F, Shimoni E, Klein E, Rousseau M, Bourrat X, Lopez E, Addadi L, Weiner S. 2008. Forming nacreous layer of the shells of the bivalves *Atrina rigida* and *Pinctada margaritifera*: An environmental- and cryo-scanning electron microscopy study. *J Struct Biol* 162:290–300.
- Outka DE, Williams DC. 1971. Sequential Coccolith Morphogenesis in *Hy-menomonas carterae*. *J Eukar Microbiol* 18:285–297.
- Paasche E. 1962. Coccolith formation. *Nature* 193:1094–1095.
- Paasche E. 1964. A tracer study of the inorganic carbon uptake during coccolith formation and photosynthesis in the coccolithophorid *Coccolithus huxleyi*. *Physiologia Plantarum* 3(suppl):1–82.
- Paasche E. 2001. A review of the coccolithophorid *Emiliania huxleyi* (Prymnesiophyceae), with particular reference to growth, coccolith formation, and calcification-photosynthesis interactions. *Phycologia* 40:503–529.
- Pushkin A, Kurtz I. 2006. SLC4 base (HCO₃⁻, CO₃²⁻) transporters: classification, function, structure, genetic diseases, and knockout models. *Amer J Physiol Renal Physiol* 290:F580–599.
- Quinn P, Bowers RM, Zhang X, Wahlund TM, Fanelli MA, Olszova D, Read BA. 2006. cDNA microarrays as a tool for identification of biomineralization proteins in the coccolithophorid *Emiliania huxleyi* (haptophyta). *Appl Environ Microbiol* 72:5512–5526.
- Raven JA. 1980. Nutrient transport in microalgae. *Adv Microb Physiol* 21:47–226.
- Richier S, Kerros M-E, deVargas C, Haramaty L, Falkowski P, Gattuso J-P. 2009. Light-dependent transcriptional regulation of genes of biogeochemical interest in the diploid and haploid life cycle stages of *Emiliania huxleyi*. *Appl Environ Microbiol* 75:3366–3369.
- Rickaby REM, Schrag DP, Zondervan I, Riebesell U. 2002. Growth rate dependence of Sr incorporation during calcification of *Emiliania huxleyi*. *Global Biogeochem Cycles* 16:1006.
- Ridgwell A, Schmidt DN, Turley C, Brownlee C, Maldonado MT, Tortell P, Young JR. 2009. From laboratory manipulations to earth system models: predicting pelagic calcification and its consequences. *Biogeosciences* 6:3455–3480.
- Riebesell U, Bellerby RGJ, Engel A, Fabry VJ, Hutchins DA, Reusch TBH, Schulz KG, Morel FMM. 2008. Phytoplankton calcification in a high CO₂ world. *Science* 32:1466b.
- Riebesell U, Körtzinger A, Oschlies A. 2009. Sensitivities of marine carbon fluxes to ocean change. *Proc Natl Acad Sci* 106:20602–20609.
- Riebesell U, Zondervan I, Rost B, Tortell P, Zeebe R, Morel FMM. 2000. Reduced calcification of marine plankton in response to increased atmospheric CO₂. *Nature* 407:364–367.
- Rost B, Riebesell U, Burkhardt S, Sültemeyer D. 2003. Carbon acquisition of bloom-forming marine phytoplankton. *Limnol Oceanogr* 48:55–67.
- Sanders D, Pelloux J, Brownlee C, Harper JF. 2002. Calcium at the crossroads of signalling. *Plant Cell* 14:401–417.
- Schroeder DC, Biggi GF, Hall M, Davy J, Martínez J, Richardson AJ, Malin G, Wilson WH. 2005. A genetic marker to separate *Emiliania huxleyi* (Prymnesiophyceae) morphotypes. *J Phycol* 41:874–879.
- Sekino K, Shiraiwa Y. 1994. Accumulation and utilization of dissolved inorganic carbon by a marine unicellular coccolithophorid, *Emiliania huxleyi*. *Plant Cell Physiol* 35:353–361.
- Shi D, Xu Y, Morel FMM. 2009. Effects of the pH/pCO₂ control method on medium chemistry and phytoplankton growth. *Biogeosciences* 6:1199–1207.
- Shiraiwa Y, Danbara A, Kanke Y. 2004. Characterization of highly oxygen-sensitive photosynthesis in coccolithophorids. *Japan J Phycol* 52 (Supplement):87–94.

- Sikes CS, Roer RD, Wilbur KM. 1980. Photosynthesis and coccolith formation—Inorganic carbon-sources and net inorganic reaction of deposition. *Limnol Oceanogr* 25:248–261.
- Smith KS, Ferry JG. 2000. Prokaryotic carbonic anhydrases. *FEMS Microbiol Rev* 24:335–366.
- Soto AR, Zheng H, Shoemaker D, Rodriguez J, Read BA, Wahlund TM. 2006. Identification and preliminary characterization of two cDNAs encoding unique carbonic anhydrases from the marine alga *Emiliania huxleyi*. *Appl Environ Microbiol* 72:5500–5511.
- Sterling D, Reithmeier RAF, Casey JR. 2001. A transport metabolon. Functional interaction of carbonic anhydrase II and chloride/bicarbonate exchangers. *J Biol Chem* 276:47886–47894.
- Sze H, Liang F, Hwang I, Curran AC, Harper JF. 2000. Diversity and regulation of plant Ca^{2+} pumps: Insights from expression in yeast. *Ann Rev Plant Physiol Plant Mol Biol* 51:433–462.
- Taylor AR, Brownlee C. 2003. A Novel Cl^- inward-rectifying current in the plasma membrane of the calcifying marine phytoplankton *Coccolithus pelagicus*. *Plant Physiol* 131:1391–1400.
- Taylor AR, Russell MA, Harper GM, Collins TT, Brownlee C. 2007. Dynamics of formation and secretion of heterococcoliths by *Coccolithus pelagicus* sp. *Braarudii*. *Euro J Phycol* 42:125–136.
- Towe KM, Lowenstam H. 1967. Ultrastructure and development of iron mineralization in radular teeth of *Cryptochiton stelleri* (Mollusca). *J Ultrastruct Res* 17:1–10.
- Trimborn S, Langer G, Rost B. 2007. Effect of varying calcium concentrations and light intensities on calcification and photosynthesis in *Emiliania huxleyi*. *Limnol Oceanogr* 52:2285–2293.
- van der Wal P, de Bruijn WC, Westbroek P. 1985a. Cytochemical and x-ray-microanalysis studies of intracellular calcium pools in scale-bearing cells of the coccolithophorid *Emiliania huxleyi*. *Protoplasma* 124:1–9.
- van der Wal P, de Jong EW, Westek P, de Bruijn WC. 1983a. Calcification in the coccolithophorid alga *Hymenomonas carterae*. *Ecol Bull* 35:251–258.
- van der Wal P, de Jong EW, Westbroek P, de Bruijn WC, Mulderstapel AA. 1983b. Polysaccharide localization, coccolith formation, and golgi dynamics in the coccolithophorid *Hymenomonas carterae*. *J Ultrastruct Res* 85:139–158.
- van der Wal P, de Jong EW, Westbroek P, de Bruijn WC, Mulderstapel AA. 1983c. Ultrastructural polysaccharide localization in calcifying and naked cells of the coccolithophorid *Emiliania huxleyi*. *Protoplasma* 118:157–168.
- van der Wal P, Leunissen-Vijvelt JJM, Verkleij AJ. 1985b. Ultrastructure of the membranous layers enveloping the cell of the coccolithophorid *Emiliania huxleyi*. *J Ultrastruct Res* 91:24–29.
- von Dassow P, Ogata H, Probert I, Winker P, Da Silva C, Audic S, Claverie J-M, deVargas C. 2009. Transcriptome analysis of functional differentiation between haploid and diploid cells of *Emiliania huxleyi*, a globally significant photosynthetic calcifying cell. *Gen Biol* 10:R114.
- Wahlund TM, Hadaegh AR, Clark R, Nguyen B, Fanelli M, Read BA. 2004. Analysis of Expressed Sequence Tags from calcifying cells of marine coccolithophorid (*Emiliania huxleyi*). *Mar Biotechnol* 6:278–290.
- Weiner S. 1979. Aspartic acid-rich proteins: Major components of the soluble organic matrix of mollusk shells. *Calcified Tissue Inter* 29:163–167.
- Weiner S. 2008. Biomineralization: A structural perspective. *J Struct Biol* 163:229–234.
- Weiner S, Dove PM. 2003. An overview of biomineralization processes and the problem of the vital effect. *Rev Mineral Geochem* 54:1–29.
- Weiner S, Traub W, Parker SB. 1984. Macromolecules in mollusk shells and their functions in biomineralization. *Phil Trans Roy Soc Lond B Biol Sci* 304:425–434.
- Weiss IM, Tuross N, Addadi L, Weiner S. 2002. Mollusk larval shell formation: Amorphous calcium carbonate is a precursor phase for aragonite. *J Exper Zool* 293:478–491.
- Westbroek P, Brown CW, Vanbleijswijk J, Brownlee C, Brummer GJ, Conte M, Egge J, Fernandez E, Jordan R, Knappertsbusch M. 1993. A model system approach to biological climate forcing—The example of *Emiliania huxleyi*. *Global Planet Change* 8:27–46.
- Westbroek P, Young JR, Linschooten K. 1989. Coccolith production (biomineralization) in the marine alga *Emiliania huxleyi*. *J Protozool* 36:368–373.
- Wilbur KM, Watabe N. 1963. Experimental studies on calcification in molluscs and the alga *Coccolithus huxleyi*. *Ann NY Acad Sci* 109:82–112.
- Young JR, Davis SA, Bown PR, Mann S. 1999. Coccolith ultrastructure and biomineralization. *J Struct Biol* 126:195–215.
- Young JR, Didymus JM, Brown PR, Prins B, Mann S. 1992. Crystal assembly and phylogenetic evolution in heterococcoliths. *Nature* 356:516–518.
- Young JR, Ziveri P. 2000. Calculation of coccolith volume and its use in calibration of carbonate flux estimates. *Deep Sea Res Pt II: Topical Stud Oceanogr* 47:1679–1700.

CHAPTER 3. Expression of biomineralization-related ion transport genes in *Emiliana huxleyi*

Published in *Environmental Microbiology*

Expression of biomineralization-related ion transport genes in *Emiliana huxleyi*

Luke Mackinder,^{1,2*} Glen Wheeler,^{1,3}
Declan Schroeder,¹ Peter von Dassow,⁴
Ulf Riebesell² and Colin Brownlee¹

¹Marine Biological Association of the UK, The Laboratory, Citadel Hill, Plymouth PL1 2PB, UK.

²Leibniz Institute of Marine Science, IFM-GEOMAR, D-24105, Kiel, Germany.

³Plymouth Marine Laboratory, Prospect Place, Plymouth, UK.

⁴Departamento de Ecología, Facultad de Ciencias Biológicas, Pontificia Universidad Católica de Chile, Alameda #340, Santiago, Chile.

Summary

Biomineralization in the marine phytoplankton *Emiliana huxleyi* is a stringently controlled intracellular process. The molecular basis of coccolith production is still relatively unknown although its importance in global biogeochemical cycles and varying sensitivity to increased pCO₂ levels has been well documented. This study looks into the role of several candidate Ca²⁺, H⁺ and inorganic carbon transport genes in *E. huxleyi*, using quantitative reverse transcriptase PCR. Differential gene expression analysis was investigated in two isogenic pairs of calcifying and non-calcifying strains of *E. huxleyi* and cultures grown at various Ca²⁺ concentrations to alter calcite production. We show that calcification correlated to the consistent upregulation of a putative HCO₃⁻ transporter belonging to the solute carrier 4 (SLC4) family, a Ca²⁺/H⁺ exchanger belonging to the CAX family of exchangers and a vacuolar H⁺-ATPase. We also show that the coccolith-associated protein, GPA is down-regulated in calcifying cells. The data provide strong evidence that these genes play key roles in *E. huxleyi* biomineralization. Based on the gene expression data and the current literature a working model for biomineralization-related ion transport in coccolithophores is presented.

Introduction

Coccolithophores, unicellular calcifying marine algae, are a key component of today's ocean playing an important role in nutrient and carbon cycling, as well as contributing as much as half of current oceanic calcite production (Milliman, 1993). *Emiliana huxleyi* (division Haptophyta class Prymnesiophyceae) is the most abundant coccolithophore species, producing extensive blooms at temperate latitudes (Holligan *et al.*, 1983; Fernandez *et al.*, 1993; Holligan *et al.*, 1993). Despite the obvious importance of coccolithophores, the function of coccoliths and the cellular processes underlying coccolith formation remain largely un-resolved. The intracellular production of coccoliths of a size approaching the diameter of a single cell together with the rapid rate of coccolith production [~1 per hour (Paasche, 1962)] presents unique questions for how Ca²⁺, H⁺ and inorganic carbon (C_i) balance is regulated in the cell. Mass balance equations show that rapid rates of Ca²⁺ and C_i uptake must occur at the cell plasma membrane (PM) and at the intracellular biomineralization compartment, the coccolith vesicle (CV). The molecular identities of the transport mechanism for delivery of substrates and removal of products are urgently required for the formulation of cellular models that may help to understand the energetics of calcification and its vulnerability to changes in ocean chemistry associated with ocean acidification.

Calcite crystal growth in the CV is highly regulated and involves an organic baseplate (van der Wal *et al.*, 1983) and possible protein matrix (Corstjens *et al.*, 1998) interacting with polysaccharides (de Jong *et al.*, 1976) to control crystal growth. The mature coccolith is transported to the cell periphery and extruded onto the cellular surface. Since Paasche's pioneering work on coccolithophore biology (Paasche, 1962), a range of approaches have been applied to understand the mechanisms underlying calcification. Cell physiology studies have mainly investigated; PM transport identifying a novel Cl⁻ inward rectifying current in *Coccolithus pelagicus* (Taylor and Brownlee, 2003), pH homeostasis indicating high PM H⁺ permeability (Suffrian *et al.*, 2011) and real-time coccolith production showing that coccoliths are extruded across the PM in a single exocytotic event (Taylor *et al.*, 2007). Cell biology and molecular studies have begun to examine the cellular mechanisms of calcification,

Received 15 April, 2011; accepted 1 July, 2011. *For correspondence. E-mail lukcki@mba.ac.uk; Tel. (+44) 1752 633342; Fax (+44) 1752 633102.

including the characterization of two carbonic anhydrases (Soto *et al.*, 2006) and a vacuolar H⁺-ATPase (Corstjens *et al.*, 2001), confirming their functions and localizing the vacuolar H⁺-ATPase to an endomembrane fraction. A recent quantitative RT-PCR study has analysed putative biomineralization genes from *E. huxleyi* grown at ambient and high pCO₂ showing variation in carbonic anhydrase gene expression but insignificant expression changes in other investigated genes (Richier *et al.*, 2010). Finally, a comparative whole genome transcriptomic study of diploid calcifying cells and isogenic haploid non-calcifying flagellated cells identified many genes that were exclusively expressed in the diploid cells and that may therefore function in biomineralization (von Dassow *et al.*, 2009). The identification of multiple putative biomineralization genes in *E. huxleyi* lays a strong foundation for future investigation, although there are clearly many factors other than the process of biomineralization contributing to differential gene expression between haploid and diploid stages of the life cycle.

In the current study we have applied quantitative reverse transcriptase PCR (qRT-PCR) to analyse transcript levels of eight genes with putative roles in calcification. To examine membrane transport processes related to coccolithophore biomineralization, target genes involved in Ca²⁺, inorganic carbon (C_i) and H⁺ transport and Ca²⁺ binding were selected (Table 1). The majority of these genes were selected from the comparative transcriptomic study of gene expression between coccolithophore life cycle stages (von Dassow *et al.*, 2009), although additional genes implicated in calcification were selected from the current literature. Ca²⁺ transport genes included two putative Ca²⁺/H⁺ exchangers (*CAX3* and *CAX4*) and an ER-type Ca²⁺-ATPase (*ECA2*). Two genes with putative roles in C_i utilization were targeted: a putative HCO₃⁻ transporter belonging to the SoLute Carrier 4 family (SLC4, termed *AEL1* for anion exchanger like 1) and a gamma carbonic anhydrase (*γ-EhCA2*), which has previously been cloned and partially characterized with the authors speculating a CV location (Soto *et al.*, 2006). The H⁺ transport genes selected for investigation were a voltage gated H⁺ channel (*HVCN1*) and subunit c of the V₀ sector of a vacuolar H⁺-ATPase (*ATPvc/c'*) previously cloned from *Pleurochrysis carterae* (Corstjens *et al.*, 2001). Of these ion transporters, *CAX3* and *AEL1* are of particular interest as they were both exclusively expressed in the calcifying diploid stage of the life cycle (von Dassow *et al.*, 2009). A Ca²⁺ binding protein shown to be associated with coccolith polysaccharides known as GPA (Corstjens *et al.*, 1998) was also investigated. Here we probe further their expression patterns under different calcification scenarios, identifying key *E. huxleyi* biomineralization-related genes.

To test the role of putative biomineralization genes in *E. huxleyi*, expression patterns were examined under three different calcification scenarios. Relative gene expression patterns were initially investigated between a diploid (calcifying) and haploid (non-calcifying flagellated form) using the strains RCC1216 and RCC1217, with RCC1217 being a stable naturally occurring haploid isolate of RCC1216 that is thought to play a gametal role in the *E. huxleyi* life cycle. Next to eliminate gene expression variations due to cell ploidy level and life cycle stage, a comparison was made between the calcifying diploid strain CCMP1516 and CCMP1516NC (a stable naturally occurring non-calcifying isolate from CCMP1516). Finally to confirm that expression of the putative calcification genes was directly related to calcification, strain CCMP1516 was cultured in different Ca²⁺ concentrations to observe the effect of inhibiting calcification on gene expression.

Results

RCC1216 vs. RCC1217 and CCMP1516 vs. CCMP1516NC comparisons

The absence of calcification in the proposed non-calcifying *E. huxleyi* strains RCC1217 and CCMP1516NC, was confirmed by measurement of PIC production rates and from scanning electron microscope (SEM) images. POC production rates were similar between the calcifying strains and the non-calcifying strains. The PIC production rate was nearly twice as high in the highly calcified strain RCC1216, which produces heavily calcified R-type coccoliths, compared with the CCMP1516 strain with A-type coccoliths (Table 2 and Fig. 1). The SEM preparation method used was unsuitable for the haploid strain RCC1217 with cells disintegrating on the filter membrane during sample processing. For the diploid non-calcifying strain, CCMP1516NC SEM preparation resulted in some collapsed cells on the filter membrane (Fig. 1).

To ensure that strain variations played a minimal role in our analysis of gene expression, microsatellite loci lengths were analysed in the strains used to confirm the pairs were isogenic. Primers to five microsatellite loci were used and amplicon lengths analysed (Table 3). CCMP1516NC, a non-calcifying isolate from CCMP1516, had identical loci lengths to CCMP1516. All the loci for RCC1217, a haploid isolate from RCC1216, correlated to RCC1216, although as expected due to its haploid nature some loci were not present.

The expression of eight target genes (Table 1) was analysed using qRT-PCR. Expression was normalized to two endogenous reference genes (ERGs), actin and elongation factor like 1 protein (*EFG1*) that were shown to be the most stable of the three potential ERGs

Table 1. Target and endogenous reference genes (ERGs) with gene name used in the text, full name, putative function, sequence ID used for primer design [GS prefix denotes EST cluster from (von Dassow *et al.*, 2009) and a asterisk denotes GenBank accession number], corresponding JGI protein ID from *Emiliania huxleyi* CCMP1516 main genome assembly v1.0, primer name with corresponding sequence and amplicon size.

Gene name	Full name	Putative function	Sequence ID	JGI protein ID	Primer name	Primer sequence 5'-3'	Amplicon size
ERGs							
Actin	Actin	Cytoskeleton protein	S64188.1* S64193.1* S64192.1* S64191.1* S64190.1* S64189.1*	–	Actin_F Actin_R	GAC CGA CTG GAT GGT CAA G GCC AGC TTC TCC TTG ATG TC	96
<i>EFG1</i>	Elongation factor 1	Protein elongation during translation. Similar to EFL – elongation factor like protein	GS00217	462457	EFG1_F EFG1_R	GCT GGA AGA AGG ACT TTG TTG TCC ACC AGT CCA TGT TCT TC	101
<i>PK</i>	Pyruvate kinase	Enzyme involved in glycolysis, catalysing the phosphorylation of ADP to ATP	GS01006	439215	PK_F PK_R	ATG GAC GCA AAG GGA ATG CGA GGA TCT CGT CAA TGT TC	94
Ca ²⁺ -transport							
<i>CAX3</i>	Cation/H ⁺ exchanger 3	Transports Ca ²⁺ - against its electrochemical gradient by using a H ⁺ gradient	GS00304	416800	CAX3_F2 CAX3_R2	CTC CTC TGC GTC TTT GCA T GAG GGC GGT GAT GAG GTA	90
<i>CAX4</i>	Cation/H ⁺ exchanger 4	Transports Ca ²⁺ - against its electrochemical gradient by using a H ⁺ gradient	GS00019	415715	CAX4_F CAX4_R	GCT GCT CTT TCC GAT GAT G CCC GCG TAG AGG AGT AGA AG	108
<i>ECA2</i>	ER-type Ca ²⁺ -ATPase 2	Transports Ca ²⁺ - against its electrochemical gradient via the hydrolysis of ATP	GE194135*	522053	ECA2_F ECA2_R	TCC TCA TCA CCT GCA ACA TC TGA CGA GGT TCA CCC AGA G	108
Inorganic carbon transport							
<i>AEL1</i>	Anion exchanger like 1	HCO ₃ ⁻ transporter belonging to the SoLute Carrier 4 family (SLC4) involved in inorganic carbon transport and pH homeostasis. See text for further details	GS05051	198643	AEL1_F AEL1_R	TTC ACG CTC TTC CAG TTC TC GAG GAA GGC GAT GAA GAA TG	102
<i>γ-EhCA2</i>	Gamma carbonic anhydrase	Catalyses the reversible hydration of CO ₂	DQ644551*	432493	γCA_F γCA_R	TCT CCG CCT CAG TCA ACC AAG TTG TCG ACT GTG CAA CC	106
H ⁺ transport							
<i>ATPVc'c'</i>	Subunit c of the V ₀ sector of a Vacuolar H ⁺ -ATPase	Transports H ⁺ against its electrochemical gradient via the hydrolysis of ATP	GS03783	359783	ATPV_F ATPV_R	TAC GGC ACT GCA AAG TCT G ACG GGG ATG ATG GAC TTC	83
<i>HVCN1</i>	H ⁺ channel	Voltage gated H ⁺ channel	–	631975	HVCN1_F HVCN1_R	CAT GTT CCT CCG CTT GTG CCG CAG CTC CCT CAC TAC	109
Biominerallization							
<i>GPA</i>	Glutamic acid, proline and alanine rich Ca ²⁺ -binding protein	Acidic Ca ²⁺ -binding protein isolated from coccoliths. Linked with coccolith morphology	AF012542*	431830	GPA_F GPA_R	TTC CTC GAC AAG GTG AAG AG GCT GCC AAC CTT GGT CTC	99

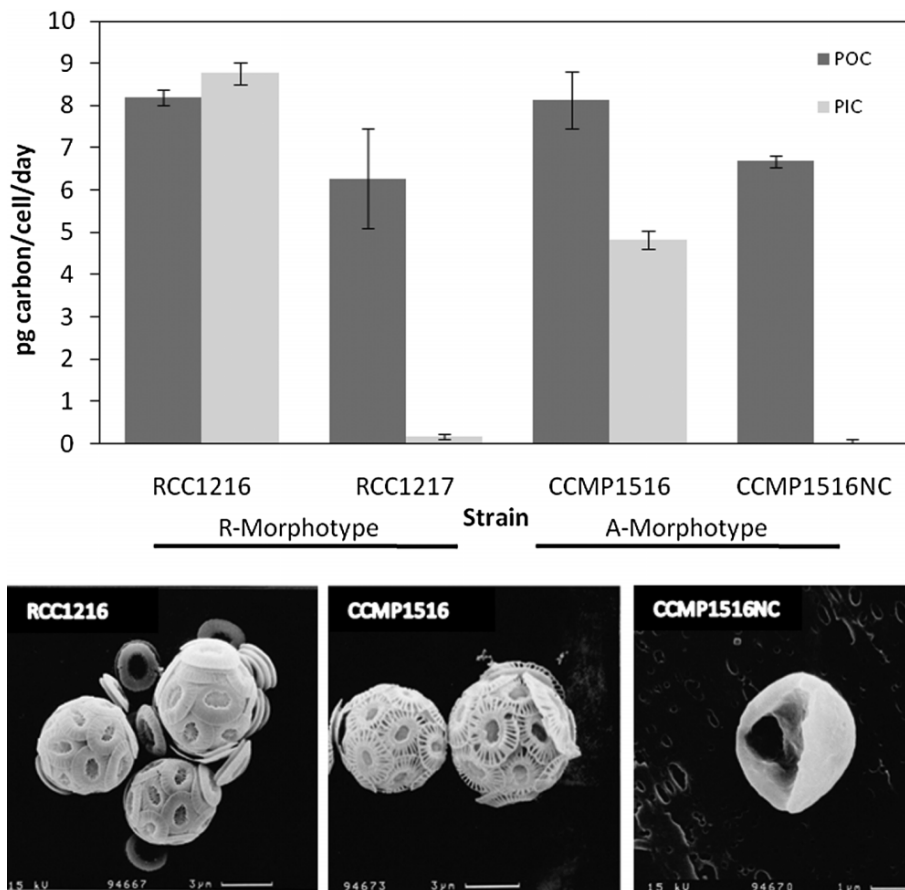
Table 2. Initial and sampling cell concentrations, sampling time after inoculation, growth rates, PIC/POC, POC production rates and calcification (PIC production) rates for the studied strains of *Emiliana huxleyi*.

Strain	Initial cell conc. $\times 10^3$	Sampling cell conc. $\times 10^5$	STDEV	Sampling time after inoculation (days)	Growth rate μ (day 2 to harvest)	STDEV	PIC : POC	STDEV	POC pg per cell per day	STDEV	Calcification rate pg carbon per cell per day	STDEV
RCC1216	0.5	1.62	0.05	5	0.81	0.03	1.07	0.03	8.20	0.19	8.76	0.27
RCC1217	0.5	1.07	0.16	5	0.66	0.05	0.03	0.05	6.28	1.19	0.18	0.06
CCMP1516	0.5	1.13	0.11	5	0.67	0.02	0.59	0.02	8.14	0.68	4.82	0.22
CCMP1516NC	0.1	1.75	0.17	9	0.60	0.01	0.00	0.01	6.68	0.14	-0.02	0.13

analysed (Actin, *EFG1* and pyruvate kinase) and also the two most stable out of all the target and ERGs analysed (geNORM analysis, data not shown (Vandesompele *et al.*, 2002).

Relative gene expression of RCC1216 (diploid, calcifying) vs. RCC1217 (haploid, non-calcifying) and CCMP1516 (diploid, calcifying) vs. CCMP1516NC (diploid, non-calcifying) is shown in Fig. 2. Of the Ca^{2+}

transporters, only *CAX3* expression correlated directly with calcification. *CAX3* gene expression was diploid specific, with no transcripts detected in the haploid RCC1217 cells, whereas *CAX4* and *ECA2* genes were expressed more highly in haploid cells. *CAX3* and *ECA2* genes were significantly upregulated twofold in the calcifying CCMP1516 relative to CCMP1516NC, but *CAX4* showed no difference in gene expression.

**Fig. 1.** Particulate organic carbon (POC) and particulate inorganic carbon (PIC) production rates (top), with SEM images of calcifying strains RCC1216 and CCMP1516 and non-calcifying strain CCMP1516NC (bottom). The flagellated haploid cells, strain RCC1217 disintegrated on the filter membrane under the used SEM protocol. Standard deviations are shown.

3254 L. Mackinder et al.

Table 3. Microsatellite analysis of *E. huxleyi* strains.

Microsatellite locus	E09	E37	F08	B12	F11
RCC1216					
Tasman Sea, South Pacific	100		148	207	123
	102		156		137
	124				
	126				
	148				
	159				
	161				
RCC1217					
Clonal isolate from RCC1216	102		156	207	137
	124				
	126				
	148				
CCMP1516					
South Pacific	96	339		212	119
	102			216	193
CCMP1516NC					
Clonal isolate from CCMP1516	96	339		212	119
	102			216	193

Five microsatellite loci were amplified and their lengths analysed. Note the increased number of products in RCC1216 against RCC1217, due to the diploid/haploid nature. Location of original strain isolation is shown.

The putative HCO_3^- transporter *AEL1* exhibited a very similar pattern of gene expression to that of *CAX3*, with specific expression in the diploid phase and strong upregulation (~3.5-fold) in calcifying CCMP1516 compared with CCMP1516NC. Note that both *CAX3* and *AEL1*, which are diploid specific genes, were expressed in CCMP1516NC supporting its identification as a non-calcifying diploid. In contrast, the carbonic anhydrase, γ -*EhCA2* did not show a significant upregulation in the diploid vs. haploid comparison but did exhibit a significant 1.71-fold upregulation in CCMP1516 relative to CCMP1516NC.

Of the two putative genes involved in H^+ transport only the vacuolar H^+ -ATPase (*ATPVc/c'*) showed consistent and significant upregulation correlating with calcification in both of the comparisons. Transcript levels for the voltage-gated H^+ channel *HVCN1* were downregulated approximately twofold in diploid RCC1216 relative to haploid RCC1217 and were stable in the CCMP1516 vs. CCMP1516NC comparison. Surprisingly, the Ca^{2+} binding protein gene isolated from coccoliths (*GPA*) was downregulated nearly twofold in diploid RCC1216 compared with haploid RCC1217 and exhibited a dramatic 26-fold downregulation in calcifying CCMP1516 compared with non-calcifying CCMP1516NC.

CCMP1516 at different Ca^{2+} concentrations

To further examine the role of these putative biomineralization genes, the calcifying strain CCMP1516 was cultured at varying Ca^{2+} concentrations to manipulate

calcification rates and relative transcript levels were monitored. The cultures showed maximum growth rates and PIC production rates at ambient (10 mM) Ca^{2+} , whereas POC production rates were maximum at 0 mM Ca^{2+} . PIC production was almost fully inhibited in the absence of Ca^{2+} and growth rates were significantly reduced. At higher than ambient Ca^{2+} levels growth rates, PIC production rates and POC production rates decreased with increased Ca^{2+} (Fig. 3). SEM images showed no noticeable variation in morphology at higher Ca^{2+} concentrations relative to 10 mM Ca^{2+} and demonstrated complete dissolution of the coccosphere at 0 mM Ca^{2+} resulting in the presence of some collapsed cells on the filter membrane (Fig. 3).

The ERGs Actin and *EFG1* were the most stable throughout the Ca^{2+} treatments. Five target genes (*CAX3*, *ECA2*, *AEL1*, *ATPVc/c'* and *GPA*) that showed significant changes in gene expression in the strain comparison analyses described above were examined at four different Ca^{2+} concentrations (Fig. 4). Gene expression is shown relative to 0 mM Ca^{2+} where calcification was nearly completely inhibited. The genes encoding the putative Ca^{2+} transporters, *CAX3* and *ECA2*, showed upregulation at 10, 35 and 60 mM Ca^{2+} when compared with zero Ca^{2+} . *CAX3* transcripts were elevated between 2.5- and 3-fold and *ECA2* showed an approximately twofold upregulation. The *AEL1* bicarbonate transporter showed transcript levels between 2.4- and 3.1-fold higher at 10–60 mM Ca^{2+} compared with 0 mM Ca^{2+} and the *ATPVc/c'* gene was slightly upregulated 1.6-fold. Therefore, all four of these ion transport genes exhibited increased expression in calcifying CCMP1516 cultures relative to the 0 mM Ca^{2+} control where calcification was severely inhibited.

In contrast, the gene expression of *GPA* was strongly (~10.8-fold) downregulated at ambient Ca^{2+} , relative to 0 mM Ca^{2+} . This downregulation in respect to 0 mM Ca^{2+} was less at higher Ca^{2+} concentrations with a 6.6-fold downregulation at 35 mM and 6.1-fold downregulation at 60 mM Ca^{2+} . Strikingly, the pattern of gene expression of cells cultured at 0 mM Ca^{2+} vs. ambient Ca^{2+} mirrors very closely that shown in the CCMP1516NC vs. CCMP1516 comparison with all investigated genes up- or downregulated to similar degrees (Figs 2B and 4).

Phylogenetic analysis

The gene expression patterns of the ion transport proteins *CAX3* and *AEL1* demonstrate a very clear positive correlation with the calcification process, although we do not know their functional characteristics. Previous phylogenetic analyses of both the Ca^{2+} /cation exchange (CaCa) and the SLC4 protein families demonstrate that transporters with different ion specificities within these families can be grouped into distinct clades (Cai and Lytton, 2004;

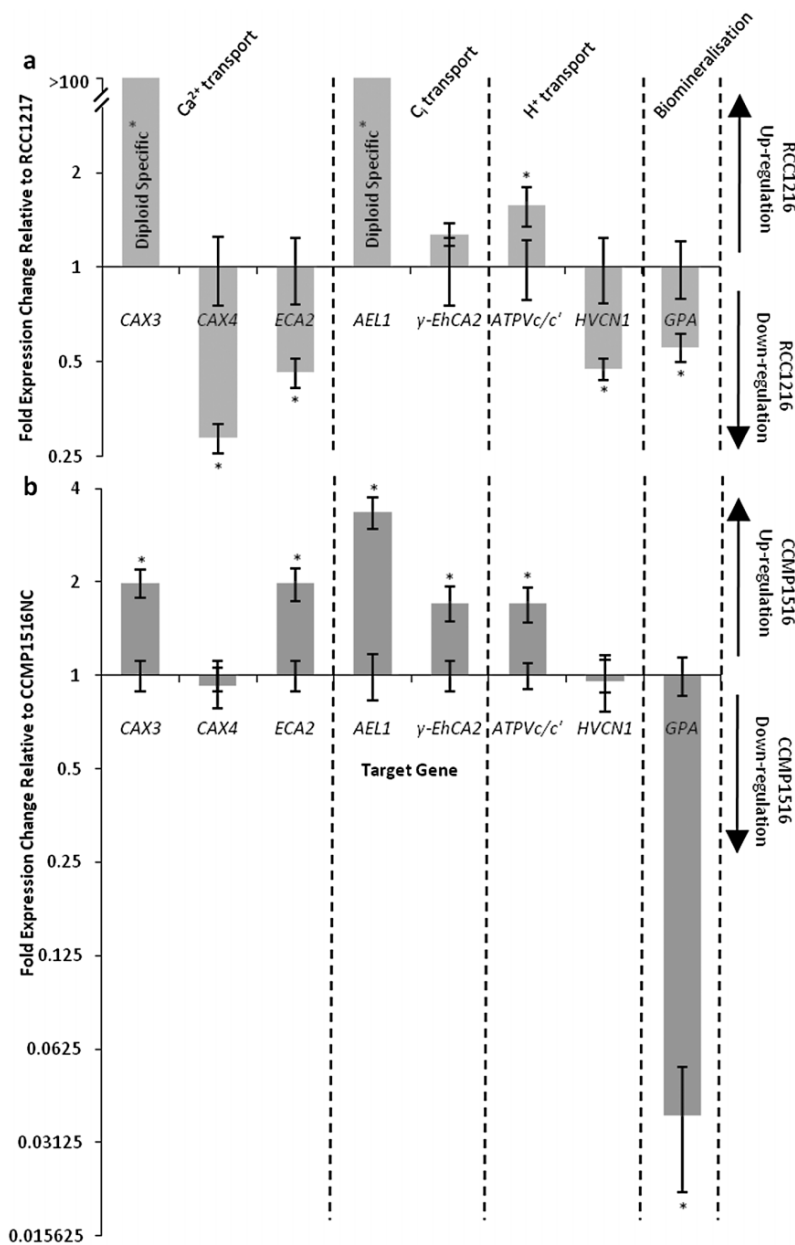


Fig. 2. Relative gene expression of putative calcification genes in (A) strain RCC1216 vs. RCC1217 (B) strain CCMP1516 vs. CCMP1516NC. Genes are grouped into putative functions. Note the y axis is logarithmic to base 2. Standard errors are shown. A * represents significant expression change, $P < 0.01$.

Pushkin and Kurtz, 2006). The CaCA superfamily includes Na⁺-dependent Ca²⁺ exchangers (NCX and NCKX), the Ca²⁺/H⁺ exchangers (CAX), the poorly characterized Ca²⁺/cation exchanger family (CCX) and the prokaryote YRBG transporters (Cai and Lytton, 2004). Phylogenetic analysis of *E. huxleyi* CAX3 and CAX4 with characterized Ca²⁺/cation antiporter (CaCA) superfamily proteins strongly supports their positioning within the CAX clade (Fig. 5A). The HCO₃⁻ transporters within the SLC4 family form two groups based on their phylogeny or three based on their function (Alper, 2006; Pushkin and Kurtz, 2006). Function-

ally these consist of Na⁺-independent Cl⁻/HCO₃⁻ exchangers [also known as anion exchangers (AE)], Na⁺-HCO₃⁻ cotransporters (NBC) and Na⁺-driven Cl⁻/HCO₃⁻ exchangers (NDCBE) (Pushkin and Kurtz, 2006). In addition to Cl_i transport, a group of SLC4 transporters identified in mammals (Human BTR1/NaBC1), plants (*Arabidopsis* BOR1) and yeast (BOR1) have been shown to preferentially transport borate against its electrochemical gradient (Takano *et al.*, 2002; Park *et al.*, 2004). Phylogenetic analysis of known SLC4 proteins indicated AEL1 forms a clade with the putative SLC4 transporter from the picoeu-

3256 L. Mackinder et al.

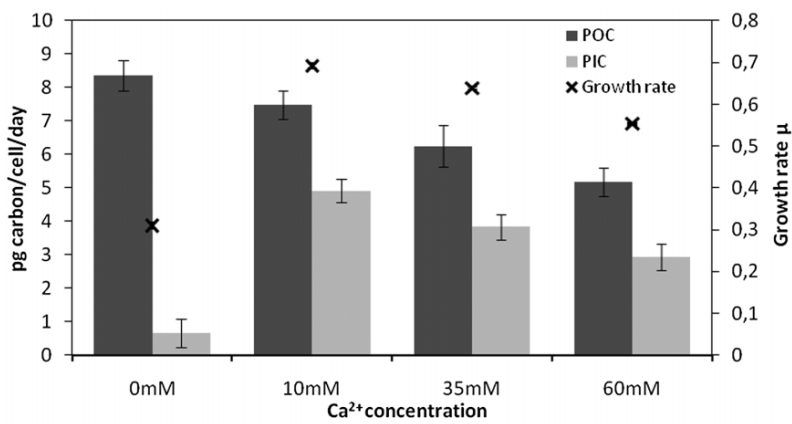
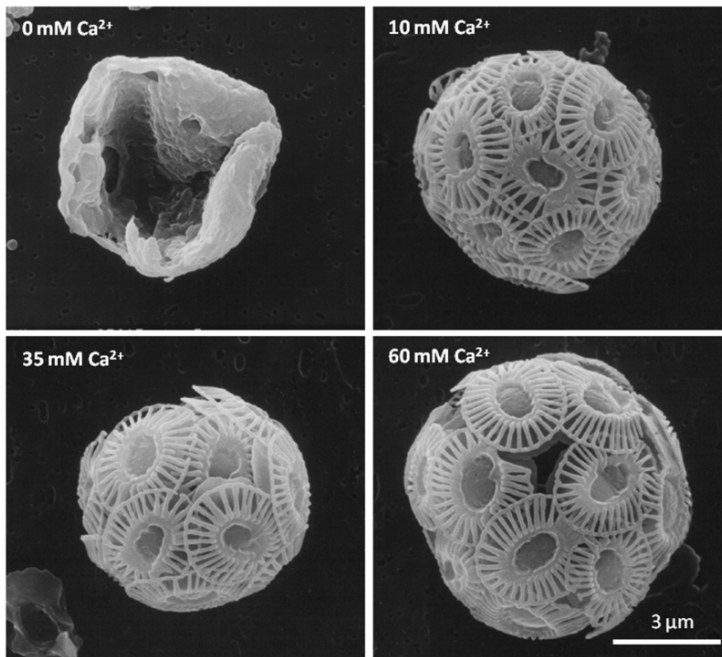


Fig. 3. Carbon fixation rates, growth rates and SEM images of CCMP1516 at different Ca²⁺ concentrations. Standard deviations are shown. For growth rates the standard deviations are smaller than the cross. SEM images are representative of each Ca²⁺ concentration, with natural variations of size and malformation seen within each treatment. Scale bar applies to all SEM images.



karyotic green algae *Micromonas* sp. RCC299, which was distinct from the plant/yeast clade of borate transporters. Although AEL1 does not group within the characterized vertebrate HCO₃⁻ transporters, it is distinct from several other *E. huxleyi* SLC4 transporters identified by Richier *et al.* (2010), which fall into the plant/yeast borate transporter clade (data not shown).

Discussion

We used qRT-PCR to study a select number of genes with putative roles in calcification in a quantifiable and repeatable manner. As calcification influences the ion fluxes and energy demands of the cell, the transcription of genes involved in processes that support calcification such as increased ATP requirements or increased membrane

cycling may also exhibit transcriptional regulation in addition to those directly involved in calcification. By comparing two independent pairs of calcifying vs. non-calcifying strains, in addition to altering calcification rates via manipulation of Ca²⁺ concentrations, we can identify genes that have a strong likelihood of a role in calcification or a calcification related process.

Ca²⁺ transport and homeostasis

Ca²⁺ transport from seawater to the intracellular coccolith forming compartment represents one of the highest trans-cellular net transport rates for Ca²⁺ with a calcifying cell transporting around five million Ca²⁺ ions every second (Mackinder *et al.*, 2010). Fig. 3 indicates that ambient Ca²⁺ (10 mM) is optimal for both calcification and growth

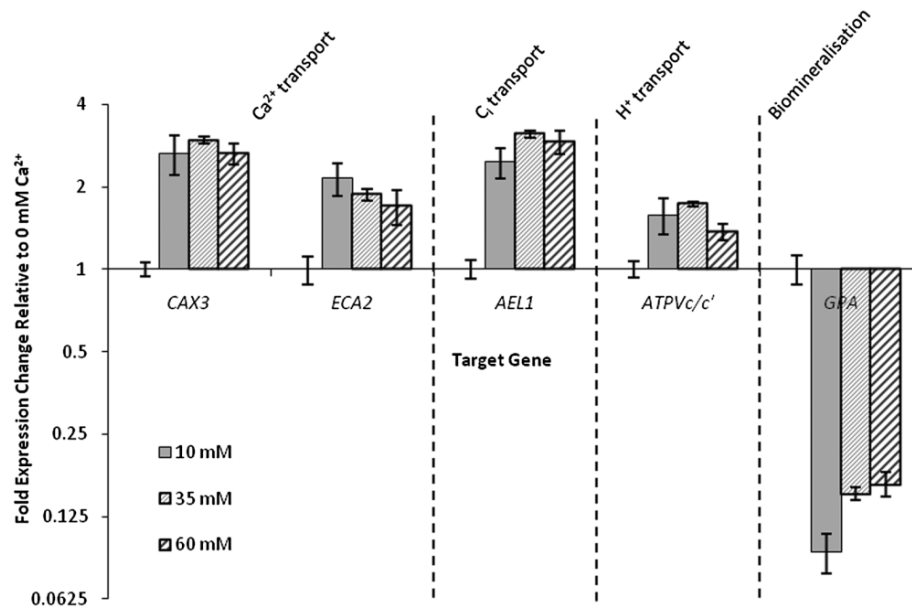


Fig. 4. Relative gene expression of putative calcification genes in CCMP1516 grown at various Ca^{2+} concentrations. Expression is relative to 0 mM Ca^{2+} where calcification was inhibited. Standard errors are shown. Note the y axis is logarithmic to base 2.

rate in *E. huxleyi* for the tested Ca^{2+} concentrations. Elevated Ca^{2+} levels resulted in a decline in PIC production, POC production and growth rate, which is in agreement with a study by Herfort and colleagues (2004) where a decline in calcification and photosynthesis was shown at 50 mM Ca^{2+} . The physiological effects of above optimal levels of Ca^{2+} is probably linked to the increased energetic costs associated with Ca^{2+} homeostasis at higher Ca^{2+} concentrations. In the absence of Ca^{2+} the decline in growth rate and a severe inhibition of PIC production concurs with previous studies which investigated lowered Ca^{2+} concentrations (Herfort *et al.*, 2004; Trimborn *et al.*, 2007; Leonardos *et al.*, 2009). The associated decrease in growth rate and PIC production with the removal of Ca^{2+} can be respectively attributed to the limited Ca^{2+} impacting essential cellular processes necessary for cell division and the lack of substrate for calcification. The removal of Ca^{2+} has a slight positive impact on POC production on a per cell basis most likely due to reduced cell division allowing the reallocation of energy to cellular growth.

Ca^{2+} for calcification most probably enters the cell down its electrochemical gradient via Ca^{2+} -permeable PM channels. Following Ca^{2+} entry a number of routes for Ca^{2+} transport to the CV are possible, the most likely pathway appears to be via the endomembrane system (Brownlee and Taylor, 2005; Mackinder *et al.*, 2010). Loading of endomembrane compartments with Ca^{2+} would require either ATP-dependent pumping or ion exchange using the electrochemical gradient of another ion species. The upregulation of *CAX3* in all the calcifying scenarios

studied here supports a potential role in calcification for Ca^{2+} loading into endomembrane compartments via a H^+ gradient. Here we confirm diploid-specific expression of *CAX3*, with levels below detection limits in haploid cells (von Dassow *et al.*, 2009). As *CAX4* is not upregulated in calcifying cells, it may play a more homeostatic house-keeping role in Ca^{2+} transport, unrelated to calcification. Phylogenetic analysis of the two *CAX* proteins investigated in the present study indicates that they are closely related, although their expression is very different. *CAX* proteins are found in plants, fungi, bacteria and lower invertebrates (Shigaki *et al.*, 2006) and have been shown to export cytosolic cations to maintain optimal chemical and ionic levels for the cell. The first *CAX* proteins to be functionally characterized were Arabidopsis *CAX1* and *CAX2* (Hirschi *et al.*, 1996). Expression of Arabidopsis *CAX1* and *CAX2* in a yeast mutant with Ca^{2+} hypersensitivity rescued the original phenotype with pH-dependent $\text{Ca}^{2+}/\text{H}^+$ exchange (Hirschi *et al.*, 1996). Further investigation of other *CAX* proteins from plants and *Chlamydomonas reinhardtii* has shown that transport is not limited to Ca^{2+} , with *CAX* proteins transporting other cations including Mn^{2+} , Na^+ , Cd^{2+} , Ba^{2+} and Co^{2+} (Kamiya and Maeshima, 2004; Kamiya *et al.*, 2005; Edmond *et al.*, 2009; Liu *et al.*, 2009; Pittman *et al.*, 2009). Regulation of *CAX* activity has been shown to be varied and complex with N-terminal auto-inhibition (Pittman and Hirschi, 2001) and interacting proteins (Cheng *et al.*, 2004a,b) playing key roles in some *CAX*s. To date all plant *CAX*s have been shown to be tonoplast localized (Shigaki and Hirschi,

exhibit a lower capacity (White and Broadley, 2003). It has been postulated that a Ca^{2+} ATPase could act in coccolithophore calcification to facilitate the direct uptake of Ca^{2+} into the CV (Araki and González, 1998). The Ca^{2+} -ATPase investigated in this study (ECA2) is related to the plant ER-type Ca^{2+} -ATPases (ECAs). Despite their name, plant ECAs are not limited to the ER membrane but have also been identified in vacuolar and PMs (Ferrol and Bennett, 1996). ECA2 was upregulated in the calcifying diploid vs. non-calcifying diploid and at ambient or higher Ca^{2+} levels when compared with 0 mM Ca^{2+} . However, ECA2 showed a twofold downregulation in the diploid vs. haploid comparison, suggesting that if it is involved in Ca^{2+} transport during calcification, its cellular role is not exclusive to calcification. Whether Ca^{2+} -ATPases, such as ECA2, move Ca^{2+} directly into the CV remains unknown, with further investigation required to determine if they play a direct role in calcification or function more generally in Ca^{2+} homeostasis.

Dissolved inorganic carbon transport

Calcification and photosynthesis require large and sustained C_i fluxes. It has been hypothesized that calcification and photosynthesis are intrinsically linked with calcification increasing CO_2 availability for ribulose biphosphate carboxylase oxygenase (Rubisco) but a recent accumulation of contrasting evidence has shown no dependence of photosynthesis on calcification. The almost complete absence of PIC fixation in cells grown at 0 mM Ca^{2+} in the present study, in conjunction with a minimal effect on POC production rate is in agreement with previous studies (Herfort *et al.*, 2002; Trimbom *et al.*, 2007; Leonardos *et al.*, 2009) and further demonstrates that photosynthesis can be completely decoupled from calcification. At current seawater pH 8.2, the dissolved C_i composition is approximately 91% HCO_3^- , 8% CO_3^{2-} and 1% CO_2 . There is strong evidence that coccolithophores utilize both CO_2 and HCO_3^- as their external C_i source for photosynthesis (Sekino and Shiraiwa, 1994; Buiteenhuis *et al.*, 1999; Herfort *et al.*, 2002; Rost *et al.*, 2003; Trimbom *et al.*, 2007) and mainly HCO_3^- for calcification (Sikes *et al.*, 1980; Nimer *et al.*, 1997; Buiteenhuis *et al.*, 1999; Herfort *et al.*, 2002). With CO_2 as the substrate for Rubisco, conversion of internalized HCO_3^- to CO_2 would be necessary to support CO_2 supply. The transport routes of the C_i components, their associated transport proteins and the C_i speciation in cellular compartments is relatively unknown. Here we report the gene expression levels of a γ carbonic anhydrase (γ -EhCA2) and a member of the SLC4 family (AEL1). γ -EhCA2 has been functionally characterized *in vitro* (Soto *et al.*, 2006) and its gene expression appears to be responsive to pCO_2/pH , with γ -EhCA2 transcripts significantly reduced (3.8-fold) in RCC1216

cells grown at an elevated pCO_2 (770 ppm relative to cells grown at 440 ppm) (Richier *et al.*, 2010). In that study, no significant change in calcification rates were observed between the treatments, indicating γ -EhCA2 gene expression is possibly more dependent on C_i availability and speciation or pH than cellular calcification. Our data show increased γ -EhCA2 gene expression under calcifying conditions for CCMP1516 compared with CCMP1516NC, but there was no significant upregulation in the diploid vs. haploid comparison. Cellular localization of CAs is key to understanding C_i fluxes and speciation, Soto and colleagues (2006) speculate on a CV location of γ -EhCA2 and external localization of δ -EhCA1. External CA activity has been recorded previously in coccolithophores (Nimer *et al.*, 1996; Herfort *et al.*, 2002), but isoform specific localization studies are essential for completely understanding their role in C_i uptake and calcification.

The use of HCO_3^- as the primary external and internal C_i species used for calcification requires facilitated transport at the PM and CV. Mammalian, fish and squid SLC4 HCO_3^- transport proteins characterized to date have been shown to play key roles in PM carbon transport and pH homeostasis (Shmukler *et al.*, 2005; Pushkin and Kurtz, 2006; Piermarini *et al.*, 2007). Phylogenetic analysis did not group AEL1 with these well-characterized animal HCO_3^- transporters, although AEL1 appears in a distinct group from the plant/yeast borate transporter group. We found that expression of the AEL1 gene was diploid specific, supporting data from von Dassow and colleagues (2009). The upregulation of AEL1 gene expression in all the calcifying scenarios strongly links this gene to a role in calcification, potentially through the provision of C_i . This distinctive gene expression pattern strongly supports further functional characterization of AEL1 in order to determine more clearly its cellular roles. A PM location for AEL1 could potentially allow an inward Na^+ gradient and/or an outward Cl^- gradient to drive C_i uptake. Interestingly, the expression of five *E. huxleyi* SLC4 genes (including AEL1) was shown to be unresponsive to changes in CO_2 (Richier *et al.*, 2010), although only a small CO_2 range was tested.

H⁺ transport and pH homeostasis

pH homeostasis is a fundamental process for all eukaryotic cells. H^+ gradients are maintained across endomembranes and the PM, with many enzymatic and transport processes being dependent on the maintenance of localized pH in different cellular compartments. In animals, ion transport across the PM is commonly energized by a Na^+ gradient, whereas land plants use primarily H^+ electrochemical gradients to drive uphill transport of solutes (Sze *et al.*, 1999). In coccolithophores, H^+ production via calcification may potentially exert significant influence on pH

3260 L. Mackinder et al.

homeostasis (Brownlee and Taylor, 2005; Suffrian *et al.*, 2011). The use of HCO_3^- as the source of inorganic carbon for calcification (Sikes *et al.*, 1980; Nimer *et al.*, 1997; Buiteenhuis *et al.*, 1999; Herfort *et al.*, 2002) produces 1 mol H^+ for each mol of calcite, which have to be removed from the cytosol or rapidly buffered. Coccolithophores possess a PM localized voltage-gated H^+ channel that plays an important role in regulating intracellular pH (Taylor, *et al.*, 2011). The *HVCN1* gene encoding the voltage-gated H^+ channel was not transcriptionally regulated by calcification, suggesting that it may serve a general role related to H^+ transport in haploid and diploid cells. Ion channels have a very high capacity relative to other ion transport mechanisms and their activity can be effectively regulated at the level of channel gating without the requirement for transcriptional regulation.

In contrast, *ATPVc/c'* encoding the *c/c'* subunit of the vacuolar H^+ -ATPase (V-ATPase) was consistently upregulated between 1.5- and 2-fold in all of the calcifying scenarios. V-ATPases are localized to both endosomal membranes and the PM and generate H^+ gradients and membrane voltage, which drive numerous ion and other transport processes (Beyenbach and Wiczkorek, 2006). A Ca^{2+} stimulated V-ATPase activity was identified in the CV containing fraction of *P. carterae* (Araki and González, 1998) and the *c* subunit was cloned and immuno-localized to the coccolith producing fraction (Corstjens *et al.*, 2001). Our results implicate V-ATPase activity in calcification in *E. huxleyi*, supporting this earlier work in *P. carterae*.

Biom mineralization

The gene expression of the coccolith-associated Ca^{2+} -binding protein GPA showed an unexpected trend. *GPA* gene transcripts were approximately twice as abundant in haploid than diploid cells, suggesting a role for GPA in the absence of calcification. von Dassow and colleagues (2009) confirmed the presence of haploid expression of *GPA* in RCC1217 via non-quantitative RT-PCR and Richier and colleagues (2009) found *GPA* expression to be relatively stable between the diploid RCC1216 and haploid RCC1217 strains. The discrepancy between our *GPA* expression data and the data presented in Richier and colleagues (2009) may relate to important differences in the normalization procedures used for gene expression, with Richier and colleagues (2009) normalizing to total RNA rather than ERGs. Remarkably, *GPA* transcripts were strongly repressed in calcifying diploid cells with a ~26-fold downregulation relative to non-calcifying diploid cells and a ~10.8 downregulation relative to cells in 0 mM Ca^{2+} . GPA was initially isolated from coccoliths and has been shown to have strong Ca^{2+} binding properties possibly related to the presence of 2 EF hand-like domains (Corstjens *et al.*, 1998). There

is also a link between gene sequence and coccolith morphology among different *E. huxleyi* morphotypes, with a genetic marker termed the coccolith morphology motif within the 3' untranslated region (3' UTR) of GPA that distinguishes between A and B morphotypes (Schroeder *et al.*, 2005). The association of GPA with coccoliths (Corstjens *et al.*, 1998) suggests a close relationship with calcification but the strong downregulation of GPA when the cell is calcifying is counter-intuitive. Three possible explanations for this downregulation need to be investigated further: (i) High concentrations of GPA may act as an inhibitor of calcification. It is possible that at low levels GPA plays a role in calcite nucleation and determining coccolith geometry, but increased cellular concentrations of GPA may result in inhibition of calcite precipitation. This explanation would seem plausible for the RCC1216 vs. RCC1217 and CCMP1516 vs. CCMP1516NC comparisons but in the low Ca^{2+} treatment when the cell cannot calcify due to lack of substrate, an upregulation in a calcite inhibitor protein does not fit. (ii) GPA protein or *GPA* mRNA may play a role in gene regulation. A possible epigenetic role could be carried out by *GPA* transcripts or their protein products acting as regulating elements on calcification related genes. However, no conserved DNA binding motif is present in the GPA peptide. The presence of the coccolith morphology motif in the 3' UTR is intriguing indicating a potentially complex and mRNA related influence of GPA on coccolith morphology. (iii) There may be a translational block. *GPA* transcripts are not translated to protein resulting in accumulation of mRNA. Understanding this unexpected result is clearly very important in determining the regulation of calcification in coccolithophores.

A conceptual model

To stimulate further investigation, Fig. 6 provides a conceptual cellular model of calcification with possible routes for C_i , Ca^{2+} and H^+ transport and the possible location of transporters investigated in this study. The model undoubtedly simplifies the transport processes involved in calcification and has not taken into account the processes of calcite nucleation and crystallization and coccolith transport involving membrane cycling. Assuming AEL1 can act as a HCO_3^- transporter, it could play a role in the uptake of C_i for calcification across the PM using either Na^+ cotransport and/or Cl^- exchange to drive HCO_3^- uptake. Alternatively, AEL1 could function intracellularly, facilitating HCO_3^- uptake into the CV. The action of CAs, such as γ -EhCA2, may aid in maintaining HCO_3^- concentrations within the cytosol and generating gradients across membranes, although the localization of the individual CA isoforms in *E. huxleyi* remain unknown. The close apposition of the peripheral ER to the PM in

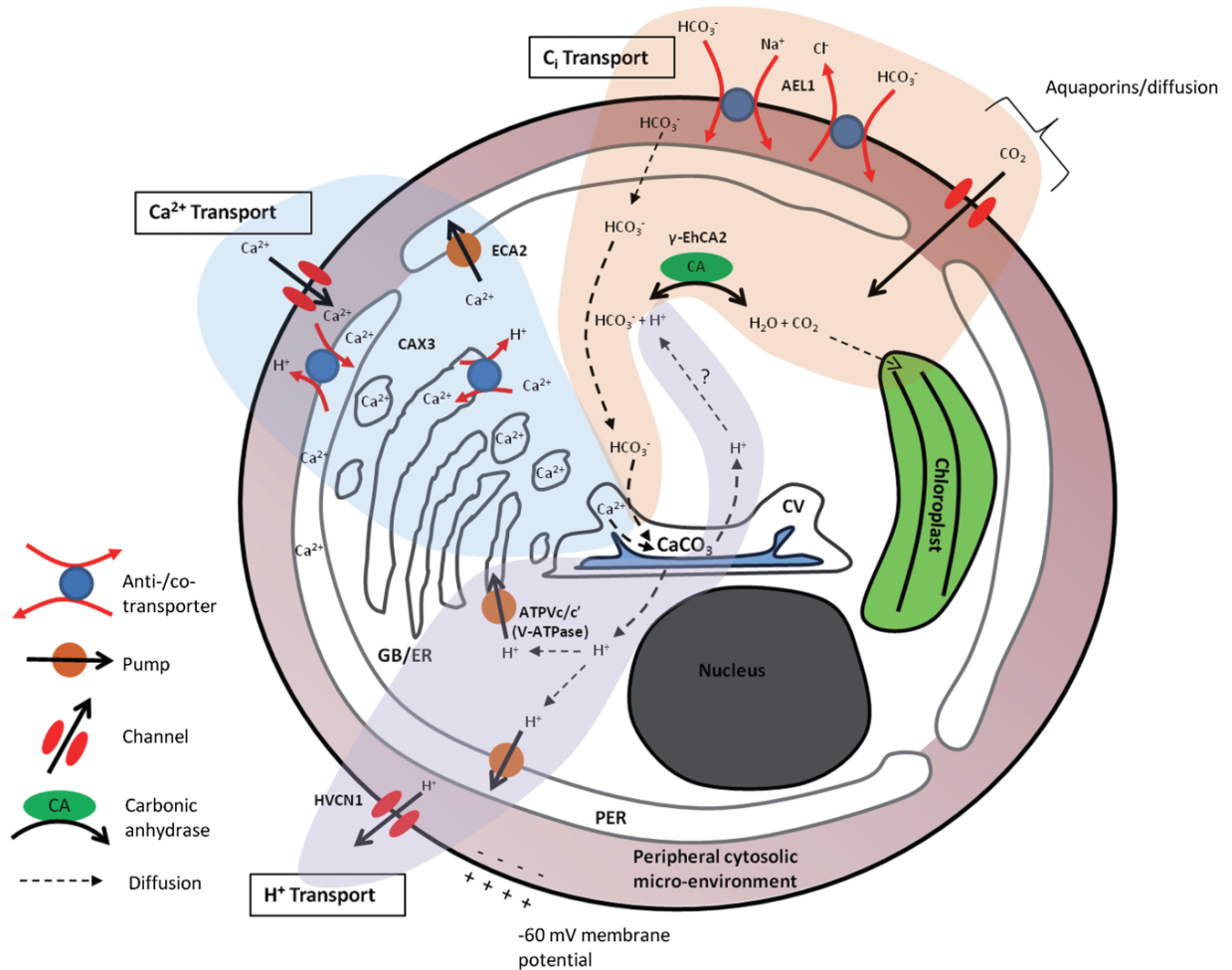


Fig. 6. A conceptual model of Ci , Ca^{2+} and H^+ transport related to calcification in coccolithophores based on transcriptomic evidence presented in this study. CV, GB/ER Golgi body/endoplasmic reticulum endomembrane network and PER-peripheral endoplasmic reticulum. See text for further details.

E. huxleyi suggests this endomembrane system may play an important role in ion transport processes. Ca^{2+} entry via PM channels would generate a micro-localized Ca^{2+} elevation between the PM and peripheral ER, facilitating Ca^{2+} uptake into the endomembrane network via Ca^{2+} exchangers. CAX3, which is specifically expressed in diploid cells, may therefore play a role in this process, presumably exchanging Ca^{2+} for H^+ . This would require a H^+ gradient across the peripheral ER relative to the cytosol, most probably generated by a V-type ATPase, such as ATPVc/c'. The action of Ca^{2+} -ATPases could also aid Ca^{2+} uptake into the peripheral ER, although the expression pattern of ECA2 suggests it most probably contributes more generally to Ca^{2+} homeostasis. From the peripheral ER, Ca^{2+} could then be transported into the maturing CV, avoiding transport across the cytosol. Within the CV and associated endomembrane network,

CaCO_3 formation from Ca^{2+} and HCO_3^- , possibly via an amorphous pre-cursor (Mackinder *et al.*, 2010), would generate H^+ . To maintain suitable conditions for calcite precipitation, H^+ must be removed from the CV, presumably into the cytosol, where excess H^+ may be released via the action of the PM localized voltage gated H^+ channel (Hv1) or may be pumped into endomembrane compartments (i.e. via an V-ATPase) to regulate cytosolic pH. Calcite nucleation and crystal growth is thought to be primarily controlled via organic molecules such as polysaccharides (de Jong *et al.*, 1976; Marsh *et al.*, 1992) and proteins (such as GPA) as well as through substrate supply and H^+ removal. Our data suggest an important role for GPA in regulating the calcification process. Elucidation of this function should provide much needed insight into the cellular mechanisms of calcification in coccolithophores.

3262 L. Mackinder et al.

Experimental procedures

Culturing

Four previously isolated clonal strains of *E. huxleyi* (CCMP1516, CCMP1516NC, RCC1216, RCC1217) were batch cultured. CCMP1516 and RCC1216 were isolated separately from the South Pacific as calcifying diploid strains. RCC1217 was subsequently isolated from RCC1216 as a naturally occurring non-calcifying haploid. Both of these strains were obtained from the Roscoff Culture Collection (RCC; Roscoff, France). The CCMP1516 strain maintained at the Centre for the Culture of Marine Phytoplankton (CCMP; Bigelow, ME) has lost the ability to calcify and is referred to in this manuscript as CCMP1516NC. However, before CCMP1516 lost the ability to calcify a subculture was sent to the Plymouth Culture Collection (PCC; Plymouth, UK) where it is identified as strain M217. The culture maintained at the PCC has retained the ability to calcify and is referred to in this manuscript as CCMP1516. All strains were cultured in sterile filtered artificial seawater containing vitamins and metals at 1/4 concentration (Guillard, 1975), 88 $\mu\text{mol kg}^{-1}$ nitrate and 5.2 $\mu\text{mol kg}^{-1}$ phosphate and 10 nmol kg^{-1} selenium and 2 ml of sterile North Sea natural sea water kg^{-1} . CO_2 fugacity ($f\text{CO}_2$) was set to 400 ppm by the addition of Na_2CO_3 and removing excess alkalinity using certified HCl to give a total alkalinity of $\sim 2325 \mu\text{mol kg}^{-1}$. Cells were grown at 15°C under a 12:12 h light:dark cycle at photon flux density 150 $\mu\text{mol m}^{-2} \text{s}^{-1}$. Culture concentration was determined as the mean of three measurements obtained with a Z series Beckman Coulter counter. Growth rates (μ) were calculated as

$$\mu = \frac{\ln C_1 - \ln C_0}{t_1 - t_0}$$

where C_1 and C_0 are concentrations at time (in days) of t_1 and t_0 respectively. Gene expression was further investigated in CCMP1516 cultured in 0, 10, 35 and 60 mM Ca^{2+} .

Sampling

Pre-cultures maintained in their exponential growth phase (for > 10 generations) were inoculated in triplicate in fresh media to give a starting cell concentration of 1×10^3 or $5 \times 10^3 \text{ cells ml}^{-1}$. Cell concentration was monitored until sampling at $1\text{--}2 \times 10^5 \text{ cells ml}^{-1}$. All sampling and cell counts were conducted within a 3 h time period between hours 5 and 8 of the light phase to minimize temporal variations.

TPC/POC/PIC

Duplicate samples for total particulate carbon (TPC, 100 ml) and particulate organic carbon (POC, 200 ml) were filtered onto pre-combusted (450°C, 6 h) GF/F filters and frozen at -20°C until analysis. POC filters were fumed in a desiccator with 37% HCl for 2–2.5 h to remove all inorganic carbon before the drying of filters (POC and TPC) for 15 h at 60°C. All filters were measured on a Euro EA Elemental Analyser (Ehrhardt and Koeve, 1999). Particular inorganic carbon (PIC) was determined by the difference between TPC and

POC. POC and PIC production rates were calculated by multiplying growth rate (μ) with POC and PIC cellular content respectively.

SEM

Approximately 2.5×10^5 cells of each strain were gently filtered onto polycarbonate filters (0.2 μm), dried for 1 h at 60°C and sputter-coated with gold-palladium. SEM images were obtained with a CamScan-CS-44 SEM.

Microsatellite data

To test for strain identity five primer pairs designed to microsatellite loci (EHMS37, P01F08, P02B12, P02F11, P02E09 (Iglesias-Rodríguez *et al.*, 2002; 2006) were ran on genomic DNA (gDNA) extracted from the four strains under study. Approximately 5×10^6 cells were filtered onto 0.45 μm cellulose acetate filters. gDNA was extracted using an Invisorb DNA extraction kit (Invitek). Briefly, 400 μl of lysis buffer and 40 μl of proteinase K were added to the filter in a 1.5 ml centrifuge tube, vortexed for 20 s followed by a 10 min water bath sonification at 52°C, then shaking (950 r.p.m.) for 50 min at 52°C. The filter was removed and discarded, DNA was bound to the columns as in the supplied protocol and eluted in 100 μl of elution buffer. DNA concentration was determined using a NanoDrop spectrophotometer. The above forward primers end-labelled with fluorescent phosphoramidite dyes (HEX or 6-FAM) were used to amplify (30 cycles) 2 ng of gDNA using pro Taq DNA polymerase (Promega). One microlitre of PCR sample was analysed on an AB3130 MSAT Genetic Analyser. Microsatellite electropherogram data were scored using the software GeneMarker (Soft Genetics, State College, PA, USA).

qRT-PCR

RNA extraction and reverse transcription. 100 ml of culture was filtered onto 0.8 μm polycarbonate filters, immediately washed off with 1 ml of RNeasy (QIAGEN) and kept on ice until frozen at -20°C . RNA was extracted using the RNeasy mini kit (QIAGEN) as follows: the supernatant was directly removed if the cells had settled out during storage (due to the density of RNeasy some cells settled out at -20°C), if this was not the case cells were centrifuged (10 000 r.p.m., 3 min) and the supernatant removed. After the removal of supernatant lysis buffer containing β -mercaptoethanol was added as in the protocol, cell lysis was achieved by a 30 s vortex, 3 min bath sonification, 30 s vortex all at room temperature. RNA was bound to columns and eluted in 40 μl of RNase free H_2O as in the provided protocol and frozen at -80°C . RNA concentration, quality and integrity was analysed on a Bio-Rad Experion. All samples had a RNA quality indicator (RQI) > 7 (except sample TQ26 1N biological replicate 2, RQI 4.5). 625 ng of RNA per sample was DNase treated then reverse-transcribed using a Quantitect kit (QIAGEN) primed with a mixture of oligo-dT and random primers. Samples for no reverse transcription control (NRTC) were removed post DNase treatment but before the RT step. The resulting cDNA and NRTCs were stored at -20°C and -80°C respectively.

Primer design. Primers were designed using Primer3Plus software (<http://www.bioinformatics.nl/cgi-bin/primer3plus/primer3plus.cgi>). Primers to the genes *EFG1*, *PK*, *CAX3*, *CAX4*, *AEL1* and *ATPVC/c'* were designed to EST clusters from von Dassow and colleagues (2009), while primers to *ECA2*, γ -*EhCA2* and *GPA* were designed to EST or complete gene sequences deposited in GenBank (Table 1). Primers to *HVCN1* correspond to sequence data (JGI protein ID 631975) provided with permission from the *E. huxleyi* Genome Project (<http://genome.jgi-psf.org/Emihu1/Emihu1.home.html>). The primers to the multi-copy gene Actin amplify identical amplicons from six different gene copies (Bhattacharya *et al.*, 1993). For clarity, gene names have been used, which correspond to the annotation in the *E. huxleyi* Genome, although these were not available for all genes (Table 1). Primers were tested on gDNA and cDNA and products ran on 1.5% agarose gel to check for single amplicons and primer dimers.

Efficiency curves. Equal amounts of cDNA from all samples were pooled and serially diluted to generate efficiency curves from five or more cDNA concentrations. All efficiency curves had a R^2 greater than 0.99 and efficiencies between 90–105%.

ERG analysis. To test for the most stable ERGs equal amounts of cDNA (2 ng of reverse transcribed RNA) were analysed with the primers for three ERGs (Actin, *EFG1* and pyruvate kinase). Threshold cycle (C_t) values were plotted per sample to show expression variation between samples. ERG stability was also tested using the program geNorm, which generates a gene expression stability value and allows ranking of genes according to their expression stability (Vandesompele *et al.*, 2002).

qPCR chemistry. 20 μ l reaction volumes were set up consisting of 10 μ l 2 \times Fast SYBR Green Master Mix (Applied Biosystems), 0.4 μ l forward and reverse primers (10 pmol μ l⁻¹), 4 μ l of sample (cDNA 2 ng of reverse transcribed RNA), NRTC (2 ng of RNA) or no template control (NTC) and 5.2 μ l of HPLC grade H₂O. All samples were ran in technical triplicates with NRTCs ran for each sample and primer pair on every plate and NTCs for each primer pair per plate. Samples were ran using the fast cycling program on an Applied Biosystems Step One Plus qPCR machine.

qRT-PCR data analysis. Before data analysis checks were carried out on the raw qPCR data. The baseline was checked and adjusted if necessary, the C_t threshold was adjusted to 0.2 and checked to ensure the crossing point was in the log phase. The standard deviations of triplicates were checked and if > 0.3 outliers were removed. Sample C_t 's were checked and in all cases were at least five C_t 's lower than the NRTC and NTC and fell within the range covered by the efficiency plots. Melt curves were checked to ensure there was no non-specific priming in samples and specific priming in NTCs.

qRT-PCR data were analysed using an efficiency corrected $\Delta\Delta C_t$ method, normalizing to the geometric mean of two ERGs (Vandesompele *et al.*, 2002). *P*-values were obtained using a pairwise fixed reallocation randomization test using

the relative expression software tool (REST) (Pfaffl *et al.*, 2002).

Phylogenetic analysis

Amino acid sequences of characterized and uncharacterized proteins belonging to the Ca²⁺/cation antiporter (CaCA) superfamily and SoLute Carrier 4 (SLC4) family respectively were aligned using ClustalW multiple sequence alignment software. Alignments were manually checked to ensure only unambiguous residues were compared. For CaCA proteins, a truncated alignment of amino acids comprising of the conserved $\alpha 1$ and $\alpha 2$ domains was used for tree construction. An alignment of amino acids encompassing the transmembrane domains was used for SLC4 phylogenetic analysis. Minimum evolution phylogenetic analysis was conducted using MEGA version 4 (Tamura *et al.*, 2007).

Acknowledgements

Thank you to Thorsten Reusch for access to laboratory facilities in Kiel, Kai Lohbeck for advice with the microsatellite work and Lennart Bach for help with *E. huxleyi* culturing and sampling. We thank Betsy Read (California State University, San Marcos, CA, USA) and co-workers at the Joint Genome Institute for access to the draft *E. huxleyi* genome. The work was funded by CalMarO a FP7 Marie Curie Initial training network, the UK NERC Oceans 2025 Strategic Research Programme and the European Project on Ocean Acidification (EPOCA: EC 211384).

References

- Alper, S.L. (2006) Molecular physiology of SLC4 anion exchangers. *Exp Physiol* **91**: 153–161.
- Araki, Y., and González, E.L. (1998) V- and P-type Ca²⁺ stimulated ATPases in a calcifying strain of *Pleurochrysis* Sp. (Haptophyceae). *J Phycol* **34**: 79–88.
- Beyenbach, K.W., and Wiczorek, H. (2006) The V-type H⁺ ATPase: molecular structure and function, physiological roles and regulation. *J Exp Biol* **209**: 577–589.
- Bhattacharya, D., Stickel, S.K., and Sogin, M.L. (1993) Isolation and molecular phylogenetic analysis of actin-coding regions from *Emiliana huxleyi*, a Prymnesiophyte alga, by reverse transcriptase and PCR methods. *Mol Biol Evol* **10**: 689–703.
- Brownlee, C., and Taylor, A.R. (2005) Calcification in coccolithophores: a cellular perspective. In *Coccolithophores: From Molecular Processes to Global Impact*. Thierstein, H., and Young, J. (eds). Berlin: Springer, pp. 31–50.
- Buitenhuis, E., de Baar, H., and Veldhuis, M. (1999) Photosynthesis and calcification by *Emiliana huxleyi* (Prymnesiophyceae) as a function of inorganic carbon species. *J Phycol* **35**: 949–959.
- Cai, X., and Lytton, J. (2004) The Cation/Ca²⁺ Exchanger Superfamily: Phylogenetic Analysis and Structural Implications. *Mol Biol Evol* **21**: 1692–1703.
- Cheng, N.-H., Pittman, J.K., Zhu, J.-K., and Hirschi, K.D. (2004a) The Protein Kinase SOS2 Activates the Arabidopsis H⁺/Ca²⁺ Antiporter CAX1 to Integrate Calcium Transport and Salt Tolerance. *J Biol Chem* **279**: 2922–2926.

3264 L. Mackinder et al.

- Cheng, N.H., Liu, J.Z., Nelson, R.S., and Hirschi, K.D. (2004b) Characterization of CXIP4, a novel Arabidopsis protein that activates the H⁺/Ca²⁺ antiporter, CAX1. *FEBS Lett* **559**: 99–106.
- Corstjens, P., van der Kooij, A., Linschooten, C., Brouwers, G.J., Westbroek, P., and de Vrind-de Jong, E.W. (1998) GPA, a calcium-binding protein in the coccolithophorid *Emiliania huxleyi* (Prymnesiophyceae). *J Phycol* **34**: 622–630.
- Corstjens, P.L.A.M., Araki, Y., and González, E.L. (2001) A coccolithophorid calcifying vesicle with a vacuolar-type ATPase proton pump: cloning and immunolocalisation of the V₀ subunit c'. *J Phycol* **37**: 71–78.
- von Dassow, P., Ogata, H., Probert, I., Wincker, P., Da Silva, C., Audic, S., et al. (2009) Transcriptome analysis of functional differentiation between haploid and diploid cells of *Emiliania huxleyi*, a globally significant photosynthetic calcifying cell. *Genome Biol* **10**: R114.
- Edmond, C., Shigaki, T., Ewert, S., Nelson, M.D., Connorton, J.M., Chalova, V., et al. (2009) Comparative analysis of CAX2-like cation transporters indicates functional and regulatory diversity. *Biochem J* **418**: 145–154.
- Ehrhardt, M., and Koeve, W. (1999) Determination of particulate organic carbon and nitrogen. In *Methods of Seawater Analysis*. Grasshoff, K., Kremling, K., and Ehrhardt, M. (eds). Weinheim: Wiley, pp. 437–444.
- Fernandez, E., Boyd, P., Holligan, P.M., and Harbour, D.S. (1993) Production of organic and inorganic carbon within a large-scale coccolithophore bloom in the northeast Atlantic-ocean. *Mar Ecol Prog Ser* **97**: 271–285.
- Ferrol, N., and Bennett, A.B. (1996) A Single Gene May Encode Differentially Localized Ca²⁺-ATPases in Tomato. *Plant Cell* **8**: 1159–1169.
- Guillard, R. (1975) Culture of phytoplankton for feeding marine invertebrates. In *Culture of Marine Invertebrates*. Smith, W., and Chanley, M. (eds). New York: Plenum, pp. 26–60.
- Herfort, L., Thake, B., and Roberts, J. (2002) Acquisition and use of bicarbonate by *Emiliania huxleyi*. *New Phytol* **156**: 427–436.
- Herfort, L., Loste, E., Meldrum, F., and Thake, B. (2004) Structural and physiological effects of calcium and magnesium in *Emiliania huxleyi* (Lohmann) Hay and Mohler. *J Struct Biol* **148**: 307–314.
- Hirschi, K.D., Zhen, R.G., Cunningham, K.W., Rea, P.A., and Fink, G.R. (1996) CAX1, an H⁺/Ca²⁺ antiporter from Arabidopsis. *PNAS* **93**: 8782–8786.
- Holligan, P.M., Viollier, M., Harbour, D.S., Camus, P., and Champagnephilippe, M. (1983) Satellite and ship studies of coccolithophore production along a continental-shelf edge. *Nature* **304**: 339–342.
- Holligan, P.M., Fernandez, E., Aiken, J., Balch, W.M., Boyd, P., Burkill, P.H., et al. (1993) A biogeochemical study of the coccolithophore, *Emiliania huxleyi*, in the North-Atlantic. *Global Biogeochem Cycles* **7**: 879–900.
- Iglesias-Rodríguez, M.D., Alberto, G.S., René, G., Keith, J.E., Jacqueline, B., Linda, K.M., and Paul, K.H. (2002) Polymorphic microsatellite loci in global populations of the marine coccolithophorid *Emiliania huxleyi*. *Mol Ecol Notes* **2**: 495–497.
- Iglesias-Rodríguez, D.M., Schofield, O.M., Batley, J., Medlin, L.K., and Hayes, P.K. (2006) Intraspecific genetic diversity in the marine coccolithophore *Emiliania huxleyi* (Prymnesiophyceae): the use of microsatellite analysis in marine phytoplankton population studies. *J Phycol* **42**: 526–536.
- de Jong, E.W., Bosch, L., and Westbroek, P. (1976) Isolation and characterization of a Ca²⁺-binding polysaccharide associated with coccoliths of *Emiliania huxleyi* (Lohmann) Kamptner. *Eur J Biochem* **70**: 611–621.
- Kamiya, T., and Maeshima, M. (2004) Residues in Internal Repeats of the Rice Cation/H⁺ Exchanger Are Involved in the Transport and Selection of Cations. *J Biol Chem* **279**: 812–819.
- Kamiya, T., Akahori, T., and Maeshima, M. (2005) Expression Profile of the Genes for Rice Cation/H⁺ Exchanger Family and Functional Analysis in Yeast. *Plant Cell Physiol* **46**: 1735–1740.
- Leonardos, N., Read, B., Thake, B., and Young, J.R. (2009) No mechanistic dependence of photosynthesis on calcification in the coccolithophorid *Emiliania huxleyi* (Haptophyta). *J Phycol* **45**: 1046–1051.
- Liu, H., Zhang, X., Takano, T., and Liu, S. (2009) Characterization of a PutCAX1 gene from *Puccinellia tenuiflora* that confers Ca²⁺ and Ba²⁺ tolerance in yeast. *Biochem Biophys Res Commun* **383**: 392–396.
- Mackinder, L., Wheeler, G., Schroeder, D., Riebesell, U., and Brownlee, C. (2010) Molecular Mechanisms Underlying Calcification in Coccolithophores. *Geomicrobiol J* **27**: 585–595.
- Marsh, M.E., Chang, D.K., and King, G.C. (1992) Isolation and characterization of a novel acidic polysaccharide containing tartrate and glyoxylate residues from the mineralized scales of a unicellular coccolithophorid alga *Pleurochrysis carterae*. *J Biol Chem* **267**: 20507–20512.
- Milliman, J.D. (1993) Production and Accumulation of Calcium Carbonate in the Ocean: Budget of a Nonsteady State. *Global Biogeochem Cycles* **7**: 927–957.
- Nimer, N.A., Merrett, M.J., and Brownlee, C. (1996) Inorganic carbon transport in relation to culture age and inorganic carbon concentration in a high-calcifying strain of *Emiliania huxleyi* (Prymnesiophyceae). *J Phycol* **32**: 813–818.
- Nimer, N.A., IglesiasRodríguez, M.D., and Merrett, M.J. (1997) Bicarbonate utilization by marine phytoplankton species. *J Phycol* **33**: 625–631.
- Paasche, E. (1962) Coccolith Formation. *Nature* **193**: 1094–1095.
- Park, M., Li, Q., Shcheynikov, N., Zeng, W., and Muallem, S. (2004) NaBC1 Is a Ubiquitous Electrogenic Na⁺-Coupled Borate Transporter Essential for Cellular Boron Homeostasis and Cell Growth and Proliferation. *Mol Cell* **16**: 331–341.
- Pfaffl, M.W., Horgan, G.W., and Dempfle, L. (2002) Relative expression software tool (REST[©]) for group-wise comparison and statistical analysis of relative expression results in real-time PCR. *Nucl Acids Res* **30**: e36.
- Piermarini, P.M., Choi, I., and Boron, W.F. (2007) Cloning and characterization of an electrogenic Na/HCO₃⁻ cotransporter from the squid giant fiber lobe. *AJP – Cell Physiology* **292**: C2032–2045.
- Pittman, J.K., and Hirschi, K.D. (2001) Regulation of CAX1, an Arabidopsis Ca²⁺/H⁺ Antiporter. Identification of an N-Terminal Autoinhibitory Domain. *Plant Physiol* **127**: 1020–1029.

- Pittman, J.K., Edmond, C., Sunderland, P.A., and Bray, C.M. (2009) A Cation-regulated and Proton Gradient-dependent Cation Transporter from *Chlamydomonas reinhardtii* Has a Role in Calcium and Sodium Homeostasis. *J Biol Chem* **284**: 525–533.
- Pushkin, A., and Kurtz, I. (2006) SLC4 base (HCO_3^- , CO_3^{2-}) transporters: classification, function, structure, genetic diseases, and knockout models. *Am J Physiol Renal Physiol* **290**: F580–F599.
- Richier, S., Kerros, M.-E., de Vargas, C., Haramaty, L., Falkowski, P.G., and Gattuso, J.-P. (2009) Light-Dependent Transcriptional Regulation of Genes of Biogeochemical Interest in the Diploid and Haploid Life Cycle Stages of *Emiliana huxleyi*. *Appl Environ Microbiol* **75**: 3366–3369.
- Richier, S., Fiorini, S., Kerros, M.-E., von Dassow, P., and Gattuso, J.-P. (2010) Response of the calcifying coccolithophore *Emiliana huxleyi* to low pH/high pCO₂: from physiology to molecular level. *Marine Biology* **158**: 551–560.
- Rost, B., Riebesell, U., Burkhardt, S., and Sültemeyer, D. (2003) Carbon Acquisition of Bloom-Forming Marine Phytoplankton. *Limnol Oceanogr* **48**: 55–67.
- Sanders, D., Pelloux, J., Brownlee, C., and Harper, J.F. (2002) Calcium at the crossroads of signaling. *Plant Cell* **14**: 401–417.
- Schroeder, D.C., Biggi, G.F., Hall, M., Davy, J., Martínez, J., Richardson, A.J., et al. (2005) A genetic marker to separate *Emiliana huxleyi* (Prymnesiophyceae) morphotypes. *J Phycol* **41**: 874–879.
- Sekino, K., and Shiraiwa, Y. (1994) Accumulation and utilization of dissolved inorganic carbon by a marine unicellular coccolithophorid, *Emiliana huxleyi*. *Plant Cell Physiol* **35**: 353–361.
- Shigaki, T., and Hirschi, K.D. (2006) Diverse functions and molecular properties emerging for CAX cation/H⁺ exchangers in plants. *Plant Biology* **8**: 419–429.
- Shigaki, T., Rees, I., Nakhleh, L., and Hirschi, K.D. (2006) Identification of Three Distinct Phylogenetic Groups of CAX Cation/Proton Antiporters. *J Mol Evol* **63**: 815–825.
- Shmukler, B.E., Kurschat, C.E., Ackermann, G.E., Jiang, L., Zhou, Y., Barut, B., et al. (2005) Zebrafish slc4a2/ae2 anion exchanger: cDNA cloning, mapping, functional characterization, and localization. *Am J Physiol Renal Physiol* **289**: F835–F849.
- Sikes, C.S., Roer, R.D., and Wilbur, K.M. (1980) Photosynthesis and coccolith formation – inorganic carbon-sources and net inorganic reaction of deposition. *Limnol Oceanogr* **25**: 248–261.
- Soto, A.R., Zheng, H., Shoemaker, D., Rodriguez, J., Read, B.A., and Wahlund, T.M. (2006) Identification and preliminary characterization of two cDNAs encoding unique carbonic anhydrases from the marine alga *Emiliana huxleyi*. *Appl Environ Microbiol* **72**: 5500–5511.
- Suffrian, K., Schulz, K.G., Gutowska, M.A., Riebesell, U., and Bleich, M. (2011) Cellular pH measurements in *Emiliana huxleyi* reveal pronounced membrane proton permeability. *New Phytol* **190**: 595–608.
- Sze, H., Li, X., and Palmgren, M.G. (1999) Energization of Plant Cell Membranes by H⁺-Pumping ATPases: Regulation and Biosynthesis. *Plant Cell* **11**: 677–690.
- Takano, J., Noguchi, K., Yasumori, M., Kobayashi, M., Gajdos, Z., Miwa, K., et al. (2002) Arabidopsis boron transporter for xylem loading. *Nature* **420**: 337–340.
- Tamura, K., Dudley, J., Nei, M., and Kumar, S. (2007) MEGA4: Molecular Evolutionary Genetics Analysis (MEGA) software version 4.0. *Mol Biol Evol* **24**: 1596–1599.
- Taylor, A.R., and Brownlee, C. (2003) A Novel Cl⁻ Inward-Rectifying Current in the Plasma Membrane of the Calcifying Marine Phytoplankton *Coccolithus pelagicus*. *Plant Physiol* **131**: 1391–1400.
- Taylor, A.R., Chrachri, A., Wheeler, G., Goddard, H., and Brownlee, C. (2011) A Voltage-Gated H⁺ Channel Underlying pH Homeostasis in Calcifying Coccolithophores. *PLoS Biol* **9**: e1001085.
- Taylor, A.R., Russell, M.A., Harper, G.M., Collins, T.T., and Brownlee, C. (2007) Dynamics of formation and secretion of heterococcoliths by *Coccolithus pelagicus* ssp. *Braarudii*. *Eur J Phycol* **42**: 125–136.
- Trimborn, S., Langer, G., and Rost, B. (2007) Effect of varying calcium concentrations and light intensities on calcification and photosynthesis in *Emiliana huxleyi*. *Limnol Oceanogr* **52**: 2285–2293.
- Vandesompele, J., De Preter, K., Pattyn, F., Poppe, B., Van Roy, N., De Paepe, A., and Speleman, F. (2002) Accurate normalization of real-time quantitative RT-PCR data by geometric averaging of multiple internal control genes. *Genome Biol* **3**: research0034.0031–0034.0011.
- Waditee, R., Hibino, T., Tanaka, Y., Nakamura, T., Incharoen-sakdi, A., and Takabe, T. (2001) Halotolerant Cyanobacterium *Aphanothece halophytica* Contains an Na⁺/H⁺ Antiporter, Homologous to Eukaryotic Ones, with Novel Ion Specificity Affected by C-terminal Tail. *J Biol Chem* **276**: 36931–36938.
- van der Wal, P., de Jong, E.W., Westbroek, P., de Bruijn, W.C., and Mulderstapel, A.A. (1983) Ultrastructural polysaccharide localization in calcifying and naked cells of the coccolithophorid *Emiliana huxleyi*. *Protoplasma* **118**: 157–168.
- White, P.J., and Broadley, M.R. (2003) Calcium in Plants. *Ann Botany* **92**: 487–511.

CHAPTER 4. Calcification and photosynthesis in *Emiliana huxleyi*: Physiological and genetic responses to individual carbonate system parameters

Lennart T. Bach⁺, Luke C. M. Mackinder^{+*}, Kai G. Schulz, Glen Wheeler, Declan C. Schroeder, Colin Brownlee, Ulf Riebesell

+ These authors contributed equally to the paper.

*Corresponding author: Luke C. M. Mackinder, lukcki@mba.ac.uk

Helmholtz-Zentrum für Ozeanforschung Kiel (GEOMAR), D-24105, Kiel, Germany (L.T.B., L.C.M.M., K.G.S., U.R.); Marine Biological Association of the UK, The Laboratory, Citadel Hill, Plymouth PL1 2PB, UK (L.C.M.M., G.W., D.C.S., C.B.); Plymouth Marine Laboratory, Prospect Place, Plymouth, PL1 3DH, UK (G.W.).

To be submitted to *Plant Physiology*

ABSTRACT

The uptake of anthropogenic carbon dioxide (CO_2) into the oceans leads to a concomitant increase in bicarbonate (HCO_3^-) and proton (H^+) concentrations and a decrease in carbonate (CO_3^{2-}) concentration. The combined effect of these changes on coccolithophores (marine calcifying phytoplankton) has been well documented but our knowledge on their individual influence on molecular, physiological and regulatory processes is still limited. This study aims to identify the influence of the individual carbonate system components on growth, organic carbon fixation, calcification and gene expression in *Emiliana huxleyi* - a key coccolithophore species. We found that calcification rates relied on HCO_3^- as the principal substrate, while growth and organic carbon fixation rates were primarily influenced by $[\text{CO}_2]$ and $[\text{H}^+]$. As external inorganic carbon decreased, calcification rates started to decrease prior to organic carbon fixation rates. This indicates that calcification does not function as a carbon concentrating mechanism (CCM) under inorganic carbon limitation, but may decline to allow the redistribution of inorganic carbon from calcification to photosynthesis. The transcription of a putative HCO_3^- transporter, four putative H^+ transporters, and three carbonic anhydrases remained largely unaffected at high inorganic carbon concentrations but were up-regulated at low $[\text{HCO}_3^-]$ and $[\text{CO}_2]$. This transcriptional profile supports the presence of a CCM in *E. huxleyi* and provides the genetic basis of a CCM in a haptophyte algae. The data presented here helps to understand the influence of changing carbonate chemistry on *E. huxleyi* at a cellular and molecular level. This is essential to comprehend how this species will respond in a changing ocean.

INTRODUCTION

Marine photoautotrophic organisms fix about 55 gigatons of carbon per year which is equal to the photosynthetic production by the terrestrial biosphere (Field et al., 1998). Coccolithophores represent an important group within marine photoautotrophs, comprising in the order of 10% of global phytoplankton biomass (Tyrrell and Young, 2009). Their unique feature is the ability to produce small scales (coccoliths) made of calcium carbonate (CaCO_3), which are formed intracellularly and subsequently exocytosed to cover the organic cellular surface. The formation of coccoliths (calcification) is of high importance in the global carbon cycle because of the accelerating effect of CaCO_3 on organic matter sinking velocities into the deep ocean (Thierstein et al., 1977). The globally most abundant coccolithophore species is *Emiliana huxleyi* playing a dominant role in carbon cycling by having the ability to form blooms up to a million square kilometres (Tyrrell and Young, 2009). *E. huxleyi* evolved from *Gephyrocapsa oceanica* about 270,000 years ago and has dominated the marine coccolithophore community for approximately the last 70,000 years (reviewed in; Paasche, 2002). Despite the global significance of *E. huxleyi*, there is only a limited understanding of important cellular processes and their response to environmental change.

Under present day conditions, marine phytoplankton growth is mostly limited by low light availability or the insufficient supply of nutrients such as fixed nitrogen, phosphorus or iron (Sarmiento and Gruber, 2006) while carbon dioxide (CO_2) is usually not considered to be limiting. Nevertheless, CO_2 diffusion rates are in most cases not high enough to account for the photosynthetic rates seen in the majority of phytoplankton (Falkowski and Raven, 2007). This discrepancy is explained by the action of carbon (or CO_2) concentrating mechanisms (CCMs), which can make use of the large bicarbonate (HCO_3^-) pool in seawater and enhance $[\text{CO}_2]$ at the active site of the CO_2 fixing enzyme Ribulose-1,5-bisphosphate Carboxylase Oxygenase (RubisCO) (Reinfelder, 2011). It is thought that nearly all marine phytoplankton operate a CCM, although the inorganic carbon species used (CO_2 and/or HCO_3^-), its regulation, cellular components and inorganic carbon affinity can vary significantly between species (Giordano et al., 2005). *E. huxleyi* was shown to possess a low affinity CCM, with a relatively high $[\text{CO}_2]$ half saturation ($K_{1/2}$) compared to other tested phytoplankton species (Rost et al., 2003), although it is able to regulate its CCM with a decreasing $K_{1/2}$ for cells cultured at low CO_2 (Rost et al., 2003). Several studies have focused on distinguishing the external inorganic carbon source for photosynthesis (Paasche, 1964; Sikes et al., 1980; Nimer and Merrett, 1992; Sekino and Shiraiwa, 1994; Rost et al., 2003; Schulz et al., 2007). All confirm that CO_2 is the primary source for photosynthesis under ambient CO_2 concentrations, although there are some

discrepancies over the importance of HCO_3^- especially at lower CO_2 concentrations and the ability of cells to accumulate inorganic carbon (Nimer and Merrett, 1992; Sekino and Shiraiwa, 1994). Some diatom species show features of a C_4 biochemical CCM. In *E. huxleyi* only a small proportion of carbon was shown to be fixed via a C_4 intermediate (Tsuji et al., 2009) indicating that the *E. huxleyi* CCM is primarily based on a C_3 biophysical mechanism. In addition to a biophysical mechanism, intra-cellular calcification has been proposed to act as a CCM by providing protons (H^+) as a by-product from calcification to support the dehydration of HCO_3^- to CO_2 (reviewed in; Paasche, 2002). Although there is considerable supporting data (Nimer and Merrett, 1992; Buitenhuis et al., 1999) other studies contradict the concept (Paasche, 1964; Herfort et al., 2004; Trimborn et al., 2007; Leonardos et al., 2009).

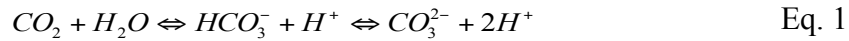
In the forthcoming centuries, on-going dissolution of increasing atmospheric CO_2 into the oceans will continuously change the surface marine carbonate chemistry - a process widely known as ocean acidification (Caldeira and Wickett, 2003). Chemically, ocean acidification leads to a strong decrease of the carbonate ion (CO_3^{2-}) concentration, a slight increase in $[\text{HCO}_3^-]$ and a strong increase in $[\text{CO}_2]$ and $[\text{H}^+]$ (Wolf-Gladrow et al., 1999). These components are thought to effect coccolithophores in varying ways with $[\text{CO}_3^{2-}]$ influencing calcite saturation levels, $[\text{H}^+]$ affecting cellular pH homeostasis, $[\text{CO}_2]$ affecting photosynthesis and $[\text{HCO}_3^-]$ influencing calcification (and photosynthesis). The potential effects of ocean acidification on calcification and photosynthesis by *E. huxleyi* have been repeatedly reported (reviewed in; Riebesell and Tortell, 2011) but the importance of changes in the individual carbonate parameters behind the observed responses is still incomplete. The present study aims to improve our conceptual understanding of the acquisition of inorganic carbon and its subsequent use in calcification and photosynthesis. In particular, we focus on the influence of the individual carbonate system parameters (e.g. CO_2 or H^+) on these metabolic processes in order to assess their potential relevance in a changing environment. Therefore we cultured *E. huxleyi* in a variety of carbonate chemistry conditions and combined measurements on calcification rates and carbon fixation rates with quantitative gene expression measurements.

Conceptual background of the experiments

At this point, it is important to explain the chemical concept of the applied experimental approach and the basic assumptions underlying our interpretations since this is critical for the understanding of this dataset.

The marine carbonate system is usually defined by the concentrations of CO_2 , HCO_3^- , CO_3^{2-} , H^+ , pCO_2 , total alkalinity (TA), dissolved inorganic carbon (DIC i.e. combined $[\text{CO}_2]$,

[HCO₃⁻] and [CO₃²⁻]), and pH (i.e. H⁺) (Zeebe and Wolf-Gladrow, 2001). Among these parameters, pCO₂, TA and DIC are physical or chemical concepts useful for the determination of the carbonate system in seawater but of no direct relevance for the cell physiology. The physiological relevant parameters of the carbonate system are [CO₂], [HCO₃⁻], [CO₃²⁻] and [H⁺] since only these can be perceived by the cell. They are connected to each other in the equilibrium reaction:



(Note that the formation of true carbonic acid is neglected in this equation because its concentration is more than two orders of magnitude lower than the concentration of aqueous CO₂ (Zeebe and Wolf-Gladrow, 2001). Since no other parameters of physiological relevance other than CO₂, HCO₃⁻, CO₃²⁻ and H⁺ were changed in the experiments (e.g. light or temperature), it is assumed that only the concentrations of these parameters can cause different physiological or genetic responses observed in between treatments. Unfortunately, CO₂, HCO₃⁻, CO₃²⁻ and H⁺ are closely connected to each other (Eq. 1) and any change in the concentration of one will according to Le Chatelier's Law lead to changes in the others. Nevertheless, it is possible to keep one of the four parameters constant between different treatments. For example, [H⁺] can be the same between two treatments but if [HCO₃⁻] is different, then [CO₂] and [CO₃²⁻] will be different as well. We made use of this feature and performed three experiments where we kept either [CO₂] or [H⁺] constant between treatments ([H⁺] was kept constant at two different levels). This allowed us to exclude the constant carbonate system parameter from being responsible for the observed physiological or genetic response (Buitenhuis et al., 1999). Note that we chose to focus on [CO₂] and [H⁺] since previous work points towards a major importance of these particular parameters in *E. huxleyi* (Schulz et al., 2007; Bach et al., 2011).

At a current ocean pH_{freescale} (pH_f) of ~8.15 the [DIC] is ~2105 μmol kg⁻¹ ([CO₂] ~15 μmol kg⁻¹, [HCO₃⁻] ~1910 μmol kg⁻¹ and [CO₃²⁻] ~180 μmol kg⁻¹). This has changed from pre-industrial times where pH_f was ~8.26 and [DIC] was ~2030 μmol kg⁻¹ ([CO₂] ~10 μmol kg⁻¹, [HCO₃⁻] ~1800 μmol kg⁻¹ and [CO₃²⁻] ~220 μmol kg⁻¹). At the current rate of fossil fuel use atmospheric CO₂ could reach 1000 parts per million (ppm) by the year 2100, this would result in a drop in ocean pH_f to ~7.79 with a corresponding increase in [DIC] to ~2255 μmol kg⁻¹ ([CO₂] ~35 μmol kg⁻¹, [HCO₃⁻] ~2130 μmol kg⁻¹ and [CO₃²⁻] ~90 μmol kg⁻¹). In order to push the physiology of the cells to understand the importance of the individual carbonate system parameters we chose a wide range of carbonate system values below, spanning and above recent past and future predicted values. Over the three experiments [CO₂] ranged from 0.8 to 135 μmol

kg⁻¹, [HCO₃⁻] from 165 to 8660 μmol kg⁻¹, [CO₃²⁻] from 7 to 1230 μmol kg⁻¹ and pH_f from 7.58 to 8.39.

By disentangling the carbonate system we show that physiological and genetic responses can be attributed to individual carbonate system parameters. Indicating that CO₂ and HCO₃⁻ are the principal driving forces behind cellular responses over the carbonate system range tested. Furthermore the data identifies the genetic basis of a coccolithophore CCM revealing novel insights into inorganic carbon uptake for photosynthesis and calcification and how inorganic carbon is distributed between these two processes.

RESULTS

Carbonate chemistry

To determine the importance of the components of the carbonate system on *E. huxleyi* physiology cells were grown in three separate experiments at constant pH 7.74, constant pH 8.34 and constant CO₂ (16 μmol kg⁻¹). The carbonate chemistry showed certain differences and similarities between the three experiments (Fig. 1). The most pronounced differences are found between the constant CO₂ and constant pH experiments. At constant CO₂, the [CO₂] remained constant with increasing DIC, while pH, [HCO₃⁻] and [CO₃²⁻] increased. In both constant pH experiments, pH remained constant while [CO₂], [HCO₃⁻] and [CO₃²⁻] increased with increasing DIC. The key difference between the two constant pH experiments was the different constant pH_f levels of 7.74 and 8.34. Furthermore, [CO₂] increased more in the constant pH_f 7.74 experiment, while [CO₃²⁻] increase was more pronounced in the constant pH_f 8.34 experiment (Fig. 1). [HCO₃⁻] was increasing almost similarly in all experiments while [CO₃²⁻] increased most pronounced at constant CO₂ and least pronounced at constant pH_f 7.74. By maintaining relatively low cell concentrations, changes in carbonate chemistry due to biological processes were kept to a minimum over the time of the experiments (see error bars in Fig. 1).

Growth, particulate organic carbon (POC) and particulate inorganic carbon (PIC) production rates and C:N

Growth, POC and PIC production rates were significantly influenced by the carbonate chemistry manipulation in all experiments while C:N ratios were only significantly influenced in the constant pH experiments (Table SI). The influence of changing carbonate chemistry was

generally most pronounced from low to intermediate HCO_3^- and CO_2 (Fig. 2) with neither pH nor CO_3^{2-} having primary influence (Fig. S1).

At low levels of DIC growth rates increased in all experiments with increasing concentrations of HCO_3^- and CO_2 until reaching maximum rates of $\sim 1.1 \text{ d}^{-1}$ where further CO_2 or HCO_3^- increases had no effect on growth rates. While there are correlations between both HCO_3^- and CO_2 with growth, the constant pH experiments allow us to differentiate between these variables. CO_2 demonstrates a good correlation with growth rate in both constant pH experiments, whereas the influence of HCO_3^- on growth rate is variable, suggesting CO_2 is the dominant DIC species determining growth inhibition at low CO_2 (Fig. 2A and B), with a decline in growth rates below a $[\text{CO}_2]$ of $\sim 7.5 \mu\text{mol kg}^{-1}$ (Fig. 2B). As manipulation of CO_2 at two different constant pH levels had a similar effect on growth, pH did not appear to affect growth rates. However, in the constant CO_2 experiment growth rates are significantly lower in the lowest HCO_3^- treatment compared to intermediate HCO_3^- treatments ($p=0.009$) even though $[\text{CO}_2]$ is above this critical threshold of $7.5 \mu\text{mol kg}^{-1}$ (Fig. 2A). This may initially appear to be due to HCO_3^- limitation, however, in the constant pH 7.7 experiment growth rates were maintained at lower $[\text{HCO}_3^-]$ (and $[\text{CO}_2]$) indicating that this is a pH effect brought about by pH_f , dropping below 7.7 in the two lowest HCO_3^- treatments in this experiment (Fig. 1). In summary, above pH 7.7 $[\text{CO}_2]$ determines growth rate but pH begins to have a negative effect below this pH.

POC production increased in all experiments from low to intermediate $[\text{HCO}_3^-]$. The increase was least pronounced at constant CO_2 and most pronounced at constant pH_f 8.34 (Fig 2C). POC production rates in both constant pH experiments were highly sensitive to HCO_3^- and CO_2 when the concentrations drop below ~ 2000 and $\sim 10 \mu\text{mol kg}^{-1}$, respectively (Fig. 2C and D). The rates appear to correlate best to CO_2 at concentrations below $\sim 5 \mu\text{mol kg}^{-1}$, although there are limited data points in this range. At a constant CO_2 the lowest HCO_3^- treatment also showed significantly lower POC production rates than at intermediate HCO_3^- ($p = 0.002$, Fig. 2C). The lowest and highest measured POC production rates of $\sim 2.8 \text{ pg}$ and $\sim 11 \text{ pg cell}^{-1} \text{ d}^{-1}$ were found in constant pH_f 8.34 at ~ 170 and $\sim 1950 \mu\text{mol HCO}_3^- \text{ kg}^{-1}$, respectively. At HCO_3^- concentrations above $\sim 2000 \mu\text{mol kg}^{-1}$ POC production rates display a slight but significantly decreasing trend with increasing HCO_3^- in the constant pH experiments (Fig. 2C; pH 8.34, $p < 0.001$; pH 7.74, $p(\text{MC}) = 0.004$). With POC production decreasing significantly by about 20 % at constant pH_f 8.34 and 10 % in constant pH_f 7.74 from intermediate (i.e. $\sim 2000 \mu\text{mol kg}^{-1}$) to highest HCO_3^- levels (i.e. ~ 9950 at constant pH_f 8.34 and ~ 7350 at constant pH_f 7.74). No significant changes occurred above $2000 \mu\text{mol HCO}_3^- \text{ kg}^{-1}$ at constant CO_2 (Fig 2C), however, the HCO_3^- range at constant CO_2 was narrower than in the constant pH experiments so that possible influences of high $[\text{HCO}_3^-]$ could have been missed. In summary POC production

showed no clear overall correlation to any of the carbonate chemistry parameters except a correlated increase at the very low CO₂ range (below ~5 μmol kg⁻¹) and a potentially HCO₃⁻ driven decrease at high HCO₃⁻ (>2000 μmol kg⁻¹).

C:N ratios were highest in the intermediate CO₂ range (~40 μmol kg⁻¹) in both constant pH experiments and decreasing to both sides of the optimum (Fig. 2F). At the left side of the optimum (low CO₂ range) C:N increased similarly with CO₂. At the right side, however, trends started to diverge. At constant CO₂, changes in C:N were not statistically significant, although there seems to be a tendency towards increasing C:N with increasing HCO₃⁻ (Fig. 2E).

Calcification rates increased similarly in all experiments with increasing [HCO₃⁻] (Fig. 2G). No signs of calcification could be found in the two lowest HCO₃⁻ treatments at constant pH_f 7.74 and in two replicates of the lowest HCO₃⁻ treatment of constant CO₂ (Table I). In these treatments Ω_{calcite} is <0.31 so post-production dissolution of coccoliths could potentially be taking place. Maximum calcification rates at constant pH_f 8.34 and 7.74 were identical but were reached at lower CO₂ in constant pH_f 8.34 indicating a poor correlation with CO₂ (Fig 2H).

Gene Expression Analysis

In order to identify the molecular basis of the physiological response of *E. huxleyi* to the individual carbonate system parameters, 15 genes with putative roles in carbon transport, pH homeostasis and biomineralization were chosen for investigation (Table SII). Gene expression analysis was performed on all samples used for the physiological data allowing a direct link between gene expression and physiology. Each gene was normalized to the three (out of the four tested) most stable endogenous reference genes (ERGs) indicated by GeNorm, identified as *ACTIN*, *α-TUBULIN* and *EFG1-α*, followed by normalization to the lowest expression treatment for that gene which was set to 1. Plotting gene expression vs. DIC indicates the transcriptional response to changes in total inorganic carbon (Fig. 3). Out of the 15 genes investigated, 11 showed a marked increase in expression when the cells became DIC limited at total DIC <1000 μmol kg⁻¹ but displayed no repression above this level. Of the selected genes with putative roles in inorganic carbon transport, *AEL1*, *αCA1*, *δCA* and *rubisco* showed a significant DIC limited up-regulation between 4-11 fold (Fig. 3A). Two genes, *βCA* and *LCIX*, had a large low DIC response with a respective 450-fold and 180-fold up-regulation at the lowest DIC value in the constant pH_f 8.34 experiment relative to the treatment with the lowest expression (Fig. 3C,D). At higher DIC levels there was no detectable expression in some samples of *βCA* after 40 amplification cycles, indicating the very low basal expression of this gene. The general trend showed increased up-regulation at low DIC, but there are large variations between treatments

and within replicates (Fig. 3C and D). Interestingly expression of βCA and $LCIX$ showed strongly correlated expression patterns with a plot of βCA vs. $LCIX$ giving a linear response with an R^2 value of 0.99 (data not shown). Of the putative H^+ transport related genes $CAX3$, $NhaA2$, $ATPvc$ and $PATP$ showed a 4-7.5 fold up-regulation (Fig. 3B). Four genes with potential roles in H^+ and DIC transport, $HVCN1$, $AQP2$, $\alpha CA2$, and γCA , showed no significant transcriptional response over the carbonate system range tested (Fig. 3E; Table SI). Above $1000 \mu mol kg^{-1}$ DIC changes in gene expression of most investigated genes was minimal with no repression of DIC responsive genes but a small but significant decrease ($p=0.02$) seen in GPA expression above $\sim 2000 \mu mol kg^{-1}$ (Fig. 3F).

Plots of gene expression vs. individual carbonate system parameters indicate which parameter(s) are potentially influencing gene expression (Fig. 4). Genes sensitive to changes in carbonate chemistry showed an up-regulation at low $[CO_2]$ and $[HCO_3^-]$, with thresholds at approximately 7.5 and $800 \mu mol kg^{-1}$, respectively (Fig. 4A and B). Although pH and CO_3^{2-} may have a synergistic effect with other factors on the expression of some genes, they do not appear to be the main driving carbonate system parameters behind any of the genetic responses (Fig. 4C and D).

Further disentangling of gene expression response to CO_2 or HCO_3^- was possible to a certain degree for some genes (Table II). Table II also highlights the putative function of each gene, its potential cellular location by experimental determination or analogy to experimentally determined genes from other organisms and its predicted location determined by Target P and WoLF PSORT.

DISCUSSION

Growth rates and POC fixation

Growth rates presented in this study correlate closely to $[CO_2]$ with pH_f playing a critical role, having a significant negative impact once it drops below $pH_f \sim 7.7$ (CO_2 constant data, Fig. S1A). A similar effect of pH was seen in Bach et al., (2011) where a drop in pH_f from $\sim 7.7 - 7.0$ resulted in a linear decrease in growth rate of *E. huxleyi*. In their study, they also show that above $pH_f 7.7$ growth rates of *E. huxleyi* are dependent on CO_2 with a similar critical threshold of $\sim 7.5 \mu mol kg^{-1}$. Hence, trends in growth rates presented in our study seem to confirm the dependence on CO_2 and H^+ shown in Bach et al. (2011) and their approximated thresholds. It should be kept in mind, however, that both studies were performed with the same *E. huxleyi* strain and under the same culture conditions (e.g. light, temperature and nutrients). Threshold

values may be different in other strains and may also depend on culture conditions. In a similar study by Buitenhuis et al. (1999) they saw no clear tightly coupled correlation between *E. huxleyi* growth rate and $[\text{CO}_2]$. Instead the authors suggest that both CO_2 and HCO_3^- are important for growth rates. The reason behind this discrepancy is unclear although a different strain (Ch 24-90) was used in their study and growth rates were only calculated over a 24 hour period unlike the full experimental period in our study.

Although POC production rates did not show a strong overall correlation to $[\text{CO}_2]$ or $[\text{HCO}_3^-]$, the rates showed a close relationship to CO_2 at concentrations below $\sim 5 \mu\text{mol kg}^{-1}$ indicating a possible role of this molecule at sub-saturating conditions. The significant drop in POC production rate for the lowest HCO_3^- level in the constant CO_2 experiment (Fig. 2C) cannot result from low $[\text{CO}_2]$ as in the constant pH experiments but is most likely due to either a limitation by other carbon sources than CO_2 (e.g. HCO_3^- being $\sim 500 \mu\text{mol kg}^{-1}$ in this treatment) or by an inhibiting effect of $[\text{H}^+]$, similar as seen for the growth rates. Again the latter is probably the most likely scenario as a negative effect of high $[\text{H}^+]$ on POC production rates was also shown by Bach et al. (2011). The decrease in POC production at high HCO_3^- concentrations is not induced by external $[\text{H}^+]$ since this parameter did not change in both constant pH experiments (see Fig. 2D). Instead, the decrease is potentially the consequence of increasing $[\text{HCO}_3^-]$ because the trend correlates best to $[\text{HCO}_3^-]$ (Fig. 2C). It has been shown that high $[\text{HCO}_3^-]$ can cause intracellular acidification (Suffrian et al., 2011), which may negatively affect cell metabolism resulting in reduced POC production rates. According to the results presented here we speculate that POC production rates are similar to growth rates, in that they are majorly influenced by $[\text{CO}_2]$ and $[\text{H}^+]$. Additionally, very high concentrations of HCO_3^- possibly reduce POC production through an unknown mechanism.

C:N changed significantly in both constant pH experiments and were highest at intermediate CO_2 levels (Fig. 2F). C:N correlated substantially better to $[\text{CO}_2]$ than to any other carbonate system parameter suggesting a key role of this molecule on cellular C:N in *E. huxleyi*. Differences in C:N between treatments probably reflect variable cellular amounts of nitrogen-free relative to nitrogen-rich organic compounds. In *E. huxleyi* 40 - 60% of the total cellular carbon is in the form of lipids (Fernandez et al., 1994) with the largest part of cellular nitrogen expected to be present in proteins ($\sim 75\%$ of total cellular nitrogen is stored in proteins in *Isochrysis galbana* a species belonging to the same order as *E. huxleyi* (Lourenço et al., 1998)) which contribute only $\sim 20\%$ of total cellular carbon (Fernandez et al., 1994). With an approximate C:N ratio in proteins of 4:1 the cellular protein content would have to increase by more than 100% to decrease C:N from 8 to 6 as seen in our data. Such a pronounced increase would contradict results by Lourenco et al. (1998) who measured a maximum increase of only

~10% under CO₂ limitation. Hence we speculate, that changes in C:N reported in our study are mainly driven by changing assimilation of lipids and polysaccharides at different carbonate chemistry conditions.

Calcification rates (PIC production)

Calcification rates are tightly correlated to [HCO₃⁻] (Fig. 2G) but there is a clear offset when plotting calcification rates of the three experiments to [CO₂] (Fig. 2H) and [CO₃²⁻] (Fig. S1). This points towards HCO₃⁻ being the primary carbon source used for CaCO₃ precipitation in *E. huxleyi* which is in agreement with previous studies (reviewed in Paasche, 2002).

Changes in the carbonate system by increasing CO₂ have been shown to negatively effect coccolithophore calcification. By performing constant TA (ocean acidification scenario) and constant pH 8 experiments, Bach et al. (2011) showed that it is an increase in [H⁺] at elevated CO₂ which negatively affects calcification rates of *E. huxleyi* (Bach et al., 2011). Under this consideration, it could be expected that calcification rates would remain consistently lower throughout the constant pH_f 7.74 experiment compared to the constant pH_f 8.34 experiment. Surprisingly, however, this is not the case. Instead, maximum calcification rates are similar in both constant pH experiments (Fig 2H). This indicates that the direct negative effect of high [H⁺] on calcification rates reported in Bach et al. (2011) can at some point be overcome by increasing availability of inorganic carbon substrate. Considering carbonate chemistry conditions of the past this data might provide a further explanation why coccolithophores were able to thrive in the early Mesozoic era, a time that was characterized by relatively low seawater pH (down to pH 7.7) and high DIC (up to 5000 μmol kg⁻¹; Ridgwell, 2005).

Calcification could not be detected at low [HCO₃⁻] (Table I) although POC production continues at relatively high rates. Due to the low Ω_{calcite} in these treatments it could be argued that post-production dissolution is taking place once the coccoliths are exposed to the sub-saturated culture media. However, low levels of PIC would still be expected due to internal coccoliths, also cross-polarized light microscopy has shown the absence of internal coccoliths under similar carbonate chemistry conditions (unpublished data) and coccoliths are found extracellularly in cultures where the carbonate chemistry is at ambient levels but Ω_{calcite} is <0.1 due to reduced Ca²⁺ (Xu et al., 2011). This evidence indicates that it is a decrease in PIC production not dissolution that is being measured. The maintenance of POC production whilst PIC production is reduced indicates a strong priority of POC over PIC production under inorganic carbon limitation (Fig. S2). Sacrificing calcification at these conditions could free up

energy and inorganic carbon substrate, which then becomes available for cells to maintain higher growth and POC production rates.

Coccolithophores have maintained calcification since coccoliths appeared in the fossil record about 220 Ma before present (Bown et al., 2004). Nevertheless, calcification stops once either calcium is removed from the growth medium (Herfort et al., 2004; Trimborn et al., 2007; Leonardos et al., 2009) or inorganic carbon substrate is reduced below certain thresholds (Buitenhuis et al., 1999; this study) with both limitations having minimal effect on growth and POC production rates (Trimborn et al., 2007; CO₂ constant experiment of this study). The inhibition of calcification by the removal of Ca²⁺ clearly shows that photosynthesis has no mechanistic dependence on calcification (Leonardos et al., 2009). The inhibition by a reduction in external DIC not only supports this but also strongly suggests that calcification does not function as a CCM at low DIC. If calcification had a CCM function it would be maintained or up-regulated to support photosynthesis as inorganic carbon became limiting (Fig. 2 and S2). Hence, if calcification has no physiological necessity to maintain high cellular growth and photosynthesis then the reason to produce coccoliths is more likely an ecological one, increasing the chance of survival in the natural environment.

The molecular transporters anion exchanger like 1 (AEL1; a putative HCO₃⁻ transporter), Ca²⁺/H⁺ exchanger 3 (CAX3) and a H⁺ pumping V-ATPase (ATPVc'/c) have previously been identified to be potentially involved in calcification (Mackinder et al., 2011). Significant down-regulation of these genes was found in non-calcifying strains or when calcification was inhibited by calcium limitation but [HCO₃⁻] as inorganic carbon source was kept constant. In contrast to the findings by Mackinder et al. (2011), inhibition of calcification through HCO₃⁻ limitation instead of calcium limitation showed the opposite trend – i.e. an up-regulation of these three genes (Fig. 3 and Table II). Here, we hypothesize that this opposing regulation pattern found under calcium and HCO₃⁻ limitation is due to a dual function of these molecular transporters. At normal seawater [CO₂] and [HCO₃⁻] (as in Mackinder et al., 2011) they would mainly be involved in calcification, with removal of calcium resulting in their down-regulation. However, in cases where inorganic carbon becomes limiting their main function may switch from serving calcification to serving as a CCM. In this case a further decrease of CO₂ and HCO₃⁻ would lead to their up-regulation with a concomitant loss of calcification (as can be seen in our data).

More specifically, AEL1 for example could be used to transport HCO₃⁻ into an intracellular pool from where, under normal conditions, it would be predominantly transported into the coccolith vesicle to supply calcification (Fig. 5A, see Table III for further information). Under low CO₂ and HCO₃⁻ availability, however, the intracellular HCO₃⁻ flux would increasingly bypass the coccolith vesicle and be diverted into the chloroplast instead (Fig. 5B). AEL1 would

be up-regulated under these circumstances to enhance the use of HCO_3^- and/or to balance the high diffusive loss of CO_2 (Rost et al., 2006). ATPVc'/c and CAX3 both which are involved in H^+ transport could play an important role in maintaining compartmental pH an essential part of CCMs (Raven, 1997).

CCM and influence of individual inorganic carbon species on gene regulation

C_3 biophysical CCMs are characterized by linking HCO_3^- and CO_2 transporters, carbonic anhydrases (CAs) and pH gradients to actively transport DIC and accumulate it as CO_2 in the proximity of RubisCO at a concentration many folds higher than external CO_2 (Badger et al., 1980). The results presented identify a defined and clear up-regulation in multiple putative CCM related genes in *E. huxleyi* as DIC becomes limiting for growth, POC and PIC production (Figure 3, Table II). The majority of genes respond by up-regulation when HCO_3^- drops below $\sim 800 \mu\text{mol kg}^{-1}$ or CO_2 falls below $\sim 7.5 \mu\text{mol kg}^{-1}$. Above these thresholds all genes (with the exception of *GPA*) showed a relatively stable level of expression over a wide range of DIC and pH levels. This transcriptional profile identifies the genetic basis of a CCM in *E. huxleyi*. The majority of the investigated genes had the capacity to be up-regulated at low DIC indicating that *E. huxleyi* operates a regulated CCM. This supports previous work by Rost et al. (2003) who showed the $K_{1/2}$ of CO_2 for photosynthetic O_2 evolution to drop from 27.3 to 9.6 $\mu\text{mol L}^{-1}$ for cells cultured at ~ 15 versus $\sim 1 \mu\text{mol CO}_2 \text{ kg}^{-1}$. Interestingly most of the DIC responsive genes were not further repressed at CO_2 above $\sim 7.5 \mu\text{mol kg}^{-1}$ ($[\text{HCO}_3^-] \sim 800 \mu\text{mol kg}^{-1}$). This indicates a potential basal level of the CCM, with a low level of active DIC transport taking place even when growth rates and POC production are saturated. The presence of active transport at ambient CO_2 and HCO_3^- is supported by Schulz et al. (2007) who show active DIC uptake even at ambient conditions. Most photosynthetic O_2 evolution curves and ^{14}C incorporation studies have indicated that photosynthesis is not saturated at ambient CO_2 (Paasche, 1964; Herfort et al., 2002; Rost et al., 2003) but in some cases would need up to 15 times greater DIC to become saturated (Paasche, 1964). However, this is not supported by Schulz et al. (2007) who show that net CO_2 fixation is close to saturation at ambient CO_2 . This is also strongly supported by our data with growth rates and organic carbon fixation both saturated at or below ambient $[\text{CO}_2]$ under light and nutrient replete conditions.

How *E. huxleyi* senses DIC limitation and regulates its CCM at a molecular level is unknown. From the presented expression data both $[\text{CO}_2]$ and $[\text{HCO}_3^-]$ could be primary signal molecules inducing a transcriptional response upon changing concentration (Fig. 4A and B). The CO_2 concentration in seawater is lower than that of HCO_3^- but in contrast to HCO_3^- , CO_2 is

uncharged and can easily diffuse through membranes (Hopkinson et al., 2011). This attribute makes this molecule the most important inorganic carbon source for carbon fixation at ambient carbonate chemistry conditions (Schulz et al., 2007). In addition to that, up-regulation of some putative CCM-related genes was less pronounced in the low DIC treatments of the constant CO₂ experiment compared to similarly low DIC treatments of the constant pH experiments. These lines of evidence make CO₂ a key candidate to regulate the expression of CCM-related genes. Further support for CO₂ was found by previous studies that have reported CO₂ sensitivity of CCM regulation in the green algae *Chlamydomonas* and *Chlorella* sp. and the diatom *Phaeodactylum tricornutum* (Matsuda and Colman, 1995; Bozzo and Colman, 2000; Matsuda et al., 2001). A summary of the potential regulation of gene expression by CO₂, HCO₃⁻, CO₃²⁻ and pH is given in table II.

Function and localization of CCM related genes

The spatial organization and regulation of CCM components is key to CCM functionality. Table II provides a summary of the putative function and predicted cellular location of the investigated genes. CAs function to speed up the reversible dehydration of HCO₃⁻ to CO₂ or vice versa depending on their chemical environment. CAs have been shown to be generally up-regulated under carbon limitation at a transcriptional level if they are associated to CCMs (Badger, 2003; Raven and Giordano, 2009). This agrees with our data with three out of the five investigated CAs being up-regulated under low DIC to varying degrees. For αCAI [CO₂] and [HCO₃⁻] appeared to contribute equally to its transcriptional response while [CO₂] seemed to have the primary influence on the transcription of βCA and δCA (Table II). Due to the diversity of the investigated CAs it is likely that they have varying cellular locations and activities.

βCA showed the largest response of all the genes investigated and is predicted to be located in the chloroplast by WoLF PSORT. CA activity has previously been demonstrated in the chloroplast fraction in the coccolithophore *Pleurochrysis* sp. with most activity in the stroma (Quiroga and González, 1993). A plastid location is further supported by Tachibana et al. (2011) who localized two βCAs in *Phaeodactylum tricornutum* to the chloroplast stroma. The likely chloroplastic location of βCA and its strong up-regulation at low DIC indicates a key role within the *E. huxleyi* CCM. Furthermore, a correlated expression with *LCIX* ($R^2 > 0.99$) indicates that these genes could be under the same transcriptional control. *LCIX* exhibits similarity to *LCIB* a gene that is induced under CO₂ limitation (Miura et al., 2004) and plays a crucial role in the *Chlamydomonas* CCM (Wang and Spalding, 2006).

The δ CA is a key candidate for an extracellular CA, due to it containing a potential membrane anchor (Soto et al., 2006) and a δ CA has been immuno-localized to the cell surface of the marine dinoflagellate *Lingulodinium polyedrum* (Lapointe et al., 2008). Extracellular CA activity in *E. huxleyi* is generally thought to be low in exponential growing cells (Nimer et al., 1994; Elzenga et al., 2000) however increased activity has been shown at very low CO₂ (pH 8.7, [CO₂] ~2 μ M) (Nimer et al., 1997) and once cells reach the stationary phase (Nimer et al., 1994). The up-regulation at low [CO₂] and [HCO₃⁻] found in our experiments indicates that δ CA maybe the genetic basis of this CA activity. Assuming an extracellular location, the δ CA could accelerate HCO₃⁻ to CO₂ equilibration close to the cell plasma membrane, thereby quickly resupplying incorporated CO₂ playing a key role within the CCM. Strong up-regulation at low CO₂ has also been demonstrated in TWCA1, a δ CA from *Thalassiosira weissflogii* (McGinn and Morel, 2008), suggesting that these enzymes are involved in CCMs of other taxa too.

The investigated γ CA showed no change in expression over the wide carbonate chemistry range tested. This agrees with Soto et al. (2006) who found no change in expression between high and low HCO₃⁻ (although their manipulation of the carbonate system is unclear). Nevertheless, Soto et al. (2006) observed a large up-regulation of this gene in the dark which indicates a possible function independent of photosynthesis and calcification, one possibility is a role in respiration. This is supported by the mitochondrial location of γ CAs in Arabidopsis (Parisi et al., 2004) and the diatom *Phaeodactylum tricornutum* (Tachibana et al., 2011).

α CA1 was up-regulated at low CO₂ which points towards an involvement of the corresponding α CA enzyme in the CCM of *E. huxleyi*. In *Chlamydomonas* α CAH3 has been shown to be a fundamental part of the CCM responsible for the dehydration of HCO₃⁻ to release CO₂ in the thylakoid lumen (Karlsson et al., 1998). Two other *Chlamydomonas* α CAs (CAH1 and CAH2) that are linked to the CCM (Spalding, 2008) have been shown to be located in the cell wall region (Coleman et al., 1984; Fujiwara et al., 1990). In the diatoms *P. tricornutum* and *Thalassiosira pseudonana*, putative α CAs were located in the four layered plastid membrane system and inside the chloroplast, respectively (Tachibana et al., 2011).

Interestingly *rubisco* shows an up-regulation at low DIC although it could be expected that a decrease in substrate for RubisCO would rather lead to a reduced transcription. However, due to the oxygenase activity of RubisCO the efficiency of RubisCO decreases as CO₂ decreases. This is due to an increased competitive advantage of O₂ over CO₂ for RubisCO's active site, which leads to increased photorespiration – a loss of fixed carbon. To avoid this the cell can operate a CCM to keep RubisCO saturated for CO₂ or increase the amount of RubisCO to compensate for its decrease in efficiency. It appears that *E. huxleyi* does both, initially up-regulating *rubisco* (Table II) followed by up-regulation of the CCM. If the CCM was 100%

efficient it would be expected that RubisCO would stay saturated with respect to CO₂ and no *rubisco* up-regulation would be necessary. However this is not the case with *rubisco* transcription increased indicating a level of futility in the CCM.

Possible scenario for CCM function and regulation in *E. huxleyi*

The CCM of *E. huxleyi* shows a number of differences to those of other partially characterized eukaryotic algae. One outstanding feature is its low affinity for CO₂ even for low CO₂ acclimated cells. Rost et al. (2003) measured a K_{1/2} of 9.6 μmol kg⁻¹ CO₂ for cells grown at 1 μmol kg⁻¹ CO₂. This is considerably higher than the K_{1/2} for the diatom *Skeletonema costatum* of 0.3 or the Prymnesiophyte *Phaeocystis globosa* of 2.4 μmol kg⁻¹ CO₂ (Rost et al., 2003). The K_{1/2} for other diatom species has also been shown to be considerably lower than that of *E. huxleyi* (Johnston and Raven, 1996; Trimborn et al., 2009). Another feature of the *E. huxleyi* CCM is that up-regulation of molecular components is induced only when very low CO₂ levels are encountered. This is strikingly different to diatoms and *Chlamydomonas* where molecular CCM components are already strongly induced at ambient CO₂ and even above (Miura et al., 2004; Harada et al., 2005).

Although the *E. huxleyi* CCM may be of a lower affinity many of the components are still similar to other eukaryotic algae. Genome analysis shows that *E. huxleyi* has 9 putative CAs belonging to the α, β, γ and δ families. This is similar to the diatom CA repertoire with *P. tricornutum* also having 9 CAs spreading across the same 4 families (Tachibana et al., 2011). There are also strong similarities with *Chlamydomonas*, which has 10 putative CAs in its genome belonging to the α, β and γ families (Spalding, 2008). Furthermore HCO₃⁻ transporters belonging to the SLC4 family are present in the genomes of *P. tricornutum* and *T. pseudonana* although absent in *Chlamydomonas*. Also, the presence of proteins in *E. huxleyi* with possible homology to *LciB* family proteins previously thought to be confined to green algae (Wang and Spalding, 2006) is an interesting similarity that warrants further investigation.

The expression data supports an increasing use of HCO₃⁻ at low DIC with transporters belonging to the SLC4 family (e.g. AEL1), which could actively transport this ion across the plasma-membrane. The increased expression of proton pumps (ATP_{Vc}'/c and PATP) and cation/H⁺ exchangers (NhaA2 and CAX3) suggests an increased demand of these transporters to maintain pH homeostasis, membrane potential or alter compartmental pH in order to promote changes in CO₂:HCO₃⁻ ratios. More alkaline regions would maintain DIC as HCO₃⁻ which is one million times less permeable to membranes than CO₂ (Moroney et al., 2011). This could prevent CO₂ loss via diffusion across membranes while more acidic regions in the proximity of RubisCO

would result in a shift to CO_2 (Raven, 1997). In cyanobacteria there is an absence of CA in the cytosol resulting in an accumulation of HCO_3^- , that once transported to the carboxysome is dehydrated to CO_2 catalyzed by CA in the proximity of RubisCO (Price et al., 2008). A cytosolic location for CAs also seems unlikely because the cytosolic pH in *E. huxleyi* is close to pH 7 (Dixon et al., 1989) and the presence of CA would accelerate HCO_3^- to CO_2 equilibration, which would subsequently leak out of the cell before it reaches the site of fixation (Badger and Price, 1989). Experimental evidence also supports the lack of CA activity in the cytosol, with the cytosolic fraction actually inhibiting CA activity (Quiroga and González, 1993).

In microalgae operating CCMs there is strong evidence that HCO_3^- accumulates in the alkaline stroma (Spalding, 2008). Upon transport to the thylakoid lumen or pyrenoid the more acidic environment and presence of CA rapidly shifts the equilibrium to CO_2 , which then diffuses to RubisCO. The importance of CA in this mechanism has been highlighted in *Chlamydomonas* (Karlsson et al., 1998). An analogous scenario is possible for *E. huxleyi* with the expression data supporting CA up-regulation of a potential chloroplast located βCA and several H^+ pumps and exchangers which could alter compartmental pH and therefore shift the $\text{HCO}_3^-:\text{CO}_2$ inside the stroma.

Although *E. huxleyi* has a regulated CCM it is insufficient to maintain growth rates and POC fixation at low CO_2 at the same level as seen under ambient carbonate chemistry conditions (Fig. 2B, D). This inability to fully compensate can potentially be due to increasing CO_2 leakage at low external $[\text{CO}_2]$. Leakage in *E. huxleyi* has been measured to be $\sim 79\%$ at ambient CO_2 (Schulz et al., 2007) and shown to increase as CO_2 decreased (Rost et al., 2006). By operating a CCM the cell actively accumulates HCO_3^- and CO_2 at a higher concentration in the proximity of RubisCO than externally. Inorganic carbon has to be presented to RubisCO as CO_2 , so ultimately HCO_3^- accumulated for carbon fixation will have to be converted to CO_2 . If the external CO_2 concentration is very low, the diffusion gradient from the chloroplast to the outside will be large and leakage increases (Rost et al., 2006). Thus, although it appears that HCO_3^- use becomes increasingly important at low CO_2 it is actually external CO_2 concentration that determines how much carbon from HCO_3^- stays within the cell due to the strong inside to out CO_2 gradient and high permeability of membranes to CO_2 (Raven and Lucas, 2005; Rost et al., 2006; Bach et al., 2011).

Extrapolation to the real ocean

The above data is derived from monoclonal culture experiments and provides a key insight into carbon usage in *E. huxleyi* under controlled conditions. In the following we discuss whether our

results are useful to: (A) apply results to other coccolithophores; (B) understand CCM use in the natural environment; (C) understand changing calcification rates in future and past carbonate chemistry conditions.

A) *E. huxleyi* and its close relative *G. oceanica* are taxonomically and morphologically (e.g. no remnants of a *haptonema*, the presence of a reticular body and the absence of calcification in the haploid phase) quite different from other extant calcifying haptophytes having diverged from them over 150M years ago (De Vargas et al., 2007). Despite pronounced taxonomic and morphological differences, there are also important consistencies between *E. huxleyi* and other coccolithophores. The response of calcification rates to changing carbonate chemistry is a good example for such a consistency. Over a large CO₂ range at constant TA, all species, which have been tested for this, showed an optimum curve response (Langer et al., 2006; Bach et al., 2011; Krug et al., 2011; Sett et al. for *G. oceanica*, unpublished). Although the optimum carbonate chemistry conditions for calcification rates varied in between species, the general pattern was similar.

It is also feasible that general gene regulation patterns are similar between different coccolithophore species. Whether the thresholds at which they start to be up-regulated, or the factors which induce their up-regulation are similar is much less clear, especially because there is virtually no genetic data available on other coccolithophores. However, from other taxa (e.g. cyanobacteria) we know that the CCM genes present and the CCM regulation is related to the conditions within the natural habitat of the particular species rather than their taxonomic belonging (Badger et al., 2006; Price et al., 2008).

B) The expression data indicates an up-regulation of the CCM occurring at low inorganic carbon ([CO₂] ~7.5 μmol kg⁻¹) suggesting that an inducible CCM is redundant under current oceanic [CO₂] (~16 μmol kg⁻¹). However, in their natural habitat, it is possible that cells sporadically experience [CO₂] below 7.5 μmol kg⁻¹ in particular at the end of a bloom where [CO₂] is reduced due to photosynthetic carbon draw-down. Values as low as ~5 μmol kg⁻¹ were seen in a mesocosm experiment where a *E. huxleyi* bloom occurred after a *Phaeocystis* sp. and diatom bloom (Purdie and Finch, 1994). Furthermore, [CO₂] was significantly lower before the onset of anthropogenic CO₂ release approximately 200 years ago so that limiting inorganic carbon concentrations might have occurred more frequently in the past. A third aspect, which has to be considered, is a possible variability in the threshold DIC concentration below which the CCM is up-regulated. At very high light conditions, for example, it is possible that the CCM becomes up-regulated at a higher CO₂ threshold due to the cell having a larger inorganic carbon demand.

C) Increased pCO₂ has been shown to affect intracellular processes like calcification and photosynthesis in coccolithophores (Riebesell et al., 2000; Langer et al., 2006; Langer et al., 2009). Despite these physiological responses, our data suggests that the regulatory response to these changes on a genetic basis is very limited. CO₂ and/or HCO₃⁻ only induced enhanced transcription of genes when they decreased significantly below modern ocean concentrations, which is opposite to what will happen in the coming decades. Furthermore, none of the investigated genes – even putative H⁺ pumps - seemed to respond to increasing seawater [H⁺]. There are two possible explanations for this lack of regulatory response. 1) We have simply missed the critical genes and other genes that are not investigated here show a response to increasing [H⁺] and [CO₂]. 2) *E. huxleyi* does indeed entirely lack a regulatory machinery to cope with ocean acidification. To address these possibilities future studies need to focus on the transcriptome and proteome of *E. huxleyi* at variable carbonate chemistry conditions. If these future studies, however, support the latter, then the inability to regulate could be the reason why calcification and photosynthesis are negatively affected above certain thresholds.

MATERIALS AND METHODS

Experimental design and basic setup

Three experiments have been conducted in this study to test the physiological and molecular response of *E. huxleyi* to individual carbonate chemistry parameters. Therefore, DIC was increased in all experiments in between different treatments, while either pH (8.34 or 7.74 on free scale) or CO₂ (16 μmol kg⁻¹) was kept constant. In all experiments, monoclonal cells of *E. huxleyi* (strain B92/11) were grown in dilute batch cultures (LaRoche et al., 2010) at 15°C and 150 μmol m⁻² s⁻¹ incident photon flux density at a 16/8 light dark cycle. The growth medium was artificial seawater prepared as described in Kester et al. (1967) but without the addition of NaHCO₃, which was added in a later step (see following section). Artificial seawater was enriched with ~64 μmol kg⁻¹ nitrate, 4 μmol kg⁻¹ phosphate, f/8 concentrations of a trace metal and vitamin mixture (Guillard and Ryther, 1962), 10 nmol kg⁻¹ of SeO₂, and 2 mL kg⁻¹ of natural North Sea water to avoid nutrient limitation during the whole experiment. Concentrations of nitrate and phosphate were measured at the beginning and the end of the experiments according to Hansen and Koroleff (1999). The nutrient enriched but DIC and total alkalinity (TA) free seawater was sterile filtered into sterile polycarbonate bottles where the carbonate chemistry was manipulated. After taking samples for carbonate chemistry measurements (see following section) the seawater was split carefully into three sterile 2.3 L polycarbonate bottles. The culture

medium was brought to 15°C prior to inoculations with *E. huxleyi* cells to avoid a potential thermal shock of the cultures. Cells were acclimated to exponential growth and carbonate chemistry conditions for at least 7 generations.

Carbonate chemistry manipulation and determination

In the constant CO₂ experiment, DIC levels were adjusted by adding calculated amounts of NaHCO₃. CO₂ was then set to a constant level of ~16 (±2) μmol kg⁻¹ through additions of calculated amounts of hydrochloric acid (3.571 molar) or sodium hydroxide. In the constant pH_f 7.74 and constant pH_f 8.34 experiments, carbonate chemistry was adjusted by adding 2 mmol kg⁻¹ of 2-[4-(2-Hydroxyethyl)-1-piperazinyl]-ethanesulfonic acid (HEPES, adjusted to target pH_f levels) and calculated amounts of NaHCO₃ to reach target DIC levels. The small pH change in the buffered seawater medium due to the addition of NaHCO₃ was compensated by additions of calculated amounts of either hydrochloric acid or sodium hydroxide to reach constant pH_f levels of 7.74 (±0.004) and 8.34 (±0.008).

Carbonate chemistry in the constant CO₂ experiment was determined by measuring TA and pH_f while in both constant pH experiments it was determined from pH_f and DIC. Carbonate chemistry samples were taken at the beginning and the end of the experiments and were always the first samples to be taken to minimize potential CO₂ exchange with the atmosphere. Samples for TA were filtered (0.7 μm) into 500 mL polyethylene bottles, poisoned with saturated HgCl₂ solution (0.5 ‰ final concentration) and stored at 4°C until measured (Dickson et al., 2003). Samples with TA higher than 4700 μmol kg⁻¹ were too high to get accurate results from the applied method and therefore diluted with double de-ionised water (containing no alkalinity). The ratio of diluent relative to the sample was determined on a balance (SARTORIUS) with a precision of ±0.01g.

Samples for DIC were sterile filtered (0.2 μm) by gentle pressure into 4 mL borosilicate bottles, closed air-tight without headspace and subsequently measured as described in Stoll et al. (2001). DIC samples lower than 1000 or higher than 3000 μmol kg⁻¹ could not be reliably measured with the applied method without previous treatment. These samples were mixed with artificial seawater of the same salinity and known DIC in clean 50 mL polypropylene tubes to reach target concentrations of ~1800-2200 μmol kg⁻¹. The ratio between sample and artificial seawater of known DIC was determined on a high accuracy balance with a precision of ± 0.01 mg (SARTORIUS). The whole procedure was performed in less than two minutes and headspace in polypropylene tubes was reduced to ~1 mL to minimize CO₂ exchange with the

atmosphere during mixing. After mixing the samples, they were processed, stored and measured as described above.

Samples for pH_f were measured potentiometrically at 15°C with separate glass and reference electrodes (METROHM) calibrated with reference seawater, certified for TA and DIC (Prof. A. Dickson, La Jolla, California). pH_f of the reference material was calculated from given DIC, TA, phosphate, silicate, and salinity with the software CO2SYS (Lewis and Wallace, 1998) applying equilibrium constants determined by Roy et al. (1993). Measured electromotive force (E) of the samples and standards were used to calculate the pH_f of the sample according to Dickson et al. (2007) as

$$\text{pH}_f = \text{pH}_{f_reference} + \frac{E_s - E_x}{R \times T \times \frac{\ln 10}{F}}$$

where $\text{pH}_{f_reference}$ is the calculated pH_f of the certified reference material, E_s and E_x are the measured electromotive forces in Volts of the reference material and the sample, respectively, T is the temperature of the sample in Kelvin, R is the universal gas constant and F the Faraday constant. The application of reference material certified for TA and DIC was possible, since the salinity of the reference material ($S=33.3$) is close to the salinity in the culture medium ($S=35$).

Carbonate chemistry parameters which were not directly measured were calculated from two measured values (DIC and TA or DIC and pH_f) and known salinity, temperature, and phosphate concentrations with the software CO2SYS (Lewis and Wallace, 1998) using equilibrium constants determined by Roy et al. (1993). Biological response data is plotted against the means of the initial and final values of the carbonate chemistry. Error bars in plotted carbonate chemistry parameters denote the mean change of the three replicates of the particular carbonate chemistry parameter from the beginning of the experiment to the end.

Sampling, measurements and calculations of growth, organic and inorganic carbon production rates

Sampling started two hours after the onset of the light period and lasted not longer than two and a half hours. Duplicate samples for total particulate carbon (TPC) and particulate organic carbon (POC) were filtered with gentle underpressure (200 mbar) onto pre-combusted (5 hours at 500°C) GF/F filters and stored at -20°C until measurements. TPC and POC samples of both constant pH experiments were rinsed with 60 mL of artificial seawater medium supersaturated with respect to calcium carbonate and free of HEPES buffer immediately after filtration. This was

necessary because the HEPES buffer in the remaining seawater medium would have otherwise contributed about 40 μg of carbon per filter to the measurements. POC filters were stored for two hours in a desiccator containing fuming hydrochloric acid to remove all inorganic carbon and then dried for ~ 6 hours at 60°C . TPC filters were dried under the same conditions but in a separate oven and without the acid treatment. The carbon content of TPC and POC samples was measured using an elemental analyzer (HEKATECH) combined with an isotope ratio mass spectrometer (FINNIGAN). Particulate inorganic carbon (PIC) was calculated as the difference between TPC and POC.

Cell numbers were determined with a Coulter Counter (Z Series – BECKMAN Coulter) at the beginning and the end of the experiments approximately 4 hours after the onset of the light period. Growth rates (μ) were calculated from measured cell concentrations as

$$\mu = \frac{\ln(t_{fin}) - \ln(t_0)}{d}$$

where t_0 and t_{fin} is the cell number at the beginning and the end of the experiments, respectively, and d is the growth period in days. POC and PIC production rates were calculated by multiplying growth rates with the cellular POC or PIC contents.

Treatments with PIC production rates below $0.5 \text{ pg C cell}^{-1} \text{ d}^{-1}$ were further analysed by scanning electron microscopy (SEM) to reassure whether calcification was occurring. Therefore, 7-10 mL of sample were filtered by gravity on polycarbonate filters ($0.2 \mu\text{m}$ poresize) and dried for 2 hours at 60°C . Samples were sputtered with gold-paladium and processed with a scanning electron microscope (Phantom). Cells within investigated treatments were assumed to be actively calcifying if coccoliths could be found.

For gene expression analysis, approximately 10 million cells were filtered (200 mbar) on polycarbonate filters with a poresize of $0.8 \mu\text{m}$ and subsequently rinsed off the filters with 1 mL RNAlater (QIAGEN). This cell suspension was kept on ice until storage at -20°C .

Quantitative Reverse-Transcriptase Polymerase Chain Reaction (qRT-PCR)

Quantitative Reverse Transcriptase Polymerase Chain Reaction (qRT-PCR) was performed to quantify gene expression. 15 target genes with putative roles in carbon acquisition, pH homeostasis and calcite precipitation were analysed. Each sample was measured in triplicate. Experimental procedures were performed as described previously (Mackinder et al., 2011). Briefly, RNA was extracted from cell pellets using the RNeasy mini kit (QIAGEN), eluted in

RNase free H₂O, aliquoted and stored at -80 °C. RNA concentration, quality and integrity was determined using a BIO-RAD EXPERION, with all samples having a RNA quality indicator (RQI) value >7.5. 380 ng of totalRNA was DNase treated and reverse transcribed using a Quantitect kit (QIAGEN). No reverse transcription control (NRTC) aliquots were removed after DNase treatment and reverse transcription was primed with a mixture of oligo-dT and random primers. The resulting cDNA was stored at -20 °C until qPCR.

Primers were designed to EST clusters from von Dassow et al. (2009), the *E. huxleyi* Genome Project (<http://genome.jgi-psf.org/Emihu1/Emihu1.home.html>) or from the current literature (Table SII). Amplicon length and the presence of primer dimers were tested using PCR followed by analysis on 1.5% agarose gel. Efficiency curves for each primer pair were generated using serial dilutions on pooled cDNA from all samples. All primers except β CA had efficiencies between 90 to 105% and generated curves with R² values > 0.99. β CA efficiency remained undetermined due to the low cycle threshold (C_T) values of pooled cDNA even at undiluted levels. For relative expression calculations its efficiency was assumed to be 100%. This assumption results in a potential decrease in the accuracy of the absolute fold changes but the trend of expression and the magnitude will remain unaffected. SYBR green chemistry was used for qPCR (2x Fast SYBR Green Master Mix; APPLIED BIOSYSTEMS). 20 μ l reaction volumes consisting of 10 pmol μ l⁻¹ forward and reverse primers and cDNA (2-20 ng of RT RNA) were ran using the fast cycling program on an Applied Biosystems Step One Plus qPCR machine. All samples were ran in triplicate with NRTCs ran to check for DNA contamination for each sample and NTCs ran per primer pair on each plate to check for between well contamination. For each primer pair all samples were ran across three plates, in order to allow for the correction of between plate variation two standards in triplicate were ran on each plate. GeNorm (Vandesompele et al., 2002) was used to test the stability of four potential endogenous reference genes (ERGs).

Analysis of qRT-PCR data was done using an efficiency corrected $\Delta\Delta C_t$ method, normalizing to the geometric mean of three ERGs (Vandesompele et al., 2002). For each gene all samples were plotted relative to the sample with lowest expression from all three experiments. The sample with the lowest expression level was normalized to 1 allowing the expression ratios between samples to be easily identified.

Localization of putative CCM proteins

The intracellular localization of the investigated regulatory enzymes was approximated with the software tools TargetP and WoLF PSORT (Emanuelsson et al., 2007; Horton et al., 2007)

Protein targeting by TargetP is based on identification of N-terminal amino acid sorting sequence while WoLF PSORT predicts subcellular location based on sorting signal peptides and homology to other localized proteins (Horton et al., 2007). It has to be noted that there are 2 limitations that should be taken into account when interpreting the results of these localization predictions for *E. huxleyi*. 1) Incorrect gene models resulting in false prediction of coding region initiation sites. Although the genes were manually annotated some lacked experimental data (namely ESTs) in the 5' region which may result in truncated or extended N-terminal protein sequences used for prediction. 2) The software is principally designed and trained on green plant networks which can make localization predictions for secondary endosymbionts, like *E. huxleyi* that contain additional membranes surrounding their plastid, less accurate.

Statistical analysis

We tested if the carbonate chemistry had a statistically significant effect on individual physiological and molecular response parameters with either an one-factorial analysis of variance (ANOVA) in case the data subsets were normally distributed or with a permutational multivariate analysis of variance (PERMANOVA) in case they were not. Normality was tested with Shapiro-Wilk's test and accepted if the p-value of this test was larger 0.05. Non-normally distributed subsets were Box-Cox transformed and tested with Shapiro Wilk's test afterwards again. Subsets which remained non-normally distributed after Box-Cox transformation were further analysed with the PERMANOVA.

The ANOVA was performed using Statistica version 8 (STATSOFT). Results were assumed to be significantly influenced by the carbonate chemistry if the p-value was smaller 0.05. The difference of individual treatments within an experiment was tested with Turkey's honest significance difference post-hoc test. Homogeneity of variance was tested using Levene's test and was accepted if the p-value was larger 0.05. In case p was smaller, the significance level (p-value of the ANOVA and the post-hoc test) was decreased to 0.01. Subsets treated this way are marked in Table SI.

The PERMANOVA analysis was conducted using PRIMER 6 (including PERMANOVA+, Primer-e, Ltd). Here, a resemblance matrix was created using the Euclidian distance function and further processed with a one-factorial PERMANOVA design choosing type III partitioning of the sum of squares. In case statistically significant differences were detected, a pair-wise comparison of treatments (analogue to a post-hoc test) was conducted in a second PERMANOVA run. The numbers of permutations for each run are given in Table SI. In pair-wise PERMANOVA runs, these numbers were not sufficiently high (below 100) to get

reasonable results for p , so that an additional Monte Carlo test was conducted. Significance levels of the PERMANOVA analysis are the same as for the ANOVA but by convention termed $p(\text{perm})$ for the permutation p -value and $p(\text{MC})$ for the Monte Carlo p -value to distinguish them.

ACKNOWLEDGEMENTS

Silke Lischka is acknowledged for support on statistics and Janett Voigt for support during sampling.

AUTHOR CONTRIBUTIONS

L.T.B, L.C.M.M and K.G.S designed the experiments. L.T.B and L.C.M.M performed the experiments and analysed the data. L.T.B, L.C.M.M, K.G.S, D.C.S, G.W, C.B and U.R wrote the manuscript.

LITERATURE CITED

- Bach LT, Riebesell U, Georg Schulz K** (2011) Distinguishing between the effects of ocean acidification and ocean carbonation in the coccolithophore *Emiliana huxleyi*. *Limnology and Oceanography* **56**: 2040-2050
- Badger M** (2003) The roles of carbonic anhydrases in photosynthetic CO₂ concentrating mechanisms. *Photosynthesis Research* **77**: 83-94
- Badger MR, Kaplan A, Berry JA** (1980) Internal Inorganic Carbon Pool of *Chlamydomonas reinhardtii*. Evidence for a CO₂-Concentrating Mechanism. *Plant Physiology* **66**: 407-413
- Badger MR, Price GD, Long BM, Woodger FJ** (2006) The environmental plasticity and ecological genomics of the cyanobacterial CO₂ concentrating mechanism. *Journal of Experimental Botany* **57**: 249-265
- Bown PR, Lees JA, Young JR** (2004) Calcareous nannoplankton evolution and diversity through time. In HR Thierstein, JR Young, eds, *Coccolithophores—From Molecular Processes to Global Impact*. Springer Verlag, pp 481–505.
- Bozzo GG, Colman B** (2000) The induction of inorganic carbon transport and external carbonic anhydrase in *Chlamydomonas reinhardtii* is regulated by external CO₂ concentration. *Plant, Cell and Environment* **23**: 1137-1144
- Buitenhuis E, de Baar H, Veldhuis M** (1999) Photosynthesis and calcification by *Emiliana huxleyi* (Prymnesiophyceae) as a function of inorganic carbon species. *Journal of Phycology* **35**: 949-959
- Caldeira K, Wickett ME** (2003) Anthropogenic carbon and ocean pH. *Nature* **425**: 365
- Coleman JR, Berry JA, Togasaki RK, Grossman AR** (1984) Identification of Extracellular Carbonic Anhydrase of *Chlamydomonas reinhardtii*. *Plant Physiology* **76**: 472-477
- De Vargas C, Aubry M-P, Probert I, Young J** (2007) Origin and evolution of coccolithophores: From coastal hunters to Oceanic farmers. In PG Falkowski, AH Knoll, eds, *Evolution of primary producers in the sea*. Elsevier, London
- Dickson AG, Afghan JD, Anderson GC** (2003) Reference materials for oceanic CO₂ analysis: a method for the certification of total alkalinity. *Marine Chemistry* **80**: 185-197
- Dickson AG, Sabine CL, Christian JR** (2007) Determination of the pH of sea water using a glass/reference electrode cell. In AG Dickson, CL Sabine, JR Christian, eds, *Guide to best practices for ocean CO₂ measurements*. PICES Special Publication, pp 1-7
- Dixon GK, Brownlee C, Merrett MJ** (1989) Measurement of internal pH in the coccolithophore *Emiliana huxleyi* using 2',7'-bis-(2-carboxyethyl)-5-(and-6)carboxyfluorescein acetoxymethylester and digital imaging microscopy. *Planta* **178**: 443-449
- Elzenga JTM, Prins HBA, Stefels J** (2000) The Role of Extracellular Carbonic Anhydrase Activity in Inorganic Carbon Utilization of *Phaeocystis globosa* (Prymnesiophyceae): A Comparison with other Marine Algae Using the Isotopic Disequilibrium Technique. *Limnology and Oceanography* **45**: 372-380
- Emanuelsson O, Brunak S, von Heijne G, Nielsen H** (2007) Locating proteins in the cell using TargetP, SignalP and related tools. *Nature Protocols* **2**: 953-971
- Falkowski PG, Raven J** (2007) *Aquatic Photosynthesis*, Ed 2. Princeton University Press, Princeton
- Fernandez E, Balch WM, Maranon E, Holligan PM** (1994) High rates of lipid biosynthesis in cultured, mesocosm and coastal populations of the coccolithophore *Emiliana huxleyi*. *Marine Ecology Progress Series* **22**: 13-22
- Field CB, Behrenfeld MJ, Randerson JT, Falkowski P** (1998) Primary Production of the Biosphere: Integrating Terrestrial and Oceanic Components. *Science* **281**: 237-240

- Fujiwara S, Fukuzawa H, Tachiki A, Miyachi S** (1990) Structure and differential expression of two genes encoding carbonic anhydrase in *Chlamydomonas reinhardtii*. *PNAS* **87**: 9779-9783
- Giordano M, Beardall J, Raven JA** (2005) CO₂ concentrating mechanisms in algae: Mechanisms, Environmental Modulation, and Evolution. *Annual Review of Plant Biology* **56**: 99-131
- Guillard R, Ryther J** (1962) Studies of marine planktonic diatoms. I. *Cyclotella nana* Hustedt, and *Detonula confervacea* (Cleve) Gran. *Canadian Journal of Microbiology* **8**: 229-239
- Hansen HP, Koroleff F** (1999) Determination of nutrients. In K Grasshoff, K Kremling, M Ehrhardt, eds, *Methods of Seawater Analysis*, Ed 3. Wiley-VCH Verlag GmbH, Weinheim, pp 159-228
- Harada H, Nakatsuma D, Ishida M, Matsuda Y** (2005) Regulation of the Expression of Intracellular beta-Carbonic Anhydrase in Response to CO₂ and Light in the Marine Diatom *Phaeodactylum tricornutum*. *Plant Physiology* **139**: 1041-1050
- Herfort L, Loste E, Meldrum F, Thake B** (2004) Structural and physiological effects of calcium and magnesium in *Emiliana huxleyi* (Lohmann) Hay and Mohler. *Journal of Structural Biology* **148**: 307-314
- Herfort L, Thake B, Roberts J** (2002) Acquisition and use of bicarbonate by *Emiliana huxleyi*. *New Phytologist* **156**: 427-436
- Horton P, Park K-J, Obayashi T, Fujita N, Harada H, Adams-Collier CJ, Nakai K** (2007) WoLF PSORT: protein localization predictor. *Nucleic Acids Research* **35**: W585-W587
- Johnston AM, Raven JA** (1996) Inorganic carbon accumulation by the marine diatom *Phaeodactylum tricornutum*. *European Journal of Phycology* **31**: 285-290
- Karlsson J, Clarke AK, Chen Z-Y, Huggins SY, Park Y-I, Husic HD, Moroney JV, Samuelsson G** (1998) A novel alpha-type carbonic anhydrase associated with the thylakoid membrane in *Chlamydomonas reinhardtii* is required for growth at ambient CO₂. *EMBO J* **17**: 1208-1216
- Kester DR, Duedall IW, Connors DN, Pytkowicz RM** (1967) Preparation of artificial seawater. *Limnology and Oceanography* **12**: 176-179
- Langer G, Geisen M, Baumann K-H, Kläs J, Riebesell U, Thoms S, Young JR** (2006) Species-specific responses of calcifying algae to changing seawater carbonate chemistry. *Geochemistry Geophysics Geosystems* **7**: 10.1029/2005gc001227
- Langer G, Nehrke G, Probert I, Ly J, Ziveri P** (2009) Strain-specific responses of *Emiliana huxleyi* to changing seawater carbonate chemistry. *Biogeosciences* **6**: 4361-4383
- Lapointe M, MacKenzie TDB, Morse D** (2008) An External delta-Carbonic Anhydrase in a Free-Living Marine Dinoflagellate May Circumvent Diffusion-Limited Carbon Acquisition. *Plant Physiology* **147**: 1427-1436
- LaRoche J, Rost B, Engel A** (2010) Bioassay, batch culture and chemostat experimentation. In U Riebesell, V Fabry, L Hansson, JP Gattuso, eds, *Guide for best practices for ocean acidification research and data reporting*. Publications Office of the European Union, pp 81-94
- Leonardos N, Read B, Thake B, Young JR** (2009) No mechanistic dependence of photosynthesis on calcification in the coccolithophorid *Emiliana huxleyi* (Haptophyta). *Journal of Phycology* **45**: 1046-1051
- Lewis E, Wallace DWR** (1998) Program Developed for CO₂ Systems Calculations Program Developed for CO₂ Systems Calculations. ORNL/CDIAC-105, Carbon Dioxide Information Analysis Centre, Oak Ridge National Laboratory, U.S. Department of Energy, Oak Ridge, Tennessee *In*,
- Lourenço SO, Barbarino E, Marquez UML, Aida E** (1998) Distribution of Intracellular Nitrogen in Marine Microalgae: Basis for the calculation of specific nitrogen-to-protein conversion factors. *Journal of Phycology* **34**: 798-811

- Mackinder L, Wheeler G, Schroeder D, von Dassow P, Riebesell U, Brownlee C** (2011) Expression of biomineralization-related ion transport genes in *Emiliana huxleyi*. *Environmental Microbiology* **13**: 3250–3265
- Matsuda Y, Colman B** (1995) Induction of CO₂ and bicarbonate transport in the green alga, *Chlorella ellipsoidea*. II. Evidence for induction in response to external CO₂ concentration. *Plant Physiology* **108**: 253-260
- Matsuda Y, Hara T, Colman B** (2001) Regulation of the induction of bicarbonate uptake by dissolved CO₂ in the marine diatom, *Phaeodactylum tricornutum*. *Plant, Cell & Environment* **24**: 611-620
- McGinn PJ, Morel FM** (2008) Expression and regulation of carbonic anhydrases in the marine diatom *Thalassiosira pseudonana* and in natural phytoplankton assemblages from Great Bay, New Jersey. *Physiologia Plantarum* **133**: 78-91
- Miura K, Yamano T, Yoshioka S, Kohinata T, Inoue Y, Taniguchi F, Asamizu E, Nakamura Y, Tabata S, Yamato KT, Ohyama K, Fukuzawa H** (2004) Expression Profiling-Based Identification of CO₂-Responsive Genes Regulated by CCM1 Controlling a Carbon-Concentrating Mechanism in *Chlamydomonas reinhardtii*. *Plant Physiol.* **135**: 1595-1607
- Moroney J, Ma Y, Frey W, Fusilier K, Pham T, Simms T, DiMario R, Yang J, Mukherjee B** (2011) The carbonic anhydrase isoforms of *Chlamydomonas reinhardtii*: intracellular location, expression, and physiological roles. *Photosynthesis Research* **109**: 133-149
- Nimer NA, Guan Q, Merrett MJ** (1994) Extracellular and intracellular carbonic-anhydrase in relation to culture age in a high-calcifying strain of *Emiliana huxleyi* Lohmann. *New Phytologist* **126**: 601-607
- Nimer NA, IglesiasRodriguez MD, Merrett MJ** (1997) Bicarbonate utilization by marine phytoplankton species. *Journal of Phycology* **33**: 625-631
- Nimer NA, Merrett MJ** (1992) Calcification and utilization of inorganic carbon by the coccolithophorid *Emiliana huxleyi* Lohmann. *New Phytologist* **121**: 173-177
- Paasche E** (1964) A tracer study of the inorganic carbon uptake during coccolith formation and photosynthesis in the coccolithophorid *Coccolithus huxleyi*. *Physiologia Plantarum* **3(suppl)**: 1-82
- Paasche E** (2002) A review of the coccolithophorid *Emiliana huxleyi* (Prymnesiophyceae), with particular reference to growth, coccolith formation, and calcification-photosynthesis interactions. *Phycologia* **40**: 503-529
- Parisi G, Perales M, Fornasari Ma, Colaneri A, Schain N, Casati D, Zimmermann S, Brennicke A, Araya A, Ferry J, Echave Jn, Zabaleta E** (2004) Gamma carbonic anhydrases in plant mitochondria. *Plant Molecular Biology* **55**: 193-207
- Price GD, Badger MR, Woodger FJ, Long BM** (2008) Advances in understanding the cyanobacterial CO₂-concentrating-mechanism (CCM): functional components, Ci transporters, diversity, genetic regulation and prospects for engineering into plants. *Journal of Experimental Botany* **59**: 1441-1461
- Purdie DA, Finch MS** (1994) Impact of a coccolithophorid bloom on dissolved carbon dioxide in sea water enclosures in a Norwegian fjord. *Sarsia* **79**: 379-387
- Quiroga O, González EL** (1993) Carbonic anhydrase in the chloroplast of a coccolithophorid (Prymnesiophyceae). *Journal of Phycology* **29**: 321-324
- Raven J** (1997) Putting the C in phycology. *European Journal of Phycology* **32**: 319-333
- Raven JA, Giordano M** (2009) Biomineralization by photosynthetic organisms: evidence of coevolution of the organisms and their environment? *Geobiology* **7**: 140-154
- Reinfelder JR** (2011) Carbon Concentrating Mechanisms in Eukaryotic Marine Phytoplankton. *Annual Review of Marine Science* **3**: 291-315
- Ridgwell A** (2005) A Mid Mesozoic Revolution in the regulation of ocean chemistry. *Marine Geology* **217**: 339-357

- Riebesell U, Tortell PD** (2011) Effects of Ocean Acidification on Pelagic Organisms and Ecosystems. In J-P Gattuso, L Hansson, eds, Ocean Acidification, Ed 1. Oxford University Press, Oxford, pp 99-121
- Riebesell U, Zondervan I, Rost B, Tortell PD, Zeebe RE, Morel FMM** (2000) Reduced calcification of marine plankton in response to increased atmospheric CO₂. *Nature* **407**: 364-367
- Rost B, Riebesell U, Burkhardt S, Sültemeyer D** (2003) Carbon Acquisition of Bloom-Forming Marine Phytoplankton. *Limnology and Oceanography* **48**: 55-67
- Rost B, Riebesell U, Sültemeyer D** (2006) Carbon acquisition of marine phytoplankton: Effect of photoperiod length. *Limnology and Oceanography* **51**: 12-20
- Roy RN, Roy LN, Vogel KM, Porter-Moore C, Pearson T, Good CE, Millero FJ, Campbell DM** (1993) The dissociation constants of carbonic acid in seawater at salinities 5 to 45 and temperatures 0 to 45 °C. *Marine Chemistry* **44**: 249-267
- Sarmiento J, Gruber N** (2006) Ocean Biogeochemical Dynamics. Princeton University Press, Princeton
- Schulz KG, Rost B, Burkhardt S, Riebesell U, Thoms S, Wolfgladrow DA** (2007) The effect of iron availability on the regulation of inorganic carbon acquisition in the coccolithophore *Emiliana huxleyi* and the significance of cellular compartmentation for stable carbon isotope fractionation. *Geochimica et Cosmochimica Acta* **71**: 5301-5312
- Sekino K, Shiraiwa Y** (1994) Accumulation and utilization of dissolved inorganic carbon by a marine unicellular coccolithophorid, *Emiliana huxleyi*. *Plant and Cell Physiology* **35**: 353-361
- Sikes CS, Roer RD, Wilbur KM** (1980) Photosynthesis and coccolith formation - inorganic carbon-sources and net inorganic reaction of deposition. *Limnology and Oceanography* **25**: 248-261
- Soto AR, Zheng H, Shoemaker D, Rodriguez J, Read BA, Wahlund TM** (2006) Identification and preliminary characterization of two cDNAs encoding unique carbonic anhydrases from the marine alga *Emiliana huxleyi*. *Applied and Environmental Microbiology* **72**: 5500-5511
- Spalding MH** (2008) Microalgal carbon-dioxide-concentrating mechanisms: Chlamydomonas inorganic carbon transporters. *Journal of Experimental Botany* **59**: 1463-1473
- Suffrian K, Schulz KG, Gutowska MA, Riebesell U, Bleich M** (2011) Cellular pH measurements in *Emiliana huxleyi* reveal pronounced membrane proton permeability. *New Phytologist*: DOI: 10.1111/j.1469-8137.2010.03633.x
- Tachibana M, Allen A, Kikutani S, Endo Y, Bowler C, Matsuda Y** (2011) Localization of putative carbonic anhydrases in two marine diatoms, *Phaeodactylum tricornerutum* and *Thalassiosira pseudonana*. *Photosynthesis Research* **109**: 205-221
- Thierstein HR, Geitzenauer KR, Molfino B, Shackleton NJ** (1977) Global synchronicity of late Quaternary coccolith datum levels Validation by oxygen isotopes. *Geology* **5**: 400-404
- Trimborn S, Langer G, Rost B** (2007) Effect of varying calcium concentrations and light intensities on calcification and photosynthesis in *Emiliana huxleyi*. *Limnology and Oceanography* **52**: 2285-2293
- Trimborn S, Wolf-Gladrow D, Richter K-U, Rost B** (2009) The effect of pCO₂ on carbon acquisition and intracellular assimilation in four marine diatoms. *Journal of Experimental Marine Biology and Ecology* **376**: 26-36
- Tsuji Y, Suzuki I, Shiraiwa Y** (2009) Photosynthetic Carbon Assimilation in the Coccolithophorid *Emiliana huxleyi* (Haptophyta): Evidence for the Predominant Operation of the C₃ Cycle and the Contribution of beta-Carboxylases to the Active Anaplerotic Reaction. *Plant Cell Physiol.* **50**: 318-329
- Tyrrell T, Young JR** (2009) Coccolithophores. In JH Steele, KK Turekian, SA Thorpe, eds, Encyclopedia of Ocean Sciences, Ed 2. Academic Press, San Diego, pp 3568-3576

- Vandesompele J, De Preter K, Pattyn F, Poppe B, Van Roy N, De Paepe A, Speleman F** (2002) Accurate normalization of real-time quantitative RT-PCR data by geometric averaging of multiple internal control genes. *Genome Biology* **3**: research0034.0031 - research0034.0011
- von Dassow P, Ogata H, Probert I, Wincker P, Da Silva C, Audic S, Claverie J-M, de Vargas C** (2009) Transcriptome analysis of functional differentiation between haploid and diploid cells of *Emiliana huxleyi*, a globally significant photosynthetic calcifying cell. *Genome Biology* **10**: R114
- Wang Y, Spalding MH** (2006) An inorganic carbon transport system responsible for acclimation specific to air levels of CO₂ in *Chlamydomonas reinhardtii*. *PNAS* **103**: 10110-10115
- Wolf-Gladrow DA, Riebesell U, Burkhardt S, Bijma J** (1999) Direct effects of CO₂ concentration on growth and isotopic composition of marine plankton. *Tellus B* **51**: 461-476
- Xu K, Gao K, Villafañe VE, Helbling EW** (2011) Photosynthetic responses of *Emiliana huxleyi* to UV radiation and elevated temperature: roles of calcified coccoliths. *Biogeosciences* **8**: 1441-1452
- Zeebe RE, Wolf-Gladrow D** (2001) CO₂ in Seawater: Equilibrium, Kinetics, Isotopes, Ed 1. Elsevier, Amsterdam

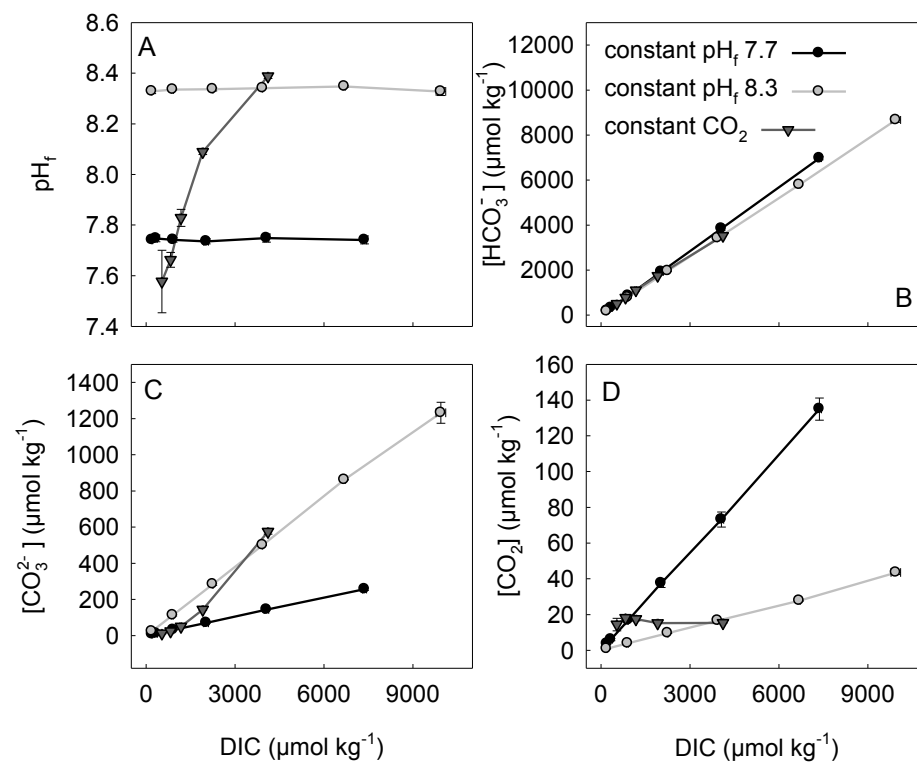


Figure 1. Physiologically relevant carbonate chemistry parameters in relation to DIC. (A) pH_f . (B) $[\text{HCO}_3^-]$. (C) $[\text{CO}_3^{2-}]$. (D) $[\text{CO}_2]$. Error bars account for the mean change (mean of triplicates) of the particular carbonate chemistry parameter in the course of the experiments.

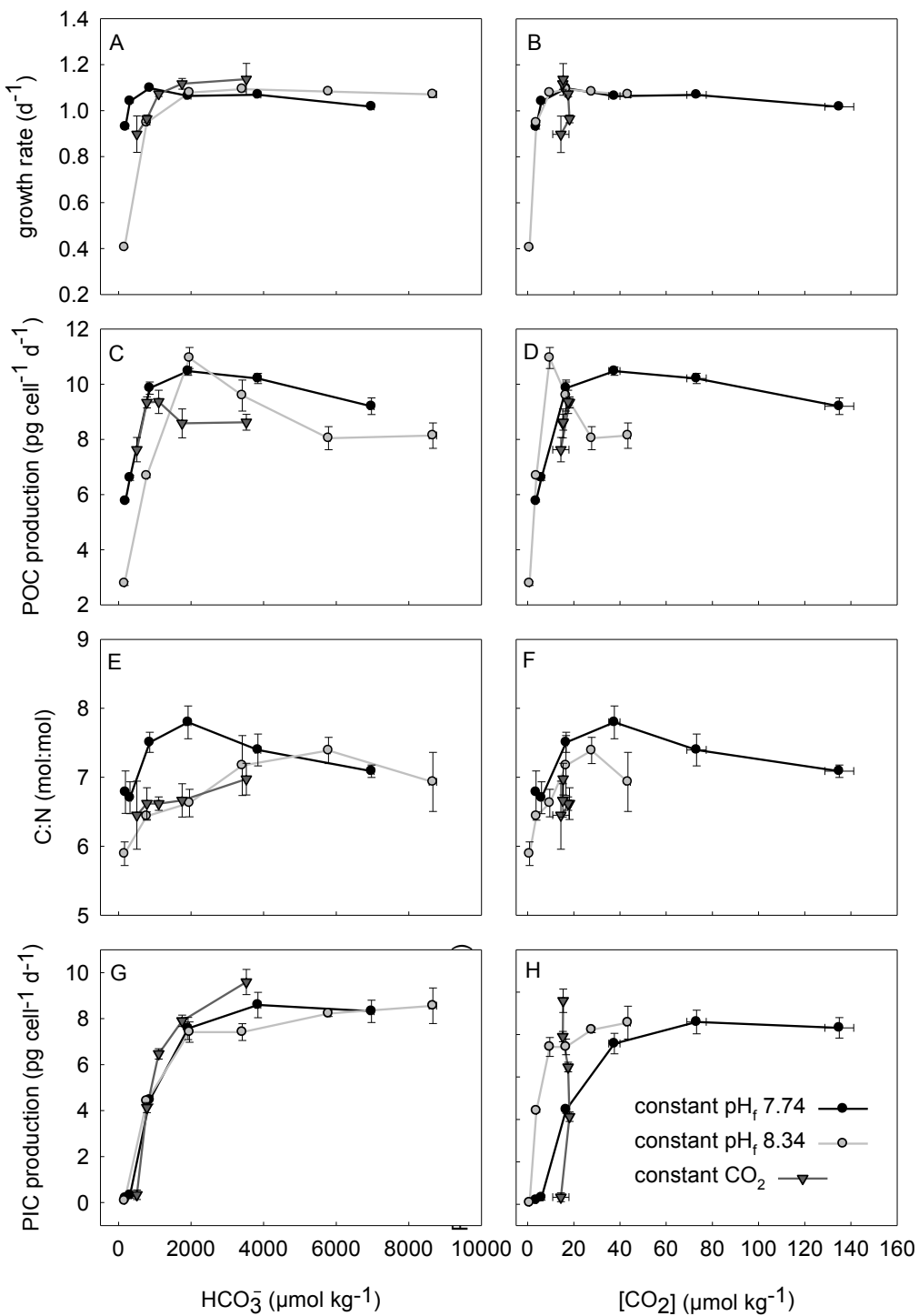


Figure 2. Physiological response parameters in relation to $[\text{HCO}_3^-]$ (left column) or $[\text{CO}_2]$ (right column). (A), (B) growth rates. (C), (D) POC production. (E), (F) C:N. (G), (H) PIC production. Vertical error bars denote the standard deviation of three replicates. Horizontal error bars show the mean change in $[\text{HCO}_3^-]$ or $[\text{CO}_2]$ (mean of triplicates) from the beginning to the end of the experiments.

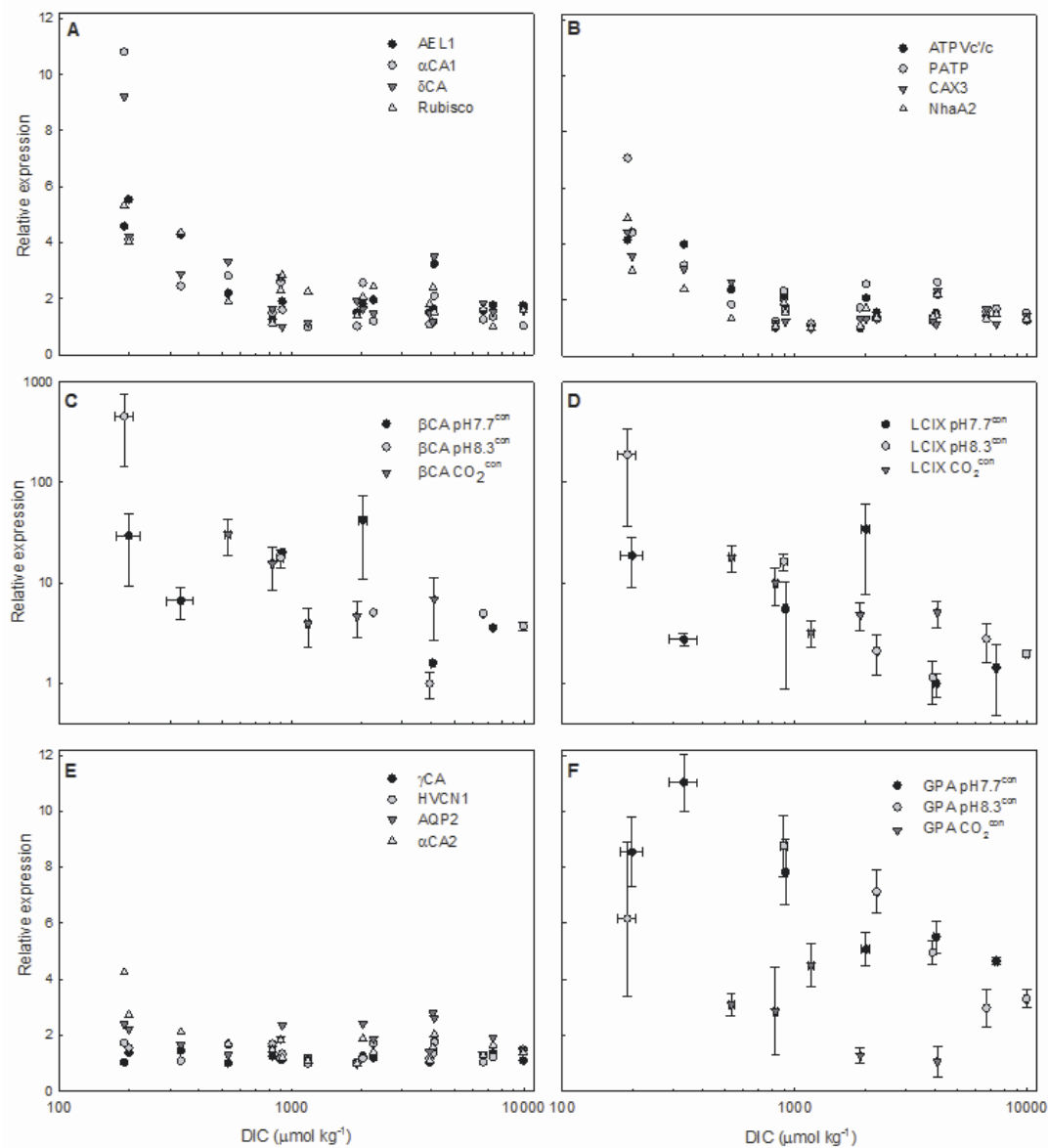


Figure 3. Relative expression of investigated genes plotted against dissolved inorganic carbon (DIC). Plot (A), (B), (C) and (D) are inorganic carbon transport and H^+ transport genes that were DIC responsive. (E) shows non-responsive genes over the DIC ranges tested. (F) is GPA which showed no clear trend over the DIC range tested. Plots (C), (D) and (F) show expression in the 3 individual experiments with standard errors shown (Y-axis) and the mean change in DIC from the beginning to the end of the experiment (X-axis). Note the logarithmic Y-axis for plots (C) and (D). (A), (B) and (E) are combined data from the constant pH_f 7.74, constant pH_f 8.34 and constant CO_2 experiments for each gene. Error bars have been omitted to improve clarity. The absence of error bars for some samples in (C) is due to undetectable levels of βCA transcripts in some of the biological replicates.

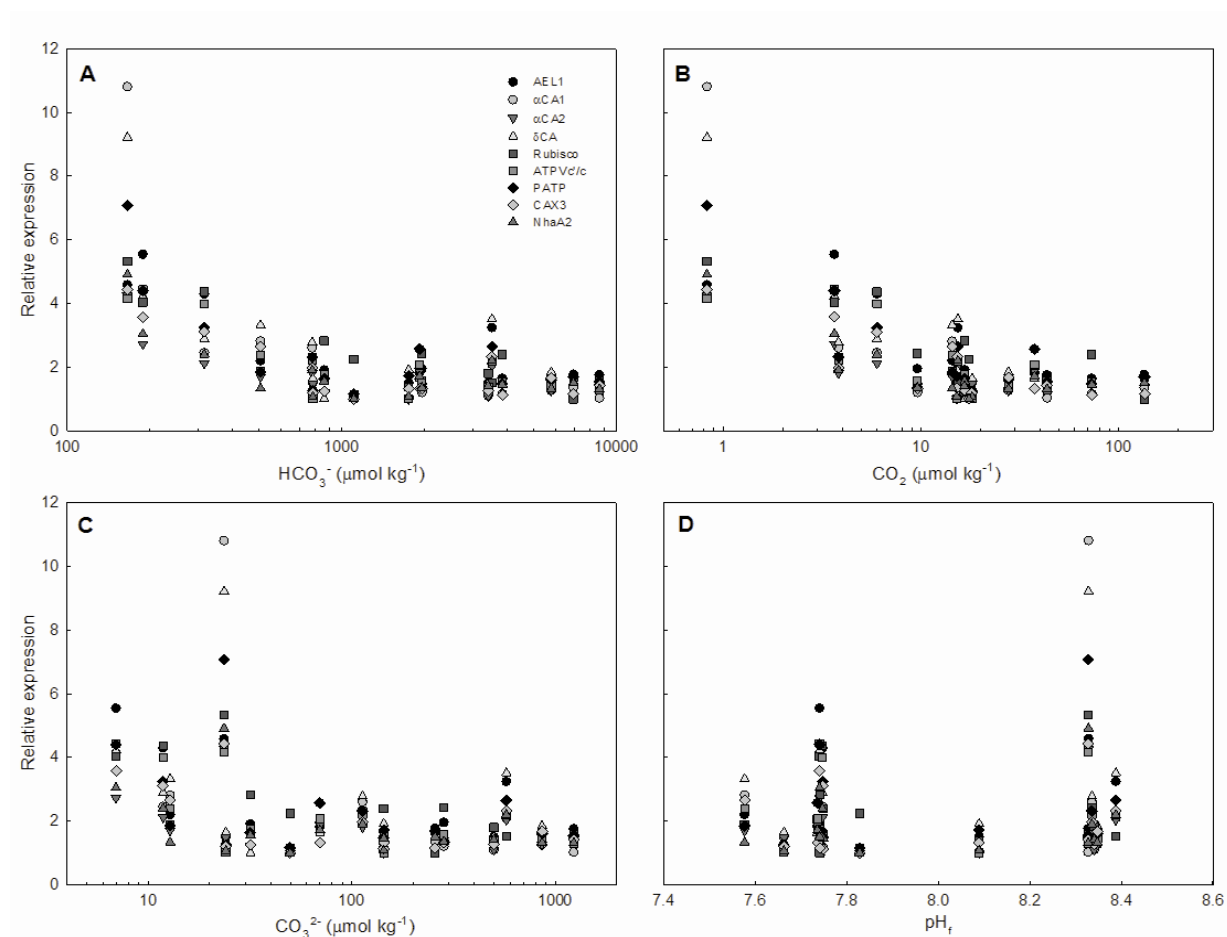


Figure 4. Plots of gene expression vs. the individual components of the carbonate system for 9 DIC responsive genes. Error bars have been omitted to improve clarity. (A) vs. HCO_3^- . (B) vs. CO_2 . (C) vs. CO_3^{2-} . (D) vs. pH_f .

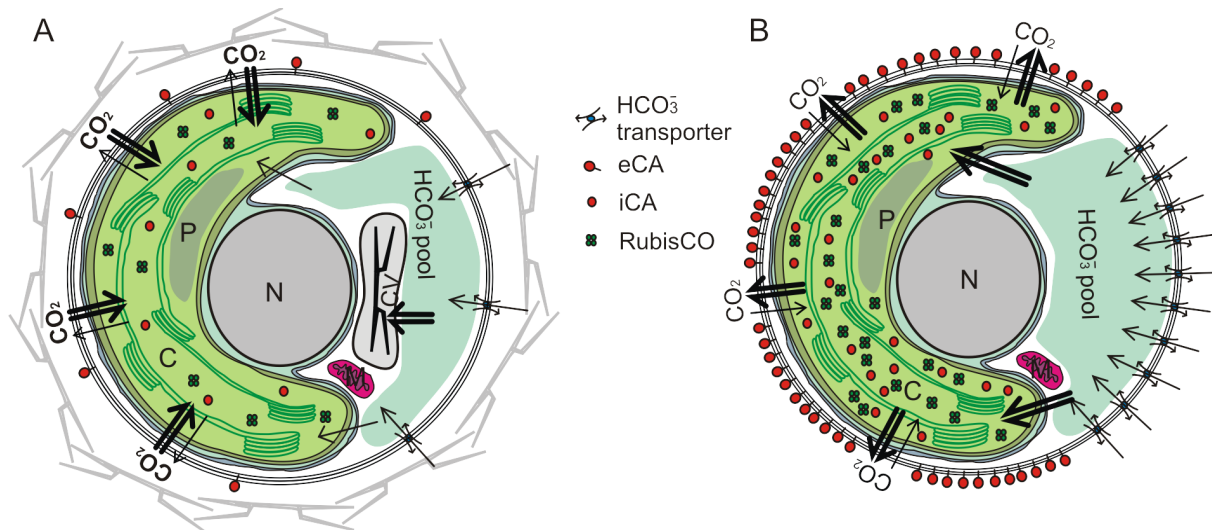


Figure 5. A conceptual model of inorganic carbon uptake at (A) high and (B) low DIC. The model is based on the data presented in this manuscript and previous studies (see Table III for all assumptions within the model). (A) With increasing CO_2 , the CO_2 gradient into the cell becomes at some point sufficient to saturate photosynthesis and maintain maximum POC fixation and growth rates. Hence CO_2 is the most important external substrate for photosynthesis at high CO_2 while HCO_3^- is the main substrate for calcification with a putative HCO_3^- exchanger AEL1 playing a key role. (B) At low CO_2 , HCO_3^- becomes more and more important as the inorganic carbon source for photosynthesis. Therefore, HCO_3^- and its uptake mechanism shifts from providing inorganic carbon for calcification to photosynthesis, leading to a reduction and eventually to a deactivation of calcification. Furthermore, the CCM (including the shown components: RubisCO, external and internal CAs) is up-regulated to support inorganic carbon supply. Although HCO_3^- becomes the dominant external carbon source for photosynthesis, external CO_2 still determines growth rates and POC fixation due to increasing CO_2 leakage as external CO_2 decreases (see text for details). C = Chloroplast, P = Pyrenoid, N = Nucleus, M = Mitochondrion, CV = coccolith vesicle, eCA = external Carbonic anhydrase, iCA = internal Carbonic anhydrase.

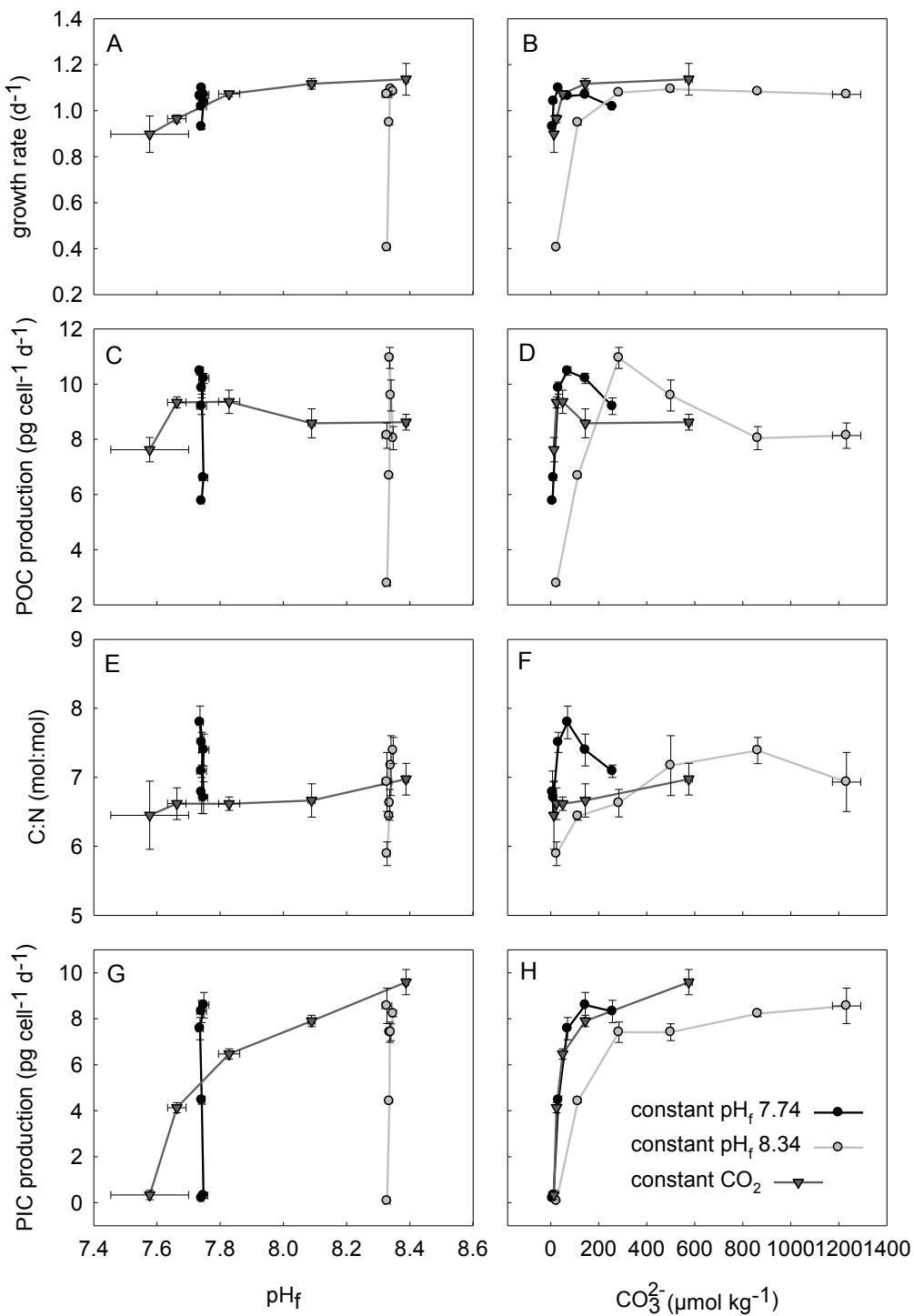


Figure S1. Physiological response parameters in relation to $[pH_f]$ (left column) or $[CO_3^{2-}]$ (right column). (A), (B) growth rates. (C), (D) POC production. (E), (F) C:N. (G), (H) PIC production. Vertical error bars denote the standard deviation of three replicates. Horizontal error bars show the mean change in $[HCO_3^-]$ or $[CO_2]$ (mean of triplicates) from the beginning to the end of the experiments.

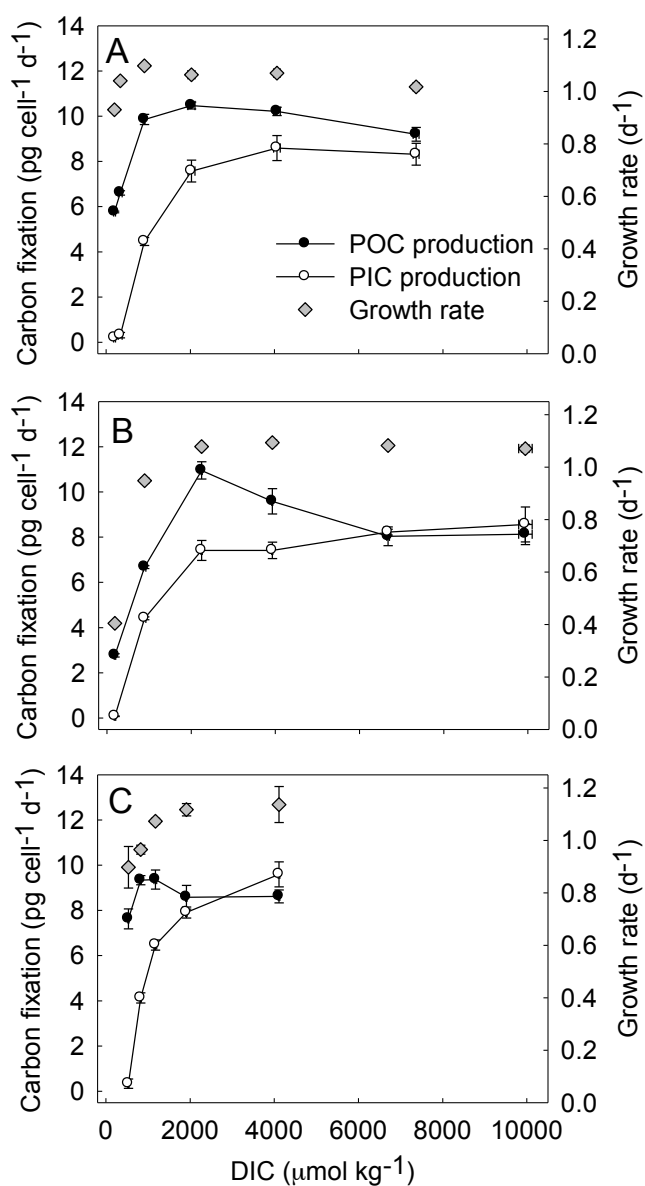


Figure S2. PIC production, POC production and growth rates plotted against DIC. (A) at constant pH_f 7.74 (B) at constant pH_f 8.34 (C) at constant [CO₂] ~16 $\mu\text{mol kg}^{-1}$. Vertical error bars denote the standard deviation of three replicates. Horizontal error bars show the mean change in [DIC] (mean of triplicates) from the beginning to the end of the experiments.

Table I. Results of SEM investigations. Shown in this table is each replicate of treatments where PIC production was below $0.5 \text{ pg cell}^{-1} \text{ d}^{-1}$. Note that coccoliths were found in all treatments and replicates not listed in this table.

Experiment	HCO_3^- ($\mu\text{mol kg}^{-1}$)	H^+ (nmol kg^{-1})	Coccoliths found?
Constant pH_f 7.74	200	18.2	No
	160	18.2	No
	200	18.2	No
	300	17.8	No
	330	17.8	No
	320	17.8	No
Constant pH_f 8.34	170	4.8	Yes
	160	4.7	Yes
	170	4.7	Yes
Constant CO_2	520	30.9	No
	510	26.3	No
	490	22.9	Yes*

*cell concentrations were higher in this replicate at the end of the experiment (76.000 compared to $36000 \text{ cell mL}^{-1}$ in first replicate). This caused a stronger decrease in $[\text{HCO}_3^-]$ and $[\text{H}^+]$.

Table II. Genetic response to carbonate system manipulations. A summary of the response of gene expression to the individual carbonate system parameters and associated physiological responses. Additional columns show putative function, possible location by experimentation or analogy and predicted location by the software Target P and WoLF PSORT. Cellular location are abbreviated as follows: plasmamembrane,(PM), cytosol (Cyto), nucleus (Nuc), chloroplast (Chloro), mitochondrium (Mito), Secretory pathway (Sec).

Gene	Correlation to carbonate system parameter							Function and Location		
	Full name	CO ₂ (μmol kg ⁻¹)	HCO ₃ ⁻ (μmol kg ⁻¹)	CO ₃ ²⁻ (μmol kg ⁻¹)	pH _i	Purative Function	Possible location - experimentally or by analogy	Predicted location Target p/WoLF PSORT		
AE11	Anion Exchanger Like 1	↑	↑	↑	-	HCO ₃ ⁻ transport, probably coupled to Na ⁺ , Cl ⁻ and/or H ⁺ transport	Plasmamembrane or chloroplast	- /PM		
αCA1	α Carbonic Anhydrase 1	↑	↑	↑	-	HCO ₃ ⁻ + H ⁺ ↔ CO ₂ + H ₂ O	αCAs are distributed throughout all Kingdoms of life. In <i>Chlamydomonas</i> they are found in the periplasmic space and the thylakoid lumen.	- /Nuc, Cyto		
αCA2	α Carbonic Anhydrase 2	↑	↑	↑	-	HCO ₃ ⁻ + H ⁺ ↔ CO ₂ + H ₂ O	Associated with the pyrenoid in the diatom <i>Phaeodactylum tricornutum</i>	Mito/Nuc		
βCA	β Carbonic Anhydrase	↑	↑	↑	-	HCO ₃ ⁻ + H ⁺ ↔ CO ₂ + H ₂ O	Mitochondrial location in <i>Arabidopsis</i> and <i>Phaeodactylum tricornutum</i> . γ-type CAs are found in the cyanobacteria carboxysome	- /Chloro		
γCA	γ Carbonic Anhydrase	-	-	-	-	HCO ₃ ⁻ + H ⁺ ↔ CO ₂ + H ₂ O	Plasmamembrane location based on dinoflagellate βCAs	Mito/Cyto		
δCA	δ Carbonic Anhydrase	↑	↑	↑	-	HCO ₃ ⁻ + H ⁺ ↔ CO ₂ + H ₂ O contains a possible membrane anchor	Chloroplast	- /PM		
Rubisco	Rubisco	↑	↑	↑	↑	Carbon fixation	Chloroplast	Chloro		
HVCN1	H ⁺ channel	-	-	-	-	H ⁺ channel	Plasmamembrane	- /Cyto		
ATPvc/c	Vacuolar-type H ⁺ pump	↑	↑	↑	-	Vacuolar Type ATP driven H ⁺ pump	Endomembrane system, possibly CV associated membrane fraction	Sec/Vac		
PATP	Plasma membrane type H ⁺ pump	↑	↑	↑	-	"PM"-type ATP driven H ⁺ pump	Plasmamembrane	- /PM		
CAX3	Ca ²⁺ /H ⁺ exchanger 3	↑	↑	↑	-	Ca ²⁺ /H ⁺ exchanger – driven by H ⁺ gradient	Endomembrane	- /Cyto		
NhaA2	Na ⁺ /H ⁺ exchanger 2	↑	↑	↑	-	Na ⁺ /H ⁺ exchanger maintain cellular pH and membrane potential	Plasmamembrane	Chloro/Nuc, Cyto		
LCIX	Low CO ₂ induced gene	↑	↑	↑	-	Putative Low CO ₂ induced gene found in <i>Chlamydomonas</i>	Chloroplast but no transmembrane regions	- /Nuc		
AQP2	Aquaporin 2	-	-	-	-	H ₂ O permeable channel. Some are CO ₂ permeable.	Membrane	- /PM		
GPA	Ca ²⁺ binding	↑	↓	↑	↑	Ca ²⁺ binding protein	Coccolith vesicle	- /Nuc		

↑ up-regulated

↓ down-regulated

↑ Best Correlation

↑ Possible correlation

Table III: Assumptions within the conceptual model

Assumption	Basis of Assumption	Reference
Cellular Organelle location and approximate relative sizes	Transmission Electron Micrographs	Gutowska et al. (Unpublished)
CO ₂ principal inorganic carbon source for photosynthesis	¹⁴ C labeling studies; Membrane Inlet Mass spectrometry measurements	Sikes et al., 1980; Schulz et al., 2007
Increasing HCO ₃ ⁻ over CO ₂ usage for photosynthesis at low CO ₂	Membrane Inlet Mass spectrometry identifies increasing HCO ₃ ⁻ :CO ₂ uptake ratio for cells acclimated to low CO ₂ conditions; Up-regulation of AEL1 at low CO ₂	Rost et al., 2003; This Study
HCO ₃ ⁻ pool and dual function of AEL1 in calcification and CCM	AEL1 previously shown to have a role in calcification; Up-regulation at low DIC.	Mackinder et al., 2011; This study
Up-regulation of CAs at low DIC	Three out of five investigated CAs showed an up-regulation in expression at low DIC.	This study
Location of δCA at plasma membrane	Presence of putative membrane anchor; Localization of a dinoflagellate δCA to the plasma membrane; Prediction of PM localization by WoLF PSORT.	Soto et al., 2006; Lapointe et al., 2008; This study
Up-regulation of extracellular CA low DIC	Increased extracellular CA activity at low DIC/high pH; Up-regulation of δCA at low DIC	Nimer et al., 1997; This study
Localization of βCA to the chloroplast	Two βCAs from diatoms have been shown to localize to the chloroplast – specifically the pyrenoid; Chloroplast predicted location by WoLF PSORT.	Kitao et al., 2008 and Tachibana et al., 2011; This study
Probable absence of cytosolic CA	Cytosolic acidification at high HCO ₃ ⁻ - presence of CA would result in rapid buffering; Cytosolic CA would increase cytosolic CO ₂ leading to increased leakage at low external CO ₂ . Expression of a human CA in the cytoplasm of cyanobacteria resulted in a high CO ₂ requiring phenotype.	Price and Badger, 1989; Suffrian et al., 2011
Switching off of calcification at low DIC to increase inorganic carbon availability for photosynthesis	The decrease in calcification before a reduction in POC and growth rates. The complete termination of calcification at low DIC and pH _f	Bach et al., 2011; This study
HCO ₃ ⁻ is the principal substrate for calcification	Previous ¹⁴ C labeling studies; Strong correlation of calcification with HCO ₃ ⁻ concentration.	Sikes et al., 1980 and Nimer et al., 1997; Buitenhuis et al., 1999 and this study
The use of pH gradients within the CCM	Up-regulation of putative H ⁺ transporters at low DIC	Raven et al., 1997; This study
Increase in RubisCO	Up-regulation of RubisCO to compensate for its decrease in efficiency due to an increased oxygenase:carboxylase ratio at low CO ₂	This Study

Table SI: Applied Statistics. The data was analysed with either an ANOVA (A) in case of normal distribution or else with a PERMANOVA (P). Numbers in brackets behind P denote the number of permutations. Data that became normally distributed after BOX-COX transformation is assigned with the corresponding lambda value. Degrees of freedom (df). F- and p-values of ANOVA (F, p) or PERMANOVA (Pseudo-F, p(perm)). Bold values are statistically significant. β CA could not be analyzed since some replicates were below detection limit. Where there is a * the significance level was changed to 0.01 due to non-homogeneous variances.

Measured variable	constant pH, 7.74						constant pH, 8.34						constant CO ₂					
	method (perms)	Lambda	df	Pseudo-F	p/ p(perms)	Levene's p	method (perms)	Lambda	df	Pseudo-F	p/ p(perms)	Levene's p	method (perms)	Lambda	df	Pseudo-F	p/ p(perms)	Levene's p
growth rate	P(9956)		5	331.55	0.0001		P(9882)		5	2656.20	0.0001		A		4	13206.0	0.0005	0.022
POC production	P(9953)		5	346.44	0.0001		A		5	166563.0	0.0000	0.115	A		4	9833.0	0.0017	0.345
PIC production	P(9948)		5	332.86	0.0001		P(9956)		5	43.19	0.0001		A		4	383854.0	0.0000	0.079
C:N	A		5	11.54	0.0003	0.358	A		5	11.00	0.0004	0.243	A		4	1316.0	0.3287	0.072
AEL1	A	-0.74	5	8.80	0.0011	0.099	A	-0.68	5	5.24	0.0088	0.052	A	-0.62	4	4.99	0.0180	0.167
αCA1	A	-0.66	5	4.23	0.0190	0.018	A	-1.46	5	16.20	0.0001	0.079	A	-0.41	4	9.61	0.0019	0.180
αCA2	A		5	1.74	0.2001		A	-0.12	5	1.30	0.3253		A	-0.45	4	2.10	0.1555	
YCA	P(9945)		5	0.78	0.5722		A		5	0.61	0.6973		A	-1.39	4	3.28	0.0580	
δCA	P(9949)		5	20.45	0.0002		A	-0.88	5	9.29	0.0008	0.009	A	0.48	4	10.82	0.0012	0.419
Rubisco	A		5	3.19	0.0464	0.094	A	0.12	5	2.55	0.0855		A	-0.09	4	1.01	0.4469	
HVCN1	A	-0.53	5	0.32	0.8890		A		5	0.75	0.5993		A	-0.65	4	1.66	0.2358	
ATPvc/c	A	-0.98	5	11.62	0.0003	0.048	A	-0.89	5	8.27	0.0014	0.039	A	-0.67	4	8.96	0.0024	0.041
PATP	A	-0.30	5	5.36	0.0081	0.345	A	-1.25	5	8.31	0.0013	0.043	A	-0.24	4	3.90	0.0369*	0.013
CAX3	A	-0.65	5	8.89	0.0010	0.074	A	-1.85	5	11.22	0.0003	0.057	A	-0.07	4	6.03	0.0098	0.161
NhaA2	A	-1.66	5	110.60	0.0004	0.024	A	-2.05	5	5.50	0.0073	0.069	A	-0.71	4	5.35	0.0144	0.125
LCIX	A	-0.10	5	2.75	0.0699		A	-0.16	5	4.55	0.0171	0.056	A	-0.51	4	2.05	0.1635	
AQP2	A		5	0.21	0.9506		A	-0.08	5	0.08	0.9945		A	0.08	4	1.95	0.1786	
GPA	A	-0.66	5	8.92	0.0010	0.277	A		5	2.99	0.0558		A	0.17	4	2.81	0.0844	

Table SII. Target and Endogenous Reference Gene Information. Gene name, protein ID/accession number, primer sequence and amplicon size for the selected target genes.

Gene	Full Name	Protein ID/GenBank accession number ¹	Primer Name	Primer Sequence 5'-3'	Amplicon size	Reference
<i>EFG1</i>	Elongation Factor 1	462457	EFG1_F	GCT GGA AGA AGG ACT TTG TTG	101	Mackinder et al. 2011
			EFG1_R	TCC ACC AGT CCA TGT TCT TC		
<i>Actin</i>	Actin	S64188.1 ¹ , S64189.1 ¹ , S64190.1 ¹ , S64191.1 ¹ , S64192.1 ¹ , S64193.1 ¹	Actin_F	GAC CGA CTG GAT GGT CAA G	96	Mackinder et al. 2011
			Actin_R	GCC AGC TTC TCC TTG ATG TC		
<i>αTUB</i>	α Tubulin	Multiple Copy	αTUB_F	GCA TCG CCG AGA TCT ACT C	84	This Study
			αTUB_R	TCG CCG ACG TAC CAG TG		
<i>18S</i>	18S Ribosomal RNA	Ribosomal	18S_F	TGC AGG AGT TCC CGA CTC AC	62	Bruhn et al. 2010
			18S_R	CGG AGA CCG GTT TGG TTT CT		
<i>AEL1</i>	Anion Exchanger Like 1	99943	AEL1_F	TTC ACG CTC TTC CAG TTC TC	102	Mackinder et al. 2011
			AEL1_R	GAG GAA GGC GAT GAA GAA TG		
<i>αCA1</i>	α Carbonic Anhydrase 1	437452	αCA1_F	CTC TCC CAG TTC TTC GAT CAG	125	This Study
			αCA1_R	CCT CGC AAG CCG TAG TAA C		
<i>αCA2</i>	α Carbonic Anhydrase 2	456048	αCA2_F	AGA GCA GAG CCC TAT CAA CA	134	Richier et al. 2010
			αCA2_R	TCG TCT CGA AGA GCT GGA A		
<i>βCA</i>	β Carbonic Anhydrase	469462	βCA_F	ATG GAG CTG CTG CTC AAG TC	118	This Study
			βCA_R	GGT GCT CGC CAA AGA ATC		
<i>γCA</i>	γ Carbonic Anhydrase	432493	γCA_F	TCT CCG CCT CAG TCA ACC	106	Mackinder et al. 2011
			γCA_R	AAG TTG TCG ACT GTG CAA CC		
<i>δCA</i>	δ Carbonic Anhydrase	436031	δCA_F	ACG AGC ACG AGA TGT TCA AG	87	This Study
			δCA_R	TCT CGC CAA CCA TCA TCT C		
<i>RubisCO</i>	RubisCO	RbcL, Plastid	RB_F	CAA TCG GTC ACC CAG ATG GTA	100	Bruhn et al. 2010
			RB_R	GCG ATA TAA TCA CGG CCT TCG		
<i>HVCN1</i>	H ⁺ channel	631872	HVCN1_F	CAT GTT CCT CCG CTT GTG	109	Mackinder et al. 2011
			HVCN1_R	CCG CAG CTC CCT CAC TAC		
<i>ATPVc'/c</i>	Vacuolar-type H ⁺ pump	359783	ATPV_F	TAC GGC ACT GCA AAG TCT G	83	Mackinder et al. 2011
			ATPV_R	ACG GGG ATG ATG GAC TTC		
<i>PATP</i>	Plasma membrane type H ⁺ pump	67081	PATPase_F	GAG CAC AAG TTC CTC ATC GTC	105	This Study
			PATPase_R	CAC GTC GGC CTT CTT GAG		
<i>CAX3</i>	Ca ²⁺ /H ⁺ exchanger 3	416800	CAX3_F2	CTC CTC TGC GTC TTT GCA T	90	Mackinder et al. 2011
			CAX3_R2	GAG GGC GGT GAT GAG GTA		
<i>NhaA2</i>	Na ⁺ /H ⁺ exchanger 2	447659	NhaA2_F	CTC GTC TGC TAT GGC ATC TC	80	This Study
			NhaA2_R	GTT GCT CGC GTC CAT TC		
<i>LCIX</i>	Low CO ₂ induced gene	457739	LCIX_F	CAG CAG TCG TGG CTC AAG	94	This Study
			LCIX_R	CGT AAG CGA CGT GGA TCA G		
<i>AQP2</i>	Aquaporin 2	75635	AQP2_F	GCC TGG GTT CAA ATG GAA G	135	This Study
			AQP2_R	CCT TCT GTG GTT ACC GAG TG		
<i>GPA</i>	Ca ²⁺ binding	431830	gpaBR_F	AGG CCT TCT CCA GCA TCA T	70	Richier et al. 2009
			gpaBR_R	GTT CAG CGT GCT CTC CGA G		

CHAPTER 5. Ion transport associated with calcification and inorganic carbon acquisition in coccolithophores: Insights from the *Emiliana huxleyi* genome

Luke C. M. Mackinder*, Declan C. Schroeder, Ulf Riebesell, Colin Brownlee and Glen Wheeler

*Corresponding author: Luke C. M. Mackinder, lukcki@mba.ac.uk

Helmholtz-Zentrum für Ozeanforschung Kiel (GEOMAR), D-24105, Kiel, Germany (L.C.M.M., U.R.); Marine Biological Association of the UK, The Laboratory, Citadel Hill, Plymouth PL1 2PB, UK (L.C.M.M., G.W., D.C.S., C.B.); Plymouth Marine Laboratory, Prospect Place, Plymouth, PL1 3DH, UK (G.W.).

To be submitted to *BMC Genomics*

ABSTRACT

Background – Coccolithophores are unicellular marine phytoplankton, that by fixing inorganic carbon through photosynthesis and calcification play a major role in global carbon cycling. As the surface ocean CO₂ concentration increases due to the anthropogenic release of CO₂ both ocean acidification and ocean carbonation are taking place. To understand the impact of these ocean changes on coccolithophores, it is essential that we rapidly increase our knowledge of the cellular processes underlying coccolithophore physiology.

Results – This study analyzes the recently sequenced genome of the coccolithophore *Emiliania huxleyi* for genes involved in Ca²⁺, inorganic carbon (Ci) and H⁺ transport that are potentially involved in calcification and photosynthesis. Multiple genes encoding channels, exchangers, symporters, pumps and regulatory proteins were identified. This included the presence of genes exhibiting similarity to the low CO₂-induced B (LCIB) family of genes found in *Chlamydomonas reinhardtii*. This group of genes are an essential part of the carbon concentrating mechanism (CCM) in *Chlamydomonas*. They were previously thought to be confined to the green algae, but are widely distributed amongst eukaryotic phytoplankton. The presence of almost exclusively animal Na⁺/Ca²⁺ exchangers and plant-related Ca²⁺/H⁺ exchangers in the *E. huxleyi* genome indicates that coccolithophores have the potential to use both H⁺ and Na⁺ electrochemical gradients to drive secondary transport.

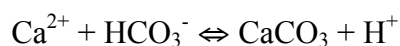
Conclusions - This study indicates that *E. huxleyi* has a diverse range of Ci, Ca²⁺ and H⁺ transporters, from classical plant, animal and bacterial families. The presence of LCIB-family proteins in coccolithophores suggests that this gene family arose in the common ancestral photosynthetic eukaryote, providing a basis for investigating the evolution of CCMs in eukaryotic algae. Finally, this work offers a strong platform for future research in coccolithophore physiology and evolution both critical to understanding how coccolithophores will adapt in a changing ocean.

INTRODUCTION

Coccolithophores are unicellular calcifying marine phytoplankton. The model species is *Emiliana huxleyi*, widely studied due to its global biogeochemical importance through the formation of extensive blooms that play a fundamental role in carbon cycling [1]. The recent sequencing of *E. huxleyi* strain CCMP1516 has made vast quantities of genomic data (<http://genome.jgi-psf.org/Emihu1/Emihu1.home.html>) available, which is driving the rapid advancement of coccolithophore cell biology research. The anticipated release of the genome paper along with current and future transcriptomic studies should provide an essential insight into coccolithophore physiology. This will aid in our understanding of how coccolithophores came to play a pivotal role in our current oceans and also their capacity to adapt and perform in the future ocean under pressures such as ocean acidification.

The genome will help in understanding the key biological question of the role and mechanisms of coccolithophore calcification - a process thought to be the basis of their evolutionary success. Apart from being an intriguing biological question, increased knowledge of the calcification process would aid in understanding why coccolithophores are sensitive to ocean acidification [2]. It would also be extremely beneficial in the understanding of the “vital effect” an unknown process that alters the Sr/Ca ratios in coccoliths relative to the surrounding seawater, making the interpretation of Sr/Ca ratios as a proxy for past coccolithophore productivity and calcification rates complex [3].

Calcification in coccolithophores is a stringently controlled process. The intracellular nature of calcification in an internal endomembrane compartment termed the coccolith vesicle (CV) means the complete isolation of calcite precipitation from the external seawater. This has posed three key cell physiological questions: 1) How are large quantities of Ca^{2+} transported from the external environment to the CV whilst Ca^{2+} homeostasis is maintained? [4, 5] 2) What is the mechanism of inorganic carbon (Ci) acquisition and its distribution between calcification and photosynthesis? [6] and 3) How do cells regulate cytosolic pH? This is potentially a major problem as utilizing HCO_3^- as the carbon source for calcification leads to an equimolar H^+ release (Equation 1) [7]. Multiple studies have focused on answering these questions, forming a strong basis of our knowledge of coccolithophore calcification and proposing feasible hypotheses. However, particularly at the molecular level, there are still many gaps in our knowledge.



Equation 1.

Acquiring the large quantities of Ca^{2+} required for calcification should not be a problem for coccolithophores. By maintaining a cytosolic Ca^{2+} concentration approximately 10^5 times lower than that of seawater, Ca^{2+} almost certainly enters down its electrochemical gradient through Ca^{2+} permeable channels into the cell [5]. However, once within the cell uptake into the CV poses a regulatory and energetic problem, requiring stringent control of cytosolic Ca^{2+} levels and active transport. Currently, there is good evidence from transcriptional studies for the involvement of a $\text{Ca}^{2+}/\text{H}^+$ exchanger (CAX3) [8, 9] potentially driven by H^+ gradients maintained by a vacuolar type ATPase H^+ pump [8, 10]. Substantial data supports HCO_3^- as the Ci source for calcification and CO_2 as the source for photosynthesis [reviewed in 6]. Whereas the majority of CO_2 is thought to enter through diffusion [11], the uptake of HCO_3^- is expected to require a certain level of active transport. Currently the sole transporter with supportive evidence for providing HCO_3^- for calcification is Anion Exchange Like 1 (AEL1), a putative HCO_3^- transporter belonging to the SoLute Carrier 4 (SLC4) family [8]. Alongside active Ci transport, carbonic anhydrases (CAs) play a fundamental role in carbon metabolism in photosynthetic organisms [12] and in calcification [13]. Two *E. huxleyi* CAs belonging to the γ and δ have been partially characterized in *E. huxleyi* with γ CA having a potential CV location [14] but its expression appears to be unrelated to cellular calcification [8]. H^+ transport and pH regulation is key to maintaining suitable environments for calcification and other cellular processes. With calcification being a strong source of H^+ , excess H^+ have to be buffered or removed. The identification and characterization of a voltage-gated H^+ channel (HVCN1) shows that it plays a fundamental role in pH homeostasis, removing H^+ produced from calcification out of the cytosol in coccolithophores [7].

As discussed, several of the genes involved in inorganic carbon uptake, calcification and related transport processes have been identified, however the majority of genes that perform these functions are unknown. The *E. huxleyi* genome is comprised of approximately 39,000 gene models, a large number compared to other algae (*Chlamydomonas reinhardtii* (referred to as *Chlamydomonas*): 15,143, *Ostreococcus tauri*: 8,166), plant (*Arabidopsis thaliana*: 26,341) and even human (~23,000) genomes, however it is expected that this number will decrease as the assembly and gene models improve with further sequencing and analysis. Of the current gene models ~1,250 are for transport related genes involved in all cellular processes. In depth analysis to provide a platform for further experimental work has the potential to identify 100's of key components involved in calcification and Ci uptake mechanisms. In this study we perform an *in silico* analysis of the *E. huxleyi* genome identifying through homology genes involved in Ca^{2+} , Ci and H^+ transport. The potential roles of these genes in calcification and carbon acquisition are discussed, hopefully stimulating further research to understand these fundamental processes and

their associated ion transport in coccolithophores.

RESULTS AND DISCUSSION

Ca²⁺ transport

In all eukaryotic cells, Ca²⁺ is a fundamental signaling molecule mediating numerous cellular processes. The ability of this molecule to successfully induce rapid intracellular responses is partly due to the diverse range of Ca²⁺-selective channels, pumps and exchangers that can elevate, dissipate and remove Ca²⁺, rapidly initiating and terminating downstream events. To maintain cytosolic [Ca²⁺] at ~100 nM [5] whilst performing calcification it is hypothesized that *E. huxleyi* uses a complex network of Ca²⁺ channels and transporters.

Sixteen putative Ca²⁺-permeable channels from 6 distinct families are present in the *E. huxleyi* genome that could potentially play a role in cellular Ca²⁺ uptake (Table I). Of these 7 belong to the Voltage-gated Ion Channel (VIC) superfamily which includes the 4-domain voltage-dependent Ca²⁺ channels (Ca_v), bacterial-type Na⁺ channels (Na_vBac) and two-pore Ca²⁺ channels (TPC). Of these 4 are Na_vBac channels, a group of classical bacterial Na⁺ channels that can have Ca²⁺ permeability. Na_vBac channels are absent from animals, green plants and red and green algae, only appearing in diatoms [15] and coccolithophores. Evidence for voltage gated Ca²⁺ uptake is supported by physiological data, with patch clamp electrophysiological experiments on *Coccolithus pelagicus* indicating plasma membrane (PM) depolarization-activated cation entry that could be Ca²⁺ mediated [16]. Also identified in the genome were 6 Transient Receptor Potential (TRP) channels, 2 inositol-1,4,5-trisphosphate receptor (IP₃R) channels and 1 cyclic nucleotide-gated channel (CNGC).

Once Ca²⁺ has entered the cell it is hypothesized that it is rapidly sequestered into the Golgi and/or endoplasmic reticulum (ER) derived endomembrane network that is potentially linked to a precursor of the CV [4, 17]. To ensure a low cytosolic Ca²⁺ level is maintained, this Ca²⁺ transit through the cytosol would have to be rapid and spatially separated from the bulk cytosol – possibly resulting in isolated Ca²⁺ elevated microenvironments in proximity to the PM. In animal cells rapid replenishment of endomembrane Ca²⁺ stores takes place via store-operated Ca²⁺ entry, which is mediated by Ca²⁺ release-activated Ca²⁺ current (CRAC) channels in the PM [18]. Analysis of the *E. huxleyi* genome for components of this mechanism failed to identify any gene homologues such as *Orai1* and *Stim1*. Instead it is thought that Ca²⁺ uptake into the endomembrane network is most likely driven by ATP requiring Ca²⁺ pumps and/or by exchangers using the electrochemical potential of other cations to drive the uphill transport of

Ca²⁺ against its electrochemical gradient.

The *E. huxleyi* genome contains a diverse range of primary and secondary energized Ca²⁺ transporters belonging to the P-ATPase superfamily of ATP driven ion translocators and cation/Ca²⁺ (CaCA) superfamily, respectively. P-type ATPases are a diverse group of transporters that carry out many fundamental cellular processes, including muscle contractions, maintenance of membrane potential, removal of toxic ions and cellular signaling. They can transport a wide range of molecules including small cations (H⁺, Ca²⁺, Na⁺, K⁺ and Mg²⁺), 'soft' transition metals (Cu⁺, Ag⁺, Cd²⁺, Pb²⁺ and Zn²⁺) and phospholipids [19]. Within the P-type ATPase superfamily, the type IIA and type IIB families are Ca²⁺ pumps. Type IIA ATPases belong to the ER-type Ca²⁺-ATPases (ECAs) that are generally ER located and play an essential role in maintaining the relatively high total Ca²⁺ concentration (5-10 mM) of the ER essential for ER biochemical processes and as a store for Ca²⁺ based signals [20].

Analysis of the *E. huxleyi* genome for Ca²⁺ transporting P-type ATPases identified 8 potential candidates (Table I). Phylogenetic tree analysis (Fig. 1) groups two of these (Joint Genome Institute number (JGI#) 522052 and 522053) with *Oryza sativa* and *Arabidopsis thaliana* type IIA Ca²⁺-ATPases. Expression of *EhECA2* (JGI# 522053) in relation to calcification was investigated in Mackinder et al. (2011) [8] with no clear-cut connection made. Although *EhECA2* was up-regulated in diploid calcifying cells relative to non-calcifying cells of strain CCMP1516, and down-regulated when Ca²⁺ was removed from the media, it was also up-regulated in non-calcifying haploid cells relative to isogenic diploid calcifying cells, indicating that its role is probably not limited to calcification. Surprisingly, no *E. huxleyi* proteins fell within the type IIB Ca²⁺-ATPase clade of autoinhibited Ca²⁺-ATPases (ACAs), a group that is highly represented in *A. thaliana* with a total of 10 ACAs that are generally associated with the PM playing essential homeostatic roles [20].

Three putative P-type ATPases (JGI# 62350, 101130 and 466567) formed a distinct group that did not fall within the type IIA or type IIB subfamily clades but showed highest similarities to type II ATPases possibly hinting towards them possessing Ca²⁺ transport properties. A comparative transcriptomic study by von Dassow et al. (2009) [9] mapped ESTs to 2 of these genes (JGI# 62350 and 466567) with the latter being more highly represented in diploid cells than haploid, indicating a potential role in Ca²⁺ transport in the diploid phase. A further 3 *E. huxleyi* proteins (JGI# 426283, 76123 and 67081) did not fall within the type II Ca²⁺-ATPases but grouped with the type IIIA H⁺-pumps, classing them as putative H⁺ pumps. It has to be noted that other P-type pumps belonging to families other than type II or type IIIA may have been missed using the applied screening approach.

Cation exchangers mediate Ca^{2+} transport across membranes by using the electrochemical gradient of an ion (generally H^+ , Na^+ or K^+) to drive the uphill transport of Ca^{2+} . Ca^{2+} exchangers belong to the CaCA superfamily, which is made up of 5 phylogenetic and functionally distinct groups: K^+ dependent $\text{Na}^+/\text{Ca}^{2+}$ exchangers (NCKX), K^+ independent $\text{Na}^+/\text{Ca}^{2+}$ exchangers (NCX), cation/ Ca^{2+} exchangers (CCX), $\text{Ca}^{2+}/\text{H}^+$ exchangers (CAX; also known as cation/ H^+ exchangers) and the bacterial and archaea YRBG transporters [21]. Genome and phylogenetic tree analysis of *E. huxleyi* indicates that it has sixteen exchangers belonging to the CaCA superfamily with members in all branches except the YRBG group (Table I, Fig. 2).

The *E. huxleyi* genome contains 3 putative NCKXs and 1 NCX (Table I) although the gene model for one NCKX protein (JGI# 354606) is severely truncated excluding it from further phylogenetic analysis. NCX and NCKX families are thought to be primarily of animal origin [21], with none present in the *A. thaliana* or *O. sativa* genomes. This is due to plants generally using H^+ gradients to drive secondary transport at the PM, whereas animals generally rely on Na^+ and K^+ electrochemical gradients [22]. One identified putative NCKX (JGI# 354606) was shown to be diploid specific with 8 expressed sequence tags (ESTs) (cluster ID: GS00463) present in the calcifying diploid state supporting a potential role in calcification [9].

Seven of the identified CaCA members fell within the CAX family of $\text{Ca}^{2+}/\text{H}^+$ exchangers (Fig. 2). CAXs are found in a wide range of taxa including fungi, plants, bacteria and most animals although they are absent from mammals, archaeobacteria and insects [23]. They were initially identified as fungi and plant $\text{Ca}^{2+}/\text{H}^+$ exchangers that reside in the vacuolar membrane to mediate Ca^{2+} removal from the cytosol [24], although it has now become clear that they transport a diverse range of cations in exchange for H^+ and some locate to other organelles [25]. Six of the CAX members contain the conserved GNxxE motif in the $\alpha 1$ and $\alpha 2$ region [21]. Whilst the seventh (JGI# 103021) shows high levels of similarity it varies slightly in the CAX signature region with SNxxE in the $\alpha 1$ region and GNxxT in the $\alpha 2$ region (Data not shown). The low affinity high capacity $\text{Ca}^{2+}/\text{H}^+$ exchange of CAXs makes them ideal candidates for the loading of endomembrane compartments for calcification following localized Ca^{2+} elevation in the cytosol. By using a H^+ gradient generated by the H^+ production of calcification and the action of H^+ -pumps, CAX proteins could be a rapid and energy efficient mechanism for the loading of Ca^{2+} into the CV precursor and endomembrane network [17]. *E. huxleyi* CAX3 has been putatively associated with calcification whilst CAX4 transcription is not regulated by calcification [8]. Two of the CAXs are nearly identical at both the DNA and protein level (JGI# 66584 and 315097) and are potentially gene duplications or a genome assembly error. Six out of

the 7 have EST data indicating that they are actively expressed and show varying haploid and diploid expression specificity [9](Table I).

Also present in the *E. huxleyi* genome are 2 CaCA proteins (JGI# 203920 and 449053) belonging to the CCX family of proteins with unknown substrate specificities [21], and 3 proteins (JGI# 461099, 219401 and 199067) that do not fall within any of the CaCA subfamilies (Fig. 2).

The presence of several H⁺ coupled and Na⁺ coupled transporters in *E. huxleyi* indicates that coccolithophores potentially rely on both H⁺ and Na⁺ gradients for Ca²⁺ transport. It can be hypothesized that H⁺ gradients most probably drive Ca²⁺ uptake into endomembrane systems whereas Na⁺ gradients would be used at the PM for Ca²⁺ efflux. Therefore, taking advantage of the high Na⁺ concentration of their surrounding environment to drive secondary transport across the PM. It is also feasible that the ability to use both H⁺ and Na⁺ gradients could have given coccolithophores an evolutionary advantage to deal with large and controlled Ca²⁺ fluxes through the cell essential for calcification whilst maintaining Ca²⁺ at optimum levels for cellular signaling.

Inorganic carbon transport

Unlike most photosynthetic organisms, coccolithophores have two large cellular demands for Ci - photosynthesis and calcification. Carbon fixation into calcite can equal and even exceed that of organic carbon fixation [26] potentially placing a large pressure on the cell to maintain adequate Ci uptake rates. Our understanding of Ci transport in algae is principally based on studies in non-calcifying algae, with the basis of our knowledge coming from work on the green algae *Chlamydomonas*, diatoms and cyanobacteria. It is known that *E. huxleyi* operates a low affinity Ci uptake mechanism in comparison to investigated species of diatoms, non-calcifying Haptophytes, green algae and cyanobacteria [27-29]. Although of low affinity, this uptake system is regulated by Ci availability [27] and involves active transport of HCO₃⁻ and potentially CO₂ [11, 27]. At ambient Ci levels, external CO₂ is the substrate for photosynthesis [11, 27, 30, 31] and HCO₃⁻ for calcification [30, 31]. Multiple genes involved in Ci transport and metabolism are present in the genome (Table I).

Active HCO₃⁻ transport in mammalian cells is predominantly via SLC4 and SLC26A family proteins [32]. *E. huxleyi* possesses 8 putative SLC4 and 5 putative SLC26A transporters (Table I). It is thought that SLC4 and SLC26A transporters have distinct evolutionary origins [33] with phylogenetic analysis of putative SLC4 and SLC26A transporters highlighting this (Fig. 3). None of the *E. huxleyi* SLC4 transporters fall within the well-characterized

electroneutral $\text{Cl}^-/\text{HCO}_3^-$ exchangers or the Na^+ -coupled HCO_3^- transporters from metazoans. However, 4 (JGI# 120259, 99943, 198643 and 200137) group with the photosynthetic marine picoeukaryote *Micromonas* sp. forming their own clade distinct from the metazoan HCO_3^- transporters but also distinct from borate transporters identified in a wide range of species (Fig. 3). These paralogs are structurally very similar, showing 81% amino acid similarity (excluding the C terminal tail of JGI# 120259), with only large variations at the N and C terminals along with several amino acid changes and insertions/deletions at intron exon boundaries (data not shown). The similarity at the nucleotide level is highlighted by data from von Dassow et al. (2009) [9] showing that reads from the same cluster IDs hit all 4 genes (Table I). Bearing this in mind, they are probably derived from recent gene duplication events or may be genome assembly errors (i.e. represent the same gene). Members of this group of SLC4 genes have been shown to increase in expression during calcification [8, 9, 34]. This, along with the support of inhibitor studies [35] provides strong evidence that this family plays a key role in Ci supply for calcification and photosynthesis. However, further characterization is essential to determine their HCO_3^- affinity, stoichiometry and cellular role in coccolithophores. SLC4 proteins are also known to have borate transport capabilities [36, 37] with two *E. huxleyi* transporters (JGI# 436956 and 466232) grouping with borate transporting proteins (Fig. 3).

SLC26A transporters were originally identified as sulfate transporters [38], however increasing experimental data has shown that many facilitate HCO_3^- transport [33]. Five putative SLC26A transporters were identified in the genome. Two of these (JGI# 249865 and 441761) grouped with a alkaliphilic bacteria BicA and a cyanobacterial BicA, which is a known Na^+ dependent HCO_3^- transporter [39] (Fig. 3). Whether the *E. huxleyi* homologues are selective for HCO_3^- or sulfate requires further experimental data. However, their role in providing Ci for calcification is unlikely, as expression of both JGI# 249865 and 441761 appears to be higher in non-calcifying haploid cells than calcifying diploid cells [9, 34]. Of the other 3 putative SLC26A transporters, JGI# 453061 branches off at the base where the human SLC26A $\text{Cl}^-/\text{HCO}_3^-$ transporters and the BicA transporters diverge, and 2 structurally similar *E. huxleyi* transporters (JGI# 460215 and 455488) are phylogenetically distinct from the other investigated SLC4 and SLC26A members.

Depending on the coupled ion, SLC4 and SLC26A transporters require Cl^- or Na^+ electrochemical gradients to drive transport. It is expected that in coccolithophores there is a strong inwards Na^+ electrochemical gradient that could drive HCO_3^- uptake through symport. In mammalian cells Na^+ gradients across the PM are primarily maintained by Na^+/K^+ ATPases. In addition to Na^+/K^+ ATPases coccolithophores could also potentially use NCX or NCKX

proteins, which use the strong Ca^{2+} gradient to drive Na^+ efflux, or Na^+ pumps that use ATP to maintain Na^+ gradients. If Cl^- was the coupled ion, elevated cytosolic Cl^- could be maintained through H^+/Cl^- exchange by Chloride Channel (ClC) family proteins [40, 41], of which there are 7 present in the genome (data not shown).

Due to the importance of HCO_3^- transporters in supplying Ci for photosynthesis, several have been characterized from the model microalgae *Chlamydomonas* and the widely studied cyanobacteria. Examination of the *E. huxleyi* genome for cyanobacterial Ci transporters (other than BicA) yielded negative results with the absence (no hits from BlastP $< E^{-05}$) of protein homologues to SbtA, a high affinity Na^+ dependent HCO_3^- transporter [42], BCT1 (cmpA) an inducible HCO_3^- transporter belonging to the ABC superfamily [43] and NDH-I a multimeric CO_2 uptake system [44]. In *Chlamydomonas* a number of transporters have been identified as low Ci-inducible genes with several shown to have important roles related to Ci transport [45]. Exploration for genes exhibiting similarity in *E. huxleyi* identified multiple candidates with similarities to low CO_2 induced A (LCIA), low CO_2 induced B (LCIB) and multi-drug resistant 1 (MRP1/HLA3) proteins. Four homologues to LCIA were identified in the genome (Table I). *Chlamydomonas* LCIA belongs to the FNT family of transporters mostly associated with nitrite transport. It was initially proposed as a potential HCO_3^- transporter due to its regulation by CO_2 availability rather than nitrogen source and its predicted chloroplast location [46]. Expression in *Xenopus* oocytes confirmed its ability to transport HCO_3^- , however it also had nitrite transport capacity [47]. Of the four FNT proteins identified in *E. huxleyi* one has a severely truncated C-terminus gene model and was not included in the phylogenetic analysis. Of the other 3, only one (JGI# 64600) showed similarity to CrLCIA, although a monophyletic origin was not supported by boot-strapping values (Fig. 4). Furthermore, as the majority of FNT genes are involved in nitrite transport, its role in HCO_3^- uptake is tenuous. Searches for MRP1/HLA3, a member of the ATP-binding cassette family (ABC), homologues returned >100 potential hits. A large percentage of these are gene duplicates potentially due to genome assembly errors. Phylogenetic analysis indicates a diverse range of proteins with 2 members (JGI# 264051 and 40721) showing a relatively high similarity to MRP1/HLA3 (data no shown).

In *Chlamydomonas*, genes belonging to the LCIB family are known to form an essential part of the carbon concentrating mechanism (CCM). *Chlamydomonas* mutants lacking *LciB* have an “*air-dier*” phenotype, where they show wild-type growth at high and very low CO_2 but fail to acclimate to air levels of CO_2 resulting in a fatal phenotype [48]. Although the function of LCIB and other family members is unknown, its chloroplastic location and predicted solubility indicate a potential regulatory role in Ci transport [45]. As these genes were previously thought to be confined to green microalgae [49], the presence of 3 putative LCIB family homologues in *E.*

huxleyi (JGI# 121287, 238489 and 285668) is very interesting. Searches for homologues in other organisms identified putative members in other unicellular algae including the diatoms *Phaeodactylum tricornutum* and *Thalassiosira pseudonana* and the green algae *O. tauri*, *Ostreococcus lucimarinus*, *Volvox carteri*, *Chlorella variabilis* and *Micromonas pusilla*. ClustalW alignments show that they have a conserved N terminus region with other putative LCIB-type proteins but limited or no similarity at the C-terminus (Fig. 5). Figure 6 indicates that LCIB proteins fall within 2 clades, those of the Archaeplastida (Green algae) and the Chromalveolates (diatoms and coccolithophores). Whether related through divergent or convergent evolution is uncertain, with further sequences from microalgae belonging to the Rhizaria, Alveolate and Stramenopile divisions [50] necessary. If through divergent evolution, this gene family would have been present in ancestral photosynthetic algae prior to the secondary endosymbiosis events, which led to photosynthesis in the Chromalveolates [51]. Providing an interesting gene for investigating the evolution of CCMs in eukaryotes.

CAs are known key components of Ci carbon metabolism in all organisms catalysing the reversible hydration of CO_2 to HCO_3^- . Genome analysis shows that *E. huxleyi* has 9 putative CAs belonging to the α (4), β (1), γ (2) and δ (2) families (Table I). This is similar to the diatom CA repertoire with *P. tricornutum* also having 9 CAs spreading across the same 4 families and *T. pseudonana* possessing 13 CAs belonging to the α , β , γ , δ and ζ families [52]. There are also strong similarities with *Chlamydomonas*, with 10 putative CAs in its genome belonging to the α , β and γ families [45]. No CAs belonging to the cadmium binding ζ family [53] were found in the *E. huxleyi* genome. Interestingly one of the δ CAs (JGI# 469783) is potentially fused to a SLC4-type HCO_3^- transporter, however the gene model requires further experimental data to confirm this. The understanding of the roles of CAs in Ci uptake for photosynthesis is gradually becoming clearer [12, 54] but whether they play a fundamental role in Ci transport for coccolithophore calcification is unclear.

Although membranes are permeable to small uncharged molecules like CO_2 , diffusion rates can be increased through the presence of selective channels [55]. CO_2 selective aquaporin and Rhesus proteins have been found in plants and animals [56]. With the tobacco aquaporin NtAQP1 demonstrated to substantially enhance the CO_2 permeability of the PM and innerchloroplast membrane of tobacco leaf cells [55, 57] and human AQP1 shown to increase the CO_2 permeability of the PM [58]. Also a Rhesus protein (RHP) found in *Chlamydomonas* functions as a bidirectional CO_2 channel, which is essential for wild-type growth at high CO_2 when the CCM is not active [56]. Close examination of the *E. huxleyi* genome indicates the absence of Rhesus proteins, however 7 putative aquaporins/aquaglyceroporins are present. Phylogenetic analysis identified 3 of these as putative *E. huxleyi* aquaporin proteins that show a

relatively close similarity to NtAQP1 (Fig. 7). With protein ID 458101 being up-regulated in calcifying diploid cells vs. haploid cells [9].

H⁺ transport

Calcification and Ci carbon metabolism both require highly regulated pH within specific endomembrane compartments. In calcification pH has a direct effect on the calcite saturation state, therefore by regulating pH in conjunction with regulatory organic molecules (i.e. acidic polysaccharides [59]) the cell can exert control over calcite precipitation. H⁺ transporting genes belong to a wide variety of families. These can be broadly classed into two groups, those energized directly by ATP or pyrophosphate (PPi; H⁺ pumps) and those driven by an electrochemical gradient of a coupled ion (exchangers/symporters). The *E. huxleyi* genome encompasses H⁺ pumps from three major families, the P-type ATPases, V-type ATPases and the H⁺-pyrophosphatases (H⁺-PPases). V-type ATPases are multi-subunit proteins containing up to 14 polypeptides forming an integral V₀ and peripheral V₁ subcomplex [60]. V-ATPases are thought to be present in virtually every eukaryotic cell [60], with *E. huxleyi* being no exception by possessing the necessary subunits to form a complete V-ATPase complex (Table I). V-ATPases are primarily involved in the acidification of intracellular compartments to support secondary transport and cellular processes such as proteolytic cleavage [60]. Microarray data from a haploid vs. diploid comparison indicates that multiple subunits are up-regulated in the calcifying diploid stage, with quantitative reverse-transcriptase PCR showing that ATPVA (JGI# 439538) was >1,000 fold up-regulated in diploid cells [34]. Furthermore the immunolocalization of V-ATPase subunit ATPVc/c' to the CV [10] in conjunction with calcification linked expression of this subunit [8] indicates a role for a V-type ATPase in calcification, potentially by maintaining a H⁺ gradient to drive Ca²⁺/H⁺ exchange [17].

Whereas V-type ATPases are multimeric, P-type H⁺-ATPases and H⁺-PPases are monomeric. Due to the similarity of P-type Ca²⁺ ATPases and P-type H⁺ ATPases, 3 P-type-III A H⁺-ATPases were identified in the blast searches using characterized Ca²⁺-ATPases (Table I, Fig.1, see *Ca²⁺ transport* section). In plants P-type H⁺-pumps are almost solely located to the PM [19] where they play a fundamental role in maintaining pH homeostasis and in control of the membrane potential. Unless it is regulated, the increased production of H⁺ during calcification (Equation 1) would alter these fundamental housekeeping processes. Rokitta et al. (2011) [34] identified the up-regulation of a putative P-type H⁺-ATPase (JGI# 426283) in calcifying diploid cells indicating a potential role in the maintenance of cytosolic pH. H⁺-PPases are found in vacuolar, Golgi and PM membranes where they form homodimers that use the energy of the

phosphoanhydride bond of PPi to drive H⁺ transport [61]. Four H⁺-PPases were identified in the genome of which 2 have EST evidence from diploid calcifying cells, with JGI# 439740 potentially preferentially expressed in diploid cells [9] (Table I). Secondary H⁺ transporters play an influential role in cellular pH regulation. Although not a focus of this analysis, unless directly related to Ca²⁺ transport, multiple members coupled to a wide range of ions are present in the genome including 10 Na⁺/H⁺ exchangers with 6 belonging to the eukaryotic Na⁺/H⁺ exchangers (NHE/NHX) and 4 to the bacterial Na⁺/H⁺ exchanger family (Nha) along with 4 highly conserved K⁺/H⁺ transporters.

H⁺ transport is not solely confined to pumps and exchangers but can also be mediated by channels. The identification and characterization of a voltage-gated H⁺ channel, HVCN1, from both *C. pelagicus* and *E. huxleyi* highlights the importance of rapid H⁺ efflux in pH homeostasis during calcification (Table I) [7].

Conclusions

Calcification and its associated transport is a complex process requiring multiple genes with diverse functions. Analysis of the genome has identified a large and diverse group of genes involved in the transport of Ci, Ca²⁺ and H⁺ that could play fundamental roles in calcification and Ci supply for photosynthesis. The presence of transport proteins classically found in bacteria (i.e. Na_vBac channels and Nha Na⁺/H⁺ exchangers) and animals (i.e. NCKX and NCX exchangers) is of particular interest indicating that coccolithophores may have ion transport properties not generally associated with plants/algae. If coccolithophores use both H⁺ and Na⁺ gradients to drive secondary transport it could be hypothesized that H⁺ driven exchangers such as CAX function in endomembranes using the low pH of the ER, Golgi or vacuole to drive counter ion uptake. Whereas Na⁺ coupled exchangers could function in the PM using the strong inward Na⁺ gradient to drive the efflux of toxic ions (i.e. Ca²⁺) or the uptake of essential substrates (i.e. HCO₃⁻).

The presence of multiple Ci transport and metabolism genes in the *E. huxleyi* genome that are homologous to genes found in *Chlamydomonas* and diatoms indicates that fundamental cellular processes underlying Ci acquisition may be conserved between these species. This is further supported by the discovery of LCIB-family homologues suggesting that this gene family was present in the common ancestral primary endosymbiont. Therefore some key components of eukaryotic algal CCMs may have been conserved since the evolution of the “red” algal lineage ~1.2 billion years ago [51].

Whole genome transcriptomic approaches combined with physiological characterization of individual genes and gene families is now essential to understand the fundamental cellular processes underlying calcification and Ci uptake in coccolithophores. Furthermore due to the lowering of seawater pH and increase in Ci through the uptake of anthropogenic released CO_2 by the oceans [62], the understanding of the molecular components behind calcification, pH regulation and Ci acquisition are essential in understanding the response of coccolithophores in the future ocean.

MATERIALS AND METHODS

Ca²⁺ transport - The *E. huxleyi* genome (<http://genome.jgi-psf.org/Emihu1/Emihu1.home.html>) was analysed for Ca^{2+} pumps, exchangers and channels (Table 1). To identify potential P-type Ca^{2+} -ATPases and H^+ -ATPases, AtECA1, OsECA1, AtACA1 and AtAHA1 protein sequences were blasted against *E. huxleyi* protein models using BlastP. Hits with E-value scores lower than 1×10^{-10} were used for further analysis. Retained sequences were checked and any duplicates, originating from allelic copies or potential genome assembly errors, and severely truncated gene models were removed. The remaining sequences were aligned with P-type ATPases from *A. thaliana* and *O. sativa* using ClustalW and non-conserved regions were deleted. CaCA exchangers and Ca^{2+} channels were identified in the *E. huxleyi* genome from BlastP searches using characterized family members. Identified putative *E. huxleyi* CaCAs were aligned with CaCA proteins from the literature using ClustalW. The $\alpha 1$ and $\alpha 2$ conserved domains of CaCA proteins were used for the CaCA tree construction. Phylogenetic analysis was performed using the minimum evolution function in MEGA version 4 [63] to investigate protein function and classification.

Inorganic carbon transport – Potential transporters belonging to the SLC4 and SLC26A families in the *E. huxleyi* genome were identified using BlastP of known characterized family members from both families (e.g. HsAE1, HsSLC26A4) against the *E. huxleyi* genome. The same E-values and gene model stringency checks were carried out as above. All identified *E. huxleyi* protein sequences were aligned using ClustalW with characterized and other representative SLC4 and SLC26A proteins available from databases and other genome websites. Phylogenetic tree analysis was performed as above. Two CAs have previously been cloned from *E. huxleyi* [14]. Further CAs were identified through the same process as above, using characterized representative members from each of the five families (α , β , γ , δ and ζ) to blast against the *E. huxleyi* genome. Aquaporins in the genome were found by blasting characterized plant and

human members against the genome, with phylogenies constructed as described above. The presence of potential Cl^- transport proteins belonging to other gene families was investigated. Genes expressing proteins with homology to two cyanobacteria HCO_3^- transporters BCT1 and SbtA were not found. Rhesus family proteins were also absent.

H⁺ transport – Due to H^+ pumps belonging to the P-type ATPases family having a relatively high degree of similarity to P-type Ca^{2+} pumps these were analysed alongside the P-type Ca^{2+} pumps. PPase H^+ pumps were identified through BlastP searches using *A. thaliana* AVP2 and the bacterium *Streptomyces coelicolor* ScPP. Feasible gene models were checked as described above. V-ATPases are comprised of up to 14 subunits with genome annotation having identified the presence of all necessary subunits for a functional transporter.

REFERENCES

1. Tyrrell T, Young JR: **Coccolithophores**. In: *Encyclopedia of Ocean Sciences*. Edited by Steele JH, Turekian KK, Thorpe SA, 2 edn. San Diego: Academic Press; 2009: 3568-3576.
2. Riebesell U, Zondervan I, Rost B, Tortell PD, Zeebe RE, Morel FMM: **Reduced calcification of marine plankton in response to increased atmospheric CO₂**. *Nature* 2000, **407**(6802):364-367.
3. Langer G, Gussone N, Nehrke G, Riebesell U, Eisenhauer A, Kuhnert H, Rost B, Trimborn S, Thoms S: **Coccolith Strontium to Calcium Ratios in *Emiliana huxleyi*: The Dependence on Seawater Strontium and Calcium Concentrations**. *Limnol Oceanogr* 2006, **51**(1):310-320.
4. Berry L, Taylor AR, Lucken U, Ryan KP, Brownlee C: **Calcification and inorganic carbon acquisition in coccolithophores**. *Funct Plant Biol* 2002, **29**(3):289-299.
5. Brownlee C, Davies M, Nimer N, Dong LF, Merrett MJ: **Calcification, photosynthesis and intracellular regulation in *Emiliana huxleyi***. *Bull Inst Oceanogr Monaco* 1995, **14**:19-35.
6. Paasche E: **A review of the coccolithophorid *Emiliana huxleyi* (Prymnesiophyceae), with particular reference to growth, coccolith formation, and calcification-photosynthesis interactions**. *Phycologia* 2002, **40**(6):503-529.
7. Taylor AR, Chrachri A, Wheeler G, Goddard H, Brownlee C: **A voltage-gated H⁺ channel underlying pH homeostasis in calcifying coccolithophores**. *PLoS Biol* 2011, **9**(6):e1001085.

8. Mackinder L, Wheeler G, Schroeder D, von Dassow P, Riebesell U, Brownlee C: **Expression of biomineralization-related ion transport genes in *Emiliana huxleyi*.** *Environ Microbiol* 2011, **13**(12):3250–3265.
9. von Dassow P, Ogata H, Probert I, Wincker P, Da Silva C, Audic S, Claverie JM, de Vargas C: **Transcriptome analysis of functional differentiation between haploid and diploid cells of *Emiliana huxleyi*, a globally significant photosynthetic calcifying cell.** *Genome Biol* 2009, **10**(10):R114.
10. Corstjens PLAM, Araki Y, González EL: **A coccolithophorid calcifying vesicle with a vacuolar-type ATPase proton pump: cloning and immunolocalisation of the V₀ subunit c¹.** *J Phycol* 2001, **37**(1):71-78.
11. Schulz KG, Rost B, Burkhardt S, Riebesell U, Thoms S, Wolfgladrow DA: **The effect of iron availability on the regulation of inorganic carbon acquisition in the coccolithophore *Emiliana huxleyi* and the significance of cellular compartmentation for stable carbon isotope fractionation.** *Geochim Cosmochim Acta* 2007, **71**(22):5301-5312.
12. Badger M: **The roles of carbonic anhydrases in photosynthetic CO₂ concentrating mechanisms.** *Photosynth Res* 2003, **77**:83-94.
13. Weiss IM, Marin F: **The Role of Enzymes in Biomineralization Processes.** In: *Biomineralization*. John Wiley & Sons, Ltd; 2008: 71-126.
14. Soto AR, Zheng H, Shoemaker D, Rodriguez J, Read BA, Wahlund TM: **Identification and preliminary characterization of two cDNAs encoding unique carbonic anhydrases from the marine alga *Emiliana huxleyi*.** *Appl Environ Microbiol* 2006, **72**(8):5500-5511.
15. Verret F, Wheeler G, Taylor AR, Farnham G, Brownlee C: **Calcium channels in photosynthetic eukaryotes: implications for evolution of calcium-based signalling.** *New Phytol* 2010, **187**(1):23-43.
16. Taylor AR, Brownlee C: **A Novel Cl⁻ Inward-Rectifying Current in the Plasma Membrane of the Calcifying Marine Phytoplankton *Coccolithus pelagicus*.** *Plant Physiol* 2003, **131**:1391-1400.
17. Mackinder L, Wheeler G, Schroeder D, Riebesell U, Brownlee C: **Molecular Mechanisms Underlying Calcification in Coccolithophores.** *Geomicrobiol J* 2010, **27**(6):585 - 595.
18. Parekh AB, Putney JW: **Store-Operated Calcium Channels.** *Physiol Rev* 2005, **85**(2):757-810.

19. Kuhlbrandt W: **Biology, structure and mechanism of P-type ATPases.** *Nat Rev Mol Cell Biol* 2004, **5**(4):282-295.
20. Sze H, Liang F, Hwang I, Curran AC, Harper JF: **Diversity and regulation of plant Ca²⁺ pumps: Insights from expression in yeast.** *Annu Rev Plant Physiol Plant Mol Biol* 2000, **51**:433-462.
21. Cai X, Lytton J: **The Cation/Ca²⁺ Exchanger Superfamily: Phylogenetic Analysis and Structural Implications.** *Mol Biol Evol* 2004, **21**(9):1692-1703.
22. Sze H, Li X, Palmgren MG: **Energization of Plant Cell Membranes by H⁺-Pumping ATPases: Regulation and Biosynthesis.** *Plant Cell* 1999, **11**(4):677-690.
23. Manohar M, Shigaki T, Hirschi KD: **Plant cation/H⁺ exchangers (CAXs): biological functions and genetic manipulations.** *Plant Biology* 2011, **13**(4):561-569.
24. Hirschi KD, Zhen RG, Cunningham KW, Rea PA, Fink GR: **CAX1, an H⁺/Ca²⁺ antiporter from Arabidopsis.** *PNAS* 1996, **93**:8782-8786.
25. Manohar M, Mei H, Franklin AJ, Sweet EM, Shigaki T, Riley BB, MacDiarmid CW, Hirschi K: **Zebrafish (*Danio rerio*) Endomembrane Antiporter Similar to a Yeast Cation/H⁺ Transporter Is Required for Neural Crest Development.** *Biochemistry* 2010, **49**(31):6557-6566.
26. Langer G, Geisen M, Baumann K-H, Kläs J, Riebesell U, Thoms S, Young JR: **Species-specific responses of calcifying algae to changing seawater carbonate chemistry.** *Geochemistry Geophysics Geosystems* 2006, **7**(9):10.1029/2005gc001227.
27. Rost B, Riebesell U, Burkhardt S, Sültemeyer D: **Carbon Acquisition of Bloom-Forming Marine Phytoplankton.** *Limnol Oceanogr* 2003, **48**(1):55-67.
28. Trimborn S, Wolf-Gladrow D, Richter K-U, Rost B: **The effect of pCO₂ on carbon acquisition and intracellular assimilation in four marine diatoms.** *J Exp Mar Biol Ecol* 2009, **376**(1):26-36.
29. Giordano M, Beardall J, Raven JA: **CO₂ concentrating mechanisms in algae: Mechanisms, Environmental Modulation, and Evolution.** *Annu Rev Plant Biol* 2005, **56**(1):99-131.
30. Nimer NA, Merrett MJ: **Calcification and utilization of inorganic carbon by the coccolithophorid *Emiliania huxleyi* Lohmann.** *New Phytol* 1992, **121**(2):173-177.
31. Sikes CS, Roer RD, Wilbur KM: **Photosynthesis and coccolith formation - inorganic carbon-sources and net inorganic reaction of deposition.** *Limnol Oceanogr* 1980, **25**(2):248-261.
32. Romero M, Fulton C, Boron W: **The SLC4 family of HCO₃ - transporters.** *Pflug Arch Eur J Phy* 2004, **447**(5):495-509.

33. Cordat E, Casey JR: **Bicarbonate transport in cell physiology and disease.** *Biochem J* 2009, **417**:423–439.
34. Rokitta SD, de Nooijer LJ, Trimborn S, de Vargas C, Rost B, John U: **Transcriptome Analyses Reveal Differential Gene Expression Patterns between the Life-Cycle Stages of *Emiliana huxleyi* (Haptophyta) and Reflect Specialization to Different Ecological Niches.** *J Phycol* 2011, **47**(4):829-838.
35. Herfort L, Thake B, Roberts J: **Acquisition and use of bicarbonate by *Emiliana huxleyi*.** *New Phytol* 2002, **156**(3):427-436.
36. Takano J, Noguchi K, Yasumori M, Kobayashi M, Gajdos Z, Miwa K, Hayashi H, Yoneyama T, Fujiwara T: **Arabidopsis boron transporter for xylem loading.** *Nature* 2002, **420**(6913):337-340.
37. Park M, Li Q, Shcheynikov N, Zeng W, Muallem S: **NaBC1 Is a Ubiquitous Electrogenic Na⁺-Coupled Borate Transporter Essential for Cellular Boron Homeostasis and Cell Growth and Proliferation.** *Mol Cell* 2004, **16**(3):331-341.
38. Markovich D: **Physiological roles and regulation of mammalian sulfate transporters.** *Physiol Rev* 2001, **81**(4):1499-1533.
39. Price GD, Woodger FJ, Badger MR, Howitt SM, Tucker L: **Identification of a SulP-type bicarbonate transporter in marine cyanobacteria.** *PNAS* 2004, **101**(52):18228-18233.
40. Miller C: **ClC chloride channels viewed through a transporter lens.** *Nature* 2006, **440**(7083):484-489.
41. Scheel O, Zdebik AA, Lourdel S, Jentsch TJ: **Voltage-dependent electrogenic chloride/proton exchange by endosomal CLC proteins.** *Nature* 2005, **436**(7049):424-427.
42. Shibata M, Katoh H, Sonoda M, Ohkawa H, Shimoyama M, Fukuzawa H, Kaplan A, Ogawa T: **Genes essential to sodium-dependent bicarbonate transport in cyanobacteria: function and phylogenetic analysis.** *J Biol Chem* 2002, **277**(21):18658-18664.
43. Omata T, Price GD, Badger MR, Okamura M, Gohta S, Ogawa T: **Identification of an ATP-binding cassette transporter involved in bicarbonate uptake in the cyanobacterium *Synechococcus* sp. strain PCC 7942.** *PNAS* 1999, **96**(23):13571-13576.
44. Shibata M, Ohkawa H, Kaneko T, Fukuzawa H, Tabata S, Kaplan A, Ogawa T: **Distinct constitutive and low-CO₂-induced CO₂ uptake systems in cyanobacteria: Genes**

- involved and their phylogenetic relationship with homologous genes in other organisms. *PNAS* 2001, **98**(20):11789-11794.
45. Spalding MH: **Microalgal carbon-dioxide-concentrating mechanisms: *Chlamydomonas* inorganic carbon transporters.** *J Exp Bot* 2008, **59**(7):1463-1473.
46. Miura K, Yamano T, Yoshioka S, Kohinata T, Inoue Y, Taniguchi F, Asamizu E, Nakamura Y, Tabata S, Yamato KT *et al*: **Expression Profiling-Based Identification of CO₂-Responsive Genes Regulated by CCM1 Controlling a Carbon-Concentrating Mechanism in *Chlamydomonas reinhardtii*.** *Plant Physiol* 2004, **135**(3):1595-1607.
47. Mariscal V, Moulin P, Orsel M, Miller AJ, Fernandez E, Galvan A: **Differential regulation of the *Chlamydomonas* Nar1 gene family by carbon and nitrogen.** *Protist* 2006, **157**(4):421-433.
48. Wang Y: **An inorganic carbon transport system responsible for acclimation specific to air levels of CO₂ in *Chlamydomonas reinhardtii*.** *PNAS* 2006, **103**(26):10110-10115.
49. Grossman AR, Croft M, Gladyshev VN, Merchant SS, Posewitz MC, Prochnik S, Spalding MH: **Novel metabolism in *Chlamydomonas* through the lens of genomics.** *Curr Opin Plant Biol* 2007, **10**(2):190-198.
50. Baldauf SL: **An overview of the phylogeny and diversity of eukaryotes.** *Journal of Systematics and Evolution* 2008, **46**(3):263-273.
51. Falkowski PG, Katz ME, Knoll AH, Quigg A, Raven JA, Schofield O, Taylor FJ: **The evolution of modern eukaryotic phytoplankton.** *Science* 2004, **305**(5682):354-360.
52. Tachibana M, Allen A, Kikutani S, Endo Y, Bowler C, Matsuda Y: **Localization of putative carbonic anhydrases in two marine diatoms, *Phaeodactylum tricoratum* and *Thalassiosira pseudonana*.** *Photosynth Res* 2011, **109**(1):205-221.
53. Lane TW, Saito MA, George GN, Pickering IJ, Prince RC, Morel FMM: **Biochemistry A cadmium enzyme from a marine diatom.** *Nature* 2005, **435**(7038):42-42.
54. Moroney J, Ma Y, Frey W, Fusilier K, Pham T, Simms T, DiMario R, Yang J, Mukherjee B: **The carbonic anhydrase isoforms of *Chlamydomonas reinhardtii*: intracellular location, expression, and physiological roles.** *Photosynth Res* 2011, **109**(1):133-149.
55. Uehlein N, Otto B, Hanson DT, Fischer M, McDowell N, Kaldenhoff R: **Function of *Nicotiana tabacum* Aquaporins as Chloroplast Gas Pores Challenges the Concept of Membrane CO₂ Permeability.** *Plant Cell* 2008, **20**(3):648-657.
56. Soupene E, Inwood W, Kustu S: **Lack of the Rhesus protein Rh1 impairs growth of the green alga *Chlamydomonas reinhardtii* at high CO₂.** *PNAS* 2004, **101**(20):7787-7792.

57. Uehlein N, Lovisolo C, Siefritz F, Kaldenhoff R: **The tobacco aquaporin NtAQP1 is a membrane CO₂ pore with physiological functions.** *Nature* 2003, **425**(6959):734-737.
58. Nakhoul NL, Davis BA, Romero MF, Boron WF: **Effect of expressing the water channel aquaporin-1 on the CO₂ permeability of *Xenopus* oocytes.** *AJP - Cell Physiology* 1998, **274**(2):C543-548.
59. Marsh ME: **Polyanion-mediated mineralization — assembly and reorganization of acidic polysaccharides in the Golgi system of a coccolithophorid alga during mineral deposition.** *Protoplasma* 1994, **177**(3):108-122.
60. Beyenbach KW, Wiczorek H: **The V-type H⁺ ATPase: molecular structure and function, physiological roles and regulation.** *J Exp Biol* 2006, **209**(4):577-589.
61. Schumacher K: **Endomembrane proton pumps: connecting membrane and vesicle transport.** *Curr Opin Plant Biol* 2006, **9**(6):595-600.
62. Caldeira K, Wickett ME: **Anthropogenic carbon and ocean pH.** *Nature* 2003, **425**(6956):365.
63. Tamura K, Dudley J, Nei M, Kumar S: **MEGA4: Molecular Evolutionary Genetics Analysis (MEGA) software version 4.0.** *Mol Biol Evol* 2007, **24**:1596-1599.

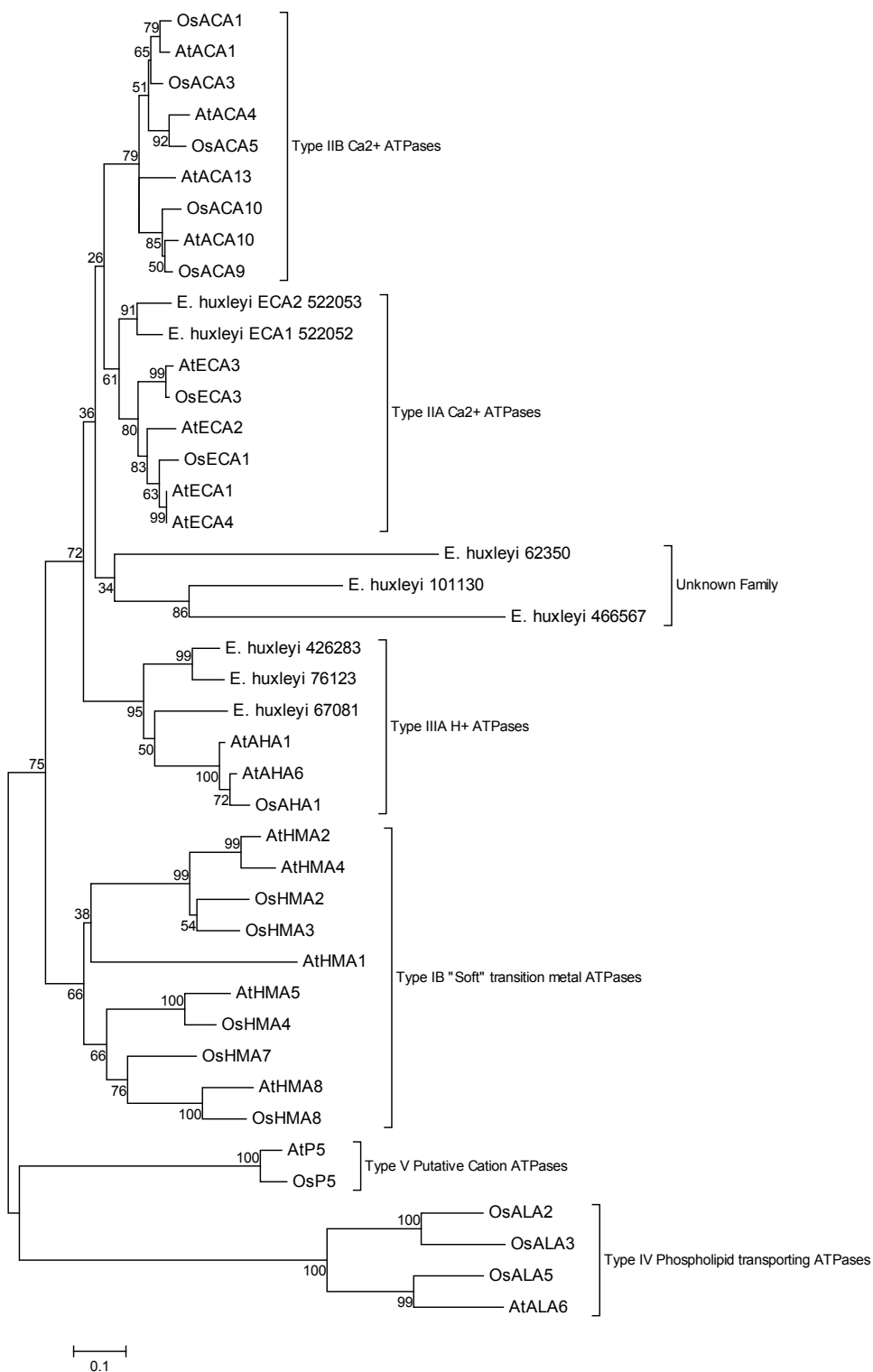


Figure 1. Phylogenetic analysis of putative *E. huxleyi* Ca²⁺-ATPases. Ca²⁺-ATPases were identified by blasting characterized Ca²⁺-ATPases against the *E. huxleyi* genome. Identified *E. huxleyi* proteins were aligned using ClustalW with representatives of *Arabidopsis thaliana* (At) and *Oryza sativa* (Os) from each of the five families making up the P-type ATPase superfamily. The tree was drawn using the Minimum Evolution algorithm (1000 bootstraps).

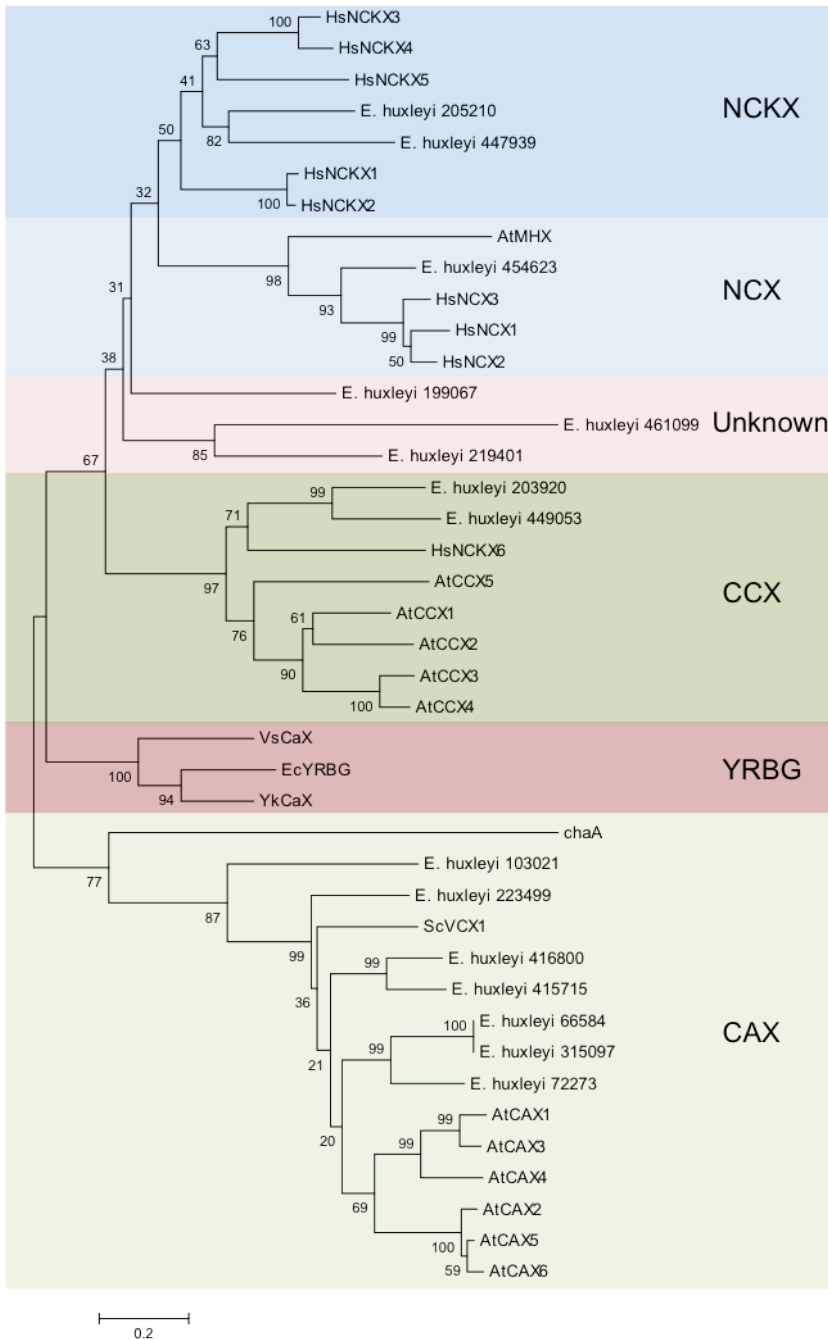


Figure 2. Phylogenetic analysis of Ca^{2+} /cation antiporter (CaCA) superfamily proteins. Putative *E. huxleyi* CaCAs were analysed with functionally characterized *Arabidopsis thaliana* (At) and human (Hs) CaCAs, yeast VCX1, *Escherichia coli* EcYRBG, *E. coli* chaA and two uncharacterized bacterial CaCAs (Vs, *Vibrio splendidus* and Yk, *Yersinia kristensenii*). The tree is based on ClustalW alignment of the $\alpha 1$ and $\alpha 2$ regions (Minimum evolution tree-1000 bootstraps).

Figure 3. Phylogenetic analysis of *E. huxleyi* SLC4 and SLC26A proteins with representative members from human (Hs), yeast (Sc, *Saccharomyces cerevisiae*), *Arabidopsis thaliana* (At), squid (sq, *Loligo pealei*), Rainbow trout (Om, *Oncorhynchus mykiss*) and skate (Le, *Leucoraja erinacea*), a picoeukaryotic algae (*Micromonas sp.*), California Sea Urchin (Sp, *Strongylocentrotus purpuratus*), diatoms (Tp, *Thalassiosira pseudonana*) and (Pt, *Phaeodactylum tricornutum*), two putative bacterial SLC4 proteins (Sr, *Segniliparus rugosus* and Nc, *Nitrococcus mobilis*), putative alkaliphilic bacteria (aa, *Alkalimonas amylolytica*) and a cyanobacterial SLC26A protein (Ssp., *Synechococcus sp.*). JGI protein ids are given for *E. huxleyi* proteins. The tree is based on ClustalW alignment followed by gap removal (Minimum evolution tree - 1000 bootstraps).

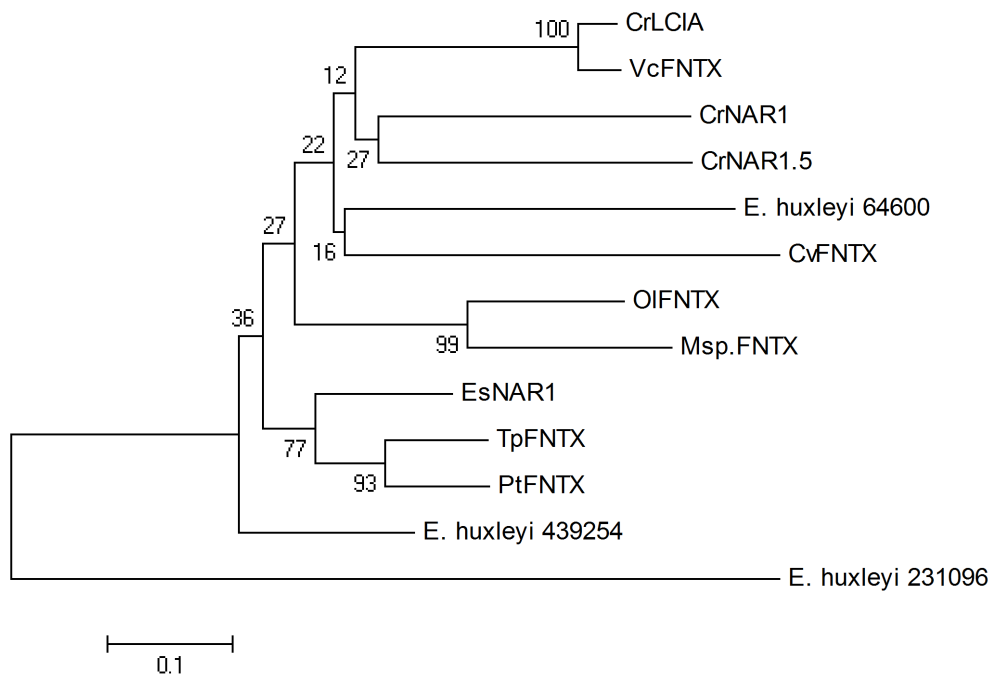


Figure 4. Phylogenetic analysis of *E. huxleyi* putative LCIA-type proteins from the diatoms *Phaeodactylum tricornutum* (Pt) and *Thalassiosira pseudonana* (Tp) and the green algae *Chlamydomonas reinhardtii* (Cr), *Ostreococcus lucimarinus* (Ol), *Volvox carterii* (Vc), *Chlorella variabilis* (Cv) and *Micromonas* sp. (Msp) and the brown algae *Ectocarpus siliculosus* (Es). Minimum evolution tree with bootstrapping (1000).

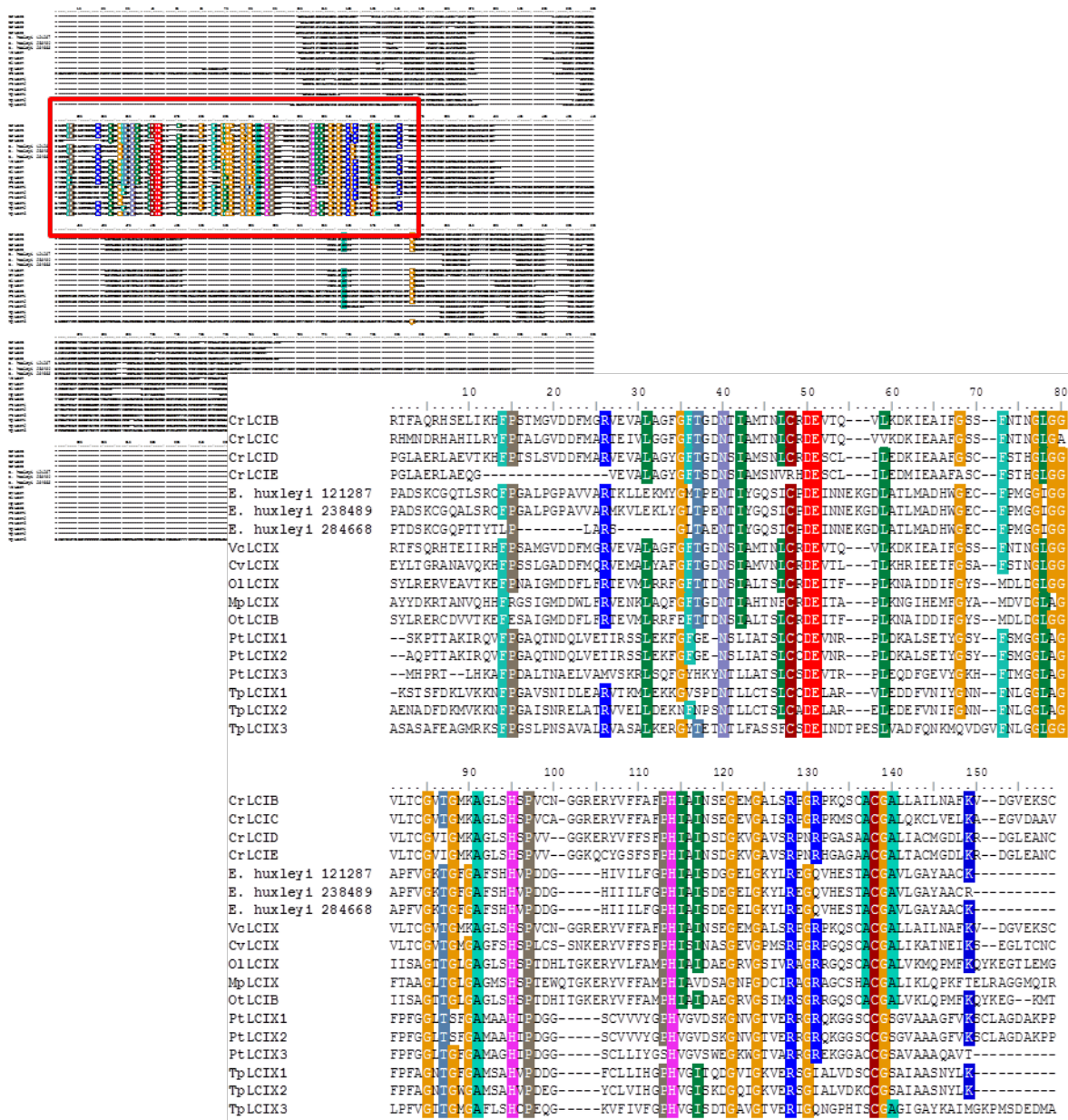


Figure 5. ClustalW alignment of putative LCIB family proteins from the diatoms *Phaeodactylum tricornutum* (Pt) and *Thalassiosira pseudonana* (Tp) and the green algae *Chlamydomonas reinhardtii* (Cr), *Ostreococcus taurii* (Ot), *Ostreococcus lucimarinus* (Ol), *Volvox carterii* (Vc), *Chlorella variabilis* (Cv) and *Micromonas pusilla* (Mp). The conserved N-terminal region is magnified. Aligned amino acids with >65% similarity are highlighted.

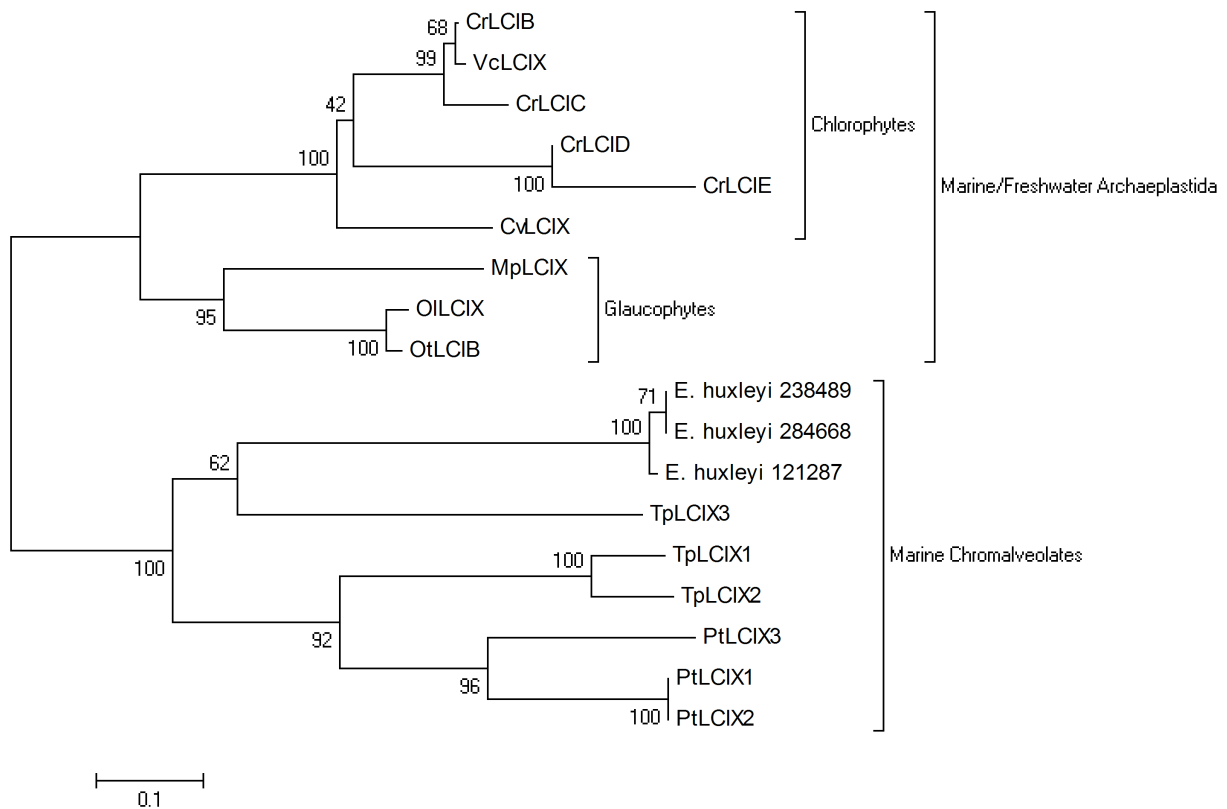


Figure 6. Phylogenetic analysis of LCIB family proteins from the diatoms *Phaeodactylum tricornutum* (Pt) and *Thalassiosira pseudonana* (Tp) and the green algae *Chlamydomonas reinhardtii* (Cr), *Ostreococcus taurii* (Ot), *Ostreococcus lucimarinus* (Ol), *Volvox carterii* (Vc), *Chlorella variabilis* (Cv) and *Micromonas pusilla* (Mp). Two clear clades are formed consisting of the Archaeplastida (green/red algae) and the Chromalveolates (diatoms and coccolithophores). Minimum evolution tree with bootstrapping (1000).

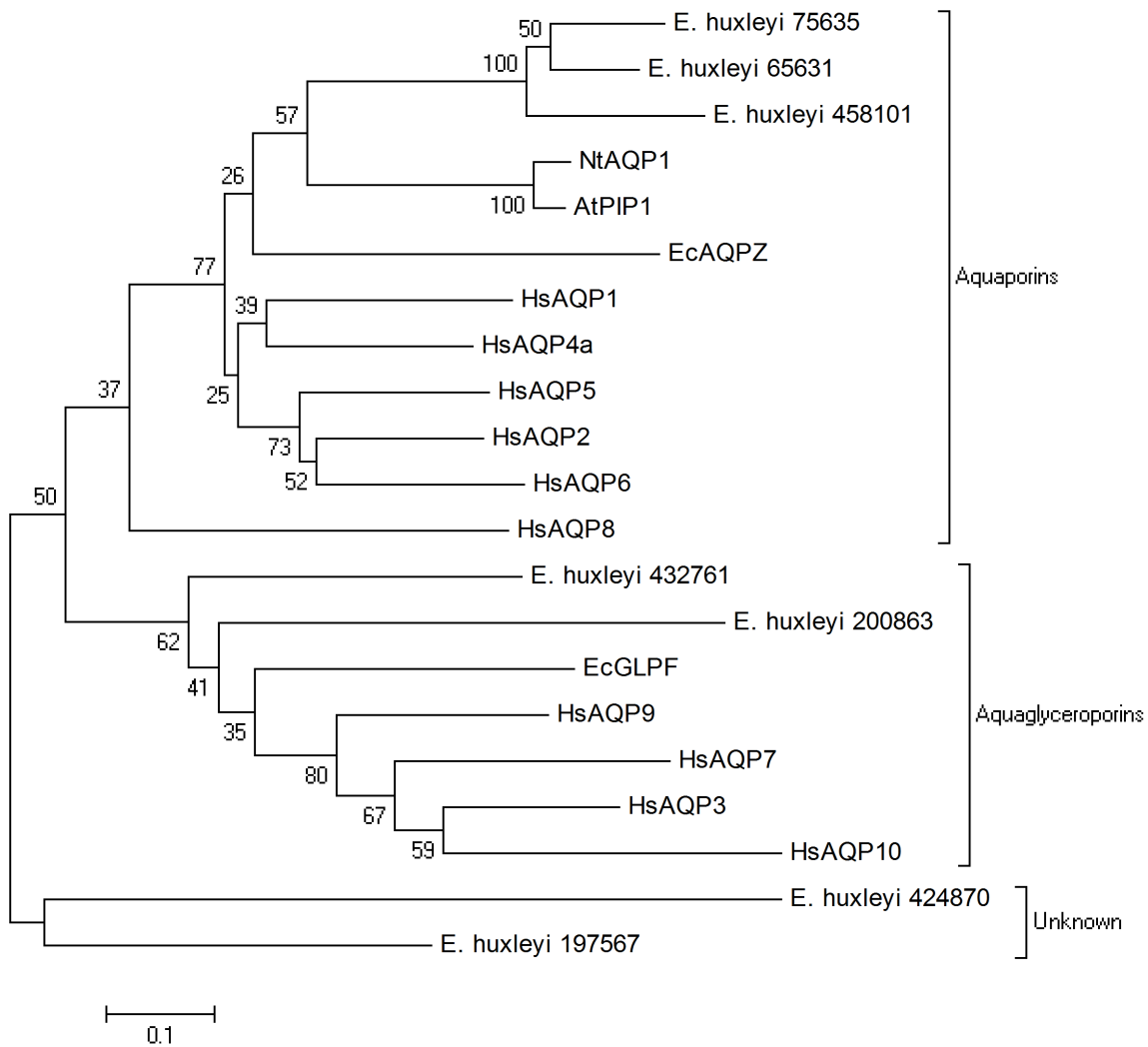


Figure 7. Phylogenetic tree analysis of aquaporin family proteins in the *E. huxleyi* genome analyzed with all human (Hs) aquaporins and representatives from *Arabidopsis thaliana* (At), *Escherichia coli* (Ec) and *Nicotiana tabacum* (Nt). The tree is based on ClustalW alignment followed by gap removal (Minimum evolution tree - 1000 bootstraps).

Table I. *Emiliania huxleyi* genome analysis for genes with putative roles in Ca^{2+} , inorganic carbon and H^+ transport. Also included are the corresponding cluster IDs from Von Dassow et al. (2009). The last two columns are the number of expressed sequence tag (EST) reads from 1N non-calcifying haploid and 2N calcifying diploid cells [9] and whether the gene was significantly up-regulated in a similar microarray comparison using the same strains [34].

Annotated Name	Protein JGI#	Location in <i>E. huxleyi</i> genome	Protein Length	Cluster ID from Von Dassow et al. 2009	1N reads	2N reads
Ca^{2+} TRANSPORT						
CATION/Ca^{2+} EXCHANGERS						
H^+/Ca^{2+} exchanger (CAX)						
CAX1	72273	scaffold_175:82681-83842	367	GS00976	2	1
CAX2	66584	scaffold_51:315048-316317	376	GS00617	3	0
CAX2'	315097	scaffold_234:21788-23057	372	GS00617	3	0
CAX3	416800	scaffold_72:205197-207212	410	GS00304	0	4/+
CAX4	415715	scaffold_27:809479-811791	432	GS00019	7	1
CAX5	522037	scaffold_110:91155-93480	327	GS06500	0	1
-	103021	scaffold_46:134344-136490	504	-	-	-
Cation/Ca^{2+} exchanger (CCX)						
CCX1	203920	scaffold_20:565364-567957	467	-	-	-
CCX2	449053	scaffold_12:1194786-1197340	542	-	-	-
K^+ dependent Na^+/Ca^{2+} exchangers (NCKX)						
NCKX1	205210	scaffold_23:819807-821288	448	-	-	-
NCKX2	447939	scaffold_4:853456-856555	624	-	-	-
-	354606*	scaffold_28:691632-693520	230	GS00463	0	8/+
K^+ independent Na^+/Ca^{2+} exchangers (NCX)						
NCX1	454623	scaffold_117:250185-253716	878	-	-	-
Possible Cation/Ca^{2+} exchanger members						
-	461099	scaffold_1:2783977-2787120	380	GS00834	4	3
-	219401	scaffold_86:95235-96675	373	-	-	-
-	199067	scaffold_9:674275-676474	611	GS02609	1	0
Ca^{2+} PUMPS						
Ca^{2+}-ATPases (P-type ATPases)						
ECA1	522052	scaffold_143:112851-116971	1033	-	-	-
ECA2	522053	scaffold_21:344465-348504	1060	GS01511	4	5
-	62350	scaffold_9:389594-393626	1021	GS07761	1	0
-	101130	scaffold_28:63012-67300	1301	-	-	-
-	466567	scaffold_107:104713-110992	1224	GS01412	2	5
Ca^{2+} CHANNELS						
Transient Receptor Potential channels (TRP)						
-	449985	scaffold_21:481448-486952	1295	GS04572	0	1/+
-	468587	scaffold_201:29095-36476	885	-	-	-
-	455760	scaffold_156:70632-75959	1341	-	-	-
-	107737	scaffold_95:88859-94606	1320	-	-	-
-	462171	scaffold_11:596711-600437	693	GS12720	0	1
-	114254	scaffold_211:100862-103899	690	-	-	-
4 domain Voltage-dependent Ca^{2+} channels (Ca_v)						
CAV1	448907	scaffold_11:956337-963485	1930	GS06882	0/+	1
CAV2	448526	scaffold_8:821120-825951	1303	-	-	-
Bacterial-type Na^+ channels (Na₁Bac)						
VDC1	97870	scaffold_11:1177161-1178294	378	GS06640	1/+	0
VDC2	196523	scaffold_4:1581467-1583231	523	GS04318	2	0
VDC3	522022	scaffold_749:16526-19222	569	-	-	-
VDC4	522033	scaffold_276:24914-27034	556	-	-	-
Two-pore Ca^{2+} channel (TPC)						
-	452741	scaffold_67:500766-503545	729	-	-	-
Inositol-1,4,5-triphosphate receptors (IP₃R)						
IPR1	209909	scaffold_40:674058-682938	2713	-	-	-

-	248526	scaffold_676:2973-8239	1616	-	-	-
Cyclic nucleotide-gated channels (CNGC)						
CNG1	213957	scaffold_59:438423-442989	1473	-	-	-
INORGANIC CARBON TRANSPORT						
SLC4 HCO₃⁻ Transporters						
SLC4	436956	scaffold_51:177552-181259	594	GS03121	0	1
EhAE3	450694	scaffold_31:94994-102202	552	GS09941	0	1
-	466232	scaffold_95:394699-398786	899	GS10424	0/+	1
AE	99943	scaffold_21:549597-551556	620	GS05051	0	7/+
AE	198643	scaffold_8:980652-982640	586	GS05051	0	4
AE	200137	scaffold_11:769855-771930	611	GS05051	0	1
AE	120259	scaffold_603:7442-11246	780	GS05051	0	3
AE	210210 [*]	scaffold_41:693996-695718	436	GS05509	0	1
SLC26A HCO₃⁻ Transporters						
-	249865	scaffold_835:6501-8679	644	GS01795	4	0
SUL1	441761	scaffold_163:232174-235881	502	-	-/+	-
-	453061	scaffold_73:477262-479712	713	-	-	-
-	460215	scaffold_914:5065-8495	764	-	-	-
-	455488	scaffold_144:281672-285321	842	-	-	-
Carbonic Anhydrases						
gamma_CA_2	373149	scaffold_1232:9443-11137	160	GS10593	0	1
gamma_CA_1	432493	scaffold_5:297449-299764	236	GS10593	0	1
- (α)	456048	scaffold_166:123920-125564	254	-	-	-
AE (δ)	469783	scaffold_322:82332-90355	636	-	-	-/+
CA (α)	233460	scaffold_191:241570-242153	165	-	-	-
Eh CA1 (α)	437452	scaffold_60:16316-18236	378	GS00014	1	2
Beta CA	469462	scaffold_287:5333-7868	477	GS01744/GS00157	1/12	3/0
Alpha CA	62679	scaffold_11:980601-981575	302	-	-	-
Delta CA_1	436031	scaffold_36:835339-840039	656	GS07947	0	1
LCIA (Formate/Nitrite Transporter (FNT) family)						
-	373579 ⁵	scaffold_1891:231-591	120	-	-	-
NAR3	439254	scaffold_97:90524-92476	296	GS04367	3	4
NAR4	64600	scaffold_24:578645-579562	306	GS00399	5	20
NAR2	231096	scaffold_169:241844-243923	326	GS03581	0	1
LCIB						
-	121287	scaffold_835:5102-6016	305	GS03176	1	0
-	238489/ 457739	scaffold_271:86005-88659	404	-	-	-
-	284668	scaffold_408:72631-73682	279	-	-	-
Aquaporins						
-	458101	scaffold_300:83263-85260	373	GS00451	0	7/+
-	75635	scaffold_390:42327-43193	289	-	-	-/+
-	65631	scaffold_37:208252-208935	228	GS00630	5	0
MIP1	432761	scaffold_5:1969208-1970256	318	-	-	-
-	200863	scaffold_13:90652-91552	265	-	-	-
-	197567	scaffold_5:1854915-1855717	224	-	-	-
MIP2	424870	scaffold_386:519-2181	441	-	-/+	-
H⁺ TRANSPORT						
H⁺-ATPases (P-type ATPases)						
-	426283	scaffold_10:1019394-1022905	948	-	-	-/+
-	67081	scaffold_58:229676-232188	613	-	-	-
-	76123	scaffold_461:21298-23444	671	-	-	-
H⁺-PPase						
-	415047	scaffold_13:1080548-1083606	876	GS09796	0	1
-	439740	scaffold_107:168745-172751	905	GS07432	0	4
-	51239	scaffold_162:92097-94199	710	-	-	-
-	75032	scaffold_334:16534-20539	733	-	-	-
V-ATPase subunits (non-exhaustive)						
ATPvc/c'	359783	scaffold_88:93746-95218	171	GS03783+GS01934	4	5/+
ATPva2	464767	scaffold_56:191424-195276	933	GS02526	1	4
ATPvc''	313800	scaffold_147:287868-288766	185	GS01501	4	0/+
ATPvd	413949	scaffold_75:287683-289374	345	GS00290	7	5
ATPVA	439538	scaffold_103:83090-85896	605	GS01727	2	5/+
ATPVB	435128	scaffold_25:24122-27231	485	GS08492	0	1/+
ATPVC	558234	scaffold_7:365993-367983	353	GS00316	6	4

ATPVD1	420005	scaffold_1062:8737-9513	160	-	-	-/+
ATPVE	433060	scaffold_8:1103926-1105618	170	GS00924	1	1/+
ATPVF	352209	scaffold_15:307437-309376	102	GS09780	0	4/+
ATPVG	369392	scaffold_365:46608-47417	112	GS01820	1	5
Voltage gated H⁺ channel						
HVCN1	631975	scaffold_69:513958-515612	261	-	-	-

[%] possibly fused to adjacent 210209 gene model at C-terminus

[§] C-terminal truncated - possible poor gene model

* Not included in phylogenetic analysis due to poor gene model

**CHAPTER 6. The cloning and partial
characterization of two calcification related
genes, AEL1 a putative HCO_3^- transporter and
CAX3 a putative $\text{Ca}^{2+}/\text{H}^+$ exchanger, from the
coccolithophore *Emiliana huxleyi***

Luke C. M. Mackinder*, Declan C. Schroeder, Ulf Riebesell, Colin Brownlee and Glen Wheeler

*Corresponding author: Luke C. M. Mackinder, lukcki@mba.ac.uk

Helmholtz-Zentrum für Ozeanforschung Kiel (GEOMAR), D-24105, Kiel, Germany (L.C.M.M., U.R.); Marine Biological Association of the UK, The Laboratory, Citadel Hill, Plymouth PL1 2PB, UK (L.C.M.M., G.W., D.C.S., C.B.); Plymouth Marine Laboratory, Prospect Place, Plymouth, PL1 3DH, UK (G.W.).

Abstract

Coccolithophores are one of the dominant producers of calcium carbonate in the current ocean. They transport Ca^{2+} and inorganic carbon (Ci) to an intracellular vesicle where they precipitate calcite in a highly controlled process. In parallel to calcification they manage to maintain low cytosolic Ca^{2+} levels for cellular signalling events and acquire adequate Ci for photosynthesis. Characterization of the underlying molecular mechanisms will aid in our understanding of the calcification process and its regulation. This study focused on the characterization of a $\text{Ca}^{2+}/\text{H}^{+}$ exchanger (*CAX3*) and a HCO_3^- transporter (*AEL1*) belonging to the SoLute Carrier 4 (SLC4) family. The full-length transcripts for both genes were obtained using Rapid Amplification of cDNA Ends (RACE) followed by cloning. Phylogenetic analysis indicates that *CAX3* belongs to CAX subfamily I and that *AEL1* does not fall within the distinct $\text{Cl}^-/\text{HCO}_3^-$ exchanger or Na^+ dependent HCO_3^- transporter families but belongs to a unique clade within the SLC4 family. In order to understand the function of *CAX3* and *AEL1* heterologous expression systems were used. *CAX3* was successfully expressed in *Saccharomyces cerevisiae* but failed to complement the Ca^{2+} sensitive phenotype of a mutant lacking $\text{Ca}^{2+}/\text{H}^{+}$ exchange activity. Expression in *Escherichia coli* resulted in a lethal phenotype, which could be partially rescued by addition of Ca^{2+} . However, the data was inconclusive on the full functionality of *CAX3*. To investigate HCO_3^- transport, internal pH was monitored in HEK293 cells expressing *AEL1* using pH sensitive fluorescent dyes. *AEL1* failed to transport HCO_3^- , although this may be due to the poor localization of *AEL1* to the plasma membrane rather than the absence of HCO_3^- transport by *AEL1*.

Introduction

Coccolithophores are calcifying marine phytoplankton that often form large blooms and play a fundamental role in global carbon and nutrient cycles (Westbroek et al., 1993). The intracellular nature of calcification in an internal endomembrane compartment, termed the coccolith vesicle (CV) means the complete isolation of calcite precipitation from the external seawater. This enables calcification in coccolithophores to be a stringently controlled process. Posing the question: how are large quantities of Ca^{2+} and inorganic carbon (Ci) transported from the external environment to the CV, whilst Ca^{2+} homeostasis is maintained and the Ci carbon supply for photosynthesis is sustained? (Brownlee et al., 1995; Berry et al., 2002). Apart from being an intriguing biological question, an understanding of Ca^{2+} transport to the CV would aid in understanding Sr/Ca ratios as a proxy for past coccolithophore productivity and calcification

rates (Langer et al., 2006). Furthermore, knowledge of the mechanisms of Ci uptake and transport is critical for understanding how coccolithophores will adapt to a future ocean where $\text{CO}_2:\text{HCO}_3^-:\text{CO}_3^{2-}$ ratios will change and the oceans will become increasingly acidic.

In all eukaryotic cells free cytosolic Ca^{2+} is kept at low concentrations to prevent uncontrolled CaPO_4 precipitation and to allow for rapid cellular signalling events. Coccolithophores are no exception, maintaining a cytosolic $[\text{Ca}^{2+}]$ of ~ 100 nM (Brownlee et al., 1995). In order to sustain this low level of cytosolic Ca^{2+} whilst performing calcification it is hypothesised that Ca^{2+} destined for calcification is rapidly sequestered into the Golgi and/or the endoplasmic reticulum (ER) once entering the cytosol (Berry et al., 2002; Mackinder et al., 2010). This Ca^{2+} uptake into the endomembrane network would most likely be an energy requiring process that could be directly driven by ATP requiring Ca^{2+} pumps and/or by exchangers using the electrochemical potential of other cations to drive the uphill transport of Ca^{2+} .

Expression studies have provided strong evidence that a $\text{Ca}^{2+}/\text{H}^+$ exchanger (*CAX3*) plays a prominent role in Ca^{2+} uptake for calcification. *CAX3* (JGI# 416800) is only expressed in the diploid calcifying stage of *E. huxleyi* (von Dassow et al., 2009; Mackinder et al., 2011) and is down-regulated in diploid cells with reduced calcification (Mackinder et al., 2011). CAXs were initially identified as $\text{Ca}^{2+}/\text{H}^+$ exchangers that reside in the vacuole membrane of plants and fungi to mediate Ca^{2+} removal from the cytosol (Hirschi et al., 1996). It has now become clear that some CAX proteins locate to other organelles and they may transport a diverse range of cations in exchange for H^+ (Manohar et al., 2010). The low affinity and high capacity $\text{Ca}^{2+}/\text{H}^+$ exchange of many CAXs makes them ideal candidates for the loading of acidic endomembrane compartments for calcification. By using a H^+ gradient generated by the action of H^+ -pumps, CAX proteins could be a rapid and energy efficient mechanism for the loading of Ca^{2+} into the CV precursor and endomembrane network (Mackinder et al., 2010).

In coccolithophores, the demand for Ci for photosynthesis can be equalled and even exceeded by the demand for calcification (Langer et al., 2006). To provide cells with the required fluxes of Ci for calcification, it is expected that active transport is necessary at either the plasma membrane (PM) or the CV. There is substantial evidence that cells use HCO_3^- as the substrate for calcification (Sikes et al., 1980; Nimer and Merrett, 1992) and that active transport of HCO_3^- is taking place in *E. huxleyi* (Schulz et al., 2007). An important group of HCO_3^- transporters is the SoLute Carrier 4 (SLC4) family. To date the majority of work has focused on mammalian members with no unicellular HCO_3^- transporting SLC4 member characterized. SLC4 members can be broadly classified into 3 groups based on their function; Na^+ dependent HCO_3^- transporters, $\text{Cl}^-/\text{HCO}_3^-$ exchangers or borate transporters. Expression of an SLC4 member,

Anion Exchanger Like 1 (*AEL1*; JGI# 198643/99943), has shown to be diploid specific (von Dassow et al., 2009) and up-regulated under calcifying conditions (Mackinder et al., 2011) making it an ideal candidate for a role in HCO_3^- supply for calcification.

This study focuses on the functional characterization of *CAX3* and *AEL1*. Firstly to determine their full-length transcripts Rapid Amplification of cDNA Ends (RACE) was carried out and both *CAX3* and *AEL1* were cloned and sequenced. Secondly, their phylogeny was examined to give clues on their function and cellular roles. Finally, to examine whether they have the capacity to transport their respective ions, heterologous expression of *CAX3* in *Saccharomyces cerevisiae* (yeast) and *Escherichia coli* and *AEL1* in Human Embryonic Kidney cell line 293 (HEK293) cells was conducted. Heterologous expression has been routinely used to characterize CAX and SLC4 genes from other organisms and is essential for understanding gene function in organisms where genetic manipulations are not possible, like coccolithophores.

Results

RACE and phylogenetic analysis

Both the full-length transcripts of *CAX3* and *AEL1* were recovered using RACE, with gene specific primers designed from available expressed sequence tag (EST) data. Two allelic copies of *CAX3* were present that corresponded to JGI# 416800 with both having full-length transcripts of 1599 base pairs (bp; excluding the polyA tail; Fig. S1). There were 8 single base pair variations between the allelic copies, 7 were found in the coding sequence (CDS) with one present in the 3' untranslated region (UTR). Of the 7 CDS point mutations 6 were silent and one resulted in an amino acid change from isoleucine to valine at amino acid position 30. CAXs can be split into three distinct phylogenetic groups (Shigaki et al., 2006). Phylogenetic analysis indicates that *CAX3* falls within the type I subfamily of CAXs, potentially forming a new clade with *E. huxleyi* CAX4, which is more closely related to plant and moss CAXs than the three other protozoa and algal CAXs used in the analysis (Fig. 1).

There are 8 putative SLC4 genes in the *E. huxleyi* genome of which 4 are very similar at the nucleotide level (<http://genome.jgi-psf.org/Emihu1/Emihu1.home.html>). Of these closely related genes, EST data supported the expression of JGI# 99943 although a number of the same reads also mapped to JGI# 120259, 198643 and 200137 (von Dassow et al., 2009). To investigate whether these were allelic copies of the same gene, different genes or genome assembly errors, RACE was used to recover the full-length transcripts. RACE identified the 5'

and 3' ends of the 2 copies of *AEL1* originally thought to be allelic copies (named *AEL1* “allele 1” and *AEL1* “allele 2”). However, cloning and sequencing indicates that they are most likely different genes that have appeared through a recent duplication event. They are nearly identical except a 27 bp insertion in “allele 1” at position 223 of the alignment (Fig. S2) and 23 point mutations of which 7 result in an amino acid change (Fig. S3). Further analysis of *AEL1* “alleles” with SLC4 gene models indicates that *AEL1* “allele 1” corresponds to JGI# 99943 although there are 10 single base pair variations and a 6 G insert in the JGI# 99943 gene model at position 700 (Fig. S2). *AEL1* “allele 2” corresponds to JGI# 198643, however they both have the same 1st intron as in JGI# 99943 (Fig. S2). It is still unclear whether JGI# 120259 and 200137 are valid genes, pseudogenes, allelic copies or assembly errors. If they are valid genes they may not have been recovered during RACE due to low levels of corresponding mRNA. A synthetic construct corresponding to *AEL1* “allele 1”, with codon usage optimised for expression in mammalian cells, was generated and subsequently used for functional analysis.

ClustalW alignments of AEL1 with other SLC4 transporters indicates that AEL1 contains the necessary 9-15 transmembrane transport domains but is lacking the N-terminal cytoplasmic region of mammalian SLC4 transporters, which is involved in anchoring mammalian transporters to the cytoskeleton and the binding of interacting proteins (Pushkin and Kurtz, 2006; Romero et al., 2004). Phylogenetic analysis of the 4 *E. huxleyi* SLC4 orthologs indicates that they do not group within the distinct Cl⁻/HCO₃⁻ exchanger (AE; anion exchanger) or the Na⁺ coupled exchanger clades but form a clade with SLC4 transporters of unknown function (Fig. 2).

CAX3 yeast expression and complementation in K667

To test the hypothesized function of *CAX3* as a Ca²⁺/H⁺ exchanger, complementation studies using the Ca²⁺ hypersensitive yeast mutant strain K667 were carried out. K667 lacks the endogenous vacuolar Ca²⁺/H⁺ exchanger (VCX1), the vacuolar Ca²⁺-ATPase (PMC1) and calcineurin (CNB1). These Ca²⁺ transport defects prevent growth in elevated Ca²⁺ media. It has been shown that by expressing a functional CAX protein it complements VCX1 mediating Ca²⁺ transport into the vacuole and preventing the toxic accumulation of Ca²⁺ in the cytosol (Hirschi et al., 1996). To ensure successful expression in yeast, a yeast codon optimised *CAX3* gene (*coCAX3*) corresponding to allele 1 was synthesized (GenScript, USA) and supplied in a *pUC57* vector. To check *coCAX3* expression and subcellular localization, a *coCAX3-eGFP* construct was expressed in yeast strain K667. The *coCAX3-eGFP* protein localized predominantly to the vacuole and to a lesser extent the PM (Fig. 3).

Full-length *coCAX3* failed to complement the Ca^{2+} sensitive phenotype of K667, with *coCAX3* expressing yeast having no increased tolerance to Ca^{2+} compared to K667 expressing the empty *pUGpd* plasmid (Fig 4A). Wild-type strain K601 expressing *coCAX3* also showed no change in phenotype relative to K601 expressing the empty *pUGpd* plasmid (Fig. 4A). It is known that some full-length plant CAXs fail to function in yeast and that truncation at the N-terminus can result in successful activation (Pittman and Hirschi, 2001). To test this a *coCAX3* construct with the initial 25 amino acids removed (*5'TrcoCAX3*), that potentially formed the regulatory domain, was cloned into the *pUGpd* vector and expressed in K667 (Fig. 4B, C and D). Yeast transformed with the truncated construct showed a similar phenotype to yeast expressing either the empty vector or full-length *coCAX3* (Fig. 4B). The function of CAX proteins are known to be pH dependent (Pittman et al., 2005), if CAX3 was functioning in the PM changes in external pH could increase Ca^{2+} efflux reducing toxicity. To test this spot tests were carried out on YPD plates containing 20 mM CaCl_2 , which were buffered at pH 4, 6 and 8. Again *CAX3* expression had no effect on growth in comparison to K667 expressing the empty vector over the pH range tested (Fig. 4B). CAX proteins have been shown to transport a variety of cations reducing the toxicity of these ions to yeast strain K667 (Liu et al., 2009). To see if CAX3 was involved in sequestration of ions other than Ca^{2+} a range of cations were tested. Yeast expression of *coCAX3*, truncated *coCAX3* and *coCAX3-GFP* did not appear to increase tolerance to any of the cations tested (Fig. 4C).

E. coli expression and complementation in KNabc

Due to the inability of *CAX3* to rescue the Ca^{2+} hypersensitive phenotype of yeast strain K667, an alternative expression system was used. The *E. coli* strain KNabc had previously been used to characterize CAXs and Na^+/H^+ exchangers from prokaryotes (Waditee et al., 2004; Wei et al., 2007). KNabc is derived from the strain TG1 and is mutated in genes *nhaA*, *nhaB* and *chaA*, with NhaA and NhaB functioning as Na^+/H^+ exchangers and ChaA a bacterial homologue of CAX. In prokaryotes it is thought that CAXs localize to the PM and are involve in Ca^{2+} transport potentially related to salt tolerance. If *CAX3* functioned in a more alkaline environment than the yeast acidic vacuole, it may fail to complement yeast strain K667 but may complement a prokaryote deficient in Ca^{2+} transport. An Isopropyl β -D-1-thiogalactopyranoside (IPTG) inducible vector, *pQE60* (QIAGEN), was chosen to allow controlled expression of *CAX3*. Transformation of KNabc with *pQE60_CAX3* was successful, although growth was slightly reduced compared to KNabc transformed with empty *pQE60* (data not shown). Upon induction with IPTG, *CAX3* became toxic to *E. coli* resulting in a lethal phenotype (Fig. 5). However,

extended incubation resulted in the appearance of a small number of resistant colonies that had a wild type growth phenotype. The appearance of resistant colonies is probably caused due to the strong selection for mutations in *CAX3* or the loss of plasmid to avoid the *CAX3* lethal phenotype. Plasmid loss could occur through the development of ampicillin resistance or due to the breakdown of ampicillin over time. This occurrence of resistant colonies with atypical phenotypes makes the interpretation of results complex.

Interestingly the presence of Ca^{2+} on agar plates reduced the lethal phenotype of *CAX3* allowing stunted growth of colonies (Fig. 5A and B), although this growth was still not comparable to KNabc expressing the empty *pQE60* vector. This can be seen in both TOP10F' and KNabc cells expressing *CAX3* grown on 100 mM Ca^{2+} containing plates. Although the presence of resistant colonies on LBK and LBC plates in the absence of Ca^{2+} , affects the clarity of these results. On Ca^{2+} containing plates, growth was stunted but a large number of colonies were viable, unlike in the absence of Ca^{2+} where the growth was dominated by only a few rapidly growing colonies thought to contain mutations (Fig. 5A and B). This is also apparent by the increasing presence of colonies on LB plates containing Ca^{2+} when spotted at a density of less than an OD_{600} of 1. Also, resistant colonies did not always appear in cells expressing *pQE60_CAX3* on plates without Ca^{2+} (as seen in Figure 5B LBK pH6). Yet growth, although stunted, always occurred in cells expressing *CAX3* if Ca^{2+} was present. Two pH values of 6 and 7 were tested with KNabc generally performing slightly poorer at pH 7, although when expressing *CAX3* there was limited variation in growth between the two pHs and a possible improvement under higher salt stress at pH7 (Fig. 5A, LBC Ca^{2+} 100 mM, Na^+ 100 mM pH 7 vs. pH 6). The presence of K^+ (compared to its absence when replaced with choline) generally improved the growth of KNabc. The presence of Na^+ was detrimental to both KNabc expressing the empty vector and *CAX3*. To see if *CAX3* had the same detrimental effect in cells possessing fully functional Ca^{2+} , Na^+ and pH regulation, the *pQE60_CAX3* construct was expressed in TOP10F' cells (Fig. 5B). *CAX3* expression was still detrimental with again some partial rescue in the presence of Ca^{2+} . pH had a minimal effect although the substitution of K^+ with Na^+ slightly enhanced growth in the presence of Ca^{2+} . To test if *CAX3* could increase KNabc cells tolerance to salt, spot tests were carried out on LBK plates supplemented with 5 mM Li^+ and the pH buffered to 5.5, 6.5 or 7.5. At all pHs, TOP10F' control cells grew well with no apparent negative effects of 5 mM Li^+ . At pH 5.5 the expression of *CAX3* was detrimental to the cells relative to expression of the empty vector, which formed well populated spots for all dilutions spotted. At pH 6.5 the KNabc containing the empty vector failed to grow but some growth was present in KNabc expressing *CAX3*. At pH 7.5, 5 mM Li^+ was completely lethal to KNabc cells expressing the empty *pQE60* vector and cells expressing *CAX3* (Fig. 5C).

AEL1 expression in HEK293 cells

In this study we attempted to characterize the function of *AEL1* using the HEK293 heterologous system. To check for successful *AEL1* expression a *GFP* tagged *AEL1* was expressed in HEK293 cells. This protein showed a distinct localization pattern when compared to only *eGFP* expression. However, the localization of *AEL1-eGFP* did not show specific localization to the PM of HEK293 cells but appeared to accumulate in the endomembrane network (Fig. 6). Although *AEL1-eGFP* showed no strong evidence of localization to the PM, an undetectable amount could have been present in the PM allowing an *AEL1* phenotype to be monitored.

Due to the buffering capacity of HCO_3^- the ability of cells to recover from an acid load has become a standard approach to characterize SLC4 family HCO_3^- transporters, with the heterologous systems of HEK cells and *Xenopus* oocytes being the most used. In both systems the recovery rate of intracellular pH is recorded after internal acidification. Cells expressing a functional HCO_3^- transporter have the capacity to recover at faster rates than cells lacking HCO_3^- transport (Romero et al., 2004; Pushkin and Kurtz, 2006). Expression of *E. huxleyi AEL1* in HEK293 cells showed no improved recovery from an acid load relative to HEK293 cells containing an empty plasmid. Figure 7 demonstrates HEK293 cell recovery after internal acidification by NH_4Cl . If *AEL1* functioned as a $\text{Na}^+ \text{HCO}_3^-$ symporter, acidification in the absence of Na^+ followed by the presence of Na^+ would drive HCO_3^- uptake (for an example see Wang et al., 2000). However, this was not observed with controls showing the same phenotype as *AEL1* expressing cells (Fig. 7A). On the other hand, if *AEL1* functioned as a $\text{Cl}^-/\text{HCO}_3^-$ exchanger the rate of recovery of internal pH would be increased in the absence of Cl^- due to an outwards Cl^- electrochemical gradient driving HCO_3^- uptake. However this was also not observed (Fig. 7B).

Discussion

Functional characterization of E. huxleyi CAX3

Heterologous expression in yeast and *E. coli*, along with gene knockdown and gene knockout studies have been the main approaches for the characterization of CAXs from multiple plant species, the green algae *Chlamydomonas*, yeast and cyanobacteria (Waditee et al., 2004; Zhao et al., 2008; Manohar et al., 2011). Due to the unavailability of genetic transformation in

coccolithophores, the heterologous expression systems of yeast and *E. coli* were used to investigate *CAX3* function.

E. huxleyi *CAX3* expressed in yeast strain K667 failed to complement the absent *vcx1* yeast gene, having no effect on the Ca^{2+} sensitive phenotype compared to K667 expressing the empty vector (Fig. 4). Tests investigating the transport of various other cations were also all negative. *CAX3* was successfully expressed in yeast with the *CAX3*-eGFP construct appearing to locate to the vacuole and possibly the PM (Fig. 3). The close phylogeny of *CAX3* with other characterized CAXs would imply a similar function. However, unlike plants and yeast *E. huxleyi* lacks a large central acidic vacuole, this may explain why yeast is suitable for characterization of plant CAXs but not for *E. huxleyi* *CAX3*. Also, as research into CAXs has increased it has become increasingly apparent that post-translational regulation of CAXs is a complex process. Several plant CAXs have been shown to possess a mechanism of N-terminal autoinhibition (Pittman et al., 2002; Pittman et al., 2002) with only the truncated version having the capacity to rescue the Ca^{2+} sensitivity of yeast strains such as K667. However, a truncated *CAX3* version failed to rescue strain K667. CAXs are known to be activated and regulated by other proteins (Cheng and Hirschi, 2003; Cheng et al., 2004; Cheng et al., 2004). The lack of *CAX3* functionality in yeast may be due to the absence of essential regulatory proteins critical for its functioning or due to the unsuitable chemical environment of the yeast vacuole.

Whereas *CAX3* expression in yeast was benign, *CAX3* expression in *E. coli* was toxic. This toxicity to some extent could be counteracted by the presence of Ca^{2+} or Li^+ in the growth media, however, this appeared to be a minor effect and does not conclusively link the transport of these ions with *CAX3*. Toxicity of recombinant proteins in *E. coli* is not uncommon with multiple membrane proteins known to have severe negative effects on growth (Miroux and Walker, 1996). The ability of enhanced growth in the presence of Ca^{2+} or Li^+ indicates that although toxic, *CAX3* may have a level of functionality. With *CAX3* potentially giving KNabc cells increased Li^+ tolerance at pH 6.5 (Fig. 5C). Li^+ is widely used to perform a salt stress on cells. The ability of *CAX3* to improve growth at pH 6.5 relative to the control but not at pH 5.5 indicates that *CAX3* function involves H^+ . A feasible explanation is that *CAX3* is having an influence on the membrane permeability to ions, cellular pH regulation and/or a direct effect on membrane potential. With the presence of substrate (Ca^{2+} or Li^+) *CAX3* functions to partially counteract its toxicity, either by increasing cation export or playing a role in H^+ transport both which would be essential for regulation of membrane potential. However, it may also be feasible that *CAX3* is not functioning in transport but the presence of Ca^{2+} or Li^+ is having an influence on the toxicity of *CAX3* to *E. coli*. However, this does not explain the partial rescue seen under Li^+ stress.

It is clear that both the yeast and *E. coli* heterologous systems had limitations for the characterization of *CAX3*. In yeast this was potentially through the absence of post-translational modifications (either truncation or activation of *CAX3*) or being in an unsuitable environment and in *E. coli* the toxicity of *CAX3* and the spontaneous occurrence of resistant colonies. Although there is compelling expression data to implicate *CAX3* in calcification, for a conclusive link gene knockdown or gene knockout experiments of *CAX3* in *E. huxleyi* are essential.

Functional characterization of E. huxleyi EhAEL1

RACE followed by cloning was used to recover full-length mRNA of *AEL1*. It is likely that the two identified *AEL1* “alleles” are potentially separate genes. This is supported by an insertion/deletion and a relative large number of point mutations. Neither of the RACE products fully matched the gene models in the genome, however “allele 1” showed the highest similarity to JGI# 99943 and “allele 2” to JGI# 198643 (Fig. S2). The accuracy of the other SLC4 gene models (JGI# 120259 and 200137) should be questioned, with the potential of them being assembly errors or poorly assembled allelic copies of JGI# 99943 and JGI# 198643. However, further experimental data is essential to determine this. Phylogenetic analysis indicates that *AEL1* falls within a group of SLC4 transporters with unknown function. From expression data there is evidence that they play a role in calcification (von Dassow et al., 2009; Mackinder et al., 2011; Rokitta et al., 2011). There is also convincing inhibitor based data that supports the role of this family of transporters in HCO_3^- uptake (Herfort et al., 2002). Expression of *AEL1* showed no improvement in the rate of recovery from intracellular acidification, both in the absence of Cl^- or the presence of Na^+ . This is potentially due to the poor localization of *AEL1* to the PM of HEK293 cells with potentially none being inserted into the PM (Fig. 6). The lack of the N-terminal tail in *AEL1* is a potential reason why *AEL1* failed to successfully locate to the PM in HEK293 cells.

The use of heterologous systems

It is becoming apparent that the use of heterologous systems for characterizing coccolithophore genes is not always ideal. In addition to *CAX3* and *AEL1*, several other attempts to characterize *E. huxleyi* transport genes have failed or given unclear phenotypes in heterologous systems (Frédéric Verret, Pers. Comms.). However, this is not always the case with the recent characterization of a coccolithophore H^+ channel in HEK293 cells (Taylor et al., 2011) and the characterization of multiple *E. huxleyi* fatty acid synthesis protein in yeast (Sayanova et al.,

2011). Protein expression is a complex process involving multiple steps and associated proteins. In heterologous expression there are multiple stages that could result in the absence of expression or the presence of non-functional proteins. Poor codon usage is a potential problem, to ensure this was not an issue codon optimised genes were used for both *CAX3* expression in yeast and *AEL1* expression in HEK cells. Once translated, proteins have to be correctly folded, transported to their desired location and correctly inserted into the membrane, if transport proteins. They may also need to be in a specific environment to function, and may require co-factors, interacting proteins, glycosylation or cleavage to become fully functional (Yin et al., 2007). Protein expression in heterologous systems may lack one or more of these essential stages/elements resulting in the expression of non-functional proteins. Due to negative results being the potential outcome of target gene incompatibility with the expression system, heterologous expression has limitations by only allowing the characterization of genes via positive results. However, with the absence of a transformation system for coccolithophores, heterologous expression systems are the best available approach to understand gene function. Ultimately, to understand the role of a gene in its native environment, the ability to knockdown, knockout or increase expression is critical. With transformation systems becoming widely available in marine unicellular algae such as the diatoms and *Ostreococcus* sp., the development of this technology in coccolithophores should be feasible and is essential to ensure that coccolithophore biology is not left in the shadows.

Materials and Methods

Target Gene Identification - A comparative transcriptomic study of haploid and diploid cells identified key sets of genes that were ploidy specific (von Dassow et al., 2009). Due to the absence of calcification in haploid cells it can be hypothesized that diploid specific genes play a possible role in calcification, although it has to be noted that there are numerous other physiological differences that could attribute to differential gene expression. Based on this two diploid specific genes, a putative $\text{Ca}^{2+}/\text{H}^{+}$ exchanger (*CAX3*) and a putative HCO_3^{-} transporter (*AEL1*), were chosen for further characterization.

Rapid Amplification of cDNA Ends (RACE) - To determine the full transcript of *CAX3* and *AEL1* RNA ligase-mediated rapid amplification of 5' and 3' cDNA ends (RLM-RACE) (GeneRacer™ Kit, Invitrogen) was used. The method applied ensures that only full-length transcripts with a 5' mRNA cap and a 3' polyA tail are amplified and later sequenced. To implement RACE a section

of the target gene sequence needs to be known, this was available from von Dassow et al. (2009) and an early draft of the *E. huxleyi* genome project.

Total RNA was extracted from *E. huxleyi* strain CCMP1516 cells in the exponential growth phase. Briefly; cells were pelleted by centrifugation at 5000 rpm for 5 minutes at 15 °C. The pellet was re-suspended in RNA extraction buffer containing β -mercaptoethanol and RNA was extracted using the RNeasy kit and provided protocol (Invitrogen). RNA purity and quantity was determined using a NanoDrop (Thermo Scientific) and the integrity checked on an Agilent Bioanalyser. RNA was stored at -80 °C. RACE was carried out according to the supplied protocol: to eliminate 5' truncated mRNA and non-mRNA total RNA was treated with calf intestinal phosphatase (CIP). CIP removes 5' phosphates from RNA but has no effect on full-length transcripts with a 5' cap. The RNA was then treated with tobacco acid pyrophosphatase (TAP) which removes the 5' cap structure leaving a 5' phosphate (on only full-length transcripts) which is then used to ligate the GeneRacer™ RNA oligo to the 5' of full length RNA using T4 ligase. The ligation of this oligo provides a known sequence for GeneRacer™ PCR primers to amplify cDNA in a later step. The mRNA was then reverse transcribed using SuperScript III reverse transcriptase and GeneRacer™ oligo dT primers with a known sequence after the polyT run. This results in the first-strand cDNA having a known sequence at both the 3' and 5' end. Using primers designed to the known region of the target gene (gene specific primers, GSP), primers that complement the 5' ligated GeneRacer™ RNA oligo and the 3' GeneRacer™ oligo dT primer, the unknown regions at the 5' and 3' ends can be amplified and then cloned for sequencing. Further nested primers for both the 5' and 3' ends were needed for successful amplification and cloning (Supplementary Table SI). After successful amplification the 5' and 3' ends were gel purified (QIAEX II or QIAquick gel extraction kit) and either TOPO-cloned into the pCR4-TOPO vector (Invitrogen) or TA cloned into the pCR2.1 vector (Invitrogen).

Cloning - Primers were designed to amplify the coding sequence of *CAX3* and *AEL1* (Table SI). To minimise amplification errors that can be introduced by Taq polymerase, Platinum Taq DNA polymerase high fidelity (Invitrogen) was used for amplification from cDNA. The amplicons were cloned into pCR4-TOPO (*CAX3*) and pCR2.1 (*AEL1*) and sequenced.

Phylogenetic Analysis - To investigate the phylogenetic relationships of *CAX3* within the *CAX* subfamily type I and *AEL1* within the *SLC4* family protein sequences were aligned with respective proteins from the literature using ClustalW. For *CAX3* tree analysis the $\alpha 1$ and $\alpha 2$ conserved domains of 30 *CAX* proteins from a diverse range of organisms were used. For *AEL1* analysis conserved transmembrane regions from 27 *SLC4* proteins were used. Phylogenetic

analysis was performed using the minimum evolution function in MEGA version 4 (Tamura et al., 2007).

Codon Optimisation - The coding sequences for *CAX3* allele 1 and *AEL1* “allele 1” determined by RACE were codon optimized for yeast expression and human cell expression respectively. Full-length codon optimized genes were synthesised by GenScript (USA) and supplied in a *pUC57* vector. The constructs were named *pUC57_coCAX3* and *pUC57_coAEL1*. To allow for further restriction cloning into expression vectors the *pUC57_coCAX3* construct contained a BamHI site upstream of the ATG start codon and a NotI downstream of the stop codon and the *pUC57_coAEL1* construct had an upstream BamHI and a downstream XhoI.

CAX3 Yeast Complementation - Codon optimized *CAX3* (*coCAX3*) and modified constructs were expressed in *Saccharomyces cerevisiae* strain K667 (genotype: *MATa ade2-1 can1-100 his3-11,15 leu2-3,112 trp1-1 ura3-1 cnb1::LEU2 pmc1::TRP1 vcx1Δ*; ((Cunningham and Fink, 1996); kindly provided by Jon Pittman) and K601 the isogenic wild type strain.

CAX3 DNA constructs – Yeast expression vector *pUGpd* (kindly provided by Jon Pittman) was used for complementation studies, it contains an ampicillin resistance gene for bacterial selection and *URA3* for selection in uracil dependent yeast. To confirm expression and view cellular localization, an in frame GFP fusion was expressed (*pUGpd_coCAX3-eGFP*). To investigate the possibility of an auto-regulatory N-terminal region a 5' truncated version was also cloned (*pUGpd_5'TrcoCAX3*). Full-length *coCAX3* was directly subcloned from the *pUC57* vector into the BamHI and NotI site of the *pUGpd* MCS (multiple cloning site). Truncated *coCAX3* was cloned by amplification with primers (Supplementary Table SII) containing BamHI and NotI restriction sites and AT cloned into the general cloning vector pCR2.1 (Invitrogen). It was then directionally cloned into the BamHI and NotI sites in *pUGpd*. Cloning of the *coCAX3-eGFP* construct was performed by 3-way cloning; *coCAX3* was amplified from *pUC57_coCAX3* (destroying the stop codon) then digested at the SpeI and BamHI sites, which were inserted in the amplification step. *eGFP* was digested from *pEGFP-N2* (kindly supplied by Frederic Verret) by BamHI and NotI retaining the stop codon. *pUGpd* was restriction digested with SpeI and NotI. All three constituents were gel purified and ligated at a 1:2:2 *vector:coCAX3:eGFP* (Fig. S4). All constructs were checked by restriction digestion and sequencing.

CAX3 yeast expression and complementation tests - The different vector constructs including the empty *pUGpd* as a control were transformed into yeast strains K601 and K667 using the lithium

acetate/single-stranded DNA/PEG method (Ausubel et al., 1994) and selected on synthetic complete medium minus uracil (SC-U) agar plates at 30°C. Yeast expressing the *coCAX3-eGFP* construct were viewed using confocal microscopy on a Nikon Eclipse E1000 microscope with a Radiance 2100 confocal laser scanning system using standard GFP excitation wavelengths and filters. In conjunction Hoechst (Invitrogen) was used to stain the nucleus. Cells were incubated for 40 minutes in 1 µg ml⁻¹ Hoechst before imaging. To test for Ca²⁺ tolerance and tolerance to other cations yeast was grown in SC-U liquid media, the OD₆₀₀ was measured and dilutions were spotted onto solid YPD media containing various cations at differing concentration - CaCl₂ (20, 50, 200 mM), MnCl₂ (1.5, 5 mM), NaCl (500, 750 mM), MgCl₂ (100, 400 mM), KCl (200, 500 mM), CdCl₂ (2.5 mM), ZnCl₂ (5 mM), BaCl₂ (5 mM), SrCl₂ (5 mM), CoCl₂ (2.5 mM), FeCl₂ (5 mM) and CuCl₂ (5 mM). To see if pH had an effect on the ability of *CAX3* to rescue the Ca²⁺ hypersensitivity of K667 spot tests on 20 mM CaCl₂ plates buffered at pH 4, 6 and 8 using 155 mM Tris-HCl were carried out. All spot tests were incubated at 30°C and photographed after 3-8 days.

CAX3 E. coli expression - *CAX3* complementation was tested in the Na⁺, Ca²⁺ and alkaline sensitive *E. coli* strain KNabc (kindly provided by Terry Krulwich, Mount Sinai School of Medicine, New York). KNabc was routinely grown at pH 7.5 in LB medium containing potassium instead of sodium (LBK) and 50 µg ml⁻¹ of kanamycin (Goldberg et al., 1987). Codon optimised *CAX3* was amplified from *pUC57_coCAX3* using forward and reverse primers containing NcoI and BglII restriction sites, respectively (Table SII). The amplicon was TA cloned into pCR2.1 and transformed into TOP10F' *E. coli* (Invitrogen). The *pCR2.1_coCAX3* construct was sequenced and *coCAX3* cut out and directionally cloned into the *E. coli* expression vector *pQE60* (QIAGEN) using NcoI and BglII restriction sites. KNabc was transformed with the *pQE60_coCAX3* and empty *pQE60* vectors using the standard CaCl₂/heat-shock method (Ausubel et al., 1994). As a positive control TOP10F' *E. coli* containing an empty *pCR2.1* vector was used. Further growth tests were also conducted using TOP10F' cells expressing *pQE60* and *pQE60_coCAX3*.

To test if *CAX3* could complement the Ca²⁺, Na⁺ or alkaline sensitivity of KNabc or influence the phenotype of TOP10F', spot tests were conducted on buffered LB media containing various concentrations of Ca²⁺, K⁺ and Na⁺ concentrations with 25 mM Tris Base and 25 mM 2-(N-Morpholino)ethanesulfonic acid (MES). The pH of the media was adjusted to pH 6 or 7 using HCl. To test the influence *CAX3* had on the salt sensitivity of KNabc spot tests on LBK media containing 5mM Li⁺ were carried out at pH 5.5, 6.5 and 7.5. Growth in the absence of Na⁺, Ca²⁺, K⁺ and Li⁺ was tested by growing cells on LB choline chloride (LBC). Spot tests

using KNabc cells expressing *pQE60* or *pQE60_coCAX3* were grown on LB media containing 50 $\mu\text{g ml}^{-1}$ kanamycin and 200 $\mu\text{g ml}^{-1}$ of ampicillin, for TOP10F' cells expressing *pQE60* or *pQE60_coCAX3* kanamycin was omitted. A 1:100 serial dilution from OD_{600} 1 – 0.0001 was spotted onto plates containing 0.25 mM IPTG to induce expression of *pQE60* inserts. Spotted plates were incubated at 37 °C.

AEL1 DNA constructs and expression - For mammalian cell expression of *AEL1*, *coAEL1* was restriction digested out of *pUC57_coAEL1* using BamHI (5' end) and XhoI (3' end) and ligated into the corresponding sites of *pcDNA3.1* (Invitrogen) - a mammalian expression vector. To confirm *coAEL1* was being expressed and to assess cellular localization a *coAEL1_eGFP* fusion construct was made. *coAEL1* was amplified from *pUC57_coAEL1* (see Table SII for primer details) and cloned into the HindIII and BamHI sites of *pcDNA3.1_HVCNI-eGFP*. This removed the *HVCNI* gene and destroyed the stop codon of *coAEL1*, forming *pcDNA3.1_coAEL1-eGFP*. All constructs were checked by sequencing. For physiological and localization studies, 1 μg of *pcDNA3.1_coAEL1-eGFP* (with 0.4 μg of *pcDNA3.1-eGFP* to check successful expression) or 1 μg of *pcDNA3.1_coAEL1-eGFP* were transiently expressed in HEK293 cells using Lipofectamine LTX (Invitrogen).

AEL1 HEK293 expression – To investigate *coAEL1-eGFP* cellular location, HEK293 cells expressing *coAEL1-eGFP* were imaged with a Zeiss LSM 510 confocal microscope (the cell nucleus was stained with 5 $\mu\text{g/ml}$ of Hoechst nucleic acid stain for 20 minutes and the PM by 5 μM FM 4-64 for ~2 minutes). To investigate the function of *coAEL1*, intracellular pH was monitored in transfected HEK293 cells as they were perfused with various solutions in the presence/absence of Cl^- and Na^+ with 5 μM of the Na^+/H^+ exchanger inhibitor 5-(N-ethyl-N-isopropyl) amiloride (EIPA) (See table S3 for used solutions). Intracellular pH changes were monitored using the ratiometric dye BCECF-AM. Cells were incubated with 2.5 μM BCECF-AM for 15 minutes and pH measurements taken using a LSM 510 confocal microscope (Zeiss, Jena, Germany) by the ratio of the fluorescence emission at 525 nm when excited sequentially with 488 and 458 nm. Ratios were calculated by using the average fluorescence intensity taken from multiple regions of interest within the cytoplasm of ~10 cells.

References

- Ausubel FM, Brent R, Kingston RE, Moore DD, Seidman JG, Smith JA, Struhl K** (1994) Current Protocols in Molecular Biology. Greene Publishing Associates and Wiley-Interscience, New York
- Berry L, Taylor AR, Lucken U, Ryan KP, Brownlee C** (2002) Calcification and inorganic carbon acquisition in coccolithophores. *Functional Plant Biology* **29**: 289-299
- Brownlee C, Davies M, Nimer N, Dong LF, Merrett MJ** (1995) Calcification, photosynthesis and intracellular regulation in *Emiliania huxleyi*. *Bulletin Institute Oceanographique Monaco* **14**: 19-35
- Cheng N-H, Hirschi KD** (2003) Cloning and Characterization of CXIP1, a Novel PICOT Domain-containing Arabidopsis Protein That Associates with CAX1. *Journal of Biological Chemistry* **278**: 6503-6509
- Cheng N-H, Pittman JK, Zhu J-K, Hirschi KD** (2004) The Protein Kinase SOS2 Activates the Arabidopsis H⁺/Ca²⁺ Antiporter CAX1 to Integrate Calcium Transport and Salt Tolerance. *Journal of Biological Chemistry* **279**: 2922-2926
- Cheng NH, Liu JZ, Nelson RS, Hirschi KD** (2004) Characterization of CXIP4, a novel Arabidopsis protein that activates the H⁺/Ca²⁺ antiporter, CAX1. *FEBS Letters* **559**: 99-106
- Cunningham KW, Fink GR** (1996) Calcineurin inhibits VCX1-dependent H⁺/Ca²⁺ exchange and induces Ca²⁺ ATPases in *Saccharomyces cerevisiae*. *Molecular and Cellular Biology* **16**: 2226-2237
- Goldberg EB, Arbel T, Chen J, Karpel R, Mackie GA, Schuldiner S, Padan E** (1987) Characterization of a Na⁺/H⁺ antiporter gene of *Escherichia coli*. *Proceedings of the National Academy of Sciences* **84**: 2615-2619
- Herfort L, Thake B, Roberts J** (2002) Acquisition and use of bicarbonate by *Emiliania huxleyi*. *New Phytologist* **156**: 427-436
- Hirschi KD, Zhen RG, Cunningham KW, Rea PA, Fink GR** (1996) CAX1, an H⁺/Ca²⁺ antiporter from Arabidopsis. *Proceedings of the National Academy of Sciences* **93**: 8782-8786
- Langer G, Geisen M, Baumann K-H, Kläs J, Riebesell U, Thoms S, Young JR** (2006) Species-specific responses of calcifying algae to changing seawater carbonate chemistry. *Geochemistry Geophysics Geosystems* **7**: 10.1029/2005gc001227
- Langer G, Gussone N, Nehrke G, Riebesell U, Eisenhauer A, Kuhnert H, Rost B, Trimborn S, Thoms S** (2006) Coccolith Strontium to Calcium Ratios in *Emiliania huxleyi*: The Dependence on Seawater Strontium and Calcium Concentrations. *Limnology and Oceanography* **51**: 310-320
- Liu H, Zhang X, Takano T, Liu S** (2009) Characterization of a PutCAX1 gene from *Puccinellia tenuiflora* that confers Ca²⁺ and Ba²⁺ tolerance in yeast. *Biochemical and Biophysical Research Communications* **383**: 392-396
- Mackinder L, Wheeler G, Schroeder D, Riebesell U, Brownlee C** (2010) Molecular Mechanisms Underlying Calcification in Coccolithophores. *Geomicrobiology Journal* **27**: 585 - 595
- Mackinder L, Wheeler G, Schroeder D, von Dassow P, Riebesell U, Brownlee C** (2011) Expression of biomineralization-related ion transport genes in *Emiliania huxleyi*. *Environmental Microbiology* **13**: 3250-3265
- Manohar M, Mei H, Franklin AJ, Sweet EM, Shigaki T, Riley BB, MacDiarmid CW, Hirschi K** (2010) Zebrafish (*Danio rerio*) Endomembrane Antiporter Similar to a Yeast Cation/H⁺ Transporter Is Required for Neural Crest Development. *Biochemistry* **49**: 6557-6566
- Manohar M, Shigaki T, Hirschi KD** (2011) Plant cation/H⁺ exchangers (CAXs): biological functions and genetic manipulations. *Plant Biology* **13**: 561-569

- Miroux B, Walker JE** (1996) Over-production of Proteins in *Escherichia coli*: Mutant Hosts that Allow Synthesis of some Membrane Proteins and Globular Proteins at High Levels. *Journal of Molecular Biology* **260**: 289-298
- Nimer NA, Merrett MJ** (1992) Calcification and utilization of inorganic carbon by the coccolithophorid *Emiliana huxleyi* Lohmann. *New Phytologist* **121**: 173-177
- Pittman JK, Hirschi KD** (2001) Regulation of CAX1, an Arabidopsis $\text{Ca}^{2+}/\text{H}^{+}$ Antiporter. Identification of an N-Terminal Autoinhibitory Domain. *Plant Physiology* **127**: 1020-1029
- Pittman JK, Shigaki T, Cheng N-H, Hirschi KD** (2002) Mechanism of N-terminal Autoinhibition in the Arabidopsis $\text{Ca}^{2+}/\text{H}^{+}$ Antiporter CAX1. *Journal of Biological Chemistry* **277**: 26452-26459
- Pittman JK, Shigaki T, Hirschi KD** (2005) Evidence of differential pH regulation of the Arabidopsis vacuolar $\text{Ca}^{2+}/\text{H}^{+}$ antiporters CAX1 and CAX2. *FEBS Letters* **579**: 2648-2656
- Pittman JK, Sreevidya CS, Shigaki T, Ueoka-Nakanishi H, Hirschi KD** (2002) Distinct N-Terminal Regulatory Domains of $\text{Ca}^{2+}/\text{H}^{+}$ Antiporters. *Plant Physiology* **130**: 1054-1062
- Pushkin A, Kurtz I** (2006) SLC4 base (HCO_3^- , CO_3^{2-}) transporters: classification, function, structure, genetic diseases, and knockout models. *AJP Renal Physiology* **290**: F580-599
- Rokitta SD, de Nooijer LJ, Trimborn S, de Vargas C, Rost B, John U** (2011) Transcriptome Analyses Reveal Differential Gene Expression Patterns between the Life-Cycle Stages of *Emiliana huxleyi* (Haptophyta) and Reflect Specialization to Different Ecological Niches1. *Journal of Phycology* **47**: 829-838
- Romero M, Fulton C, Boron W** (2004) The SLC4 family of HCO_3^- transporters. *Pflügers Archiv European Journal of Physiology* **447**: 495-509
- Sayanova O, Haslam RP, Caleron MV, Lopez NR, Worthy C, Rooks P, Allen MJ, Napier JA** (2011) Identification and functional characterisation of genes encoding the omega-3 polyunsaturated fatty acid biosynthetic pathway from the coccolithophore *Emiliana huxleyi*. *Phytochemistry* **72**: 594-600
- Schulz KG, Rost B, Burkhardt S, Riebesell U, Thoms S, Wolfgladrow DA** (2007) The effect of iron availability on the regulation of inorganic carbon acquisition in the coccolithophore *Emiliana huxleyi* and the significance of cellular compartmentation for stable carbon isotope fractionation. *Geochimica et Cosmochimica Acta* **71**: 5301-5312
- Shigaki T, Rees I, Nakhleh L, Hirschi KD** (2006) Identification of Three Distinct Phylogenetic Groups of CAX Cation/Proton Antiporters. *Journal of Molecular Evolution* **63**: 815-825
- Sikes CS, Roer RD, Wilbur KM** (1980) Photosynthesis and coccolith formation - inorganic carbon-sources and net inorganic reaction of deposition. *Limnology and Oceanography* **25**: 248-261
- Tamura K, Dudley J, Nei M, Kumar S** (2007) MEGA4: Molecular Evolutionary Genetics Analysis (MEGA) software version 4.0. *Molecular Biology and Evolution* **24**: 1596-1599
- Taylor AR, Chrachri A, Wheeler G, Goddard H, Brownlee C** (2011) A voltage-gated H^{+} channel underlying pH homeostasis in calcifying coccolithophores. *PLoS Biology* **9**: e1001085
- von Dassow P, Ogata H, Probert I, Wincker P, Da Silva C, Audic S, Claverie JM, de Vargas C** (2009) Transcriptome analysis of functional differentiation between haploid and diploid cells of *Emiliana huxleyi*, a globally significant photosynthetic calcifying cell. *Genome Biology* **10**: R114
- Waditee R, Hossain GS, Tanaka Y, Nakamura T, Shikata M, Takano J, Takabe T, Takabe T** (2004) Isolation and Functional Characterization of $\text{Ca}^{2+}/\text{H}^{+}$ Antiporters from Cyanobacteria. *Journal of Biological Chemistry* **279**: 4330-4338

- Wang C-Z, Yano H, Nagashima K, Seino S** (2000) The Na⁺-driven Cl⁻/HCO₃⁻ Exchanger: Cloning, tissue distribution, and functional characterization. *Journal of Biological Chemistry* **275**: 35486-35490
- Wei Y, Liu J, Ma Y, Krulwich TA** (2007) Three putative cation/proton antiporters from the soda lake alkaliphile *Alkalimonas amylolytica* N10 complement an alkali-sensitive *Escherichia coli* mutant. *Microbiology* **153**: 2168-2179
- Westbroek P, Brown CW, Vanbleijswijk J, Brownlee C, Brummer GJ, Conte M, Egge J, Fernandez E, Jordan R, Knappertsbusch M** (1993) A Model System Approach to Biological Climate Forcing - the Example of *Emiliana huxleyi*. *Global Planet Change* **8**: 27 - 46
- Yin J, Li G, Ren X, Herrler G** (2007) Select what you need: A comparative evaluation of the advantages and limitations of frequently used expression systems for foreign genes. *Journal of Biotechnology* **127**: 335-347
- Zhao J, Barkla B, Marshall J, Pittman J, Hirschi K** (2008) The Arabidopsis *cax3* mutants display altered salt tolerance, pH sensitivity and reduced plasma membrane H⁺-ATPase activity. *Planta* **227**: 659-669

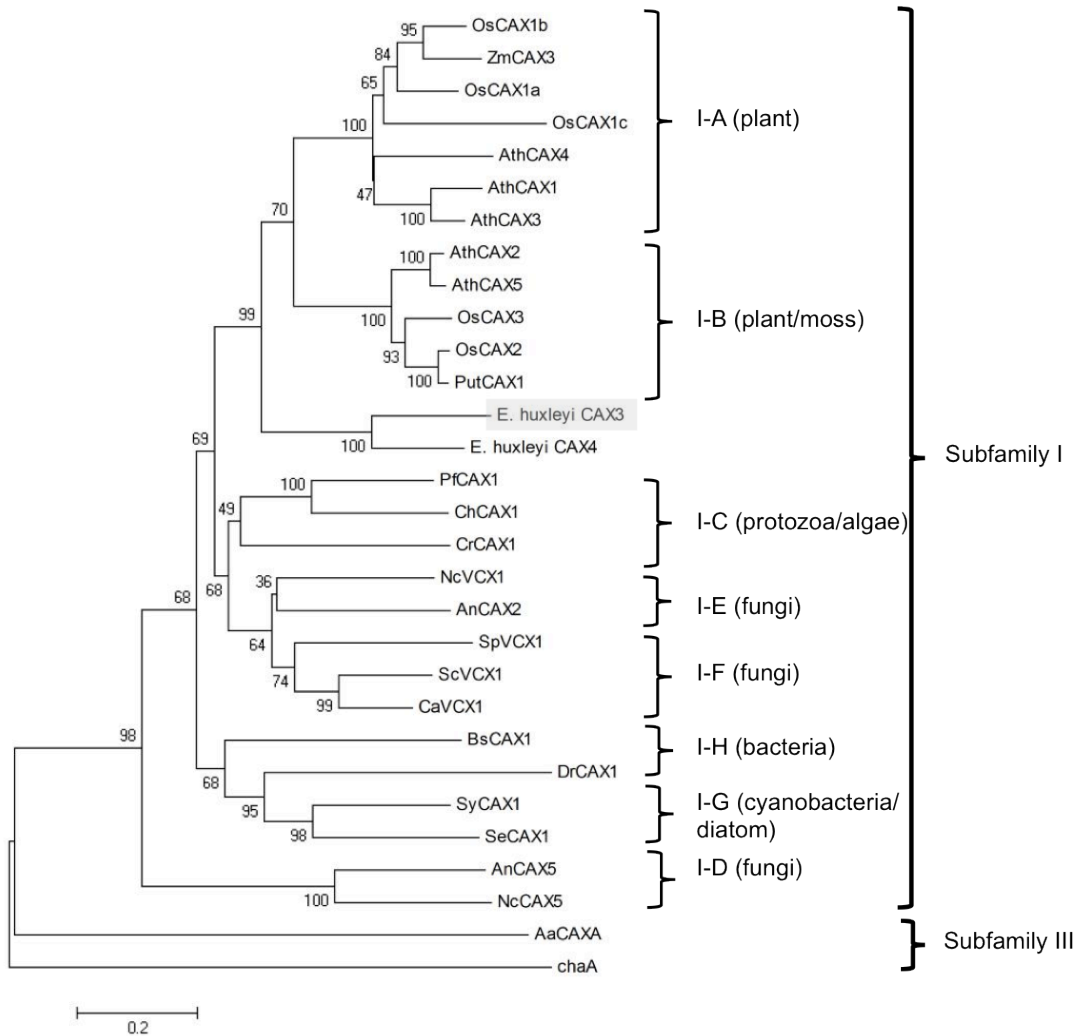


Figure 1. Phylogenetic analysis of *E. huxleyi* CAX3 analysed with CAX family proteins from *Arabidopsis thaliana* (Ath), *Oryza sativa* (Os), *Zea mays* (Zm), *Puccinellia tenuiflora* (Put), *Plasmodium falciparum* (Pf), *Cryptosporidium hominis* (Ch), *Chlamydomonas reinhardtii* (Cr), *Neurospora crassa* (Nc), *Aspergillus nidulans* (An), *Schizosaccharomyces pombe* (Sp), *Saccharomyces cerevisiae* (Sc), *Candida albicans* (Ca), *Bacillus subtilis* (Bs), *Deinococcus radiodurans* (Dr), *Synechococcus* sp. (Sy), *Synechococcus elongates* (Se), *Alkalimonas amylolytica* (Aa) and *Escherichia coli* (ChaA). *E. huxleyi* CAX3 is highlighted in grey. The tree is based on ClustalW alignment of the a1 and a2 regions (Minimum evolution tree-1000 bootstraps).

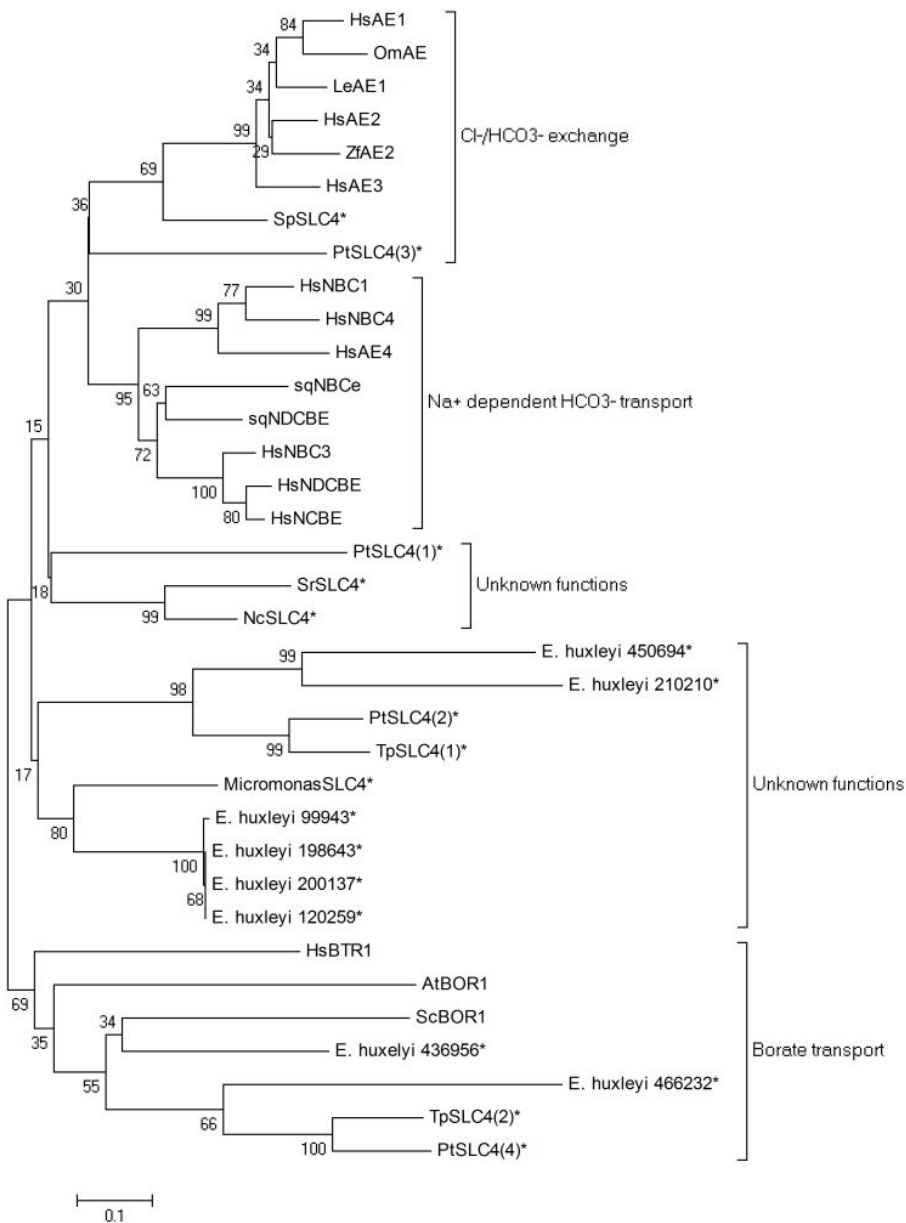


Figure 2. Phylogenetic analysis of *E. huxleyi* SLC4 proteins analyzed with characterized SLC4 transporters from human (Hs), yeast (Sc, *Saccharomyces cerevisiae*), *Arabidopsis thaliana*, (At) squid (sq, *Loligo pealei*), Rainbow trout (Om, *Oncorhynchus mykiss*) and skate (Le, *Leucoraja erinacea*) and uncharacterised SLC4 family transporters (marked with a *) including a picoeukaryotic algae (*Micromonas sp.*), California Sea Urchin (Sp, *Strongylocentrotus purpuratus*), diatoms (Tp, *Thalassiosira pseudonana*) and (Pt, *Phaeodactylum tricorutum*) and two bacterial SLC4 proteins (Sr, *Segniliparus rugosus* and Nc, *Nitrococcus mobilis*). The tree is based on ClustalW alignment of conserved domains (Minimum evolution tree-1000 bootstraps).

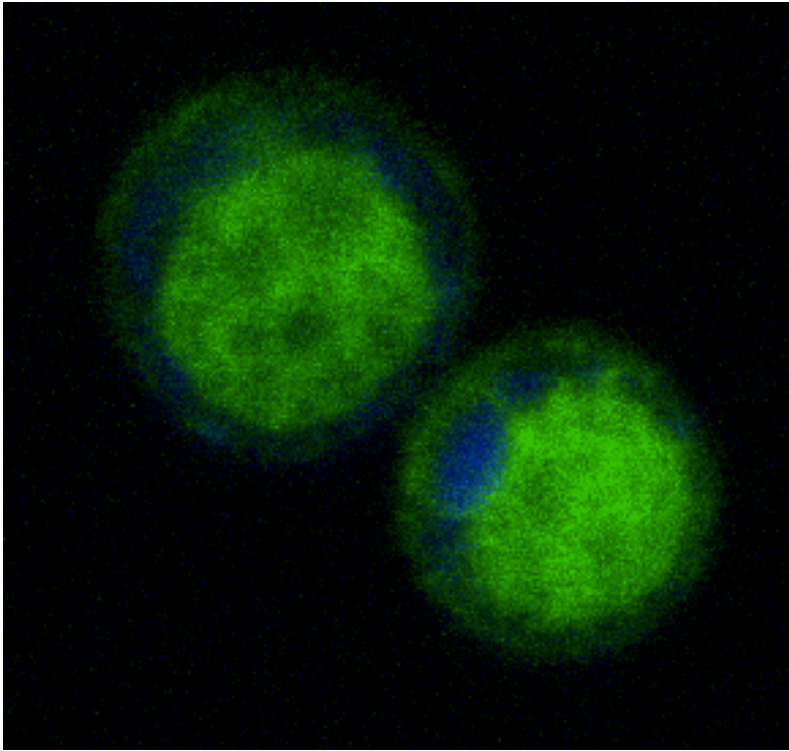


Figure 3. Yeast strain K667 expressing coCAX3-eGFP (Green) and incubated with the nucleic acid stain Hoechst (Blue). Imaged on a Nikon Eclipse E1000 microscope with a Radiance 2100 confocal laser scanning system using standard GFP and Hoechst excitation wavelengths and filters.

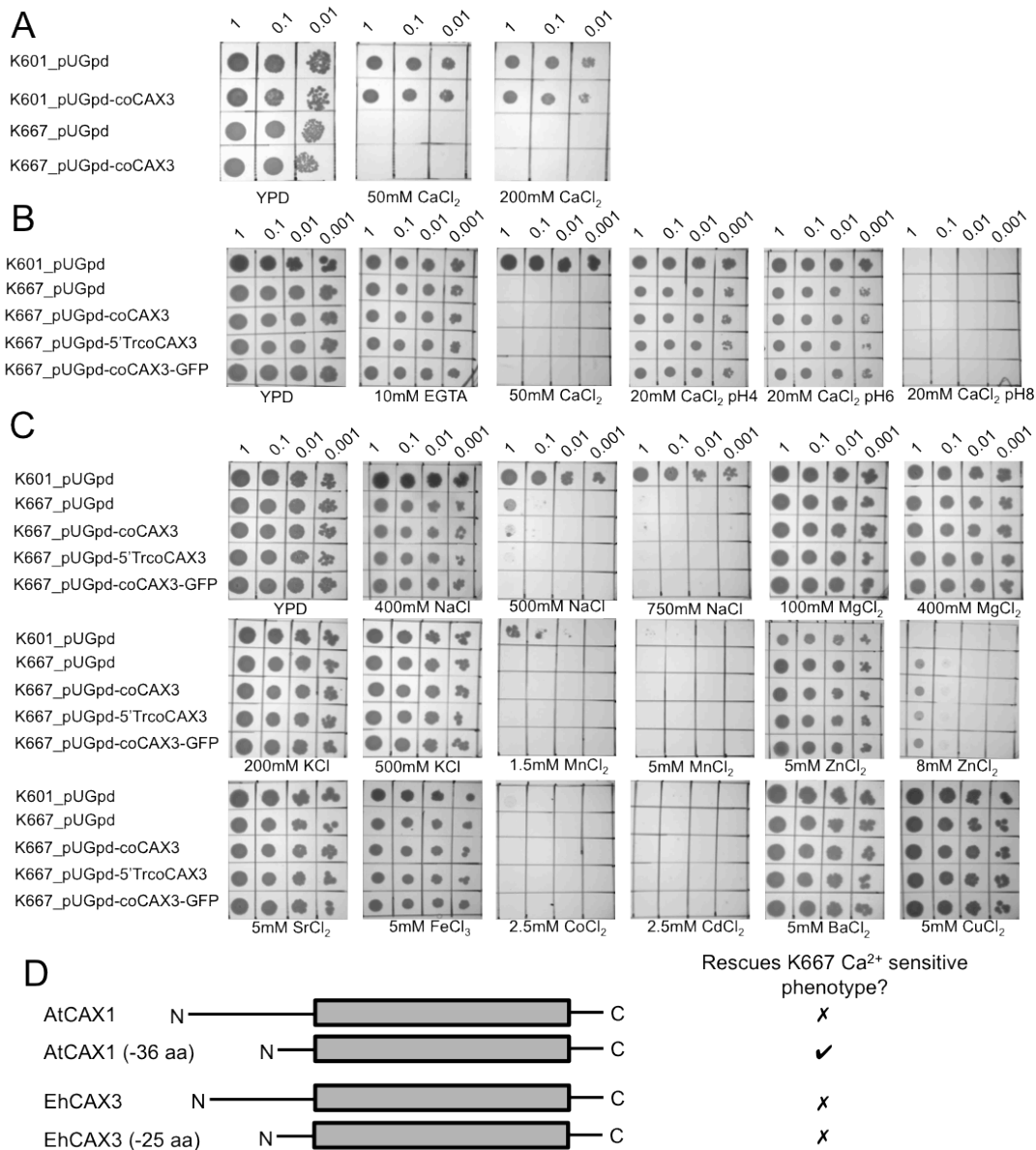


Figure 4. Spot tests of wild-type yeast strain K601 and Ca²⁺ hypersensitive yeast strain K667 expressing varying constructs of *coCAX3*. Yeast was grown in YPD liquid media and diluted to an OD₆₀₀ of 1. 1:10 serial dilutions were made and 3 μ l were spotted onto YPD media containing various cations. A) Empty *pUGpd* vector and *coCAX3* expressed in K601 and K667 on Ca²⁺ containing plates. B) K667 expressing the empty vector and *coCAX3*, 5'*TrcoCAX3* and *coCAX3-GFP* constructs on Ca²⁺ containing YPD plates buffered at different pHs. C) Yeast expressing the different constructs spotted on plates containing varying cations. D) Schematic view of how truncation of *Arabidopsis thaliana* CAX1 and *E. huxleyi* CAX3 affects the Ca²⁺ sensitive phenotype of K667. Boxed grey area represents transmembrane region. Plates were incubated at 30 °C and imaged after 3-8 days.

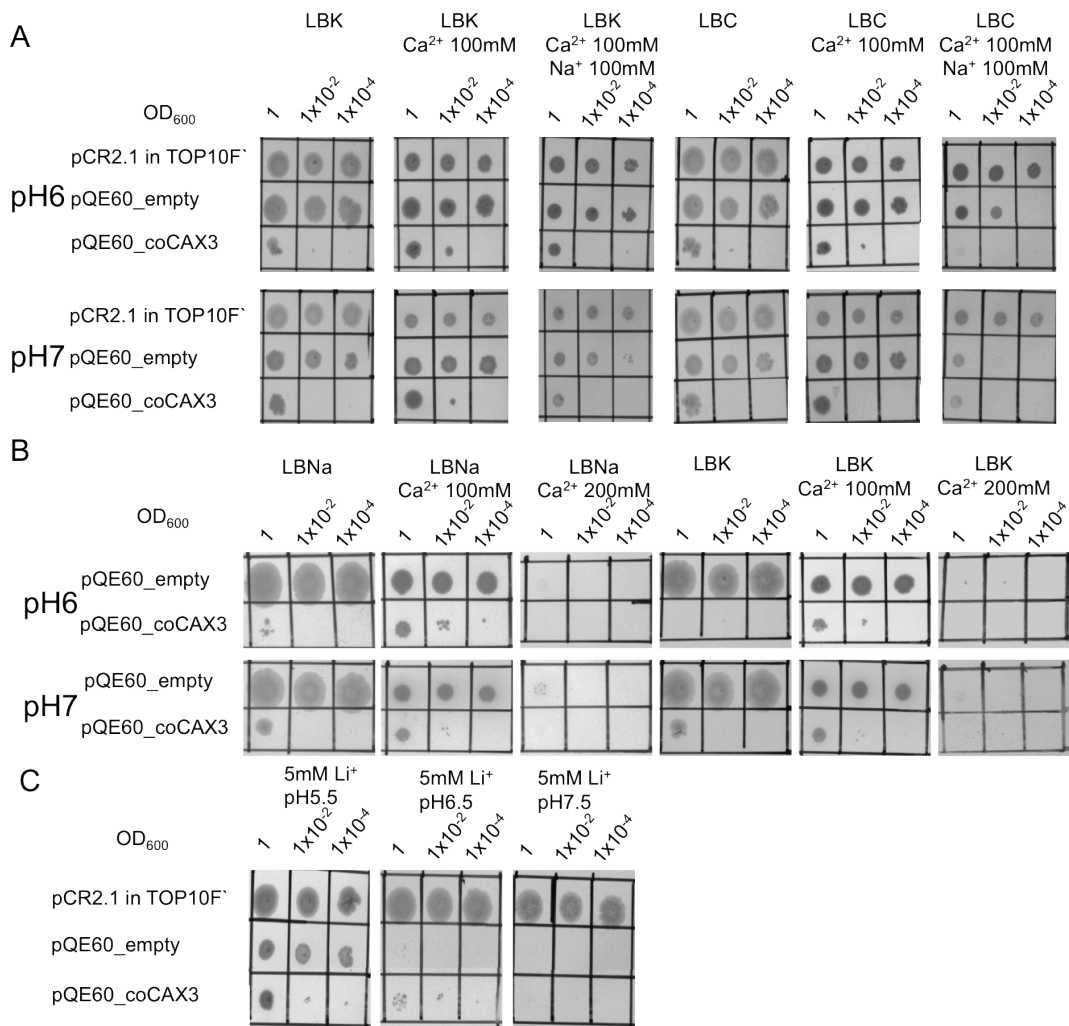


Figure 5. Spot tests of KNabc and TOP10F['] cells expressing the *pQE60* empty vector and *pQE60_coCAX3* vector. A) KNabc cells grown on LBK or LBC plus Ca²⁺ or plus Ca²⁺ and Na⁺ at pH 6 and 7. B) TOP10F['] cells grown on LBNa or LBK plus 100 mM or 200 mM Ca²⁺ at pH 6 and 7. C) KNabc cells on LBK plus 5 mM Li⁺ at pH 5.5, 6.5 and 7.5. The top row in A and C, *pCR2.1* in TOP10F['], is a positive control. A and B were imaged after 4 days and C was imaged after 5 days.

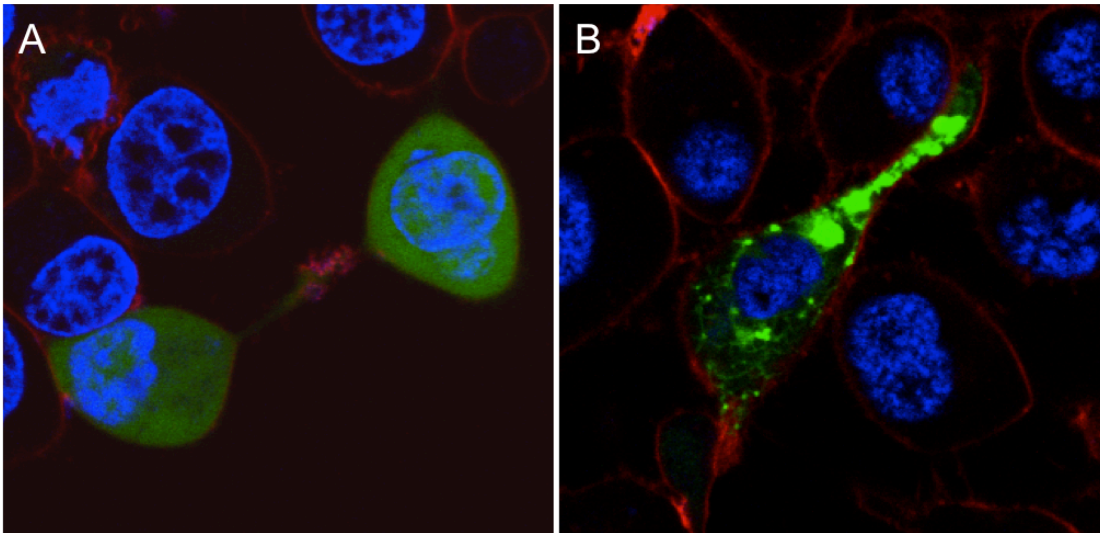


Figure 6. HEK293 cells transfected with A) *pcDNA3.1-eGFP* (green) and B) *pcDNA3.1_coAEL1-eGFP* (green). Stained with Hoechst nucleic acid stain (blue) and FM 4-64 membrane stain (red). Imaged with a Zeiss LSM 510 confocal microscope.

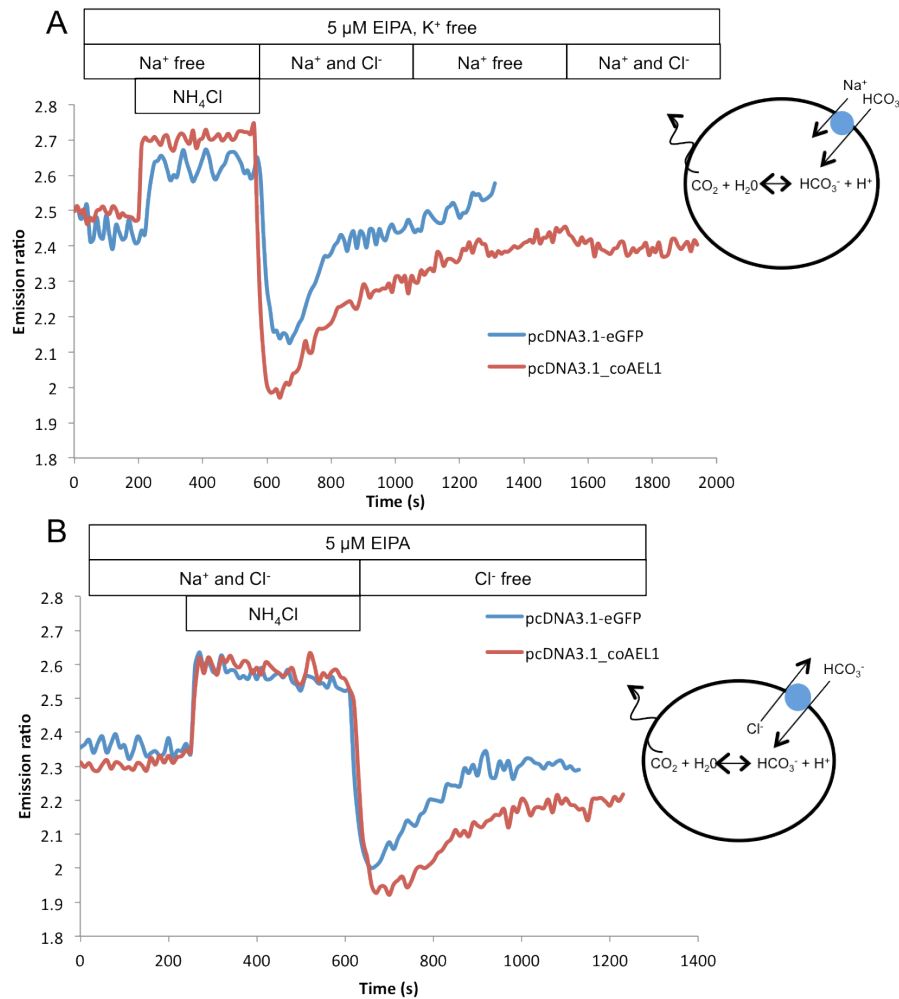


Figure 7. Representative traces of HEK293 cells recovering from an acid load. Perfusion with NH₄Cl initially leads to cellular alkalization due to an influx of NH₃. Upon removal of NH₄Cl, cellular acidification results due to diffusive loss of NH₃ driving the deprotonation of internal NH₄⁺. Each trace is the mean of ~10 regions of interest from several cells expressing either *AEL1* (red) or an empty plasmid (blue). Cells were loaded with BCECF and changes in intracellular pH were recorded from variations in the emission ratio at 525 nm when excited sequentially with lasers at 488 nm and 458 nm. In A) cells were incubated in Na⁺ free media prior to and during intracellular acidification via NH₄Cl. After the acid loading stage they were immediately perfused with Na⁺ containing media. If AEL1 functioned as a Na⁺ HCO₃⁻ co-transporter the large inwards Na⁺ gradient would drive HCO₃⁻ uptake and buffer internal pH at a faster rate than non-AEL1 transformed cells. In B) cells were incubated with Na⁺ and Cl⁻ during acid loading followed by incubation in Cl⁻ free media. In this case if AEL1 functioned as a Cl⁻/HCO₃⁻ exchanger the strong outwards Cl⁻ gradient would drive HCO₃⁻ uptake and increase the recovery rate from an acid load. EIPA was added in all experiments to inhibit the activity of endogenous Na⁺/H⁺ exchangers involved in pH homeostasis.

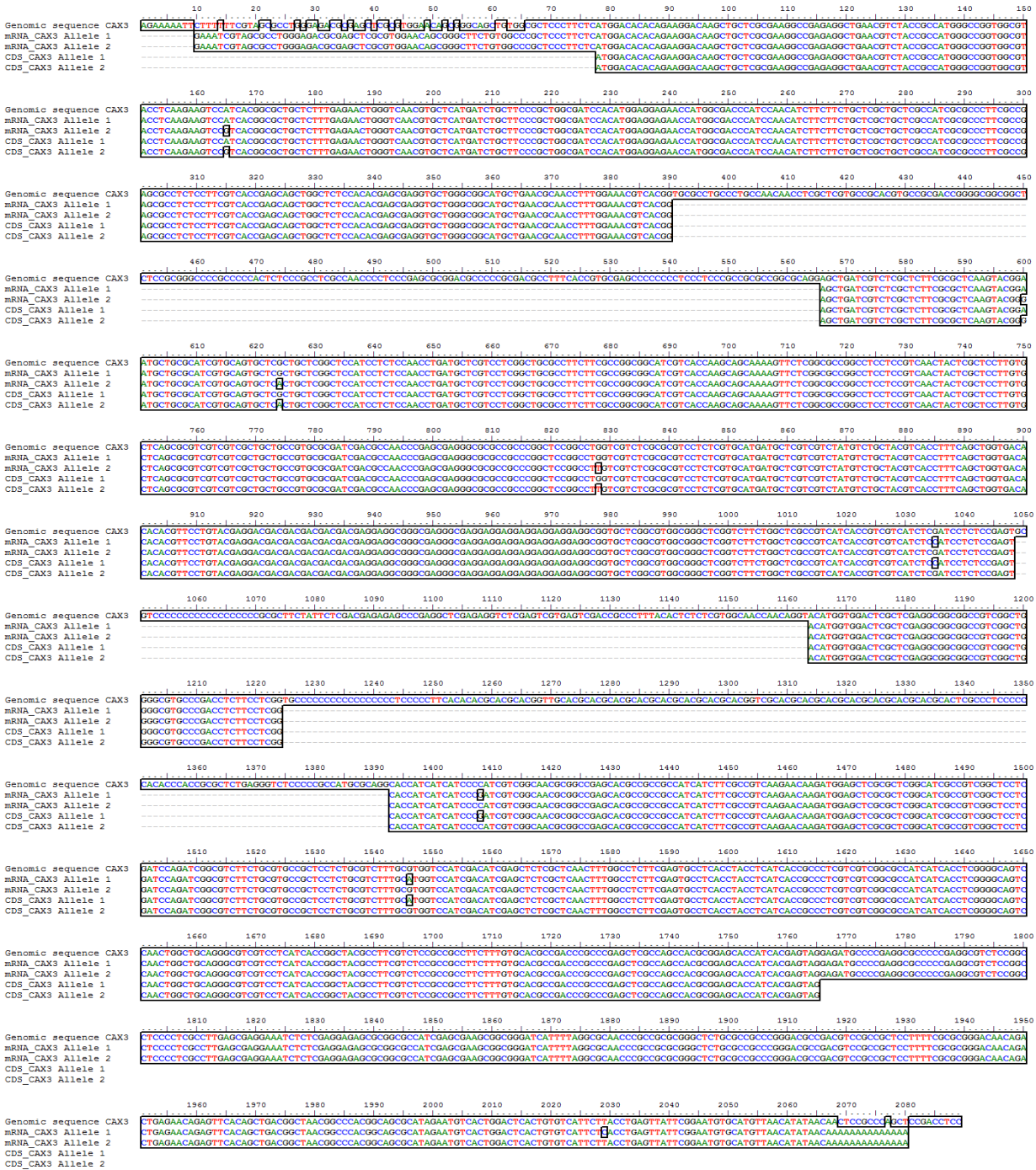


Figure S1. Full-length transcripts (mRNA) and coding regions (CDS) of both allelic copies of *CAX3* determined using Rapid Amplification of cDNA Ends (RACE). Transcripts are mapped against genomic DNA from the *E. huxleyi* genome. Allelic variations are shown.

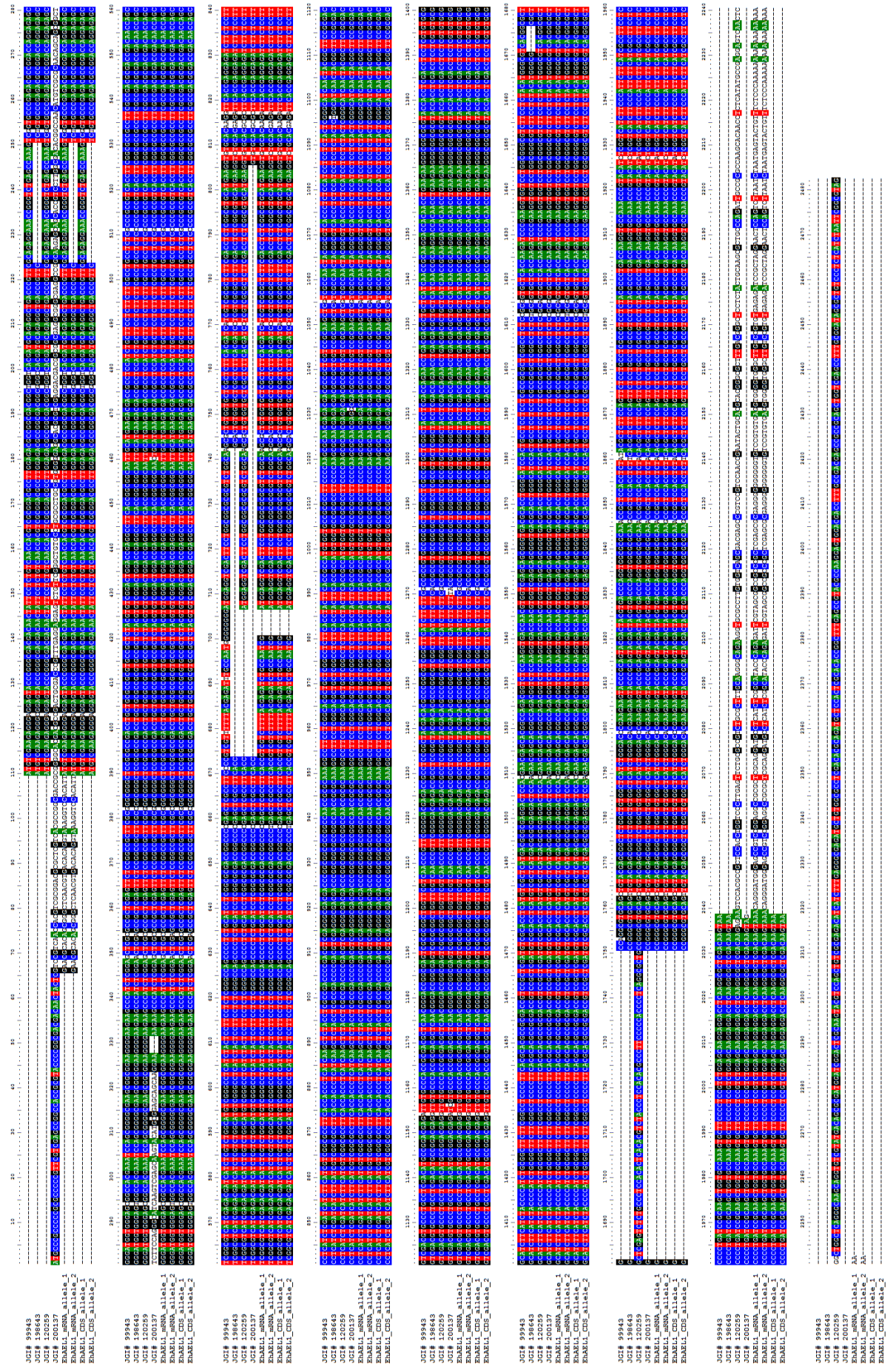


Figure S2. Alignment of *AELI* “allele 1” and “allele 2” mRNA and CDS from RACE and cloning with SLC4 genes found in the genome that show a high level of similarity. *AELI* “allele 1” corresponds to JGI# 99943 and *AELI* “allele 2” corresponds to JGI# 198643 however they both have the same 1st intron as in JGI# 99943. JGI# 120259 shows a high similarity to JGI# 99943 except a 36 bp deletion at position 674, a 69 bp insert at position 1682 and a 444 bp extended 3’ end. JGI# 200137 also shows close similarity to JGI# 99943 however it has a distinct 5’ end of 327 bp. Whether these are valid genes, alleles or assembly errors is currently unclear.

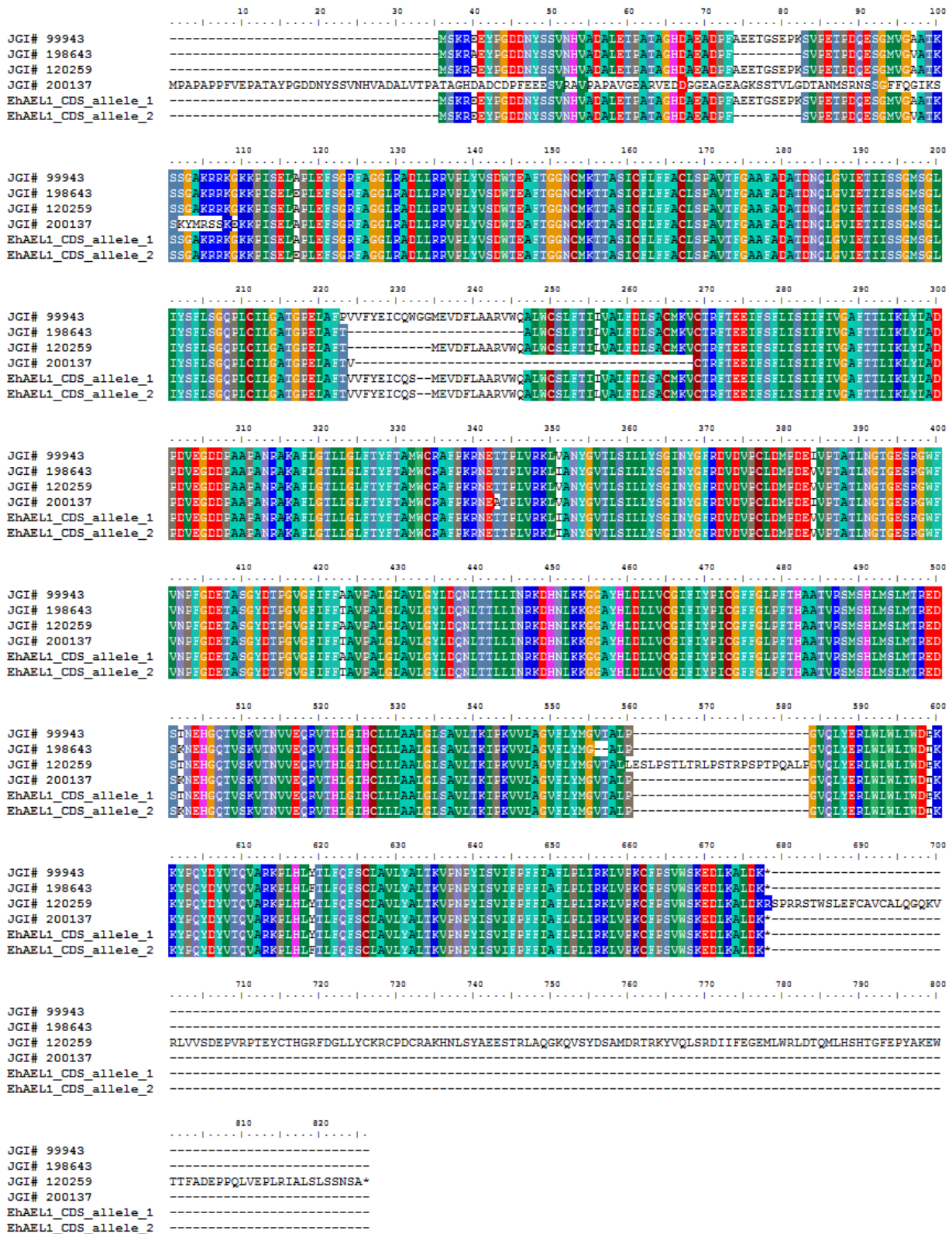


Figure S3. Amino acid sequences of *AEL1* “alleles” obtained by RACE aligned with SLC4 HCO₃⁻ transporters in the *E. huxleyi* genome that show a high level of similarity.

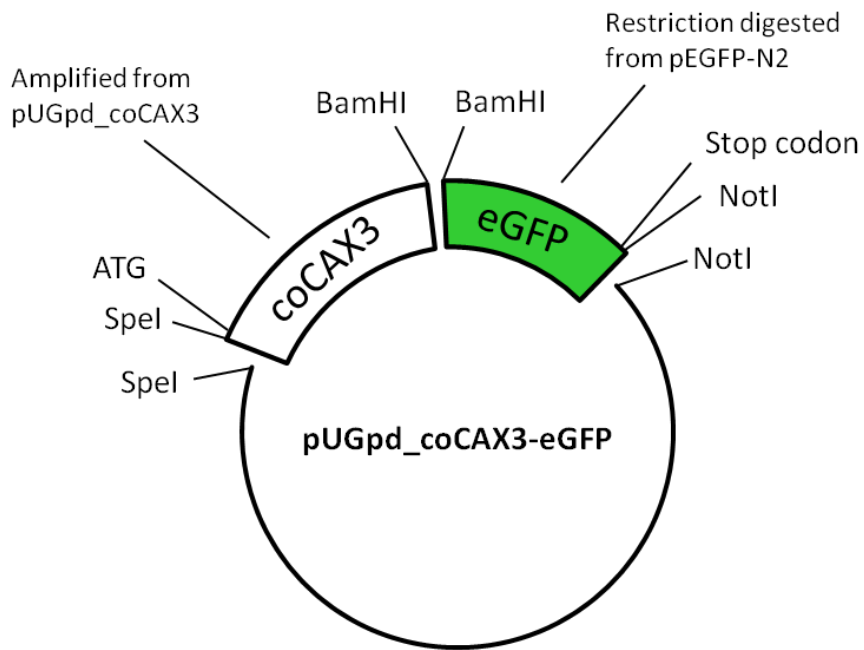


Figure S4. Diagram showing *pUGpd_coCAX3-eGFP* construct made using a three way cloning strategy.

Table SI. Primers used for RACE and cloning of *CAX3* and *AEL1* from *E. huxleyi* cDNA.

Primer	Sequence 5' – 3'
CAX3_GSP_F1	GTCTCGCGCGTCCTCTCGTG CAT
CAX3_GSP_F2_Nested	AGCTGGTGACACACACG TTC
CAX3_GSP_R1	TTGCCGACGATGGGGATGATG ATG
CAX3_GSP_R2_Nested	CGTGACGTTTCCAAAGGTTGCG TTCA
AEL1_GSP_F1	AGCGGCTCTGGCTGTGGCTCAT CTG
AEL1_GSP_F2_Nested	TTCACGCTCTTCCAGTTCTC
AEL1_GSP_R1	GGATCAGGGGGAGGAAGGCGATG AA
AEL1_GSP_R2_Nested	GATCGTGAAGAGCGAGCAC
GeneRacer_5'_Primer	CGACTGGAGCACGAGGACACTGA
GeneRacer_5'_Nested_Primer	GGACACTGACATGGACTGAAGGAGTA
GeneRacer_3'_Primer	GCTGTCAACGATACGCTACGTAACG
GeneRacer_3'_Nested_Primer	CGCTACGTAACGGCATGACAGTG
CAX3_cloning_F	GCTCCCTTCTCATGGACACACA
CAX3_cloning_R	CATGCACATTCCGAATAACTCAGG
AEL1_cloning_F	CACATTATGTCTCGAAGAGGGAGGAGT
AEL1_cloning_R	GACGGCTCCCATCCCTGTTTACT

Table SII. Primers used to create constructs of codon-optimised genes of *CAX3* and *AEL1* for expression in yeast, *E. coli* and HEK293 cells. Restriction sites are underlined and start codons are in bold.

For expression in:	Primer	Sequence 5' – 3'
Yeast	5' TrcoCAX3_F (BamHI)	AAAAGGATCC <u>ATGA</u> AGAAGAGTATAACTGCATTG
Yeast	5' TrcoCAX3_R (NotI)	TTGGGT <u>CGCGCCGC</u> CTCTTATTC
Yeast	coCAX3-eGFP_F (SpeI)	CCAATA <u>ACTAGT</u> AAAATGGATACCCAAAAAG
Yeast	coCAX3-eGFP_R (BamHI)	AAAAGGATCCCTTCATGGT <u>GATGTT</u> CTGC
HEK293	coAEL1-eGFP_F (HindIII)	CCAATA <u>AAGCTT</u> AGGAGGTGCCACCATGAGC
HEK293	coAEL1-eGFP_R (BamHI)	CCTCGAGGATCCCCTTATCCAGGGCTTTCAG
<i>E. coli</i>	coCAX3_F (NcoI)	AAAACCATGGATACCCAAAAAGACAAAT
<i>E. coli</i>	coCAX3_R (BglII)	AAAAAGATCTTTATTCATGGT <u>GATGTT</u> C

Table SIII. Media used for HEK293 *coAEL1* expression experiments.

mM	Bicarbonate buffered - K ⁺ free			Bicarbonate buffered		
	Na ⁺ and Cl ⁻	Na ⁺ and Cl ⁻ + NH ₄ Cl	Na ⁺ free	Na ⁺ and Cl ⁻	Na ⁺ and Cl ⁻ + NH ₄ Cl	Cl ⁻ free
NaCl	117.5	77.5		112.5	72.5	
Na Gluconate						112.5
Choline Chloride			117.5			
K Gluconate				5	5	5
Glucose	5	5	5	5	5	5
Ca Gluconate	1	1	1	1	1	1
Mg Gluconate	1	1	1	1	1	1
NaHCO ₃	25	25		25	25	25
Choline Bicarbonate			25			
HEPES	5	5	5	5	5	5
NH ₄ Cl		40			40	
Adjusted to pH 7.4 with:	NaOH		Choline Hydroxide	NaOH		
Osmolarity of 301 mosmol kg ⁻¹						

CHAPTER 7. Synthesis and future perspectives

The results presented in this thesis provide a significant step in understanding the genetic basis behind the transport processes of Ca^{2+} and DIC in relation to calcification and photosynthesis in coccolithophores. This section will bring together the data from chapters 2-6 placing it in context with our knowledge of calcification and DIC transport from a cellular to global level and discuss future perspectives of research in coccolithophore biology.

7.1 Calcification

Calcification is a highly complex process involving multiple genes to form a network of components, all interacting to maintain stringent control over the calcification process. This study has investigated the transport processes of the ionic substrates and products of calcification. Analysis of the *E. huxleyi* genome (Chapter 5) has identified in excess of 90 genes with known or putative functions of Ca^{2+} , inorganic carbon and H^+ transport. Chapter 3 (Mackinder et al., 2011) examined the expression of 8 of these putative calcification genes providing strong evidence for roles of *CAX3*, *AEL1*, *ATPVc/c'* and *GPA* in calcification with clear transcriptional control between calcification levels. *CAX3*, *AEL1* and *ATPVc/c'* all positively responded (up-regulation) to calcification, while *GPA* showed a consistent down-regulation upon calcification. This questions *GPA*'s role as a Ca^{2+} binding protein involved in the control of calcite precipitation (Corstjens et al., 1998). However, its strong and consistent calcification-related regulation in conjunction with the presence of the coccolith morphology motif (CMM) indicates that *GPA* plays an important but still unknown role in calcification.

To determine the function of *CAX3* and *AEL1* their full-length mRNA was recovered and sequenced. They were both subsequently cloned and heterologously expressed. However neither showed clear functionality when expressed in foreign systems. The explanation behind this is unclear but poor localization to appropriate subcellular locations and the absence of essential supporting proteins may be potential underlying reasons (see Chapter 6). Future research should have a two-pronged approach, one to identify further components involved in calcification and the second to characterize putative calcification genes. These approaches should use high-throughput whole genome methods integrating genomics, transcriptomics and proteomics. Applying these techniques to calcifying vs. non-calcifying isoforms of the same strain could identify whole networks of calcification-related genes. Furthermore, proteomics on isolated CVs and coccoliths could be used to identify non-conserved structural proteins involved in calcification. Alternative functional assays, including the use of different heterologous systems

such as *Xenopus* oocytes and biochemical assays should be explored to characterize putative calcification genes. Also the cellular localization of proteins is critical in understanding their function, making the development and application of immuno-fluorescent and immuno-TEM techniques in coccolithophores a high priority. In order to shift the focus of characterizing individual genes one at a time, the development of high-throughput screens of multiple genes in parallel should be of primary focus. However, the ultimate goal is the development of genetic transformation techniques in coccolithophores to knockout, knockdown and overexpress calcification-related genes to understand the importance of individual genes on calcification processes.

Chapter 2 (Mackinder et al., 2010) reviewed the current literature of calcification in coccolithophores at a molecular level, proposing that Ca^{2+} loading of the CV precursor could be primarily driven by $\text{Ca}^{2+}/\text{H}^+$ exchangers using a H^+ electrochemical gradient maintained by H^+ pumps. This concept is supported by the calcification related expression of *CAX3* and *ATPVc/c'* seen in Chapter 3. However, to maintain a suitable H^+ electrochemical gradient the pH of the CV would have to be relatively low, potentially providing under-saturated conditions. This could be circumvented by increasing CV pH after Ca^{2+} loading by regulating the H^+ pump *ATPVc/c'*. Chapter 2 also proposes that calcification proceeds via an amorphous calcium carbonate (ACC) phase, current data (Singleton, C., Mackinder, L., et al., unpublished) provides strong evidence that this is the case, with ACC most likely controlling calcite crystallization and preventing uncontrolled precipitation during the loading of the CV with Ca^{2+} and DIC.

Whether calcification acts as a CCM for coccolithophores has been discussed in the literature for nearly 50 years, with strong supporting and refuting evidence. In Chapter 4 we clearly show that at low DIC calcification is reduced while growth rates and POC formation are maintained. This decoupling of calcification has previously been shown by Ca^{2+} removal (Leonardos et al., 2009) and chemical inhibition of calcite production (Sekino and Shiraiwa, 1994). In these cases, DIC has been in excess and it could still be argued that calcification could act as a CCM when cells become carbon limited. However, our data clearly shows that calcification is not acting as a CCM, supporting the concept that a reduction in calcification allows the re-allocation of DIC from calcification to photosynthesis. Interestingly genes up-regulated under increased calcification (Chapter 3) were also induced under DIC limitation when calcification was decreased (Chapter 4). The accumulation of DIC into an internal pool could explain this, with both an increase in calcification or an increase in the dependence of photosynthesis (due to a decrease in CO_2 diffusion) on DIC in this internal pool leading to an up-regulation of genes. This switch of gene function between two essential cellular processes is a novel concept that warrants further investigation. Whole transcriptome studies could be used to

identify further components involved in this process and gene knockouts could prove the involvement of individual genes.

It is becoming apparent that coccolithophores follow an “Eppley” curve response to ocean acidification with a clear optimum that can vary between species and strains. This has been used to explain the contradictory responses of different coccolithophores to increasing $p\text{CO}_2$ (Ridgwell et al., 2009). However, most ocean acidification based experiments to date have used relatively small ranges of $p\text{CO}_2$ from pre-industrial (280 ppm) to IPCC 2100 worst-case scenario of ~ 1000 ppm (Meehl et al., 2007) and are unable to disentangle the biological response from the change in carbonate system parameter due to the intrinsic connected nature of the individual parameters. Chapter 4 begins to disentangle the individual components of the carbonate system. The results support Bach et al. (2011) in showing that in an ocean acidification scenario, it is pH which negatively effects calcification not the concomitant increase in $p\text{CO}_2$ or decrease in CO_3^{2-} . It also provides further evidence that HCO_3^- is the principal substrate for calcification and that if enough substrate is present calcification rates can still be saturated even if the pH is not optimal.

7.2 Inorganic carbon transport

Chapter 4 identifies for the first time the genetic basis of a CCM in Haptophytes, providing an insight into genes involved in cellular carbon fluxes. This data has been used to create a conceptual model of inorganic carbon flux in *E. huxleyi* with its associated genes (Fig. 1). However there are still many gaps in our knowledge with future studies investigating the whole transcriptome (currently underway) and the proteome in conjunction with the characterization of individual genes essential to provide a more complete picture.

CCMs are thought to be polyphyletic (Raven et al., 2012), having arisen from multiple separate evolutionary events. This is clearly the case for organisms operating C_3 vs. C_4 and crassulacean acid metabolism (CAM) photosynthesis or cyanobacterial vs. eukaryotic biophysical CCMs. In these comparisons there are fundamental differences in the mechanisms and the molecular components of the CCM (Giordano et al., 2005; Raven et al., 2012). However, whether eukaryotic C_3 biophysical based CCMs have separate evolutionary origins maybe less clear. Cyanobacteria and algal CCMs are thought to have evolved during periods of low CO_2 and high O_2 in the carboniferous ~ 300 Myrs ago (Raven et al., 2012), although they could have evolved in organisms exposed to low CO_2 microenvironments as found in microbial mats and stromatolites or during other low CO_2 episodes in the Proterozoic about 2.4, 0.75 and 0.6 billion years ago (Raven et al., 2012). Genome analysis (Chapter 5) indicates that DIC transport

components found in coccolithophores show strong similarities in both type and diversity compared to diatoms and green algae. If CCMs in eukaryotic algae have evolved from a common ancestor this would have been prior to the divergence of Stramenopiles and Haptophytes from the Archaeplastida thought to be due to a secondary endosymbiotic event ~1.2 Gyrs ago (Falkowski et al., 2004). There is limiting evidence for this as outlined in Giordano et al. (2005) and Raven et al. (2012) but gene families such as *LCIB* that are known to play fundamental roles in CCMs and found in the Archaeplastida, Stramenopiles and Haptophytes could provide useful molecular tools to investigate CCM evolution.

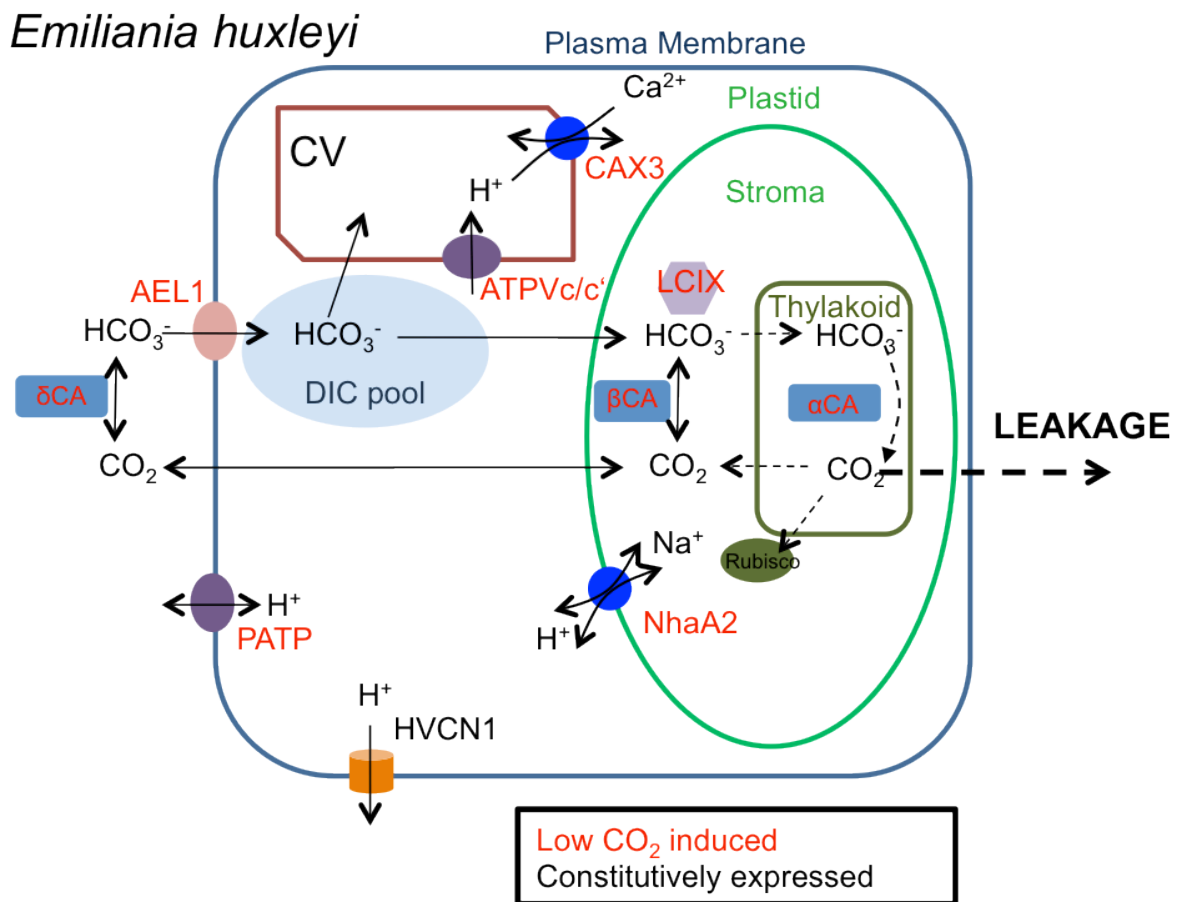


Figure 1. Simplified model of genes potentially involved in the *E. huxleyi* CCM, primarily founded on expression data from Chapter 4. The localization of genes is based on the location of homologues found in other unicellular algae and predictions by WoLF PSORT and TargetP. The cycling of HCO₃⁻ and CO₂ between the thylakoid and stroma is supported by expression data but is primarily based on *Chlamydomonas* models and concepts proposed by Raven (1997). Genes involved in H⁺ transport are hypothesized to play a crucial role in regulating compartmental pH, which determines CO₂:HCO₃⁻ ratios. Genes in red are up-regulated at low DIC.

Whether the critical values associated with CCM regulation seen in Chapter 4 apply to other coccolithophore species is uncertain. Due to the Isochrysidales having diverged from all the other extant calcifying Haptophytes ~150 Myrs ago (De Vargas et al., 2007) there could be considerable genetic variations between coccolithophore families. An insight into the genetic variation of CCMs within families can be seen in cyanobacteria with the components and regulation of the CCM being more dependent on the environment the species is found in than its genetic origins (Price et al., 2008). Thus, species that experience heavily fluctuating environments (i.e. freshwater) tend to have a more diverse set of CCM components and a higher level of CCM regulation in comparison to species in more stable environments such as oceanic oligotrophic waters (Badger et al., 2006). This may also be the deterrent of CCM presence and function in coccolithophores. The investigation of CCMs in coccolithophores that occupy different habitats (i.e. open ocean vs. coastal) and with different life-styles (i.e. bloom forming vs. non bloom forming) could provide interesting information on coccolithophore CCM diversity and activity.

Chapter 4 implies that external CO_2 concentration is the driving force behind growth rates over the complete range of tested DIC. Most CCMs are based on a HCO_3^- rather than a CO_2 economy due to it forming the bulk of DIC in seawater and its charged nature (Giordano et al., 2005). Also the active transport of CO_2 into the cell could be regarded as futile (unless rapidly converted to HCO_3^-) in a low CO_2 environment due to the high permeability of biological membranes and the strong gradient driving CO_2 out of the cell (Hopkinson et al., 2011). Bearing this in mind it would be expected that growth rates and POC fixation would become HCO_3^- dependent at low DIC, however this is not the case. Instead it is proposed that increased leakage due to a decreasing external CO_2 concentration determines growth rates, although HCO_3^- use is increased. This is potentially a larger problem for smaller cells, like *E. huxleyi*, due to the reduced distance separating the CO_2 requiring active site of RubisCO from the bulk media. This suggests that a CCM in small cells may not be very efficient due to it being short-circuited by CO_2 leakage. Further studies investigating carbon fluxes in coccolithophores of varying size could be useful in understanding CO_2 leakage in coccolithophores.

7.3 Coccolithophores in a changing ocean

The ability of the ocean to absorb anthropogenic CO_2 will decrease as global climate change proceeds, having a positive feedback on global warming (Riebesell et al., 2009). Climate model derived data from the IPCC 2007 report indicates that reductions in primary productivity by the terrestrial and ocean ecosystems result in an additional 0.1 – 1.5 °C rise in atmospheric

temperature (Meehl et al., 2007). The large uncertainty is due to the uncertainties associated with processes driving the transport of carbon in ocean and terrestrial systems. As previously discussed coccolithophores play a fundamental role in this carbon cycling. Chapter 4 indicates that *E. huxleyi* is saturated for growth rates at ambient CO₂ and HCO₃⁻ concentrations. This implies that ocean carbonation may not benefit *E. huxleyi* in respect to growth rates. Although this is generally supported by other studies (Summarized in Fig. 3 in Hoppe et al., 2011), the data from Chapter 4 disentangles changes in CO₂ concentration from changes in pH indicating that this saturation is a direct function of CO₂ and is independent of pH until it drops below ~7.7.

The isolation of calcification from the bulk seawater should allow *E. huxleyi* to fully regulate calcification independently of the external pH. However, this is not the case with a decrease in pH having negative effects on intracellular calcification. The expression data in Chapter 4 indicates that the regulatory response to changes in H⁺ concentration over a pH range of 8.3 to 7.7 is minimal. This suggests that the sensitivity of *E. huxleyi* calcification to ocean acidification may be due to the cells inability to regulate its cellular machinery to cope with pH changes. This may tentatively be connected to coccolithophores having not experienced surface-ocean pHs below 8.0 for at least the last 4 Myrs (Zeebe and Ridgwell, 2011). Future studies focusing on understanding the molecular mechanisms of H⁺ transport in coccolithophores are critical. In particular, it is important to understand why cells apparently lack strong control over intracellular pH (Suffrian et al., 2011) in the face of short-term imposed changes in external pH and whether cells change their pH regulation upon acclimation to lower pH.

A critical question in ocean acidification research is “how will organisms will adapt to increased *p*CO₂ and reduced pH?” Most ocean acidification studies are short term and therefore do not span enough generations to allow for genetic adaption. Due to the rapid division rates of most bloom forming algae, it is hypothesized that genetic change is inevitable but whether this will keep up with abiotic changes and what influence it will have on phenotypic shifts within species is uncertain (Collins, 2010). The considerable genetic variation between *E. huxleyi* strains may give it the genetic plasticity to adapt to environmental change by the selection of strains with underlying advantageous genetic traits. The presence of diverse families of genes involved in the transport of ions associated with ocean acidification along with the occurrence of multiple gene copies that have appeared in recent duplication events indicates that *E. huxleyi* may have the genetic capacity to adapt to a changing ocean on relatively short evolution time scales. However, long-term ocean acidification experiments combined with robust genetic analysis are key in understanding coccolithophore adaption in the future ocean.

Although many components of the *E. huxleyi* CCM appear to show similarities to other photosynthetic eukaryotes, its regulation with respect to DIC concentration is considerably

different. Whereas diatoms and *Chlamydomonas* up-regulate their CCMs at CO₂ levels several fold higher than current levels, *E. huxleyi* only shows a clear up-regulation at a CO₂ concentration approximately half that of current oceanic levels. These CO₂ levels may be sporadically experienced at the end of a bloom where CO₂ could drop due to photosynthetic carbon drawdown (Purdie and Finch, 1994). However it is likely that the capacity of coccolithophores to regulate their CCM is becoming increasingly redundant as *p*CO₂ increases. A long-term study investigating the phenotypic effects of *Chlamydomonas* grown at elevated *p*CO₂ for 1,000 generations indicated that the redundant aspects of the CCM mechanism could accumulate mutations that resulted in restricted growth when re-cultured at low CO₂ levels (Collins and Bell, 2004). Whether the *E. huxleyi* CCM will gradually lose its function as surface ocean *p*CO₂ increases requires further investigation, again requiring long-term experiments combined with physiological and genetic analysis.

7.4 Future directions

To understand the bigger picture of *E. huxleyi* cell biology, it is critical that powerful genomic, transcriptomic, proteomic and metabolomic techniques are run in parallel with molecular biology and physiological studies. The full integration of multiple techniques will allow the monitoring of cellular processes at multiple levels over varying time-scales providing a concise picture of cellular responses to environmental changes. The major hindrance of coccolithophore cell biology is the absence of transformation techniques. The ability to knockout, knockdown and overexpress genes has resulted in giant steps in the understanding of cellular processes in a wide range of organisms. Transformation techniques have been available in green algae for three decades (Rochaix and van Dillewijn, 1982) and are now available in several marine algae species. In diatoms they have rapidly progressed the understanding of physiological process such as CCM functioning (Hopkinson et al., 2011) and CO₂ sensing mechanisms (Harada et al., 2006). Techniques for stable transformation or RNA interference in coccolithophores are urgently needed if we want to fully understand the cellular mechanisms underlying calcification, DIC uptake and response to ocean change. Therefore their development should be one of the primary focuses of the coccolithophore research community.

One of the major unanswered questions in coccolithophore research in relation to climate change is how coccolithophores will adapt to ocean acidification. This deserves considerable research effort that should be based on collaborations between evolutionary biologists and biogeochemists. Studies should focus on understanding the genetic plasticity of coccolithophores by assessing the genetic variability between coccolithophore species and strains separated both

spatially and temporally. In parallel long-term culturing approaches combined with the latest genomic-based techniques should be used to assess genetic adaptation over 100's of generations.

In order to understand the importance of coccolithophores in ecosystem processes and the effects of future ocean changes on coccolithophores it is essential that large integrated multi-disciplinary research efforts be undertaken. These should focus on multiple aspects of coccolithophore biology from the cellular to global level working over a wide range of time-scales and concentrating on scaling cellular processes to ecosystem and global changes. Furthermore, a strong emphasis should be on the use of cutting edge techniques including a variety of -omics approaches, systems biology, long-term chemostat culturing, large open ocean mesocosm studies and the use of the latest global models. A fully integrated approach of this nature has the potential to decipher the underlying mechanisms behind coccolithophore cellular processes and how changes in these processes will impact global carbon fluxes.

References

- Bach LT, Riebesell U, Georg Schulz K** (2011) Distinguishing between the effects of ocean acidification and ocean carbonation in the coccolithophore *Emiliana huxleyi*. *Limnology and Oceanography* **56**: 2040-2050
- Badger MR, Price GD, Long BM, Woodger FJ** (2006) The environmental plasticity and ecological genomics of the cyanobacterial CO₂ concentrating mechanism. *Journal of Experimental Botany* **57**: 249-265
- Collins S** (2010) Comment on "Effects of long-term high CO₂ exposure on two species of coccolithophores" by Muller et al. (2010). *Biogeosciences Discussions* **7**: 2673–2679
- Collins S, Bell G** (2004) Phenotypic consequences of 1,000 generations of selection at elevated CO₂ in a green alga. *Nature* **431**: 566-569
- Corstjens P, van der Kooij A, Linschooten C, Brouwers GJ, Westbroek P, de Vrind-de Jong EW** (1998) GPA, a calcium-binding protein in the coccolithophorid *Emiliana huxleyi* (Prymnesiophyceae). *Journal of Phycology* **34**: 622-630
- De Vargas C, Aubry M-P, Probert I, Young J** (2007) Origin and evolution of coccolithophores: From coastal hunters to Oceanic farmers. In PG Falkowski, AH Knoll, eds, *Evolution of primary producers in the sea*. Elsevier, London
- Falkowski PG, Katz ME, Knoll AH, Quigg A, Raven JA, Schofield O, Taylor FJR** (2004) The Evolution of Modern Eukaryotic Phytoplankton. *Science* **305**: 354-360
- Giordano M, Beardall J, Raven JA** (2005) CO₂ concentrating mechanisms in algae: Mechanisms, Environmental Modulation, and Evolution. *Annual Review of Plant Biology* **56**: 99-131
- Harada H, Nakajima K, Sakaue K, Matsuda Y** (2006) CO₂ sensing at ocean surface mediated by cAMP in a marine diatom. *Plant Physiology* **142**: 1318-1328
- Hopkinson BM, Dupont CL, Allen AE, Morel FoMM** (2011) Efficiency of the CO₂-concentrating mechanism of diatoms. *Proceedings of the National Academy of Sciences* **108**: 3830-3837
- Hoppe CJM, Langer G, Rost B** (2011) *Emiliana huxleyi* shows identical responses to elevated pCO₂ in TA and DIC manipulations. *Journal of Experimental Marine Biology and Ecology* **406**: 54-62

- Leonardos N, Read B, Thake B, Young JR** (2009) No mechanistic dependence of photosynthesis on calcification in the coccolithophorid *Emiliana huxleyi* (Haptophyta). *Journal of Phycology* **45**: 1046-1051
- Mackinder L, Wheeler G, Schroeder D, Riebesell U, Brownlee C** (2010) Molecular Mechanisms Underlying Calcification in Coccolithophores. *Geomicrobiology Journal* **27**: 585 - 595
- Mackinder L, Wheeler G, Schroeder D, von Dassow P, Riebesell U, Brownlee C** (2011) Expression of biomineralization-related ion transport genes in *Emiliana huxleyi*. *Environmental Microbiology* **13**: 3250–3265
- Meehl GA, Stocker TF, Collins WD, Friedlingstein P, Gaye AT, Gregory JM, Kitoh A, Knutti R, Murphy JM, Noda A, Raper SCB, Watterson IG, Weaver AJ, Zhao Z-C** (2007) Global Climate Projections. In S Solomon, D Qin, M Manning, Z Chen, M Marquis, KB Averyt, M Tignor, HL Miller, eds, *Climate Change 2007: The Physical Science Basis. Contribution of Working Group I to the Fourth Assessment Report of the Intergovernmental Panel on Climate Change*. Cambridge University Press, Cambridge, United Kingdom and New York, NY, USA
- Price GD, Badger MR, Woodger FJ, Long BM** (2008) Advances in understanding the cyanobacterial CO₂-concentrating-mechanism (CCM): functional components, Ci transporters, diversity, genetic regulation and prospects for engineering into plants. *Journal of Experimental Botany* **59**: 1441-1461
- Purdie DA, Finch MS** (1994) Impact of a coccolithophorid bloom on dissolved carbon dioxide in sea water enclosures in a Norwegian fjord. *Sarsia* **79**: 379-387
- Raven J** (1997) Putting the C in phycology. *European Journal of Phycology* **32**: 319-333
- Raven JA, Giordano M, Beardnell J, Maberly S.** (2012) Algal evolution in relation to atmospheric CO₂: carboxylases, carbon-concentrating mechanisms and carbon oxidation cycles. *Philosophical Transactions of the Royal Society B: Biological Sciences* **367**: 493-507.
- Ridgwell A, Schmidt DN, Turley C, Brownlee C, Maldonado MT, Tortell P, Young JR** (2009) From laboratory manipulations to earth system models: predicting pelagic calcification and its consequences. *Biogeosciences Discussions* **6**: 3455-3480
- Riebesell U, Kortzinger A, Oeschlies A** (2009) Sensitivities of marine carbon fluxes to ocean change. *Proceedings of the National Academy of Sciences of the United States of America* **106**: 20602-20609
- Rochaix JD, van Dillewijn J** (1982) Transformation of the green alga *Chlamydomonas reinhardtii* with yeast DNA. *Nature* **296**: 70-72
- Sekino K, Shiraiwa Y** (1994) Accumulation and utilization of dissolved inorganic carbon by a marine unicellular coccolithophorid, *Emiliana huxleyi*. *Plant and Cell Physiology* **35**: 353-361
- Suffrian K, Schulz KG, Gutowska MA, Riebesell U, Bleich M** (2011) Cellular pH measurements in *Emiliana huxleyi* reveal pronounced membrane proton permeability. *New Phytologist*: DOI: 10.1111/j.1469-8137.2010.03633.x
- Zeebe R, Ridgwell A** (2011) Past changes in ocean carbonate chemistry In J-P Gattuso, L Hansson, eds, *Ocean Acidification*, Ed 1. Oxford University Press, Oxford, pp 21-40

Acknowledgements

Having a joint PhD between a German and a UK institution has given me the opportunity to meet many exciting people and form fruitful collaborations. I owe my kite-surfing partner Lennart Bach (GEOMAR) who through a truly collaborative set of experiments enlightened my thinking of cellular carbon transport in coccolithophores. I would like to thank my biking buddy, Kai Lohbeck (GEOMAR), for the endless discussions about coccolithophore biology, always a great source of ideas, coffee and fun. I would like to thank Dr. Kai Schulz (GEOMAR) for help and advice, Prof. Markus Bleich (Kiel University) and Prof. Thorsten Reusch (GEOMAR) for access to laboratory facilities, Dr. Peter von Dassow (Universidad Católica de Chile) for access to preliminary EST data, Dr. Reidar Andreson (Tartu University, Estonia) for our on-going collaboration analysing transcriptomic data and Matt Hall (MBA) and Katrin Beining (GEOMAR) for running efficient labs to support my research. I am in debt to my girlfriend, Caitlin Curry, who has been an endless source of support, always putting a smile on face after a long day. I would like to thank my family for always supporting me whatever I have done or wherever I have decided to go. My biggest thanks go to Dr. Glen Wheeler (MBA) who without his support, ideas, direction, time and endless enthusiasm for science I would have been lost. I am also very grateful to Dr. Declan Schroeder (MBA) for giving me the opportunity to begin my research career and to Prof. Colin Brownlee (MBA) and Prof. Ulf Riebesell (MBA) who secured the funding for the project and provided essential guidance throughout the project. I would further like to thank all of my friends in Kiel and Plymouth for all the great times I have had during my PhD outside of science, providing the balance which I truly believe makes me love what I do.

Declaration of work

Apart from my supervisor's guidance, or where clearly stated, the content and design of this thesis is the result of work completed by myself. I declare that this thesis has not been submitted to another examining body, either partially or wholly, as part of a doctoral degree. The thesis as a whole has not been published or submitted for publication. Chapters 2 and 3 have been published as they appear in this thesis. This thesis has been prepared subject to the Rules of Good Scientific Practice of the German Research Foundation.